US Army Corps of Engineers

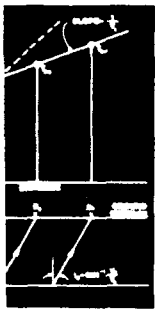

GEOTECHNICAL LABORATORY

TECHNICAL REPORT GL-89-10

IN SITU SEISMIC INVESTIGATION OF FOLSOM DAM AND RESERVOIR PROJECT

by

José L. Llopis

Geotechnical Laboratory

DEPARTMENT OF THE ARMY
Waterways Experiment Station, Corps of Engineers
3909 Halls Ferry Road
Vicksburg, Mississippi 39180-6199

September 1989
Final Report

Prepared for US Army Engineer District, Sacramento
Sacramento, California 95814-4794

Destroy this report when no longer needed. Do not return it to the originator.

The findings in this report are not to be construed as an official Department of the Army position unless so designated by other authorized documents.

The contents of this report are not to be used for advertising, publication, or promotional purposes. Citation of trade names does not constitute an official endorsement or approval of the use of such commercial products.

REPORT DOCUMENTATION PAGE

Form Approved
OMB No. 0704-0188

1a. REPORT SECURITY CLASSIFICATION Unclassified	1b. RESTRICTIVE MARKINGS
2a. SECURITY CLASSIFICATION AUTHORITY	3. DISTRIBUTION/AVAILABILITY OF REPORT Approved for public release; distribution unlimited.
2b. DECLASSIFICATION/DOWNGRADING SCHEDULE	
4. PERFORMING ORGANIZATION REPORT NUMBER(S) Technical Report GL-89-10	5. MONITORING ORGANIZATION REPORT NUMBER(S)
6a. NAME OF PERFORMING ORGANIZATION USAEWES Geotechnical Laboratory 6b. OFFICE SYMBOL (If applicable) CEWES-GG-F	7a. NAME OF MONITORING ORGANIZATION
6c. ADDRESS (City, State, and ZIP Code) 3909 Halls Ferry Road Vicksburg, MS 39180-6199	7b. ADDRESS (City, State, and ZIP Code)
8a. NAME OF FUNDING/SPONSORING ORGANIZATION US Army Engineer District, Sacramento 8b. OFFICE SYMBOL (If applicable) SPKED	9. PROCUREMENT INSTRUMENT IDENTIFICATION NUMBER
8c. ADDRESS (City, State, and ZIP Code) 650 Capital Mall Sacramento, CA 95814-4794	10. SOURCE OF FUNDING NUMBERS PROGRAM ELEMENT NO. / PROJECT NO. / TASK NO. / WORK UNIT ACCESSION NO.

11. TITLE (Include Security Classification)
In Situ Seismic Investigation of Folsom Dam and Reservoir Project

12. PERSONAL AUTHOR(S)
Llopis, Jose´ L.

13a. TYPE OF REPORT	13b. TIME COVERED	14. DATE OF REPORT (Year, Month, Day)	15. PAGE COUNT
Final report	FROM _____ TO _____	September 1989	226

16. SUPPLEMENTARY NOTATION
Available from National Technical Information Service, 5285 Port Royal Road, Springfield, VA 22161.

17. COSATI CODES			18. SUBJECT TERMS (Continue on reverse if necessary and identify by block number)
FIELD	GROUP	SUB-GROUP	Dams Folsom Dam (Calif.) Geophysical investigations

19. ABSTRACT (Continue on reverse if necessary and identify by block number)

An in situ geophysical investigation consisting of surface refraction, surface vibratory, downhole and crosshole seismic tests was performed at the man-made water retaining structures at Folsom Dam and Reservoir Project, located on the American River approximately 23 miles northeast of Sacramento, CA. More specifically the investigation was performed at Dike 5, the Right and Left Wing Dams, and at Mormon Island Auxiliary Dam. The investigation was conducted to obtain compression-, shear-, and Rayleigh-wave (P-, S-, and R-wave) velocities as a function of depth within the dike and dams and their underlying foundations for input to the seismic stability analysis of these earthen retaining structures.

20. DISTRIBUTION/AVAILABILITY OF ABSTRACT ☒ UNCLASSIFIED/UNLIMITED ☐ SAME AS RPT ☐ DTIC USERS	21. ABSTRACT SECURITY CLASSIFICATION Unclassified
22a. NAME OF RESPONSIBLE INDIVIDUAL	22b. TELEPHONE (Include Area Code) / 22c. OFFICE SYMBOL

DD Form 1473, JUN 86 *Previous editions are obsolete.*

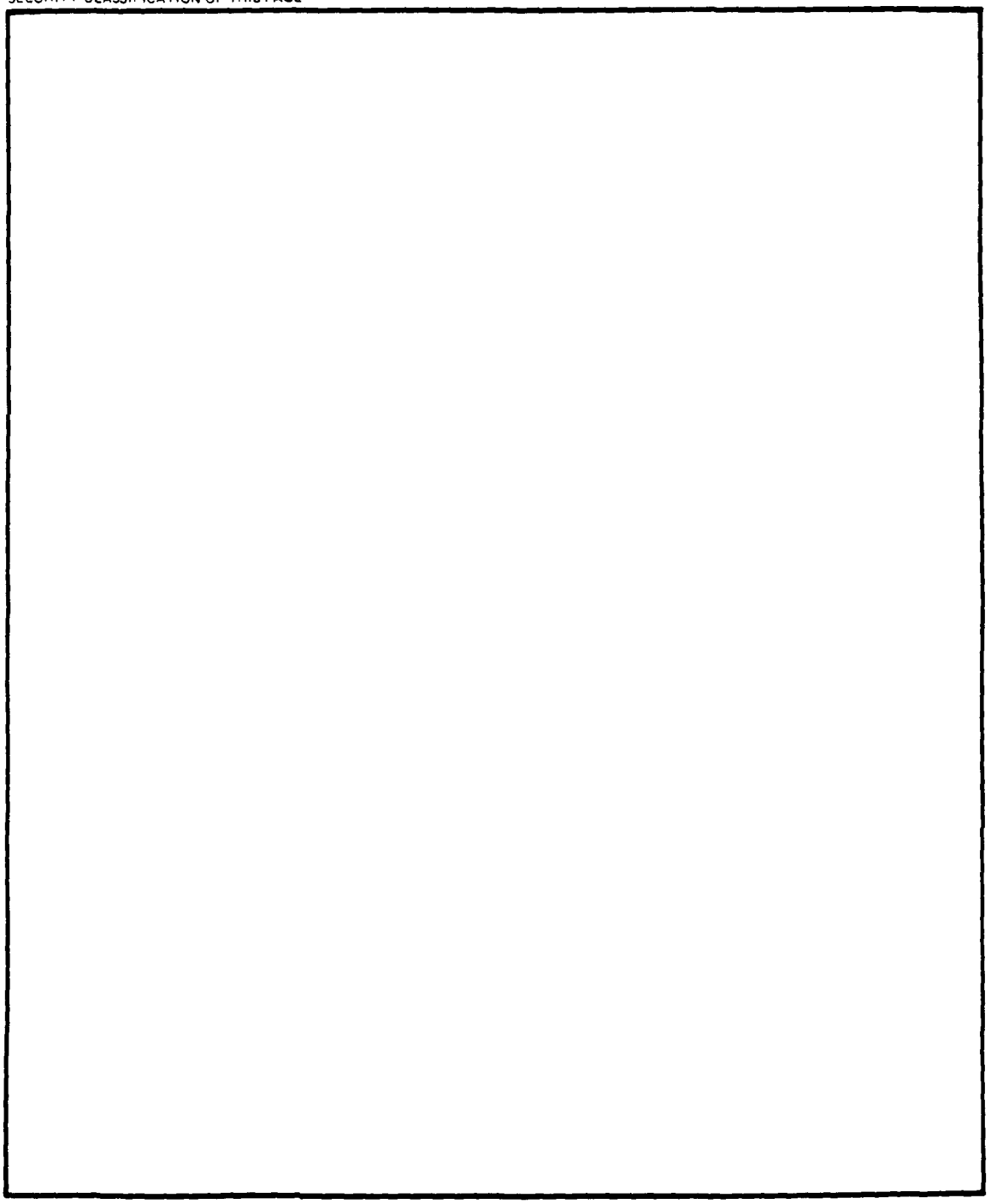

PREFACE

An in situ seismic investigation at Folsom Dam was authorized by the US Army Engineer District, Sacramento (SPK), Under Intra-Army Order for Reimbursable Services Nos. SPKED-F-82-16 dated 18 Dec 1981, SPKED-F-83-16 dated 8 Oct 1982, SPKED-F-83-16 change No. 1 dated 11 May 1983, and CESPK-ED-D-88-56 dated 24 Aug 1988.

The field investigation was performed during the periods 24 May through 4 June 1982 and 12 April through 4 May 1983. Messrs. Jose' L. Llopis, Donald E. Yule, Thomas B. Kean, Michael K. Sharp, Donald H. Douglas, Keller Golden, Ms. Mary Tinker, and LT Stephen G. Sanders of the Earthquake Engineering and Geophysics Division (EEGD), Geotechnical Laboratory (GL); and James L. Pickens of the Instrumentation Services Division (ISD), of the US Army Engineer Waterways Experiment Station (WES), were members of the field parties who carried out this project. Technical support was provided by Dr. Paul F. Hadala, Assistant Chief, GL, Dr. Mary Ellen Hynes, Messrs. Joseph R. Curro, Jr., David W. Sykora, and Ronald E. Wahl (EEGD). The analysis phase of this study was performed by Mr. Llopis under the general supervision of Dr. Arley G. Franklin, Chief, EEGD, and Dr. William F. Marcuson III, Chief, GL. This report was edited by Ms. Joyce H. Walker of the Information Technology Laboratory.

The series of eight reports which document the seismic stability evaluations of the man-made water retaining structures of the Folsom Dam and Reservoir Project, located on the American River in California, are as follows:

Report 1: Summary
Report 2: Interface Zone
Report 3: Concrete Gravity Dam
Report 4: Mormon Island Auxiliary Dam - Phase I
Report 5: Dike 5
Report 6: Right and Left Wing Dams
Report 7: Upstream Retaining Wall
Report 8: Mormon Island Auxiliary Dam - Phase II

Data reported herein were used in Reports 1, 4, 5, 6, and 8.

Commander and Director of WES during the preparation of this report is COL Larry B. Fulton, EN. Dr. Robert W. Whalin is Technical Director.

CONTENTS

CONVERSION FACTORS, NON SI-TO SI (METRIC)
UNITS OF MEASUREMENT

Non-SI units of measurement used in this report can be converted to SI (metric) units as follows:

Multiply	By	To Obtain
feet	0.3048	metres
inches	2.54	centimetres
miles (US statute)	1.609	kilometres
pounds (force)	4.4482	newtons
pounds (mass)	0.4536	kilograms

IN SITU SEISMIC INVESTIGATION OF FOLSOM DAM AND RESERVOIR PROJECT

PART I: INTRODUCTION

Background, Purpose, and Scope of Study

1. Current computerized seismic wave propagation analysis procedures for earth dams and foundations require that values of compression- and shear-wave (P- and S-wave) propagation velocities be determined as a function of depth. These seismic velocities are used in conjunction with conventional field sampling and laboratory testing to provide soil property information for a dynamic analysis of the dam and its foundation.

2. A geophysical investigation was conducted at Folsom Dam, which is located on the American River approximately 23 miles* northeast of Sacramento, California, as shown in Figure 1. More specifically the investigation was conducted at Dike 5, the Right and Left Wing Dams which flank the Concrete Gravity Dam, and at Mormon Island Auxiliary Dam all of which are shown in Figure 2. The investigation was performed to determine P- and S-wave velocities as a function of depth within the dam and underlying foundation materials. A suite of seismic test methods was used to determine true P- and S-wave velocity zonations of the embankments and their foundations for use in a dynamic analysis.

Site Geology

3. At the time of construction, the geology at the site was carefully detailed in the Foundation Reports by US Army Engineer District, Sacramento (1953a,b,c, and d, 1954, and 1955). These foundation reports and a later paper by Kiersch and Treasher (1955) are the sources for the summary of site geology provided in this section.

---

* A table of factors for converting non-SI to SI (metric) units of measurement is presented on page 4.

4. The Folsom Dam and Reservoir Project is located in the low, western-most foothills of the Sierra Nevada in central California, at the confluence of th North and South Forks of the American River. Topographic relief ranges from a maximum of 1,242 ft near Flagstaff Hill, located between the upper arms of the reservoir, to 150 ft near the town of Folsom just downstream of the Concrete Gravity Dam. The North and South Forks once entered the confluence in mature valleys up to 3 miles wide, but further downcutting of the river resulted in a V-shaped inner valley 20 to 185 ft deep. Below the confluence, the inner canyon was flanked by a gently sloping mature valley approximately 1.5 miles wide bounded on the west and southeast by a series of low hills. The upper arms of the reservoir, the North and South Forks, are bounded on the north and east by low foothills.

5. A late Pliocene-Pleistocene course of the American River flowed through the Blue Ravine and joined the present American River channel downstream of the town of Folsom. The Blue Ravine was filled with late Pliocene-Pleistocene gravels, but with subsequent downcutting and headward erosion, the Blue Ravine was eventually isolated and drainage was diverted to the present American River Channel.

6. The important formations at the damsite are: a quartz diorite granite which forms the foundation at the Concrete Gravity Dam, Wing Dams, and Saddle Dikes 1 through 7; metamorphic rocks of the Amador Group which form the foundation at Mormon Island Auxiliary Dam and Saddle Dike 8; the Mehrten Formation, a deposit of cobbles and gravels in a somewhat cemented clay matrix which caps the low hills that separate the saddle dikes and is part of the foundation at Dike 5; and the alluvium that fills the Blue Ravine at Mormon Island Auxiliary Dam.

7. Weathered granitic or metamorphic rock is present throughout the area. Figure 2 shows a geologic map of the project area. The Concrete Gravity Dam, the Wing Dams, the retaining walls, and Dikes 1 through 7 are founded on weathered quartz diorite granite. Between Dikes 7 and 8 there is a change in bedrock type. Dike 8 and Mormon Island Auxiliary Dam are underlain by metamorphic rocks of the Amador Group. The Amador Group consists predominately of schists with numerous dioritic and diabasic dikes.

Test Program

8. After a preliminary seismic test program had been planned by personnel of the US Army Engineer District, Sacramento, (SPK) it was submitted to the US Army Engineer Waterways Experiment Station (WES) for review. Pertinent information relative to the design and construction of the embankment was provided to aid in that review. The finalized test program consisted of seismic refraction, crosshole, downhole, and surface vibratory tests which would provide the geophysical data necessary to complete an analysis of Dike 5 and the dams' response to earthquake loadings. The locations of the various tests conducted for each of the embankments investigated are presented in Part II of this report.

9. The pool elevations while conducting the surface vibratory and preliminary seismic refraction tests ranged between 462 and 465 ft with an average pool elevation of 464 ft (24 May - 4 June 1982). During the performance of the crosshole, downhole, and seismic refraction surveys, the pool elevation ranged between 433 and 445 ft with an average pool elevation of 437 ft (12 April - 4 May 1983).

10. The velocity profiles presented in Hynes (1989), Hynes et al. (1988), Wahl and Hynes (1988), Wahl et al. (1989), and Wahl et al. (1988)*, were based on preliminary results from crosshole seismic tests reported by Llopis (1983) and Kean (1988). The P-wave velocity profiles presented in this report are based on results from seismic refraction, crosshole, and downhole tests; whereas, the S-wave velocity profiles are based on results from surface vibratory, crosshole, and downhole testing.

11. The P-wave velocity profiles used in Reports 1,4,5,6, and 8 are used primarily to distinguish between materials that have very low or very high levels of saturation and to delineate top of rock and geologic contacts for input to the computer program SHAKE (Schnabel, Lysmer, and Seed 1972). The S-wave velocities reported in Reports 1,4,5,6,and 8 are used in developing idealized soil profiles and determining soil moduli for input to SHAKE. Both

---

* For the remainder of this report Hynes (1989), Hynes et al. (1988), Wahl and Hynes (1988), Wahl et al. (1989), and Wahl et al. (1988) will be referred to as Reports 1,4,5,6, and 8, respectively.

the P- and S-wave velocity profiles reported in Reports 1,4,5,6, and 8 and in this report agreed very well. Minor differences between the profiles exist but they are not significant enough to affect the results of the stability analysis of Dike 5, the Wing Dams, or Mormon Island Auxiliary Dam.*

Geophysical Test Principles and Field Procedures

12. The geophysical survey procedures, including a brief description of each survey as it pertains to this investigation, are given below. These tests were run in order to obtain velocities of the materials, present at the site, as a function of depth. Further information regarding geophysical testing and interpretation procedures used in this study can be obtained in Engineer Manual EM 1110-1-1802 (Department of the Army 1979).

13. Surface seismic refraction tests. The seismic refraction method utilizes the fact that the velocity of seismic wave propagation in a material is dependent on its elastic properties. It is assumed that materials are locally homogeneous and isotropic. With this method of investigation, depth and location of bodies or layers having contrasting elastic properties and their corresponding seismic velocities are determined. In the seismic refraction method, seismic energy is imparted into the ground usually by means of explosives or by striking a metal plate, placed on the ground surface, with a sledgehammer. The location of the disturbance is considered a point source and the disturbance is transmitted through the ground as a series of waves. Geophones (velocity transducers), which are used to detect the seismic wave, are implanted into the ground surface and laid along a straight line spaced at regular intervals. The length of the line depends on the required depth of investigation; a common rule of thumb is the length of the line should be from three to four times the depth of interest. Interpretation of the seismic refraction data makes use of plots of the P-wave arrival times versus the geophone distances from the seismic source.

---

* Personal Communication, May 1989, Dr. Mary Ellen Hynes, Research Civil Engineer, and Mr. Ronald E. Wahl, Civil Engineer, US Army Engineer Waterways Experiment Station, Vicksburg, MS.

14. Crosshole tests. Crosshole tests were used to determine horizontal P- and S-wave velocities as a function of depth. One advantage of crosshole testing as opposed to surface seismic refraction is its ability to detect lower velocity layers underlying or sandwiched between layers of higher velocity. The crosshole technique is therfore considered to be inherently more definitive and accurate than the surface refraction test but has the shortcoming of requiring boreholes and not being able to cover as much areal extent; thus the techniques are used in a complementary manner. Basically, testing consists of measuring the arrival time of a P- or S-wave that has traveled from a source in one borehole to a detector in another for different test elevations. Knowing the distance between borings and the time the P- or S-waves take to travel across this distance the velocity can be computed (distance divided by time).

15. Crosshole testing on the centerline and at the downstream shoulders of the embankments and also on the downstream slope of Dike 5 was performed in boreholes cased with 4-in. ID polyvinyl chloride (PVC) pipe. The annular space between the casing and walls of the borings was grouted with a mixture of portland cement, bentonite, and water, which, after setting up, had a consistency similar to that of soil.

16. Crosshole testing in the shells of the embankments and in the dredged tailings, downstream toe of Mormon Island Auxiliary Dam, was performed in 5-in. ID steel-cased borings. The gravelly nature of the shells and dredged tailings made it necessary to use Odex equipment to drill the holes. The Odex system of drilling consists of a downhole pneumatic hammer with an expanding bit that pulls a steel casing behind the bit. When the casing is in place, the bit can be retracted and withdrawn through the casing. The Odex system was selected for the installation of the cased holes because this system does not require grouting the casing in the gravelly material as would be the case if common drilling and PVC casing were employed. It was believed that if grout had been used, the grout might have flowed through the gravel material, cementing it together, and when tested would have given erroneous results. The disturbance to the gravels when drilling these holes with the Odex system is thought to be relatively minor and allows several holes to be installed in a single day. Unfortunately, the Odex system does not provide a means of satisfactorily sampling the subsurface.

17. Borehole deviation (drift) surveys were conducted to determine the precise vertical alignment of each boring. Accurate reduction of data from the crosshole tests requires knowledge of the drift of each boring so that a straight-line distance between borings at each test depth can be established. An analysis of the crosshole data obtained at each test elevation was made with the aid of a computer program developed at WES (Butler, Skoglund, and Landers 1978).

18. Velocities were obtained by placing a detector in a receiver borehole and a source of seismic energy at the same elevation in another borehole (source hole). The detector consisted of a triaxial array of geophones (two mounted horizontally at 90 deg to each other, and one vertically oriented) housed in one container. The container housing the geophones was clamped firmly to the casing wall by means of an air-inflatable rubber bladder. An explosive charge (exploding bridgewire (EBW) detonator) was used for the crosshole P-wave tests. For the crosshole S-wave tests a downhole vibrator was used as a source of S-waves. The S-wave testing procedure consisted of lowering the vibrator in the borehole to a selected test elevation and clamping the vibrator firmly to the sidewalls of the PVC casing by means of an inflatable rubber bladder. When the vibrator was in position, the operator swept the oscillator through a range of frequencies (50 to 500 Hz) and selected one that propagated well (one with a high amplitude) through the transmitting medium. The time required for the P- and S-waves to travel from source to receiver were recorded with a portable, battery-powered, 12-channel seismograph with data-enhancement capability. Crosshole testing at each crosshole set was performed at 5-ft depth intervals.

19. Downhole tests. Downhole surveys are conducted by placing an energy source on the surface close to the mouth of a borehole, and a triaxial array of geophones placed in the borehole. In this type of survey the travel path of the seismic signal is forced to traverse all of the strata between the source and detector. Unlike the crosshole test the downhole test requires only a single boring. These surveys are useful for detecting and measuring wave velocities in blind zones or underlying zones of low velocity, which are normally not detectable in a surface refraction survey.

20. Downhole surveys are conducted by creating a seismic disturbance near the mouth of the borehole and measuring the time of arrival of this disturbance at various depths in the boring. In the case of downhole P-wave test the seismic disturbance was created by striking a steel plate, placed approximately 5 ft from the mouth of the borehole, with a sledgehammer. In the case of downhole S-wave tests the S-wave energy source was a sledgehammer impacting a large wooden plank located near the mouth of the borehole. S-wave signals of opposite polarity were generated by striking opposite ends of the plank. With reversal of polarity of the source, the polarity of the S-wave is reversed; whereas, the polarity of the P-wave is not. This allows the interpreter to pick the S-wave arrival by comparing signal wave forms measured in successive tests with reverse polarity. A triaxial geophone array (detector) placed in the borehole was used to measure the amount of time the disturbance took to travel from source to detector. This procedure was repeated at 5-ft depth increments.

21. Surface vibratory tests. These tests were conducted to determine Rayleigh-wave (R-wave) velocities of the embankments and foundation materials as a function of depth. The R-wave velocity is slightly lower than the S-wave velocity. For homogeneous media and for Poisson's ratios commonly found in soil materials, the difference in velocities is less than 9 percent (Ballard 1964). Therefore, for practical purposes, S-wave velocities and shear moduli can be determined approximately by surface vibratory tests, which generate strong R-wave trains.

22. The R-waves in this investigation were generated by a 4,000-lb force (peak) electrohydraulic vibrator with a 10- to 300-Hz frequency range. The test procedure consisted of positioning the vibrator at a selected location and placing velocity transducers (geophones) in a straight line (starting at and extending away from the vibrator) at selected intervals along the ground surface. The vibrator was then operated at discrete selected frequencies with the R-wave being monitored by the geophones (geophone nearest the vibrator served as zero time). The time lag for each geophone, referenced to the zero-time geophone, was determined and was plotted versus the respective distances that the geophones were from the the reference geophone (zero-time geophone). The R-wave velocity for each source frequency was

determined from the slope of the best-fit line obtained in the plot. With the frequency and R-wave velocity known, a corresponding wavelength was computed by dividing the velocity by the frequency. Wave velocities thus derived are assumed to be average values for an effective depth of one-half the wavelength. R-wave velocities that are determined near a high velocity contrast interface, such as a soil-rock boundary, will probably be influenced by both the higher and lower velocity materials and thus provide weighted average velocities dependent on the physical properties of the two layers.

PART II: TEST RESULTS

DIKE 5

Description

23. Dike 5 is the largest of the eight saddle dikes at the Folsom Project having a crest length of 1,920 ft and a maximum height of 110 ft. The embankment is located in a relatively steep walled topographic saddle. Two basic types of foundation conditions are present beneath the embankment. The portion of the embankment whose foundation is above elevation 450 ft is founded on the Mehrten Formation, which is composed of cobbles and gravels in a cemented clayey matrix. The remainder of the embankment is founded on a weathered quartz diorite granite.

24. The embankment is essentially homogenous and is constructed of compacted decomposed granite scraped from the weathered granite in borrow areas located in what is now the reservoir. The compacted decomposed granite, a saprolite, classifies as a silty sand according to the Unified Soil Classification (USCS). The construction specifications required that the central portion of the embankment, Zone C, receive a higher compactive effort than Zone D located in areas directly under the upstream and downstream slopes. Seepage is controlled by a downstream drainage blanket. The upstream side of the embankment has slopes of 3.25H:1.0V at below elevation 466 ft and 2.25H:1.0V between elevation 466 and 480.5 ft (crest elevation). The downstream side has one continuous slope of 2.25H:1.0V. A cross-section of Dike 5 is shown in Figure 3.

Test Results

25. Figure 4 shows the location and layout of the geophysical tests conducted at Dike 5. The geophysical program at Dike 5 consisted of seismic refraction, crosshole, downhole, and surface vibratory testing.

Surface seismic refraction tests

26. One refraction line designated R-1 was run along the downstream toe of Dike 5 between approximate Station 178+50 and 182+50, as shown in Figure 4. Line R-1 was 320 ft in length and consisted of 12 geophones spaced 25 ft apart. Shot points were offset 25 and 20 ft from the end of the line. The time-distance (TD) plot for refraction line R-1 is presented in Figure 5. The results indicate that two layers can be determined. The first or uppermost layer has a P-wave velocity of 2,110 fps and extends to an average depth of 10 ft where the second layer with true velocity of 9,930 fps is encountered. The first velocity layer corresponds to overburden or very intensely weathered granite, whereas, the second layer velocity is indicative of weathered granite.

Surface vibratory tests

27. Four 200-ft long vibratory lines, designated V-5 through V-8, were run along the crest of Dike 5, as shown in Figure 4. Lines V-5 and V-6 were run with the vibrator positioned at the highest section of the dam, Station 180+50. The measured R-wave velocities for vibratory lines V-5 and V-6 are presented in Figure 6. Vibratory lines V-5 and V-6 indicate similar velocity profiles. The R-wave velocities range between approximately 800 fps near the surface to approximately 925 fps at a depth of about 60 ft, the maximum depth of R-wave penetration. The velocities over the depth range of 0 to 60 ft were influenced entirely by the core material, compacted decomposed granite.

28. Surface vibratory lines V-7 and V-8 were run with the vibrator positioned approximately at Station 191+00. These lines were conducted on the portion of the dike that is founded on the Mehrten Formation. The average embankment height in this area is roughly 15 ft. The R-wave velocities obtained from lines V-7 and V-8 are displayed in Figure 7. The R-wave velocities increase from about 800 fps at an approximate depth of 10 ft to about 1,050 fps at a depth of 20 ft and remain essentially constant between approximate depths of 20 and 60 ft, the maximum R-wave penetration depth. The velocities measured by R-wave lines V-7 and V-8 are influenced by the relatively shallow Mehrten Formation. The results indicate that the Mehrten Formation has a higher R-wave velocity than the overlying embankment.

Crosshole tests

29. Crosshole P- and S-wave tests at Dike 5 were conducted in two pairs of boreholes near Station 180+50, as indicated in Figure 4. The boreholes designated as SS-1 and US-1 which were located on the centerline of the dike were 115 ft in depth and spaced 10 ft apart; whereas, the boreholes SS-10 and US-10 located on the downstream slope of the dike were 55 ft in depth and spaced 10 ft apart. Both borehole sets were cased with 4-in. ID PVC pipe and extended through the embankment and into the underlying weathered granite foundation.

30. P-wave tests. The calculated true P-wave velocities, as determined by the CROSSHOLE computer program, for each test elevation for the two crosshole sets, SS-US-1 and SS-US-10, are presented respectively in Figure 8 and 9. As previously mentioned, testing was conducted at 5-ft depth intervals. Figure 10 shows the P-wave velocity zones interpreted from both crosshole sets superimposed on the section of Dike 5 at Station 180+50. The interpretation indicates that the velocity of the compacted decomposed granite in the embankment ranges in velocity from 1,650 fps to 4,550 fps. Zones with velocities approaching 4,800 fps are nearly saturated. The results indicate that probably at the time of testing only the portions of the embankment just above the foundation upstream of the centerline had high degrees of saturation. The P-wave velocity of the weathered granite foundation was measured to be 9,250 and 10,175 fps.

31. S-wave tests. The calculated true S-wave velocities, as determined by the CROSSHOLE computer program, for crosshole sets SS-US-1 and SS-US-10, are respectively presented in Figures 11 and 12. The S-wave velocity zones interpreted from the crosshole sets are shown in Figure 13. In the compacted decomposed granite of the embankment the shear wave velocities generally increase with depth. The velocities measured range from 950 fps to 1,575 fps. The S-wave velocities measured in the weathered granite foundation were 2,225 fps beneath the centerline and 2,875 fps under the slope.

Downhole tests

32. Downhole P- and S-wave tests were conducted in borings SS-1 (crest) and SS-10 (downstream slope) at 5-ft depth increments as shown in Figure 4. The downhole test results are presented in conventional time versus slant distance (slant distance is nearly equal to depth) plots.

33. P-wave tests. Figures 14 and 15 present the data collected from the downhole P-wave test conducted in boring sets located on the crest and downstream slope of the dike. The P-wave velocity zones obtained from downhole testing are shown in Figure 16. Four velocity zones which ranged in velocity between 1,500 and 9,300 fps were indicated in the core material and foundation materials. Three velocity zones ranging between 1,525 and 5,500 fps were interpreted for the shell and foundation materials.

34. S-wave tests. Figures 17 and 18 respectively present the data acquired from the downhole S-wave test conducted in borings located on the crest and downstream slope of the dike. The velocity zones obtained from downhole S-wave tests are shown in Figure 19. Velocity zones of 1,000 and 1,450 fps were indicated in the core while three velocity zones with values ranging between 780 and 2,500 fps were indicated for the shell and foundation materials.

Data Consolidation

35. In order to facilitate interpretation of the data acquired at approximate Station 180+50 using the various geophysical techniques, it is convenient to present the data in composite form so that a zonal interpretation can be developed using all the available data. Such composites were prepared for P- and S-wave tests and are presented in Figures 20 and 21, respectively.

36. As shown in the P-wave composite (Figure 20), three zones of the dike were tested: the central impervious core, the downstream shell, and the foundation beneath and at the toe of the dike. Results from downhole and crosshole tests are presented for the core, shell, and foundation beneath the dike and at the downstream toe. Comparison of the results from each test for a specific zone are generally in good agreement on velocities and depths to interfaces with the exception of the downhole test conducted on the downstream

slope. For this particular test the velocity of the foundation materials is indicated as 5,500 fps which is in disagreement with values obtained for similar material as determined by other testing.

37. As depicted in the S-wave composite (Figure 21) tests were conducted in the core, shell, and foundation of the dike. Results from crosshole and downhole tests are presented for the core, shell, and foundation materials beneath the dike. Also shown are results from surface vibratory tests for the core materials. Velocities and depths to interfaces differ somewhat because of differences inherent with these test techniques.

RIGHT WING DAM

Description

38. The Right Wing Dam is a zoned embankment dam which flanks the northwest portion of the Concrete Gravity Dam. The Right Wing Dam is founded on weathered quartz diorite granite. A plan view of the Right Wing Dam is shown in Figure 22. The Right Wing Dam has a crest length of approximately 6,700 ft and a maximum height of approximately 195 ft. The core (Zone C) consists of well-compacted decomposed granite and suitable fine-grained materials from the American River channel. From Station 219+50 to Station 238+60, the zoned embankment is constructed on top of an existing homogeneous test embankment. Gravels (Zone B material) excavated from the American River channel were used as upstream and downstream transition zones. An uncompacted rock-fill shell (Zone A material) was constructed on the upstream and downstream slopes over most of the length of the dam. The upstream slopes are 2.25H:1.0V, and the downstream slopes are 2.0H:1.0V. Typical sections are shown in Figures 23 and 24.

Test Results

39. Figure 22 shows the location and layout of the geophysical tests conducted at the Right Wing Dam. The geophysical program consisted of seismic refraction, crosshole, downhole, and surface vibratory testing.

Surface seismic refraction tests

40. Three P-wave refraction lines were run along the downstream toe of the Right Wing Dam, as shown in Figure 22. Each of the three refraction lines were 325 ft in length with twelve geophones spaced 25 ft apart and 25 ft shotpoint offsets. Seismic refraction line R-4 was run along a service road on the downstream toe of the Right Wing Dam between approximate Stations 235+90 and 239+15. The TD plot for line R-4 is presented in Figure 25. The southern shotpoint (Station 239+15) was located above the filled-in North Fork Ditch which ran beneath and perpendicular to the dam. One of the short-comings of the seismic refraction method is that it assumes subsurface layers to be locally homogeneous and horizontally continuous. With the ditch being under one of the shotpoints this assumption is violated and, as a consequence, depths to layers beneath the shotpoint cannot be computed. Unfortunately, the existence of the ditch was unknown to the geophysical field party at the time of testing.

41. Results from line R-4 indicate that three velocity zones may be defined. The first layer with a velocity of 770 fps has a thickness of approximately 2.5 ft. The second layer, highly weathered granite, has a velocity of 6,140 fps and extends to a depth of approximately 28 ft where the less weathered granite is encountered with a velocity of approximately 12,790 fps.

42. Seismic refraction line R-3 was run on the downstream toe of the Right Wing Dam between approximate Stations 253+00 and 256+25. The line was run on fill material. Figure 26 presents the TD plot obtained from refraction line R-3. The data indicate three velocity zones. The topmost zone, fill and overburden material, is approximately 4 ft thick and has an average velocity of 800 fps. The second interpreted zone, which probably corresponds to the highly weathered granitic material, has a true velocity of 3,420 fps and extends to a depth of approximately 23 ft. The less altered granite is interpreted as having a true velocity of 13,730 fps.

43. Refraction line R-2 was located on the downstream toe of the Right Wing Dam between approximate Stations 267+00 and 270+25. The TD plot for refraction line R-2 is presented in Figure 27. The TD plot indicates that three P-wave velocity zones may be determined. The uppermost zone has an average velocity of 710 fps and extends to an average depth of 3 ft. The

second zone, which corresponds to highly weathered granite, has a true velocity of 5,000 fps and extends to an average depth of approximately 20 ft where the less weathered granite with a true velocity of 14,350 fps is encountered. Inspection of the TD plot indicates, as expected, a degree of variability in the thickness of the highly weathered granite.

Surface vibratory tests

44. Ten, 200-ft long, vibratory lines were run along the crest and downstream toe of the Right Wing dam as illustrated in Figure 22. The results of the vibratory tests are presented in Figures 28 through 32. Vibratory lines V-3 and V-4 were run along the crest of the Right Wing Dam with the vibrator positioned between borings US-2 and SS-2, approximate Station 235+00. The results from lines V-3 and V-4 are presented in Figure 28. The data suggest that the R-wave velocity increases slightly with depth and ranges between 900 and 1,000 fps. The depth of investigation ranged between approximately 5 and 60 ft. Vibratory lines V-1 and V-2 were run along the crest of the Right Wing Dam with the vibrator positioned between borings US-3 and SS-3, approximate Station 269+50, as shown in Figure 22. The velocity profile for lines V-1 and V-2 is presented in Figure 29 and is very similar to that of lines V-3 and V-4. These data show that the velocities increase slightly with depth and range in velocity between 900 and 1,000 fps over the 5- to 60-ft depth range. Vibratory lines V-23 and V-24 were run along the downstream toe of the Right Wing Dam with the vibrator positioned at approximate Station 240+75 and the results are presented in Figure 30. Vibratory data for line V-24, run between approximate Stations 238+75 and 240+75 is quite erratic and is felt not to be valid and, consequently, is not used in determining a best fit curve through the data. The R-wave velocity for line V-23 is approximately 1,250 fps between depths of 10 and 20 ft at which point the velocity decreases gradually with depth to approximately 1,175 fps at 40 ft where the velocity remains constant to a depth of 60 ft. Figure 31 presents the R-wave velocity versus depth for vibratory lines V-19 and V-20 which were run on the downstream toe of the Right Wing Dam between approximate Stations 251+50 and 255+50. Because of inaccessibility to the site, the vibratory line was offset approximately 300 ft from the toe of the dam and was located on an area that appeared to be backfilled with about a

10- to 20-ft thick layer of random fill. Data from line V-20 is deemed to be unusable and is not used in determining the R-wave velocity versus depth curve. R-wave velocities from line V-19 ranged from approximately 675 fps from a depth of 5 ft to 825 fps to a depth of 60 ft. Vibratory lines V-17 and V-18 were run on the downstream toe of the Right Wing Dam with the vibrator centered near approximate Station 273+00 offset approximately 150 ft from the toe of the dam. The results for lines V-17 and V-18 are shown in Figure 32. The data for these lines are somewhat erratic, probably due to the varying intensities of weathering in the granite along the survey lines; however, a trend in the velocities versus depth is evident. Figure 32 shows the R-wave velocity increasing slightly with depth from a velocity low of approximately 1,050 fps at a depth of 10 ft to a high of 1,150 fps at a depth of 60 ft.

Crosshole tests

45. A total of six sets of boreholes were used to conduct crosshole tests at Stations 235+00 and 269+50 of the Right Wing Dam, as shown in Figure 22. Tests were conducted in borings on the centerline of the dam, the downstream shoulder, and the downstream slope at each station. The boring sets on the centerline and shoulder of the embankment were cased with PVC pipe and consisted of two borings per set; whereas, the boring set on the downstream slope were cased with steel pipe and consisted of three in-line boreholes. Testing was conducted at 5-ft depth increments for each borehole set.

46. Station 235+00 is a section constructed over an existing embankment constructed of compacted decomposed granite. Borings US-2 and SS-2 were used for crosshole testing on the centerline of the embankment at Station 235+00. These borings were approximately 96 ft in depth and were designed to obtain seismic velocities representative of the compacted decomposed granite of Zone C, the underlying existing embankment, and foundation materials. Borings US-9 and SS-9, located on the downstream shoulder, were approximately 31 ft in depth and were designed to provide velocities of both the the impervious core and the embankment gravels. The crosshole tests conducted on the downstream slope were performed in borings SCB2-A, SCB2-B, and SCB2-C which were about

40 ft deep. The crosshole tests conducted on the downstream slope provided information regarding seismic velocities of the embankment gravels, Zone B, the impervious core, and the Zone A rockfill section.

47. The crosshole tests at the centerline of the dam, Station 269+50, were conducted in borings US-3 and SS-3 and were approximately 86 ft in depth. The tests performed in these borings were intended to obtain seismic velocities of the core materials, Zone C. Crosshole sets US-8 and SS-8 were located on the downstream shoulder and were approximately 26 ft in depth. These borings penetrated Zone A, B, and C materials. Borings SCB3-A, SCB3-B, and SCB3-C, used for crosshole testing on the downstream slope of the dam, were approximately 86 ft deep. These borings penetrated Zones A, B, and C and extended into the weathered granite foundation.

48. Station 235+00 P-wave tests. Plots of the calculated true P-wave velocity versus depth for each of the three crosshole sets at Station 235+00 are presented in Figures 33 through 35. Figure 36 shows the P-wave velocity zones interpreted from the three crosshole sets superimposed on the section at Station 235+00. The results of testing on the centerline of the dam (crosshole set US-SS-3) indicate that the P-wave velocities measured in the compacted decomposed granite of Zone C and the preexisting embankment generally increased with depth and ranged from 1,600 fps to 3,600 fps. The velocity of the weathered granite foundation is 9,700 fps. Results of testing on the downstream shoulder of the dam (crosshole set US-SS-9) indicate that the P-wave velocities in the upper 18 ft are 1,925 fps and are representative of the Zone A rockfill material of the shell. Between a depth of 18 and 30 ft, the tests were performed in Zone C where a velocity of 2,875 fps was measured. Testing on the downstream slope (crosshole set SCB2-ABC) indicates that Zone B consists of two velocity zones with values of 1,150 and 1,875 fps. The underlying foundation was measured as having a velocity of about 4,875 fps.

49. Station 235+00 S-wave tests. The calculated true S-wave versus depth for the three crosshole sets conducted at Station 235+00 are presented in Figures 37 through 39. Figure 40 shows the S-wave velocity zones interpreted from the three crosshole sets superimposed on the section at

Station 235+00. The tests performed on the centerline and at the downstream shoulder show that the velocities of the compacted decomposed granite in Zone C and preexisting embankment ranged between 975 and 1,300 fps. The velocities increased with depth. The velocity of Zone B was about 775 fps based on measurements taken at the downstream slope set between depths of 0 and 22 ft. The velocity for the foundation, between depths of 22 and 40 ft, was approximately 1,550 fps and was determined from testing in the downstream slope boring set. The weathered granite foundation beneath the core was determined to have an S-wave velocity of 1,950 fps.

50. Station 269+50 P-wave tests. The calculated true P-wave velocity versus depth for each of the three crosshole sets at Station 269+50 are presented in Figures 41 through 43. Figure 44 shows the P-wave velocity zones interpreted from the three crosshole sets superimposed on the section at Station 269+50. The velocities obtained from crosshole testing on the centerline of the crest (crosshole set US-SS-3) indicate that Zone C materials generally increase with depth and range between 1,625 and 3,900 fps. Results from testing on the downstream shoulder (crosshole set US-SS-8) show a velocity zone of 1,275 fps extending from the surface to a depth of about 12 ft and correlating with Zone A and B materials. The underlying Zone C material was determined to have a velocity of 2,875 fps. The crosshole results from testing on the downstream slope of the dam (SCB3-A,B,C) show that the P-wave velocity for the zone extending from the surface to a depth of approximately 8 ft has a velocity of 1,875 fps, and it is believed that this velocity may be abnormally high because of the influence of the asphalt road. The next three zones have P-wave velocities of 1,500, 1,850, and 3,575 fps and correspond to Zones A and B. The 3,575-fps velocity zone may correspond to Zone B materials or highly weathered granite. The more competent granite foundation had a velocity of 12,450 fps.

51. Station 269+50 S-wave tests. The calculated true S-wave velocities for each test elevation for the three crosshole sets at Station 269+50 are presented in Figure 45 through 47. Figure 48 shows the S-wave velocity zones interpreted from the three crosshole sets superimposed on the section at Station 269+50. Testing on the centerline of the dam indicated that the

Zone C material in the impervious core tended to increase with depth and ranged between 900 and 1,425 fps. Data acquired from the tests at the downstream shoulder and downstream slope indicate that the S-wave velocity of the Zone A rock fill ranges between 850 and 950 fps. Measurements taken in boring sets located on the downstream shoulder and downstream slope show that the velocity for the Zone B gravel ranged from 1,025 to 1,325 fps. The weathered granite foundation has an S-wave velocity between 1,700 and 1,875 fps as determined from testing in the SCB3-A,B,C borehole set located on the downstream slope of the dam.

Downhole tests

52. Downhole P- and S-wave tests were conducted in boring sets (the same boring sets used for crosshole testing) located on the crest of the dam (centerline), downstream shoulder, and the downstream slope for Stations 235+00 and 269+50 as shown in Figure 22.

53. Station 235+00 P-wave tests. Results of the downhole P-wave surveys from the centerline and downstream shoulder for Station 235+00 are presented as velocity versus slant distance (depth) and are shown in Figures 49 and 50. The downhole P-wave information collected from the downstream slope (borings SCB2-A,B,C) was not used because it appears that the waves traveled along the steel casing and also the loose nature of the near surface gravels impeded the propagation of the P-waves. Figure 51 shows the downhole P-wave velocity zones interpreted from the two boring sets superimposed on the section at Station 235+00. Figure 51 shows that Zone C materials range in velocity between 1,600 and 3,160 fps and that Zone B, the upper 10 ft tested on the downstream shoulder, has a velocity of 1,300 fps. The foundation beneath the centerline of the dam has a velocity of 9,230 fps.

54. Station 235+00 S-wave tests. Results of the downhole S-wave surveys from the centerline and downstream shoulder for Station 235+00 are presented as velocity versus slant distance and are shown in Figures 52 and 53. No downhole S-wave data is presented for the downstream slope borings. The velocity zones interpreted from downhole testing were superimposed on the section at 235+00 and are shown in Figure 54.

55. Station 269+50 P-wave tests. Results of the downhole P-wave surveys from the centerline, downstream shoulder, and downstream slope for Station 269+50 are presented as velocity versus slant distance (depth) and are shown in Figures 55 through 57. Figure 58 shows the downhole P-wave velocity zones interpreted from the three boring sets superimposed on the section at Station 269+50. The downhole P-wave results show that the core's velocity varies between 1,725 and 4,000 fps. The figure also indicates that Zone B has velocities that vary between 1,300 and 4,615 fps. Velocities between 1,300 and 2,170 fps were measured in Zone A. The granite foundation was measured as having a value of 4,615 fps.

56. Station 269+50 S-wave tests. Results of the downhole S-wave surveys from the centerline, downstream shoulder, and downstream slope for Station 269+50 are presented as velocity versus slant distance and are shown in Figures 59 through 61. The velocity zones interpreted from downhole testing were superimposed on the section at Station 269+50 and are shown in Figure 62. Figure 62 indicates that the core's velocity ranges between 875 and 1,600 fps and that the velocity increases as a function of depth. Zone B was determined to have velocities between 1,200 and 1,740 fps. Velocities of 830 and 925 fps were measured in Zone A. The granite foundation showed a velocity of 1,925 fps beneath the shell.

Data Consolidation

57. Composites of the various geophysical techniques conducted along approximate Station 235+00 were prepared for P- and S-wave velocity profiles and are presented in Figures 63 and 64, respectively. Five zones of the dam were tested at this station: the central impervious zone, the preexisting embankment, Zone A, Zone B, and foundation materials. Figures 65 and 66 present the composites prepared for P- and S-waves for the section at approximate Station 269+50. Tests performed at this station examined the same zones as were tested at Station 235+00 with the exception of the preexisting embankment.

LEFT WING DAM

Description

58. The Left Wing Dam is a zoned embankment dam which flanks the southeast portion of the Concrete Gravity Dam. The Left Wing Dam is founded on the same weathered quartz diorite granite as the Right Wing Dam. The Left Wing Dam is approximately 2,100 ft long and 167 ft high. The core consists of well compacted decomposed granite (Zone G, scraped from the weathered granite foundation), and is flanked upstream and downstream by 12-ft wide filters (Zone F). The upstream and downstream shells (Zone E) are constructed of gravels obtained from dredged tailings in the Blue Ravine. The slopes of the dam are the same as the Right Wing Dam. A plan view of the Left Wing Dam is shown in Figure 67 and a typical cross section is shown in Figure 68.

Test Results

59. Figure 67 shows the location and layout of the geophysical tests conducted at the Left Wing Dam. The geophysical program consisted of seismic refraction, crosshole, downhole, and surface vibratory testing.

Surface seismic refraction tests

60. The original geophysical plan for the Left Wing Dam consisted of running two seismic refraction tests, one line located on the centerline of the crest and another line along the downstream toe. However, detonation of one 2.5-lb charge at a depth of 5 ft at the centerline of the dam damaged the asphaltic pavement. SPK personnel directed the geophysical crew to discontinue further use of explosives on the crest for fear of further damage to the pavement and possibly to the core of the dam. No results are presented for this seismic refraction line.

61. Refraction line R-5 was run along the downstream toe of the Left Wing Dam between approximate Stations 302+25 and 306+25 as shown in Figure 67. The results of refraction line R-5 are presented in Figure 69. Line R-5 indicated two velocity layers. The first layer, which is believed to

correspond to severely weathered granite, has an average P-wave velocity of 1,780 fps and extends between 28 and 24 ft in depth. The second layer, believed to correlate with fresher granite, has a true velocity of 14,160 fps. The refraction data indicate that the contact between the weathered and fresh granite is quite irregular as expected.

Surface vibratory tests

62. Four, 200-ft long, vibratory lines were run along the centerline of the crest and downstream toe as shown in Figure 67. The results of vibratory lines V-25 and V-26, centered near Station 303+90 and run along the crest, are presented in Figure 70. These data indicate an R-wave velocity of approximately 900 fps between depths of 5 and 60 ft. Data obtained from vibratory lines V-21 and V-22 (Figure 71) centered at approximate Station 303+90 and run along the downstream toe showed a very high degree of scatter and are therefore deemed to be unusable.

Crosshole tests

63. Crosshole P- and S-wave tests at the Left Wing Dam were conducted in three sets of borings along approximate Station 303+90 as indicated in Figure 67. Borings US-4 and SS-4, which were located on the centerline of the dam, were approximately 155 ft deep and spaced 10 ft apart; whereas, borings US-5 and SS-5, located on the downstream shoulder of the crest, were 25 ft deep and 10 ft apart. These borings were cased with 4-in. ID PVC pipe. The borings located on the crest (borings US-4 and SS-4) extended through the core (Zone G) and into the granite foundation. The tests conducted in borings US-5 and SS-5 (downstream shoulder) were designed to obtain P- and S-wave velocities of the core and embankment gravels (Zone E). The third set of borings, located on the downstream slope of the dam, designated SCB4-A,B,C, consisted of three in-line borings, and were approximately 85 ft deep. They were designed to penetrate the embankment gravels (Zone E) and the granite foundation. The borings on the downstream slope were steel-cased and drilled with Odex equipment.

64. P-wave tests. The calculated true P-wave velocities, as determined by the CROSSHOLE computer program, for each test elevation for the three crosshole sets are presented in Figures 72 through 74. As previously mentioned, testing was conducted at 5-ft depth intervals.

65. Figure 75 shows the P-wave velocity zones interpreted from the three crosshole sets superimposed on the section at Station 303+90. The P-wave tests for crosshole set SS-US-4 (crest) representative of the core and foundation materials indicated nine velocity zones. The data from the centerline show that the velocities in the decomposed granite core (Zone G) generally increase with depth, with the exception of the two velocity reversals at depths of 88 and 108 ft. The velocities in the core range between 1,600 and 4,450 fps. The velocity of the granite foundation, beneath the core, was measured to be between 6,025 and 9,975 fps. The P-wave crosshole results for crosshole set US-SS-5 (downstream shoulder) indicated that the top 12 ft (Zone E) had a velocity of 1,100 fps; whereas, the interval between depths of 12 and 25 ft (Zone G) had a velocity of 2,125 fps. The P-wave test for crosshole set SCB4-A,B,C (downstream slope) representative of the shell and foundation materials indicated five velocity zones. The P-wave velocity zones between depths of 0 and 68 ft correspond to the shell materials and range between 1,150 and 2,250 fps. The 4,900-fps velocity layer encountered at an approximate depth of 68 ft corresponds to the filter blanket or highly weathered granite and is interpreted to have a thickness of approximately 6 ft. Underlying this layer is the less weathered granite foundation with a velocity of 8,900 fps.

66. S-wave tests. The calculated true S-wave velocities, as determined by the CROSSHOLE computer program, for each test elevation for the three crosshole sets are presented in Figures 76 through 78.

67. Figure 79 shows the S-wave velocity zones interpreted from the three crosshole sets superimposed on the section at Station 303+90. S-wave crosshole testing in borehole set SS-US-4 indicated six velocity zones. The crosshole data show that the S-wave velocity of the core materials increases with depth and ranges in velocity between 975 and 1,300 fps. The S-wave velocity of the granite foundation beneath the centerline of the dam ranges between 1,575 and 1,925 fps. The S-wave data for crosshole set US-SS-5 showed that Zone E materials between approximate depths of 0 and 18 ft had a velocity

of 850 fps; whereas, the Zone G materials between depths of 18 and 25 ft had a velocity of 950 fps. The S-wave test for crosshole set SCB4-A,B,C indicated four velocity zones. The first three S-wave velocity zones correspond with the gravel shells and range in velocity between 900 and 1,250 fps. The granite foundation beneath the shell has a velocity of 2,450 fps.

Downhole tests

68. Downhole P- and S-wave tests were conducted in borings SS-4 (crest), SS-5 (downstream shoulder), and SCB4-A and SCB4-C (downstream slope) as shown in Figure 67. These tests were performed at 5-ft depth increments.

69. P-wave tests. The downhole P-wave tests conducted in the three boring sets at the Left Wing Dam are presented in time versus slant distance plots in Figures 80 through 83. Figures 82 and 83 show the downhole P-wave data collected in borings SCB4-A and SCB4-C. Figure 82 presents the downhole data for the P-wave source located 5 ft from the mouth of the borings while Figure 83 presents the downhole data for a source-to-boring distance of approximately 12.7 ft. Figure 84 shows the downhole P-wave velocity zones interpreted from tests performed at the three boring sets superimposed on the section at Station 303+90.

70. S-wave tests. The downhole S-wave tests conducted in the three boring sets are presented in time versus slant distance plots in Figures 85 through 88. Figure 87 presents the downhole S-wave data collected in boring SCB4-A with a source-to-boring distance of approximately 10.7 ft while Figure 88 presents the data collected in boring SCB4-C with a source-to-boring distance of 7.0 ft. Figure 89 shows the downhole S-wave velocity zones interpreted from tests performed at the three boring sets superimposed on the section at Station 303+90.

Data Consolidation

71. The results of the tests conducted at the Left Wing Dam were superimposed on a cross section to allow comparisons. Figure 90 presents a composite of the P-wave velocity results from crosshole, downhole and seismic

refraction testing conducted at approximately Station 303+90 of the Left Wing Dam. Figure 91 presents a composite of the S-wave velocity results from surface vibratory, crosshole, and downhole testing.

MORMON ISLAND AUXILIARY DAM

Description

72. Mormon Island Auxiliary Dam was constructed in the Blue Ravine, an ancient channel of the American River, that is more than 1 mile wide at the dam site. For about 1,650 ft of its width, the Blue Ravine is filled with auriferous, gravely alluvium of Pleistocene age. The maximum thickness of the channel gravels is approximately 65 ft. The gravels have been dredged for their gold content in the deepest portion of the channel and coarser materials near the top. The remaining undisturbed alluvium is crudely stratified and slightly cemented.

73. Mormon Island Auxiliary Dam is a zoned embankment dam 4,820 ft long, 165 ft high from core trench to crest at maximum section. The shells are constructed of gravel dredged tailings from the Blue Ravine. The narrow, central impervious core is a well compacted clayey mixture founded directly on rock over the entire length of the dam to provide a positive seepage cutoff. Two transition zones, each 12-ft wide, flank both the upstream and downstream sides of the core. The transition zones in contact with the core are composed of well compacted decomposed granite which classifies as a silty-sand according to the USCS. The second transition zones are constructed of the -2 in. fraction of the dredged tailings. A plan and typical sections of the dam are shown in Figures 92 and 93.

74. From the right end of the dam, Station 412+00, to Station 441+50 and from Station 456+50 to the left end of the dam, Station 460+75, all zones are founded on rock. Between Stations 441+50 and 456+50, the undisturbed and dredged alluvium was excavated to obtain slopes of 1.0V:2.0H to found the core and most of the filter zones on rock, but the shells are founded on alluvium. The dredged portion of the alluvium begins at approximately Station 446 and continues to approximately Station 455. The slopes of the dam vary according

to the foundation conditions, with the flattest slopes in vicinity of the dredged tailings. The downstream slopes of the dam vary between 1.0V:2.0H and 1.0V:3.5H, and the upstream slopes vary between 1.0V:2.0H and 1.0V:4.5H.

Test Results

75. Figure 94 shows the location and layout of the geophysical tests conducted at Mormon Island Auxiliary Dam. The geophysical investigation consisted of seismic refraction, surface vibratory, crosshole, and downhole testing.

Surface seismic refraction tests

76. Five refraction lines were run at Mormon Island Auxiliary Dam as shown in Figure 94. Line R-1 was run along the crest of the dam and was 862 ft long. Line R-1 was a one-ended line. The reverse traverse of line R-1 was never completed to avoid any potential damage that the core might incur from further detonation of explosives. The velocities reported may not be true velocities since line R-1 was a one-ended line. This line was run in order to obtain P-wave velocity information of the core and foundation materials. The TD plot for line R-1 is presented in Figure 95.

77. Seismic refraction line MR-5 was run along the downstream toe of the dam on the left abutment as shown in Figure 94. The length of the line was 387 ft long with 20-ft geophone spacings. Line MR-5 was run to acquire information on overburden and foundation materials near the downstream left abutment of the dam. The TD plot for line MR-5 is presented in Figure 96. Analysis of the data indicates that the near surface materials are not continuous across the length of the line and therefore true velocities cannot be calculated. Depths to the tops of layers are approximate since they are calculated based on apparent velocities. Information obtained from shooting from south to north indicates that a zone with a velocity of 890 fps extends to a depth of 6 ft where a second layer with a velocity of 1,890 fps is encountered. These two velocity zones are believed to correspond to gravelly alluvium, sandstone, mudstone, and siltstone material as reported in Mormon Island Auxiliary Dam, Foundation Report 1953. The layer with a velocity of 13,570 fps encountered at a depth of approximately 32 ft corresponds to

bedrock. Shooting from north to south three velocity zones were measured. The uppermost zone, overburden materials, had a velocity of 1,130 fps and a thickness of approximately 9 ft. The second velocity zone, with a thickness of approximately 29 ft, is believed to correspond to weathered bedrock. Less weathered, fresher bedrock with a velocity of 11,350 fps is found at a depth of approximately 38 ft. The velocity of the bedrock in this area is approximately 12,360 fps.

78. Seismic refraction line MR-4 was run on the downstream toe of Mormon Island Auxiliary Dam centered approximately on borings SCB-234 as shown in Figure 94. The length of line MR-4 was 800 ft and a geophone spacing of 25 ft was used. The TD plot for line MR-4 is presented in Figure 97. Line MR-4 was run almost entirely over the area underlain by dredged tailings. The heterogeneity of the buried dredged tailings is expressed on the TD plot by the considerable amount of scatter of the arrival times. Three velocity layers were interpreted from a result of this survey. The uppermost layer has a P-wave velocity of 2,510 fps and ranges in depth from 14 ft at the southwestern shotpoint to 34 ft at the northeastern portion of the line. The second layer extends to a depth of 77 ft at the southwestern shotpoint and to 73 ft at the northeastern shotpoint and has a velocity of 5,530 fps. The first two layers correlate with the dredged gravels. Bedrock had a true velocity of 15,090 fps in this area.

79. Seismic refraction line MR-6 was run on undisturbed alluvium approximately 100 ft downstream of the toe of Mormon Island Auxiliary Dam near crosshole borings MID1 and MID2 as shown in Figure 94. This line was 75 ft in length. The TD plot for this data is shown in Figure 98 from which three velocity zones were interpreted. The first layer had a P-wave velocity of 1,070 fps and had a thickness of 1.0 to 1.5 ft. The second layer with a velocity of 1,760 fps extended to a depth of 10 ft at the southwestern shotpoint and to a depth of 14 ft at the northeastern end. These two velocity layers correspond to clayey gravel. The third layer which corresponds to undredged alluvial materials had a velocity of 4,340 fps.

80. Seismic refraction line MR-3 was run approximately 100 ft downstream of the toe of Mormon Island Auxiliary Dam as shown in Figure 94. Line MR-3 was 400 ft in length and had geophone spacings of 20 ft. This line was run to obtain the P-wave velocities for overburden, weathered rock, and

bedrock. The TD plot for line MR-3 is presented in Figure 99 from which three velocity layers were interpreted. The first layer, corresponding to overburden materials, has an average P-wave velocity of 1,910 fps and ranges in depth between 7.5 and 9 ft. The second layer encountered, with a true velocity of 3,920 fps, is believed to correspond with highly weathered bedrock. The second layer ranges in depth between 32 ft at the southwestern end to 36 ft at the northeastern end which happens to be located part way up a knoll. Fresh, unweathered bedrock is interpreted as having a true velocity of 15,550 fps.

Surface vibratory tests

81. Eight surface vibratory lines were run at Mormon Island Auxiliary Dam as shown in Figure 94. Two lines were run along the crest of the dam and six lines along the downstream toe. The length of each vibratory line was 200 ft with the exception of lines V-13 and V-14 which had respective lengths of 160 and 130 ft. Lines V-9 and V-10 were run along the crest of the dam between approximate Stations 448+00 and 452+00. Lines V-13 and V-14 were run along the downstream toe near the left abutment. Lines V-15 and V-16 were run between approximate Stations 446+50 and 450+50 on the downstream toe over dredged tailings. Vibratory lines V-11 and V-12 were run on the downstream toe between approximate Stations 423+80 and 427+80.

82. The depth versus R-wave velocity plot for lines V-9 and V-10 is presented in Figure 100. This plot shows velocities ranging between 790 and 900 fps between depths of 5 and 55 ft. Figure 101 presents a plot of R-wave velocity versus depth for lines V-13 and V-14 and it shows that R-wave velocities increased from approximately 720 fps at a depth of 5 ft to 780 fps at a depth of 41 ft. Results from lines V-15 and V-16 are presented in Figure 102. Results indicated that R-wave velocities decreased from approximately 620 fps to 550 fps between depths of 5 and 12 ft. Between depths of 12 and 45 ft velocities gradually increase to a maximum value of 680 fps. The R-wave velocities versus depth plots for lines V-11 and V-12 are presented in Figure 103. The data exhibit a general increase in R-wave velocity as a function of depth. Velocities in this area increase from approximately 600 fps to 725 fps between depths of 5 and 45 ft.

Crosshole tests

83. A total of six crosshole sets were employed at Mormon Island Auxiliary Dam for obtaining P- and S-wave velocities as a function of depth. The location of the crosshole sets are shown in Figure 94. Crosshole tests were conducted on the dam's centerline, downstream shoulder, downstream slope, and downstream toe. The boring sets which were located on the crest at approximate Station 448+00 (borings US-6 and SS-6), downstream edge at approximate Station 448+00 (borings US-7 and SS-7), and downstream toe at approximate Station 441+00 (borings MID1 and MID2) were cased with PVC pipe. Borings located on the downstream slope at approximate Station 448 (borings SCB5-A,B,C) and in the dredged area on the downstream toe at approximate Station 449 (borings SCB-2,3,4) and approximate Station 454 (borings SCB-9,5,6,7,8) were drilled with the Odex system and were cased with steel pipe.

84. Borings US-SS-6, located on the centerline of the dam, were 190 ft deep and provided velocities of the Zone 4 core material and the rock foundation. Borings US-SS-7, located on the downstream edge of the crest, were 50 ft in depth and were used to obtain velocities of the Zone 3 filter material and Zone 1 shell material. Borings SCB5-A,B,C, located on the downstream slope of the dam, were 120 ft deep and were designed to penetrate the downstream shell (Zone 1), the dredged alluvium, and bedrock. Boring sets SCB-2,3,4 (80 ft deep) and set SCB-9,5,6,7,8 (maximum boring depth 80 ft) were used to gather velocity information regarding the dredged alluvium and bedrock. Boring set MID-1,2, which was approximately 50 ft deep, was used to obtain information on the undisturbed alluvium and bedrock. Testing was conducted at 5-ft depth increments for each boring set with the exception of boring set MID-1,2 in which testing was conducted at 2.5-ft depth increments.

85. P-wave tests. The results of crosshole P-wave testing conducted at Mormon Island Auxiliary Dam are presented in depth versus velocity fashion in Figures 104 through 109. Figure 110 displays crosshole P-wave velocity zones in relationship to the various materials tested for the section at approximate Station 448. Figure 111 displays the crosshole results obtained from testing along the toe of the dam.

86. The results of crosshole testing in borings US-6 and SS-6 (crest centerline) indicated that the P-wave velocity of the core materials ranged in velocity between 1,975 and 4,500 fps and the foundation materials had a velocity of 10,850 fps. The results of testing in borings US-7 and SS-7 (downstream shoulder) show that the upper 15 ft, which corresponds to the Zone 1 materials, had a velocity of 1,800 fps. The Zone 3 materials had velocities ranging between 2,050 and 3,150 fps. Data collected in boreholes SCB5-A,B,C indicated that the P-wave velocities for the downstream shell (0 to 42 ft) ranged between 1,475 and 2,250 fps. The P-wave velocities for the dredged tailings in the downstream shell ranged between 1,075 and 5,400 fps; whereas, the foundation materials exhibited a 9,275 fps velocity. P-wave velocities measured in crosshole set SCB-5,6,7,8,9 ranged between 1,125 and 5,750 fps for the dredged tailings,whereas, bedrock, encountered at an approximate depth of 62 ft, exhibited a velocity of 10,800 fps. The results of testing conducted in borehole set SCB-2,3,4 suggest that the dredged tailings in this area have a velocity ranging between 2,600 fps to 6,575 fps; whereas, the bedrock, encountered at a depth of approximately 68 ft, had a velocity of 14,800 fps. The results of crosshole testing in borings MID-1,2 located near approximate Station 441 show that velocities ranged between 1,390 and 5,200 fps between the surface and a a depth of approximately 26 ft. These velocities correspond to overburden material (clayey gravel and undredged alluvium). Bedrock, which underlies these materials, has a P-wave velocity, depending on the degree of weathering, ranging between 7,510 and 11,260 fps.

87. S-wave tests. The results of crosshole S-wave testing conducted at Mormon Island Auxiliary Dam are presented in depth versus velocity fashion in Figures 112 through 117. Figure 118 displays crosshole S-wave velocity zones in relationship to the various materials tested for the section at approximate Station 448+00, while Figure 119 displays the crosshole results obtained from testing along the downstream toe of the dam.

88. Crosshole results from crosshole set US-SS-6 located on the centerline of the crest indicate that S-wave velocities in the core material were fairly consistent with velocities ranging between 1,000 and 1,350 fps and, in general, increased with depth. The bedrock foundation encountered at an approximate depth of 166 ft had a velocity between 3,150 and 3,750 fps.

The results of crosshole testing in crosshole set US-SS-7 indicate that S-wave velocities are fairly consistent, ranging between 900 and 1,075 fps, from the surface to a depth of approximately 42 ft at which point the velocity increases to 1,325 fps. The S-wave velocity versus depth plot for crosshole set SCB5-A,B,C located on the downstream slope shows that the shell material has velocities of between 825 and 1,200 fps to a depth of approximately 42 ft at which point the dredged tailings are encountered with a velocity of 625 fps. Bedrock is construed to correlate with the 2,900 fps velocity encountered at an approximate depth of 88 ft. Results of crosshole testing in boring set MID-9,5,6,7,8 suggest that velocities in the dredged tailings increase with depth and range from 525 to 925 fps. The underlying bedrock, with a velocity of 3,150 fps, was encountered at approximately 60 ft in depth. Testing in boring set MID-2,3,4 indicates that the velocities ranging between 400 and 475 fps correspond with the buried dredged tailings. The underlying weathered bedrock is encountered at an approximate depth of 52 ft with velocities ranging between 2,350 and 2,900 fps. Crosshole S-wave testing in boring set MID-1,2 indicates that velocities increase from 680 to 1,560 fps between the depth range of 0 and 28 ft. These velocities correspond to overburden material (clayey gravel and undredged alluvium) as previously mentioned. The underlying bedrock has a velocity range between 1,610 and 2,120 fps.

Downhole tests

89. Downhole P- and S-wave tests were conducted at each crosshole set location at Mormon Island Auxiliary Dam as shown in Figure 94. Testing was conducted at 5-ft depth intervals at each boring set with the exception of boring set MID-1,2 in which downhole tests were performed at 2.5-ft depth intervals.

90. P-wave tests. Figures 120 through 135 present the time versus slant distance plots for the downhole P-wave tests conducted at Mormon Island Auxiliary Dam. Downhole P-wave testing on the downstream slope of the dam was performed by placing geophones in borings SCB5-A and SCB5-C and recording signals from two different shot points (SP-A and SP-B), which were located on the ground surface between the borings. It was difficult to obtain good

quality data in these borings. This problem is believed to be caused by the combined effects of the steel-cased borings and the inability of the materials in the shell to propagate a P-wave signal effectively.

91. Borehole set SCB-9,5,6,7,8, located on the downstream toe of Mormon Island Auxiliary Dam (Figure 94), was divided into two subsets of borings (SCB-6,7,8 and SCB-9,5,6) for downhole P-wave testing purposes. Borings 6 and 8 were used as receiver holes and two shot points designated SP-A and SP-B were used for downhole testing in crosshole subset SCB-6,7,8. No interpretation is shown for downhole testing conducted in boring set SCB-6,7,8 because of the significant data scatter and the lack of velocity and depth agreement between the tests. Borings 6 and 9 were used as receiver holes and two shot points designated SP-A and SP-B were used for downhole testing in crosshole subset SCB-5,6,9. The inability to collect good quality data is again believed to be due to the steel casing and material properties as previously mentioned.

92. Downhole P-wave tests for crosshole set SCB-2,3,4 were performed by placing geophones in borings SCB-2 and SCB-4 and setting up two shot points designated SP-A and SP-B near the borings.

93. Downhole P-wave tests were performed in each boring of boring set MID-1,2 and are presented in Figures 134 and 135. A shot point was located midway between the borings and the resulting seismic signal was recorded in each boring at 2.5-ft depth increments.

94. Figure 136 displays downhole P-wave velocity zones in relationship to the various materials tested for the section at approximate Station 448. Averaged values from tests conducted on the downstream slope and in boring set SCB-2,3,4 are presented in this figure. Figure 137 displays the downhole results obtained from testing along the toe of the dam. The figure presents averaged values from downhole tests conducted along the toe.

95. S-wave tests. Downhole S-wave tests were conducted at each crosshole set location at Mormon Island Auxiliary Dam as shown in Figure 94. Figures 138 through 148 present the time versus slant distance plots for the downhole S-wave data collected at Mormon Island Auxiliary Dam.

96. Downhole S-wave testing on the downstream slope of the dam was conducted by placing the shear wave source approximately midway between borings SCB5-A and SCB5-C and recording the shear waves in borings SCB-5A and SCB-5C at 5-ft depth intervals until the bottom of the borings were reached.

97. Borehole set SCB-9,5,6,7,8, located on the downstream toe of Mormon Island Auxiliary Dam (Figure 94), was divided into two subsets of borings (SCB-6,7,8 and SCB-9,5,6) for downhole S-wave testing purposes. Testing at boring set SCB-6,7,8 was performed by placing the S-wave source on the ground surface, approximately halfway between borings SCB-6 and SCB-8, and recording the seismic signals at 5-ft depth increments in borings SCB-6 and SCB-8. For boring set SCB-9,5,6, the S-wave source was located approximately halfway between SCB-6 and SCB-9, which were also used as receiver holes.

98. Downhole S-wave tests for crosshole set SCB-2,3,4 (Figure 94) were performed by placing geophones in borings SCB-2 and SCB-4 and placing the S-wave source approximately halfway between borings SCB-2 and SCB-4, which were used as receiver holes. The failure to obtain good quality data was again caused by the steel-cased borings. This made the picking of accurate arrival times very difficult and thus the results of the downhole S-wave tests may be questionable.

99. Figure 149 displays downhole S-wave velocity zones in relationship to the various materials tested for the section at approximate Station 448. Results presented in this figure for testing on the downstream slope (Figures 140 and 141) and boring set SCB-2,3,4 (Figures 146 and 147) are averaged values. Figure 150 displays the downhole results obtained from testing along the toe of the dam. Results presented in this figure for testing in boring set SCB-9,5,6,7,8 (Figures 142 through 145), and boring set SCB-2,3,4 (Figures 146 and 147) are averaged values.

Data Consolidation

100. P-wave velocity composite figures were prepared for the section across approximate Station 448+00 and along the downstream toe of the dam and are presented in Figures 151 and 152, respectively. The composite sections show the results obtained from seismic refraction, crosshole, and downhole

testing. S-wave velocity composite figures were prepared for the section across approximate Station 448+00 and along the downstream toe of the dam and are respectively shown in Figures 153 and 154.

PART III: INTERPRETATION

DIKE 5

P-Wave Velocities

101. The P-wave composite (Figure 20) was analyzed and a zonal velocity interpretation was performed for Station 180+50 using weighted averaging and judgment based on data quality and the limitations and advantages of each test. Two approaches were used to present velocities for Dike 5. The first approach does not involve the extrapolation or interpolation of velocities beyond areas where measurements were made, and is presented in Figure 155. The zoning through the core and foundation materials revealed nine zones. The P-wave velocities in the core material ranged between 1,600 and 4,550 fps. The granitic material beneath the centerline of the dike had a velocity of 9,750 fps. Five velocity zones were interpreted for the shell and underlying foundation materials. The velocities in the shell ranged between 1,525 and 3,000 fps. The foundation beneath the shell has a velocity of 9,250 fps. The P-wave velocities obtained at the toe of the dike indicated two velocity zones. The first zone with a velocity of 2,110 fps corresponds to overburden material (weathered granite); whereas, the second zone encountered at an approximate depth of 10 ft had a velocity of 9,930 fps which corresponds to less weathered granite.

102. The second approach for interpreting P-wave data was to assign zonal velocities according to constructed zones of the dam and foundation materials. This involves some interpolation and extrapolation based on the principle that with other things being equal seismic wave velocities increase with effective stress. The results of this method are presented in Figure 156 for the cross section through the Station 180+50. Seven P-wave velocity zones were interpreted for the core materials and they ranged in velocity between 2,250 and 4,550 fps. The shell materials exhibited three velocity zone which ranged between 1,575 and 2,400 fps. The overburden material at the toe of the dike had a velocity of 2,110 fps. The average P-wave velocity for the granite foundation was determined to be 9,650 fps.

S-Wave Velocities

103. S-wave zonal interpretations were made in the same manner as employed for P-wave interpretations previously discussed. Figure 157 presents the S-wave zonal interpretation through the cross section at Station 180+50. Seven S-wave velocity zones were determined for the dike's core and foundation materials. The velocities in the core ranged between 975 and 1,575 fps; whereas, the foundation materials had a velocity of 2,225 fps. The shell materials exhibited two velocities of 1,000 and 1,200 fps. The granite foundation beneath the shell had a velocity of 2,700 fps. No S-wave information was obtained at the downstream toe.

104. The second interpretation approach (based on constructed zones of the dike) is presented in Figure 158. The core was divided into five velocity zones which ranged between 1,100 and 1,575 fps. The shell materials was divided into two zones. The first zone with a thickness of approximately 10 ft had a velocity of 1,000 fps. The remainder of the shell had a velocity of 1,200 fps. The foundation materials were determined to have a velocity of 2,450 fps.

RIGHT WING DAM

Station 235+00 P-Wave Velocities

105. An analysis of the P-wave composite for Station 235+00 indicated four velocity zones through the core and foundation materials as shown in Figure 159. The velocities in the core ranged between 1,600 and 3,600 fps. The velocity of the foundation beneath the core was determined to be 9,700 fps. The composite information obtained from testing in borings on the downstream shoulder of the dam indicated a velocity of 1,600 fps which corresponds to Zone B materials and a velocity of 3,025 fps corresponding to Zone C materials. The shell materials, as measured from the downstream slope borings, exhibited three velocity zones ranging between 1,150 and 4,875 fps. P-wave information at the toe of the dam was obtained from seismic refraction testing and this testing indicated 3 velocity zones for the foundation. The

770-fps layer is believed to correspond with overburden material. The 6,140-fps layer corresponds to weathered granite while the 12,790-fps velocity layer matches the velocity of fresh or slightly weathered granite.

106. The second interpretation approach (based on constructed zones of the dam) is presented in Figure 160. The core materials consisting of the test embankment and Zone C indicated three velocity zones ranging between 1,600 and 3,600 fps. Two velocity zones, 1,375 and 1,875 fps, were interpreted for Zone B. The granite foundation was divided into three velocity zones. The first zone corresponding to overburden materials, had a P-wave velocity of 770 fps and was detected only at the top of the dam by the seismic refraction method. The second velocity zone for the granite had a velocity of approximately 5,500 fps and is believed to correspond to highly weathered granite while the 11,250-fps velocity layer corresponds to fresh or slightly weathered granite.

Station 235+00 S-Wave Velocities

107. An analysis of the S-wave velocity composite indicated four velocity zones from testing along the centerline of the dam as shown in Figure 161. These tests measured velocities in Zone C and test embankment, which comprise the core, and the foundation. Velocities in the core ranged between 975 and 1,450 fps; whereas, the underlying foundation had a velocity of 2,050 fps. Tests conducted on the downstream shoulder of the dam measured the velocities of the Zone B and Zone C materials. These tests indicated a velocity of 900 fps for Zone B and a velocity of 1,125 fps for Zone C. The tests conducted in the boring sets on the downstream slope indicated that the Zone B materials had a velocity of 775 fps. The underlying weathered granite had a velocity of 1,550 fps. Rayleigh wave tests conducted at the toe of the dam exhibited velocities of 1,375 and 1,300 fps.

108. The interpretation based on constructed zones of the dam is presented in Figure 162. The figure shows three velocity zones assigned to the core materials. These velocities range in velocity from 975 fps to 1,450 fps. Zone B is shown as having a velocity of 850 fps. A 1,400-fps

velocity zone, believed to correspond to weathered granite, is shown to exist beneath the shell and extending beyond the toe of the dam. The less weathered granite was interpreted as having a velocity of 2,050 fps.

Station 269+50 P-Wave Velocities

109. An analysis of the P-wave composite for the dam at approximate Station 269+50 indicated four velocity zones for the core materials as shown in Figure 163. The P-wave velocity zones increase with depth and ranged from 1,675 to 3,150 fps. Testing conducted on the downstream shoulder of the dam measured the Zone B and Zone C velocities. The velocities for the Zone B and Zone C materials were interpreted to be 1,300 and 2,950 fps, respectively. Tests conducted on the downstream slope of the dam determined velocities for Zones A and B and underlying foundation materials. Two velocity zones with values of 1,680 and 1,825 fps were interpreted for Zone A. Velocities of 1,825 and 2,875 fps were interpreted for Zone B materials as a result of testing in borings on the downstream slope. Foundation velocities beneath the shell were interpreted to be 4,050 and 12,450 fps which correspond to weathered and slightly weathered granite. P-wave velocities at the downstream toe were obtained from seismic refraction testing and indicated three velocity zones ranging between 710 and 14,350 fps.

110. The interpretation based on the constructed zones of the dam is presented in Figure 164. Figure 164 shows the core being comprised of four velocity zones increasing in velocity as a function of depth. These velocities range between 1,675 fps and 3,150 fps. Zone B is shown as consisting of three velocity layers. The velocity zones in Zone B increase with depth and range in velocity between 1,300 and 2,875 fps. Zone A consists of two velocity layers of 1,680 fps underlain by an 1,825-fps layer. The upper 5 ft of overburden material at the toe of the dam had a velocity of 710 fps. Underlying Zone A and Zone B of the dam is a layer with a velocity of 4,525 fps. This is interpreted as being weathered bedrock material. The less weathered granite has a velocity of 13,400 fps.

Station 269+50 S-Wave Velocities

111. An analysis of the S-wave composite for the dam at approximate Station 269+50 indicates that three velocity zones exist for the core materials as shown in Figure 165. These velocities varied between 925 fps and 1,500 fps. The tests conducted on the downstream slope of the dam suggested a velocity of 925 fps for Zone B materials and a velocity of 1,200 fps for Zone C. The information collected from testing in borings on the downstream slope of the dam indicated four velocity zones ranging between 850 fps and 1,725 fps. Information gathered at the toe of the dam revealed a velocity of 1,200 fps extending to a depth of approximately 60 ft.

112. The interpretation based on constructed zones of the dam is presented in Figure 166. Materials in the core (Zone C) were interpreted as having three velocity zones ranging in velocity between 925 and 1,500 fps. Zone B is comprised of three velocity zones ranging between 900 and 1,725 fps. Zone A consisted of one velocity zone of 900 fps. The upper 20 ft of overburden material at the toe of the dam was interpreted as having an S-wave velocity of 1,200 fps. The granite beneath the dam is interpreted as having a velocity of approximately 1,900 fps.

LEFT WING DAM

P-Wave Velocities

113. Inspection of Figure 90, the P-wave velocity composite for the Left Wing Dam showed Zone G, the core of the dam, and the underlying foundation consisting of six velocity zones as shown in the zonal interpretation (Figure 167). The first four zones, which range in velocity between 1,475 fps and 3,450 fps are believed to correspond to Zone G; whereas, the 5,300- and 9,975-fps zones are believed to correspond respectively to the weathered and less weathered granite. Borings located on the downstream shoulder of the dam penetrated Zone E and Zone G. Tests conducted in these borings showed a velocity of 1,100 fps for Zone E and a velocity of 2,125 fps for Zone G. The combination of crosshole and downhole tests run in the

borings on the downstream slope acquired P-wave information regarding Zone E and its underlying foundation. These tests indicated that Zone E was comprised of two velocity zones with velocities of 1,175 and 2,175 fps. The 4,900- and 8,900-fps layers correspond to weathered and less weathered granite, respectively. P-wave velocities at the toe of the dam were obtained from seismic refraction testing. This test measured the velocities of the granite at the toe of the dam and indicated a velocity layer of 1,780 fps corresponding to highly weathered granite and a second layer with a velocity of 14,160 fps corresponding to slightly weathered granite.

114. The P-wave velocity interpretation based on the constructed zones of the dam is presented in Figure 168. Zone G is shown to be comprised of four velocity zones with velocities of 1,475, 2,225, 2,925, and 3,450 fps. Zone E is comprised of a 1,150- and a 2,175-fps velocity zone. Beneath the dam is a 5,100-fps zone that is believed to correspond to weathered bedrock. This zone is approximately 20 ft thick beneath the core and pinches out as it approaches the toe of the dam. The seismic refraction test conducted at the downstream toe of the dam failed to reveal a layer which would correspond with the 5,100 fps zone. This zone may continue beyond the toe of the dam; however, it may be too thin to be detected by the refraction method. The overburden material at the toe of the dam is shown as having thickness of approximately 25 ft and a velocity of 1,780 fps. The less weathered granite foundation has a velocity of 11,000 fps.

S-Wave Velocities

115. Figure 169 presents the S-wave interpretation for the Left Wing Dam and is based on information obtained from the velocity composite Figure 91. Interpretation of test results conducted at the centerline of the dam indicated that four S-wave velocity zones exist -- the upper two zones with velocities of 975 and 1,200 fps, correspond to the core; whereas, the zones with velocities of 1,600 and 1,925 fps pertain to foundation materials. The results from testing in borings located on the downstream shoulder of the dam revealed two velocity zones. The first zone which extends to a depth of approximately 17.5 ft had a velocity of 900 fps and corresponds to Zone E while the second velocity zone which penetrated Zone G had a velocity of

950 fps. Crosshole and downhole tests performed in borings located on the downstream slope of the dam indicated four velocity zones. The velocity of the zones increased with depth. The first three zones which range in velocity between 925 and 1,250 fps correspond to Zone E; whereas, the fourth zone with a velocity of 2,450 fps is the velocity for the foundation. Velocities for the granite varied between 1,600 and 2,450 fps. The inconsistency in velocity values in the granite is caused by the varying degrees of weathering.

116. Figure 170 presents the S-wave interpretation for the Left Wing Dam and is based on the constructed zones of the dam. Figure 170 shows approximately the upper 25 ft of Zone G with a velocity of 975 fps. From a depth of 25 ft to the foundation Zone G has a velocity of 1,200 fps. Zone E consists of three velocity zones ranging in velocity between 925 and 1,250 fps as shown in Figure 170. The foundation materials were interpreted as being comprised of two velocity zones. The first zone has a velocity of 1,600 fps which correlates with weathered granite. The second velocity zone has a velocity of 2,200 fps and corresponds with less weathered granite.

MORMON ISLAND AUXILIARY DAM

P-Wave Velocities

117. An analysis of the P-wave composite for Station 448 (Figure 151) indicates that six velocity zones exist through the core and foundation materials as shown in Figure 171. The first five zones correspond to the core material and increase in velocity as a function of depth. Velocities in the core of the dam ranged between 1,625 and 4,500 fps. The bedrock beneath the core was determined to have a velocity of 10,325 fps. The crosshole and downhole tests conducted in borings on the downstream edge of the dam acquired velocities in Zone 1 and the core. These tests indicated a velocity of 1,775 fps for Zone 1 and velocities of 2,425 and 5,275 fps for the core. Measurements made in borings, located on the downstream slope of the dam, provided velocity information for Zone 1, foundation dredge tailings, and bedrock. The interpretation of the information suggested two velocity zones having values of 1,375 and 2,400 fps for Zone 1. Three velocity zones were

determined to exist in the foundation dredge tailings. The velocities in the dredge tailings ranged between 1,575 and 5,400 fps. Bedrock was measured as having a velocity of 9,275 fps. The P-wave information shown for the toe was obtained from crosshole, downhole, and seismic refraction tests. The tests indicated that six velocity zones exist for the dredge materials and bedrock. The first four velocity zones, with velocities between 2,600 fps and 5,200 fps, correspond to the dredge tailings. The 6,050-fps layer is believed to correspond to highly weathered bedrock. The bedrock velocity was measured as 14,950 fps. It is assumed that materials are within the zone of saturation if the degree of saturation equals or exceeds 99.5 percent. This implies that the 2,600 fps encountered in the dredge tailings, at a depth of 32.5 ft, is approximately 99.87 percent saturated as illustrated in Figure 172.

118. The interpretation based on the constructed zones of the dam is presented in Figure 173. This figure shows five velocity zones for the core materials and range in velocity between 1,700 and 4,500 fps. Zone 1 is interpreted to consist of two velocity zones of 1,375 and 2,400 fps. The dredge tailings have velocities which range in velocity between 1,575 and 5,300 fps. The 6,050-fps layer shown in the figure is believed to correspond to weathered bedrock. Bedrock was interpreted as having a velocity of 11,525 fps. A zonal velocity interpretation, based on the P-wave composite along the toe of the dam (Figure 152), was constructed as shown in Figure 174.

S-Wave Velocities

119. An S-wave zonal velocity composite for Mormon Island Auxiliary Dam was constructed and is presented in Figure 175. The composite is based on an analysis of the S-wave composite (Figure 153). Eight velocity zones were determined for the core and the foundation. The velocities for the core range between 950 and 1,350 fps and consist of seven zones. In general, the velocities increase as a function of depth with the exception of the 1,125-fps layer that is sandwiched between two 1,275-fps layers. The bedrock under the core had a velocity of 3,450 fps. The combination of crosshole and downhole tests run on the downstream shoulder of the dam indicates that three velocity zones exist. The 925-fps zone, which extends to a depth of approximately

12 ft, corresponds to Zone 1 materials; whereas, the 1,075- and 1,250-fps zones correspond to the core materials. The combination of crosshole and downhole tests run on the downstream slope of the dam indicates that four velocity zones exist. The 825 and 1,200 fps were assigned to Zone 1, 625 fps to the dredge tailings and 2,900 fps to the bedrock foundation. The velocity zones obtained at the toe of the dam were the result of analyzing vibratory, downhole, and crosshole data. This analysis showed four velocity zones for the dredge tailings and bedrock materials. The zones with velocities of 525 and 900 fps correspond to the dredge tailings. The zone with a velocity of 2,350 fps is believed to correspond to weathered bedrock; whereas, the zone with 2,900 fps velocity corresponds to slightly weathered bedrock.

120. Figure 176 presents the zonal S-wave velocity interpretation based on constructed zones of the dam. Figure 176 indicates seven velocity zones ranging between 950 and 1,350 fps for the core. Zone 1 was divided into two velocity zones of 875 and 1,200 fps as shown in the figure. The dredge materials were divided into two zones with values of 575 and 900 fps. The weathered bedrock encountered beneath the toe of the dam was assigned a value of 2,350 fps. The bedrock was calculated to have a velocity of 3,075 fps. A zonal velocity interpretation, based on the S-wave composite along the toe of the dam (Figure 154), was constructed and is presented in Figure 177.

PART IV: SUMMARY

121. This report documents the results of an in situ seismic investigation conducted at Folsom Dam and Reservoir Project, located on the American River, approximately 23 miles northeast of Sacramento, California. Investigations were conducted at Dike 5, the Right and Left Wing Dam, and at Mormon Island Auxiliary Dam. The investigation was performed to determine true P- and S-wave velocity zonations of the embankments and their foundation for use in a dynamic analysis.

122. P-wave velocities were determined from seismic refraction, downhole, and crosshole testing. S-wave velocities were determined from surface vibratory, downhole, and crosshole testing. Tests were conducted on the crest, downstream slope, and downstream toe of Dike 5, the Right and Left Wing Dam, and Mormon Island Auxiliary Dam. P- and S-wave velocities were measured in the core, shells, and foundation of the embankments.

123. P- and S-wave velocity profiles were constructed for the following areas:

a. Cross section through Station 180+50, Dike 5.

b. Cross section through Station 235+00, Right Wing Dam.

c. Cross section through Station 269+50, Right Wing Dam.

d. Cross section through Station 303+90, Left Wing Dam.

e. Cross section through Station 448+00, Mormon Island Auxiliary Dam.

f. Cross section along the downstream toe of Mormon Island Auxiliary Dam.

REFERENCES

Allen, N. F., Richart, F. E., Jr., and Woods, R. D. 1980. "Fluid Wave Propagation in Saturated and Nearly Saturated Sands," Journal of the Geotechnical Engineering Division, American Society of Civil Engineers, Vol 106, No. GT3, pp 235-254.

Ballard, R. F., Jr. 1964. "Determination of Soil Shear Moduli at Depths by In Situ Vibratory Technique," Miscellaneous Paper 4-691, US Army Engineer Waterways Experiment Station, Vicksburg, MS.

Butler, D. K., Skoglund, G. R., and Landers, G. B. 1978. "CROSSHOLE: An Interpretive Computer Code for Crosshole Seismic Test Results, Documentation, and Examples," Miscellaneous Paper S-78-8, US Army Engineer Waterways Experiment Station, Vicksburg, MS.

Department of the Army 1979. Geophysical Exploration, Engineer Manual EM 1110-1-1802, Office of the Chief of Engineers, Washington D.C.

Hynes-Griffin, M. E., Wahl, R. E., Donaghe, R. T., and Tsuchida, T. 1988. "Seismic Stability of Folsom Dam and Reservoir Project; Report 4, Mormon Island Auxiliary Dam - Phase I," Technical Report GL-87-14, US Army Engineer Waterways Experiment Station, Vicksburg, MS.

Hynes, M. E. 1989. "Seismic Stability Evaluation of Folsom Dam and Reservoir Project; Report 1, Summary Report," Technical Report GL-87-14, US Army Engineer Waterways Experiment Station, Vicksburg, MS.

Kean, T. B. 1988. "Geophysical Investigation of Undredged Alluvium at Mormon Island Auxiliary Dam, California," Memorandum for Record, US Army Engineer Waterways Experiment Station, Vicksburg, MS.

Kiersch, G. A. and Treasher, R. C. 1955. "Investigations, Areal and Engineering Geology - Folsom Dam Project, Central California," Economic Geology, Vol 50, No. 3, pp 271-310.

Llopis, J. L. 1983 (Jul). "Preliminary Results of an In-Situ Seismic Investigation of Folsom Dam. California." Draft Letter Report US Army Engineer District (CESPK-ED-F), Sacramento, California, from US Army Engineer Waterways Experiment Station (CEWES-GH-I), Vicksburg, MS.

Schnabel, P. B., Lysmer, J., and Seed, H. B. 1972. "SHAKE, A Computer Program for Earthquake Response Analysis of Horizontally Layered Sites," Report No. EERC 72-12, Earthquake Engineering Research Center, College of Engineering, University of California, Berkeley, CA.

US Army Engineer District, Sacramento. 1953a. "Foundation Report, Dike 5, American River, California, Folsom Project," Sacramento, CA.

_____. 1953b. "Foundation Report, Right Wing Dam, American River, California, Folsom Project," Sacramento, CA.

US Army Engineer District, Sacramento. 1953c. "Foundation Report, Left Wing Dam, American River, California, Folsom Project," Sacramento, CA.

_____. 1953d. "Foundation Report, Mormon Island Auxiliary Dam, American River, California, Folsom Project," Sacramento, CA.

_____. 1954. "Foundation Report, Dikes 1, 2, 3, 4, and 6, American River, California, Folsom Project," Sacramento, CA.

_____. 1955. "Foundation Report, Dike 7, American River, California, Folsom Project," Sacramento, CA.

Wahl, R. E., Crawforth, S. G., Hynes, M. E., Comes, G. D., and Yule, D. E. 1988. "Seismic Stability Evaluation of Folsom Dam and Reservoir Project; Report 8, Mormon Island Auxiliary Dam - Phase II," Technical Report GL-87-14, US Army Engineer Waterways Experiment Station, Vicksburg, MS.

Wahl, R. E., and Hynes, M. E. 1988. "Seismic Stability Evaluation of Folsom Dam and Reservoir Project; Report 5, Seismic Stability Evaluation of Dike 5," Technical Report GL-87-14, US Army Engineer Waterways Experiment Station, Vicksburg, MS.

Wahl, R. E., Hynes, M. E., Yule, D. E., and Elton, D. J. 1988. "Seismic Stability Evaluation of Folsom Dam and Reservoir Project; Report 6, Right and Left Wing Dams," Technical Report GL-87-14, US Army Engineer Waterways Experiment Station, Vicksburg, MS.

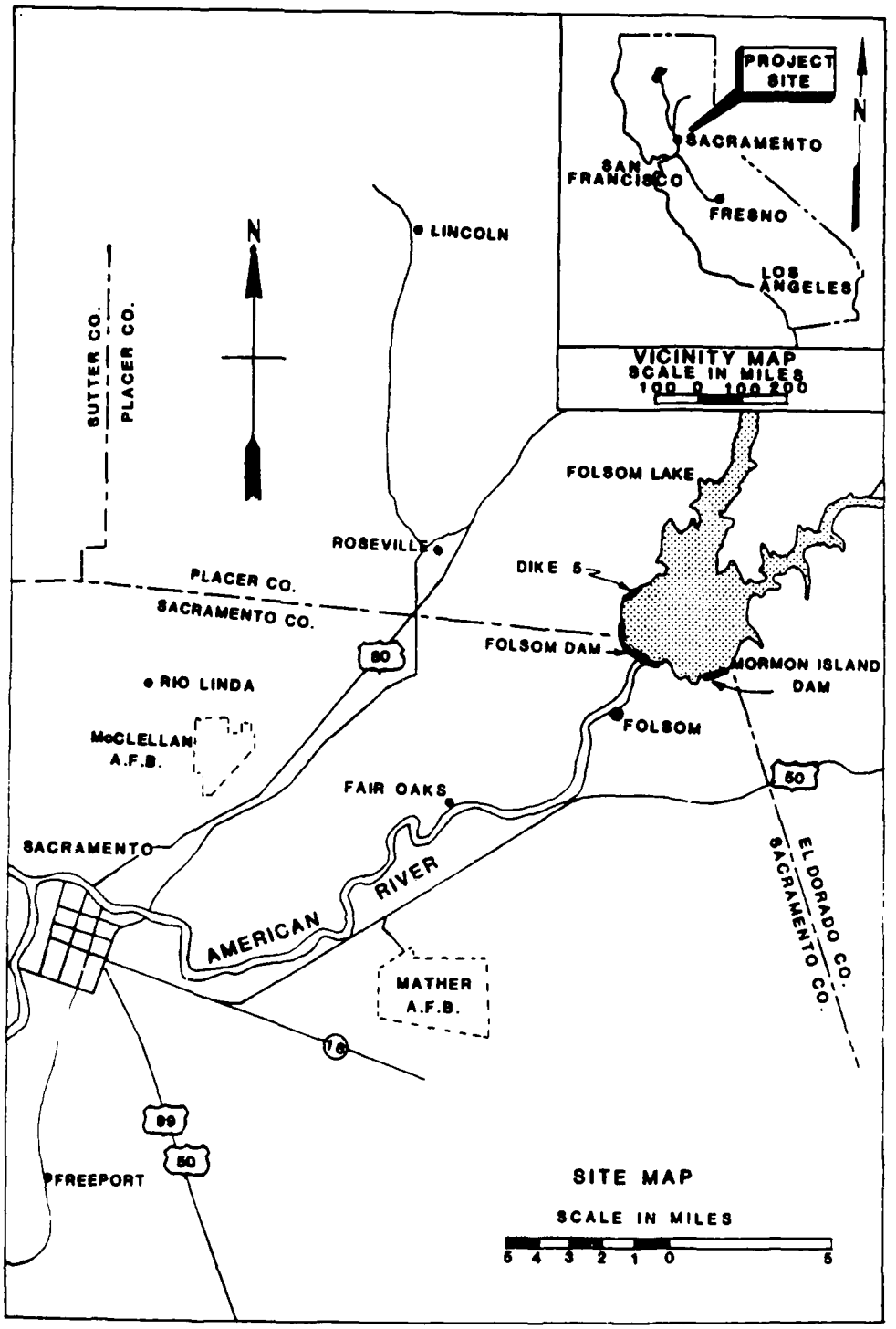

Figure 1. Location of Folsom Dam and Reservoir Project

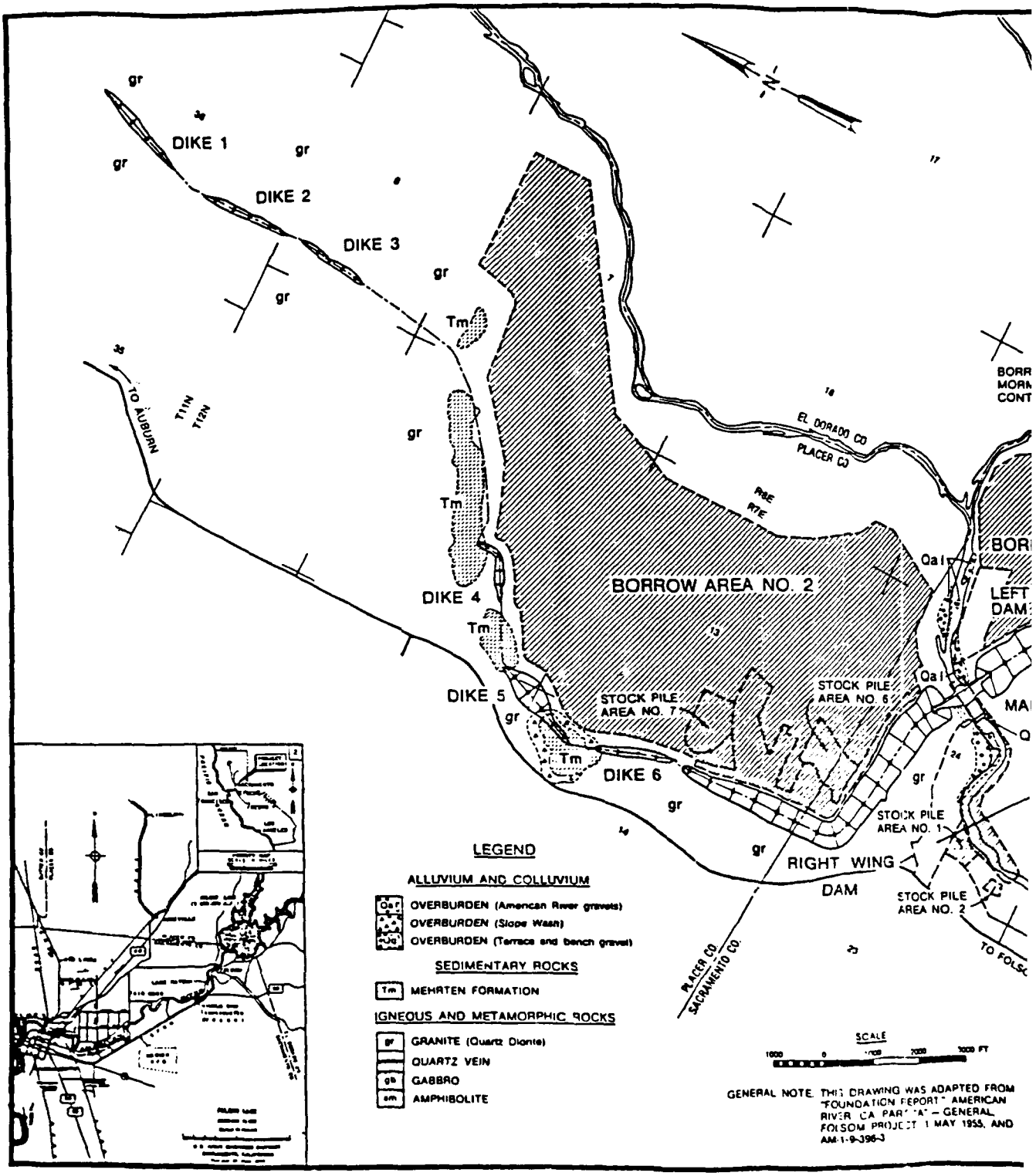

Figure 2. Geologic map of Folsom Dam and Rese

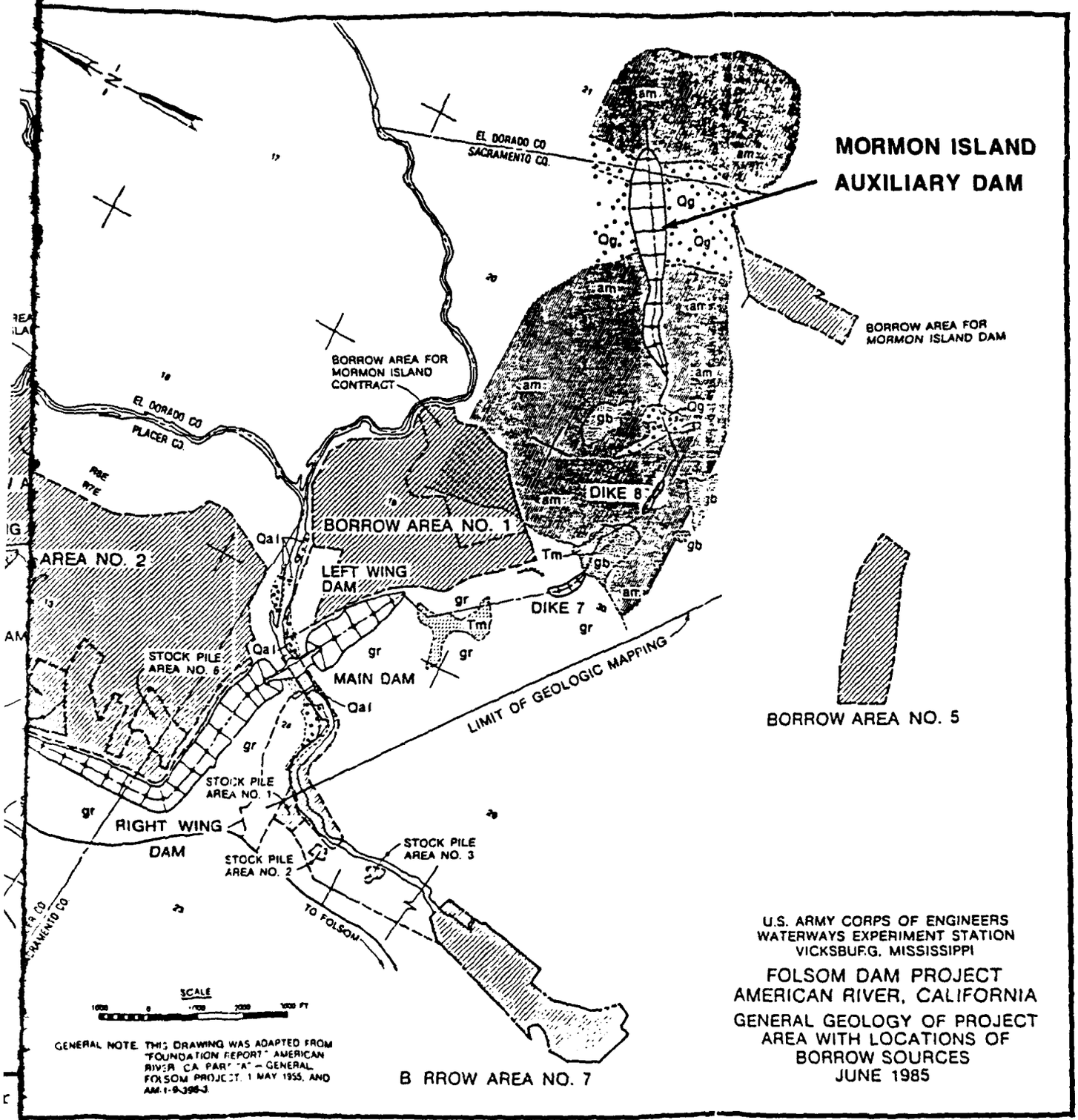

ic map of Folsom Dam and Reservoir Project

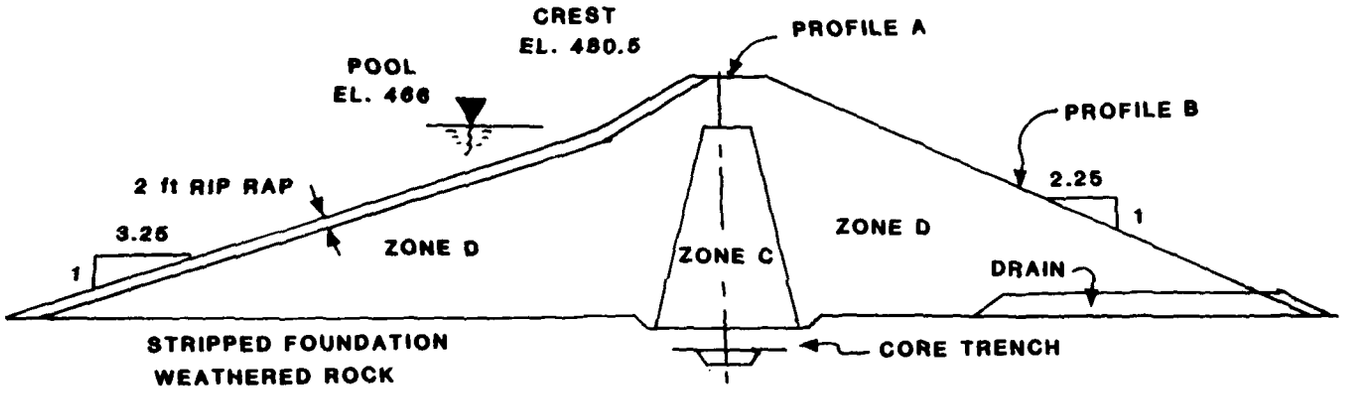

DIKE 5 - TYPICAL SECTION

Material Descriptions

Zone C - Decomposed granite from Borrow Area No. 2 and suitable fine-grained material from American river channel

Zone D - Decomposed granite from Borrow Area No. 2 - practically the same as material in Zone C.

Figure 3. Cross section of Dike 5

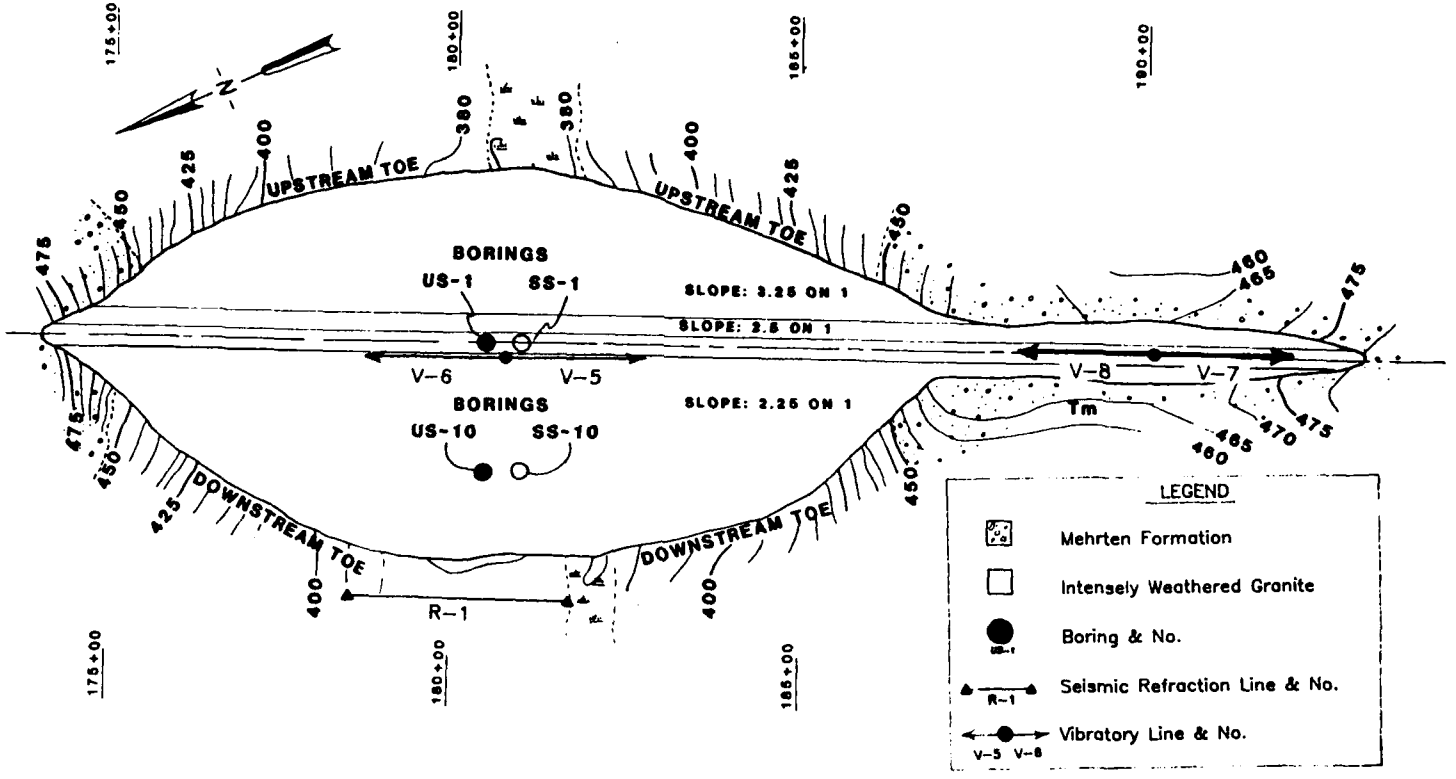

Figure 4. Plan view and test layout for Dike 5

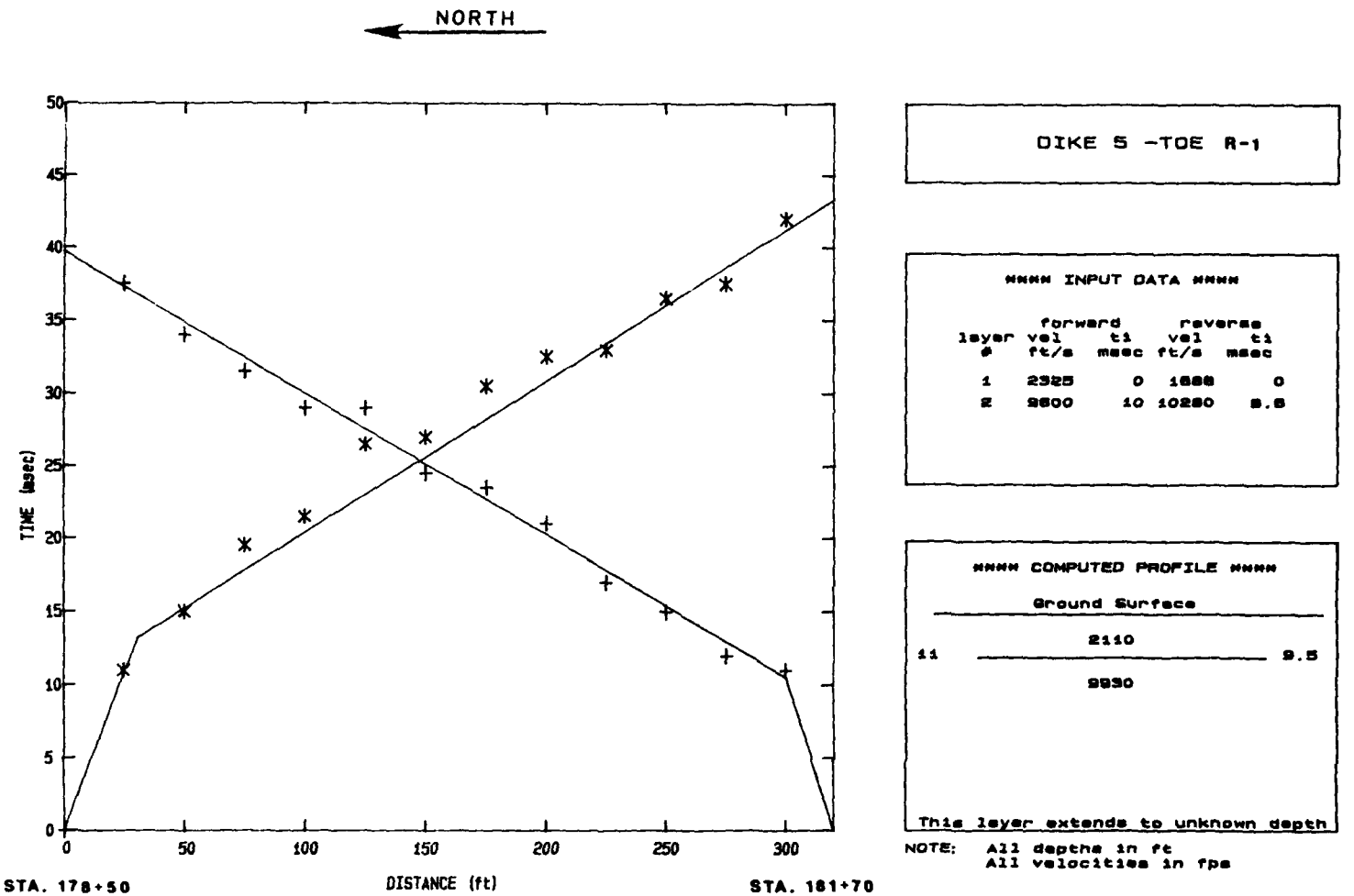

Figure 5. Seismic refraction line R-1, downstream toe of Dike 5

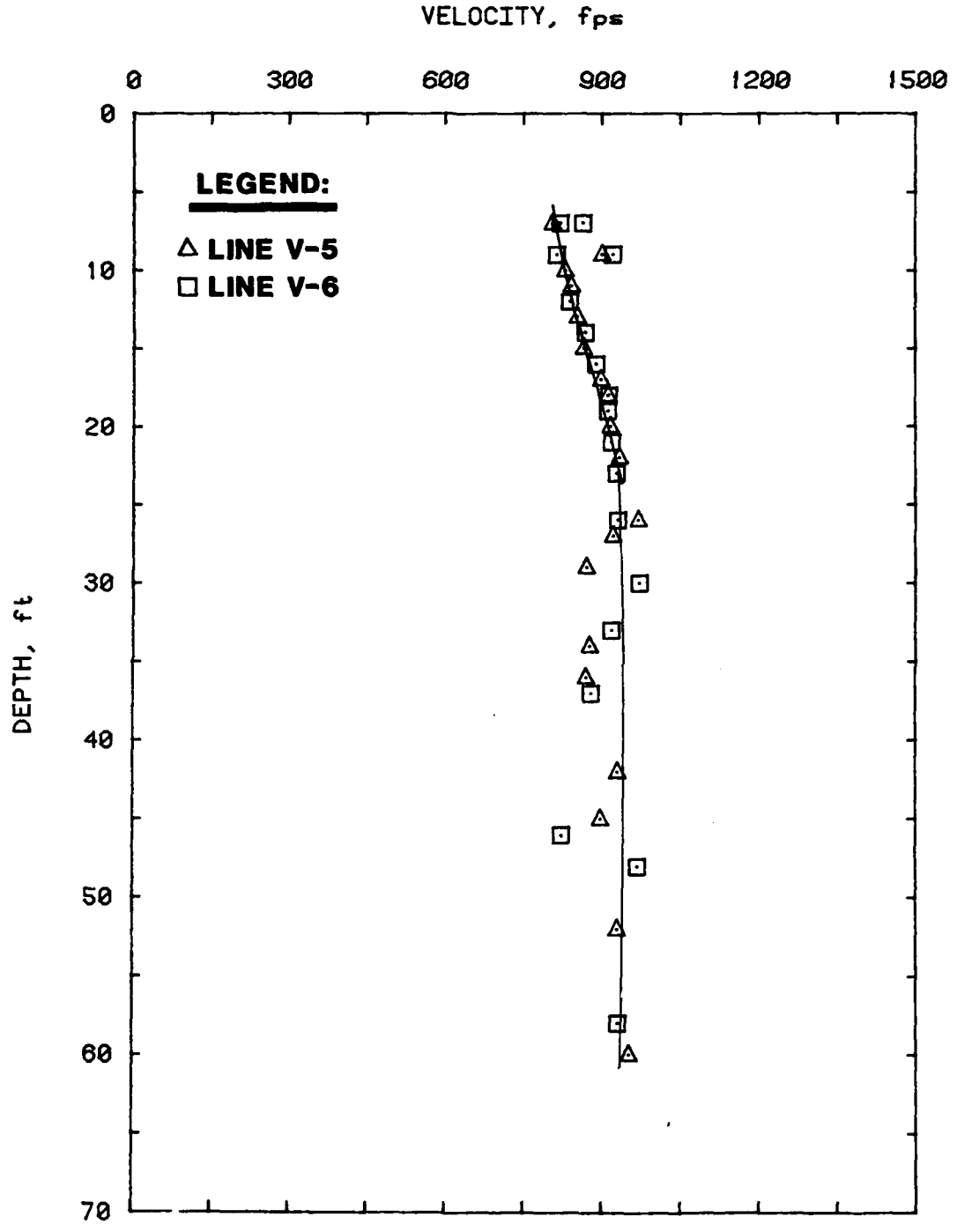

Figure 6. R-wave velocity versus depth for lines V-5 and V-6, crest of Dike 5 centered on Station 180+50

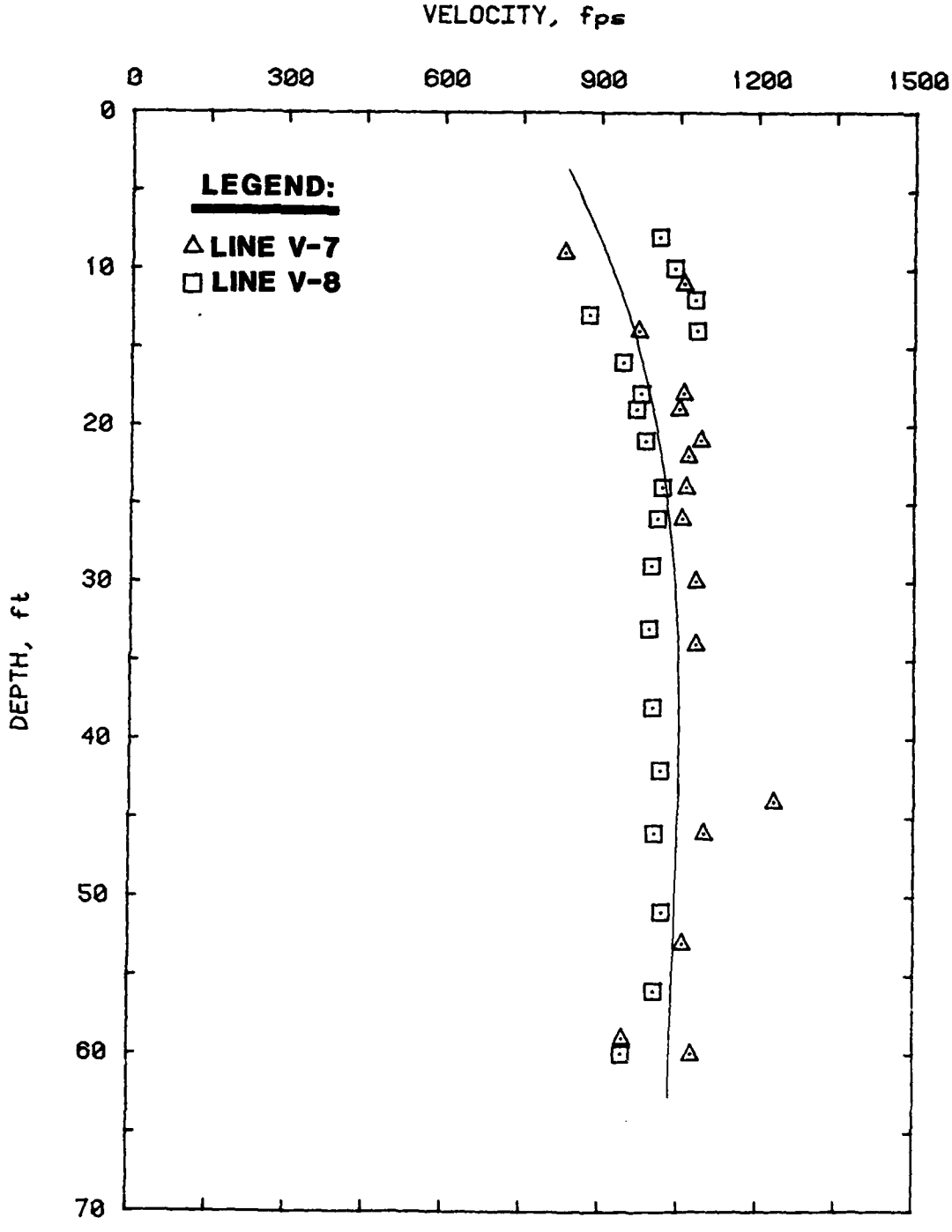

Figure 7. R-wave velocity versus depth for lines V-7 and V-8, crest of Dike 5 centered on Station 191+00

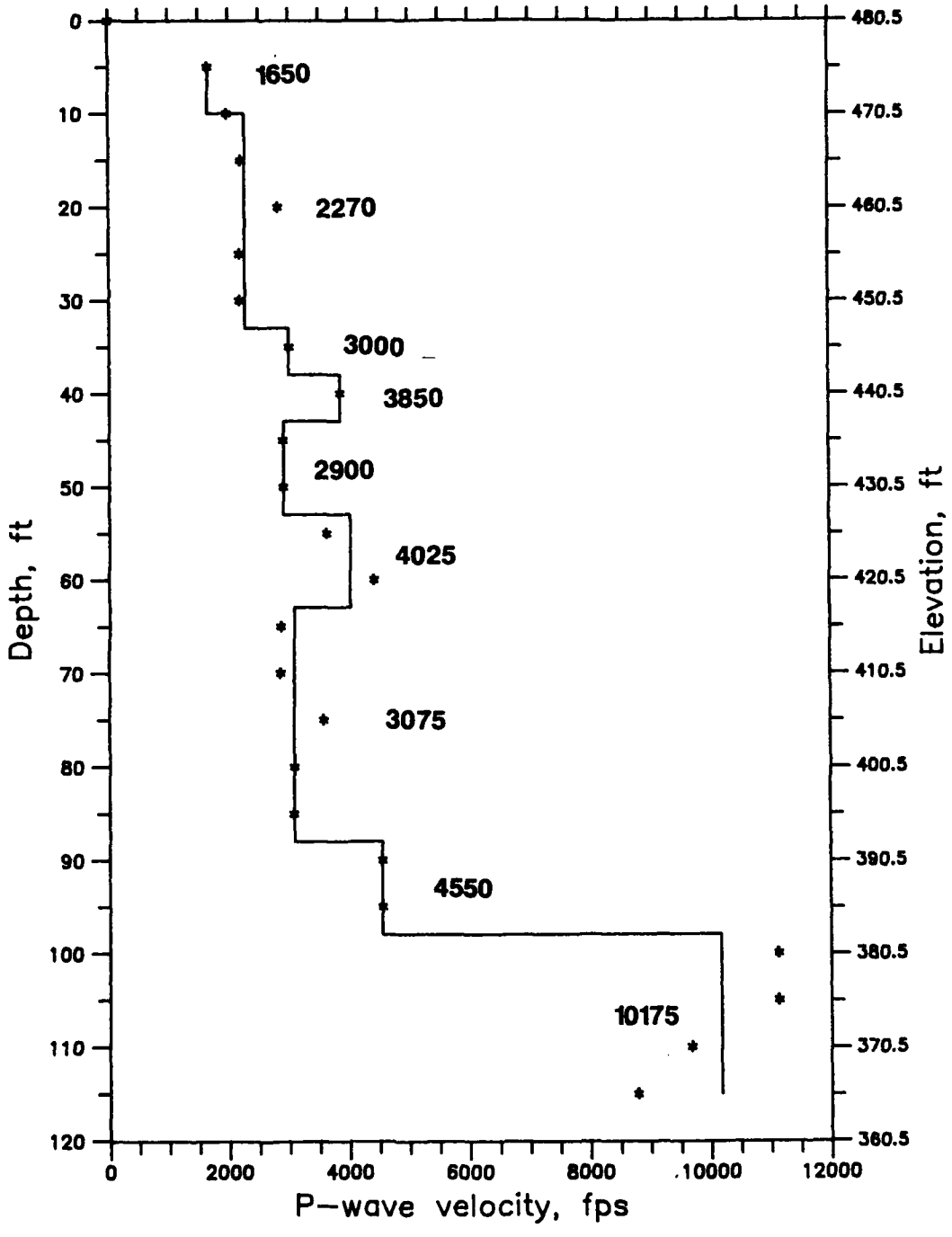

Figure 8. Crosshole P-wave results, crest of Dike 5

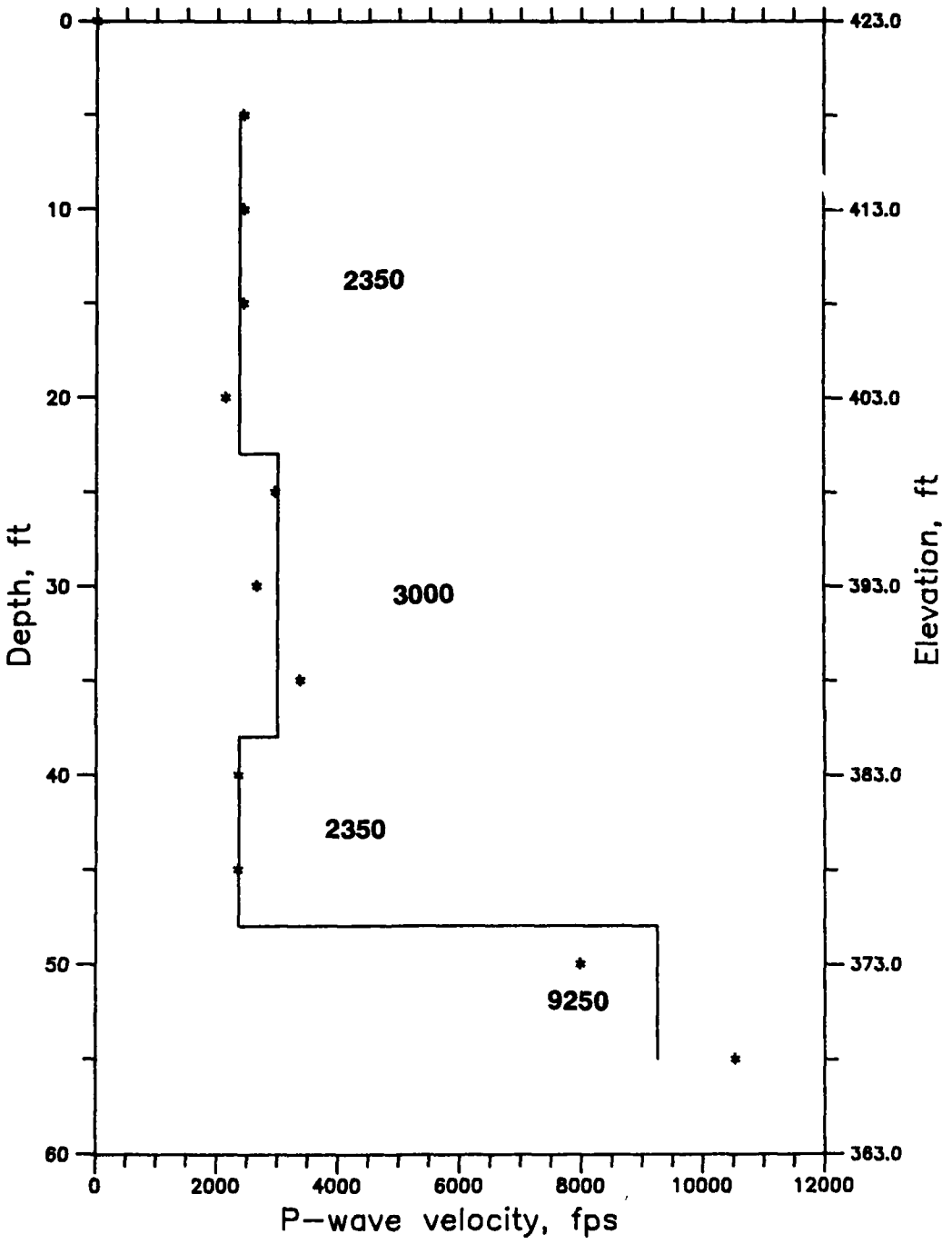

Figure 9. Crosshole P-wave results, downstream slope Dike 5

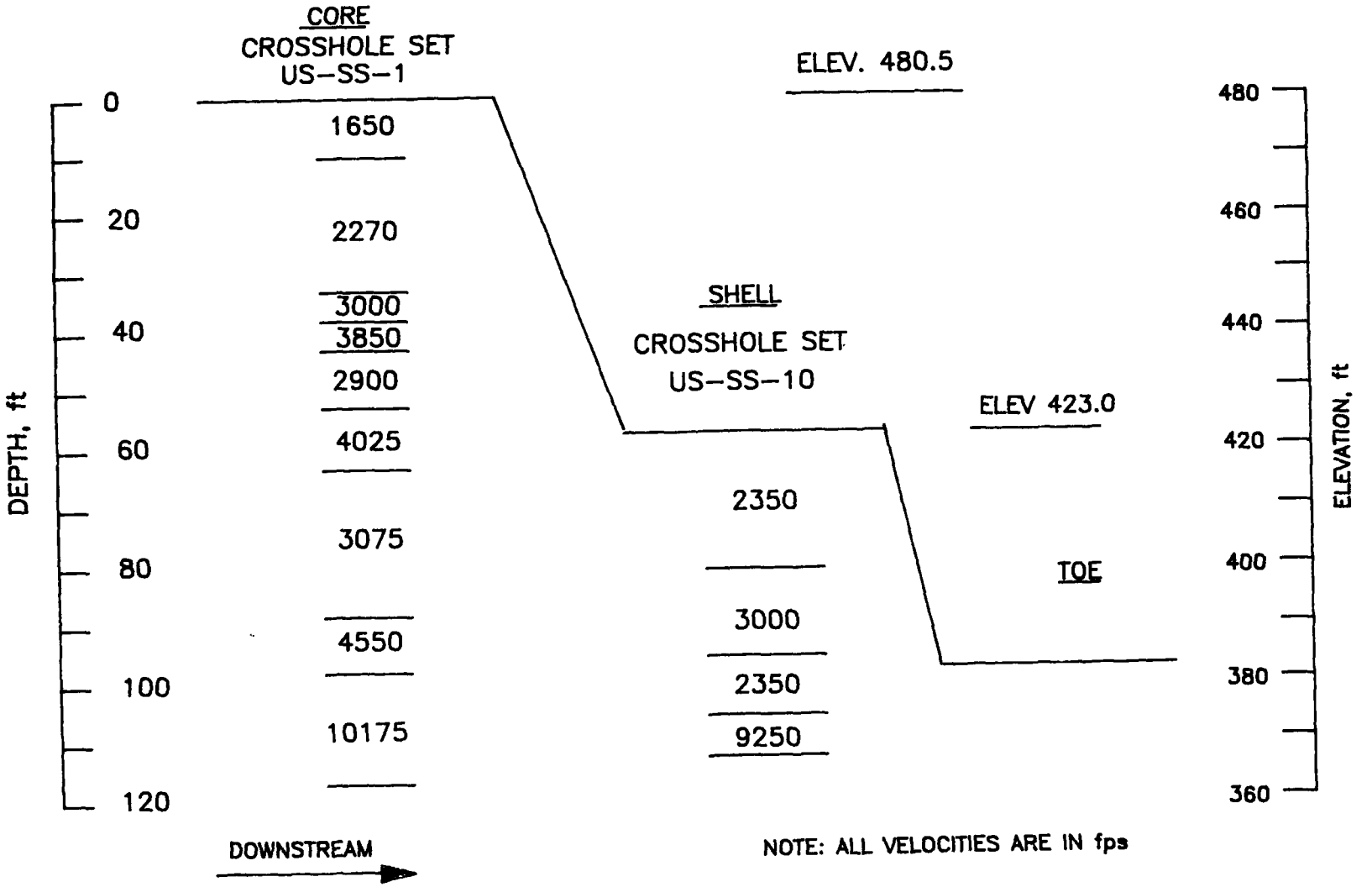

Figure 10. Interpreted P-wave profile from crosshole testing, Dike 5

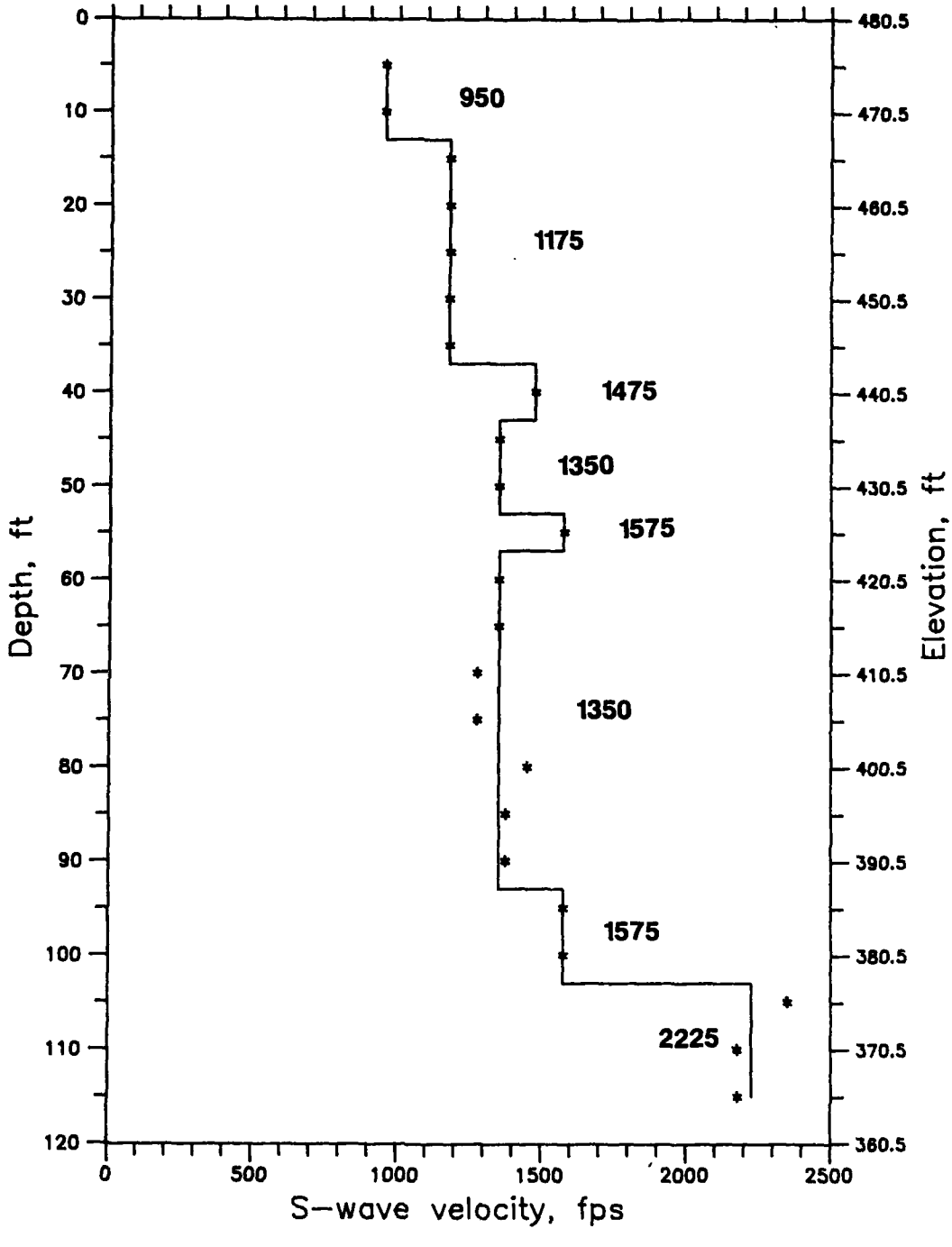

Figure 11. Crosshole S-wave results, crest of Dike 5

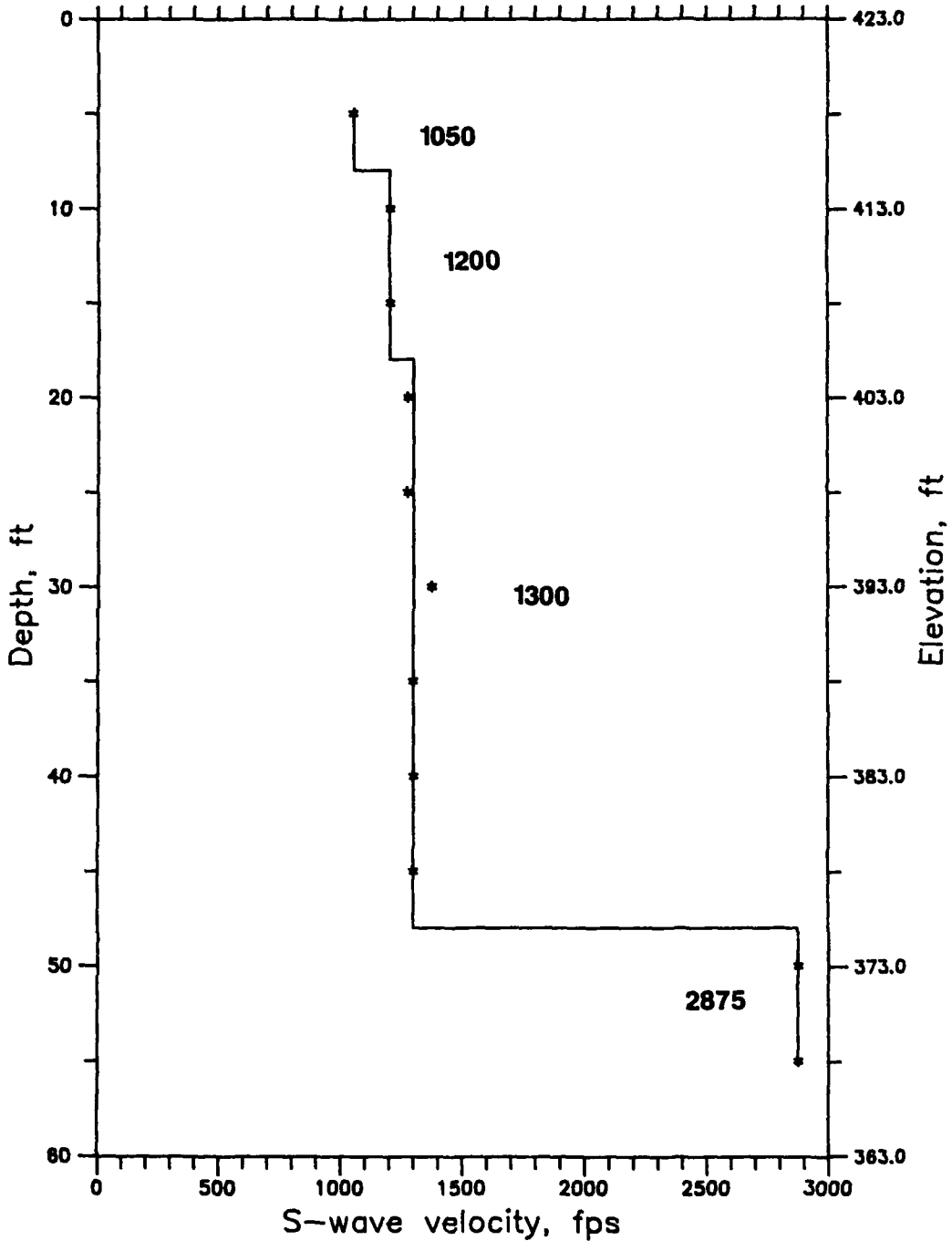

Figure 12. Crosshole S-wave results, downstream slope Dike 5

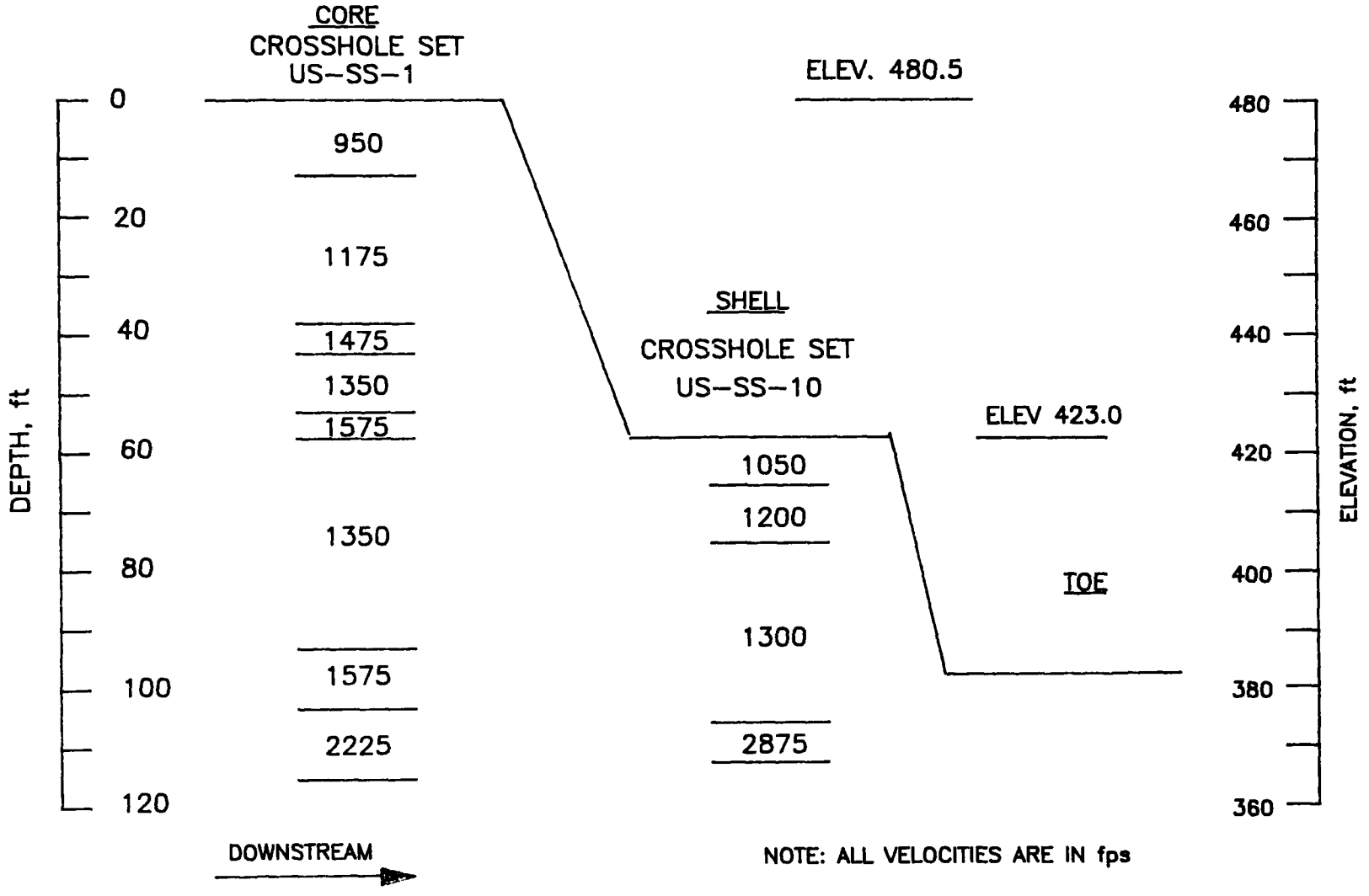

Figure 13. Interpreted S-wave profile from crosshole testing, Dike 5

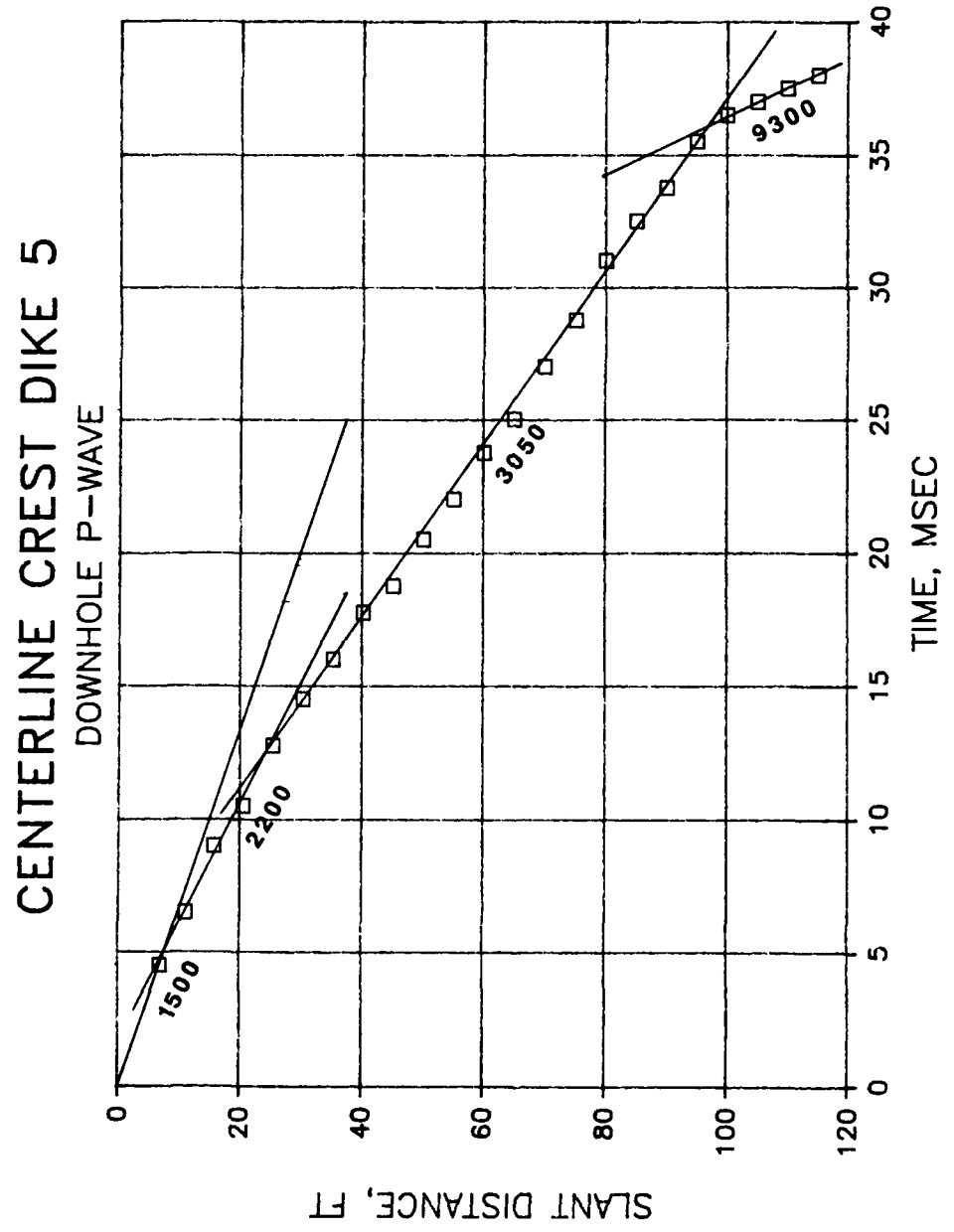

Figure 14. Downhole P-wave results, crest Dike 5

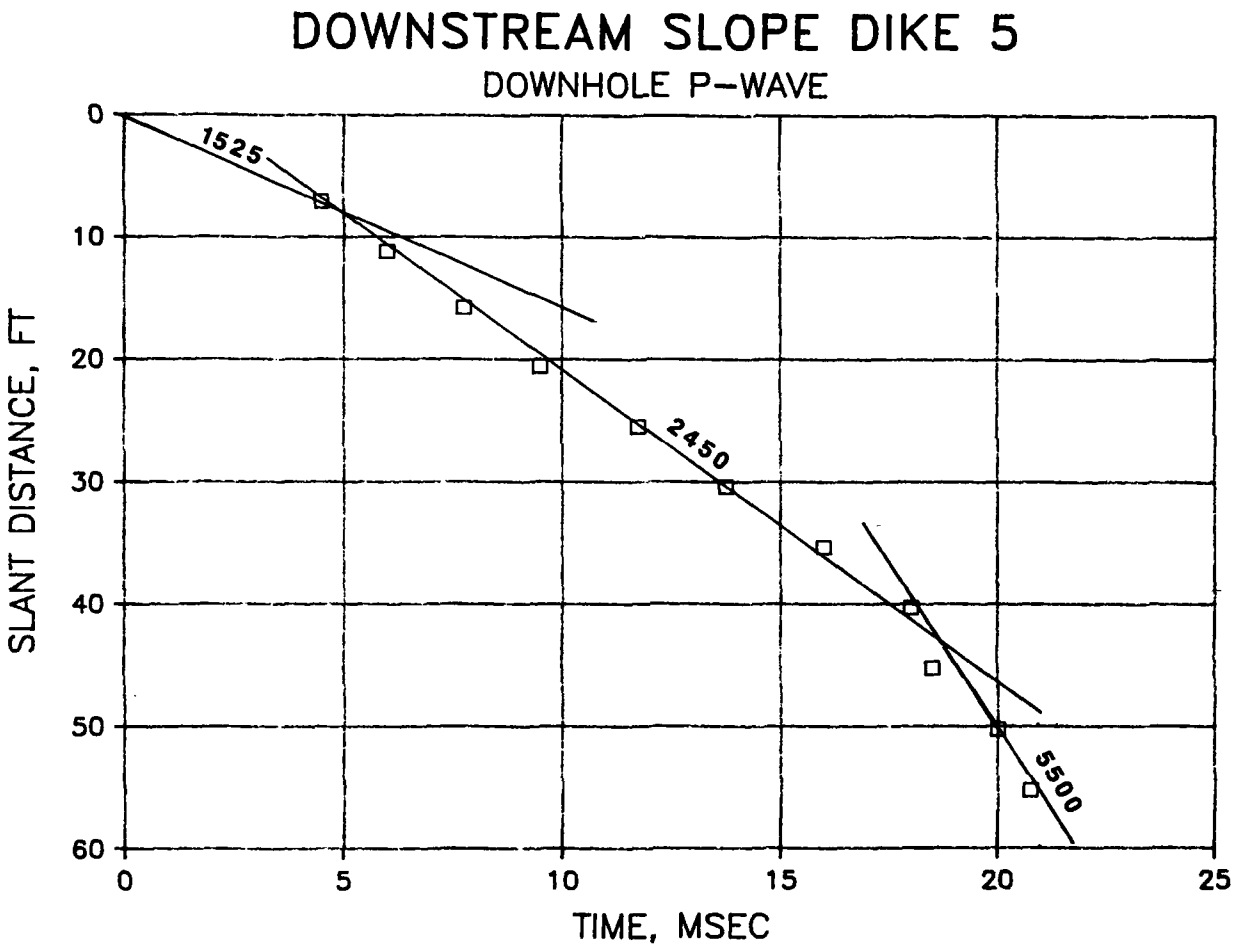

Figure 15. Downhole P-wave results, downstream slope Dike 5

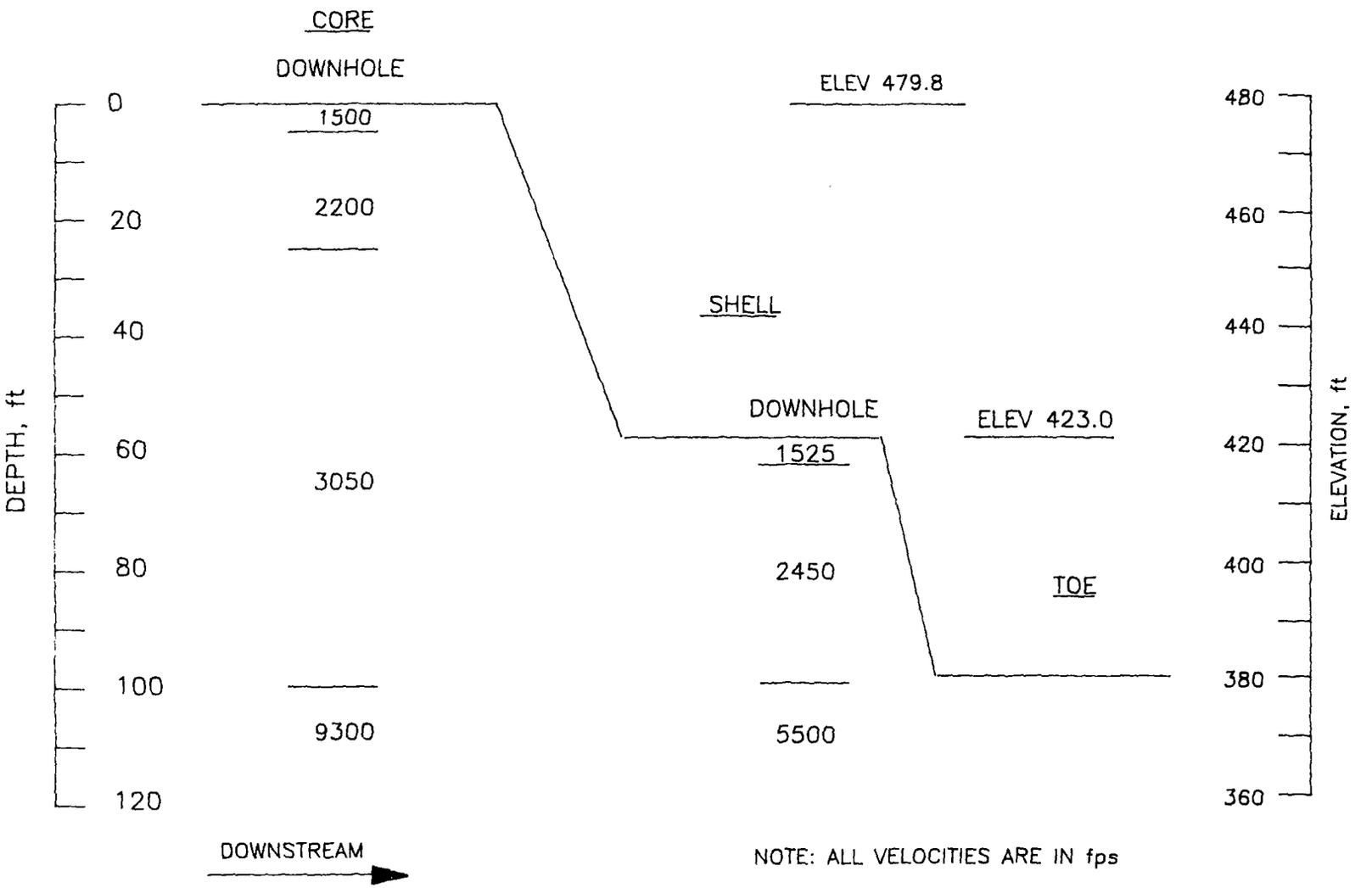

Figure 16. Interpreted P-wave profile from downhole testing, Dike 5

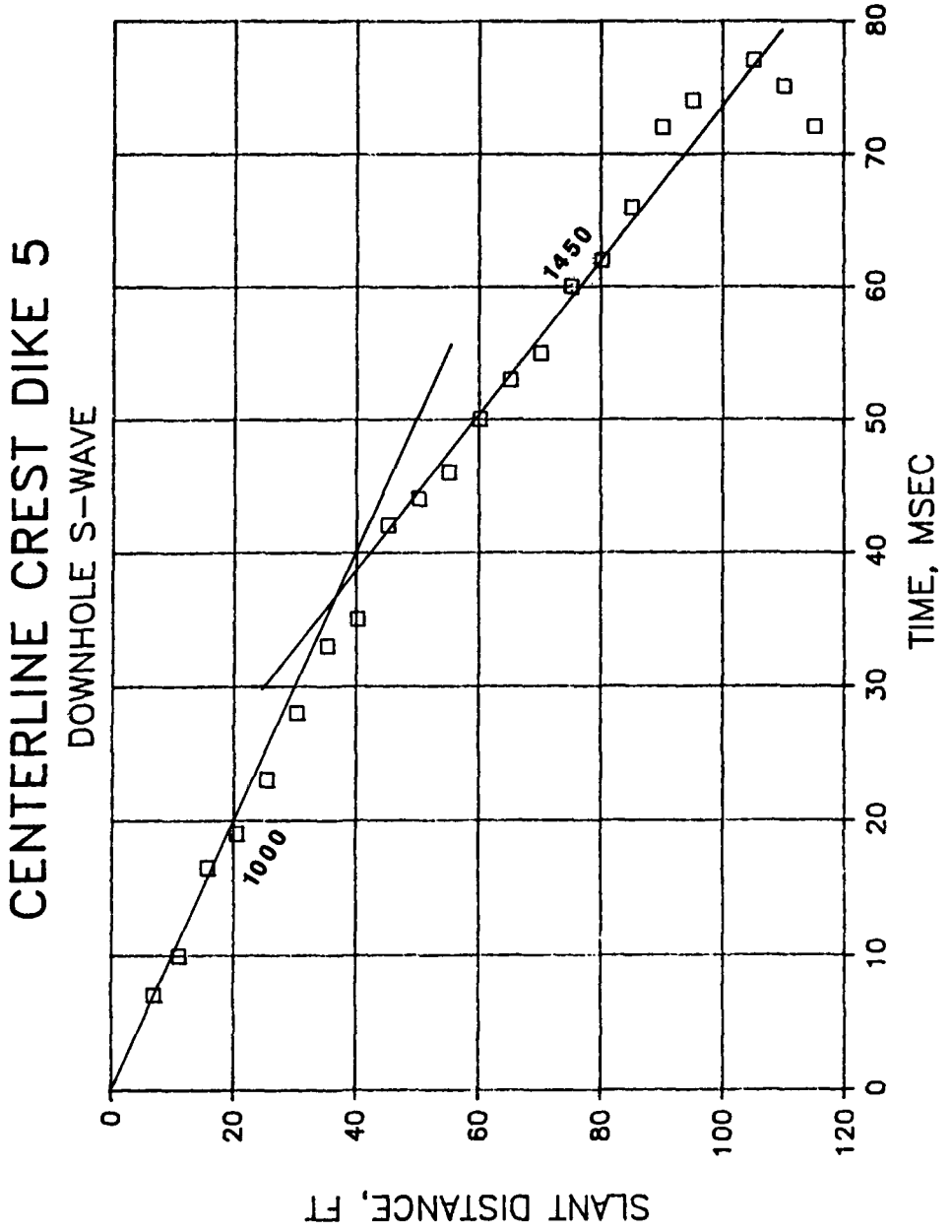

Figure 17. Downhole S-wave results, crest Dike 5

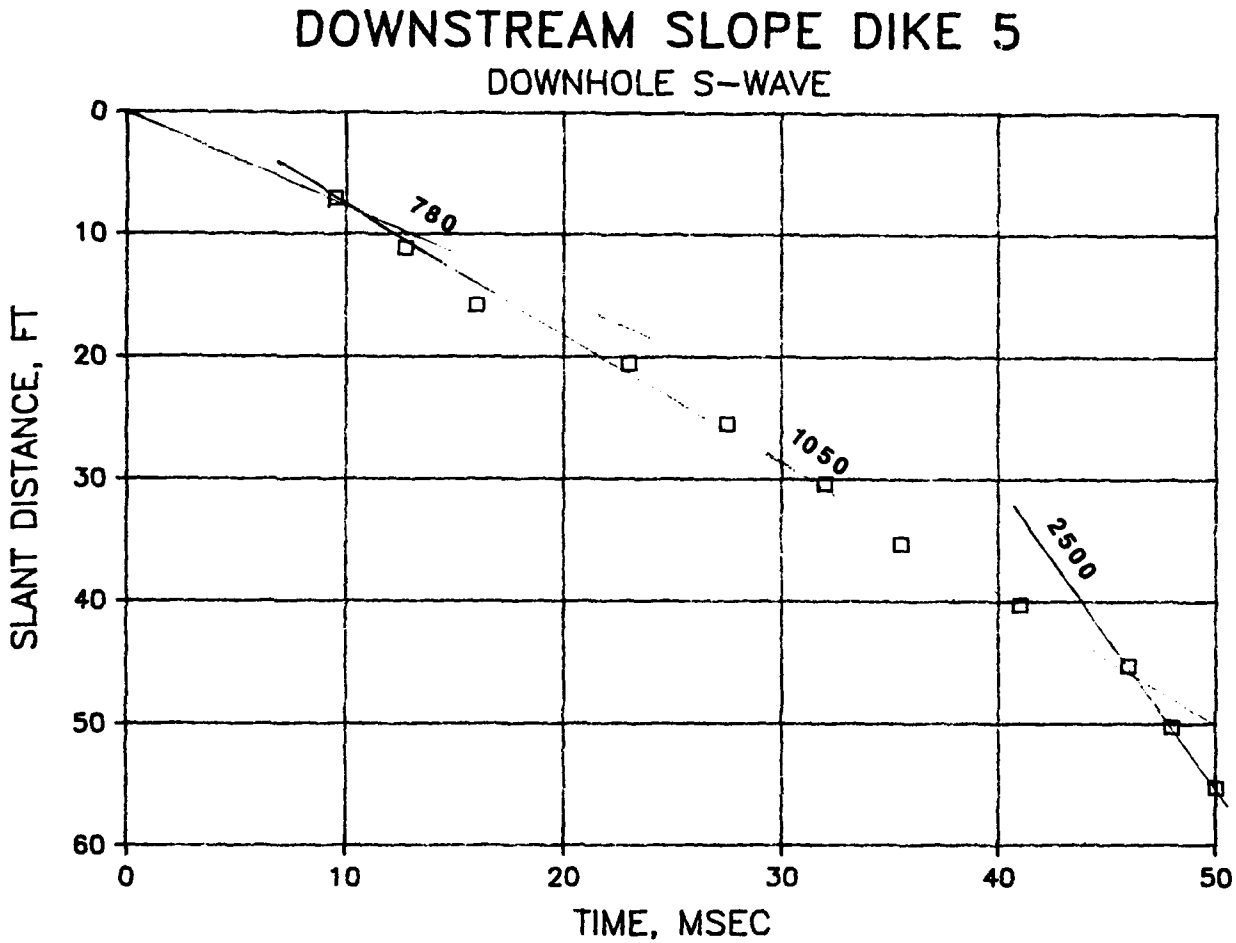

Figure 18. Downhole S-wave results, downstream slope Dike 5

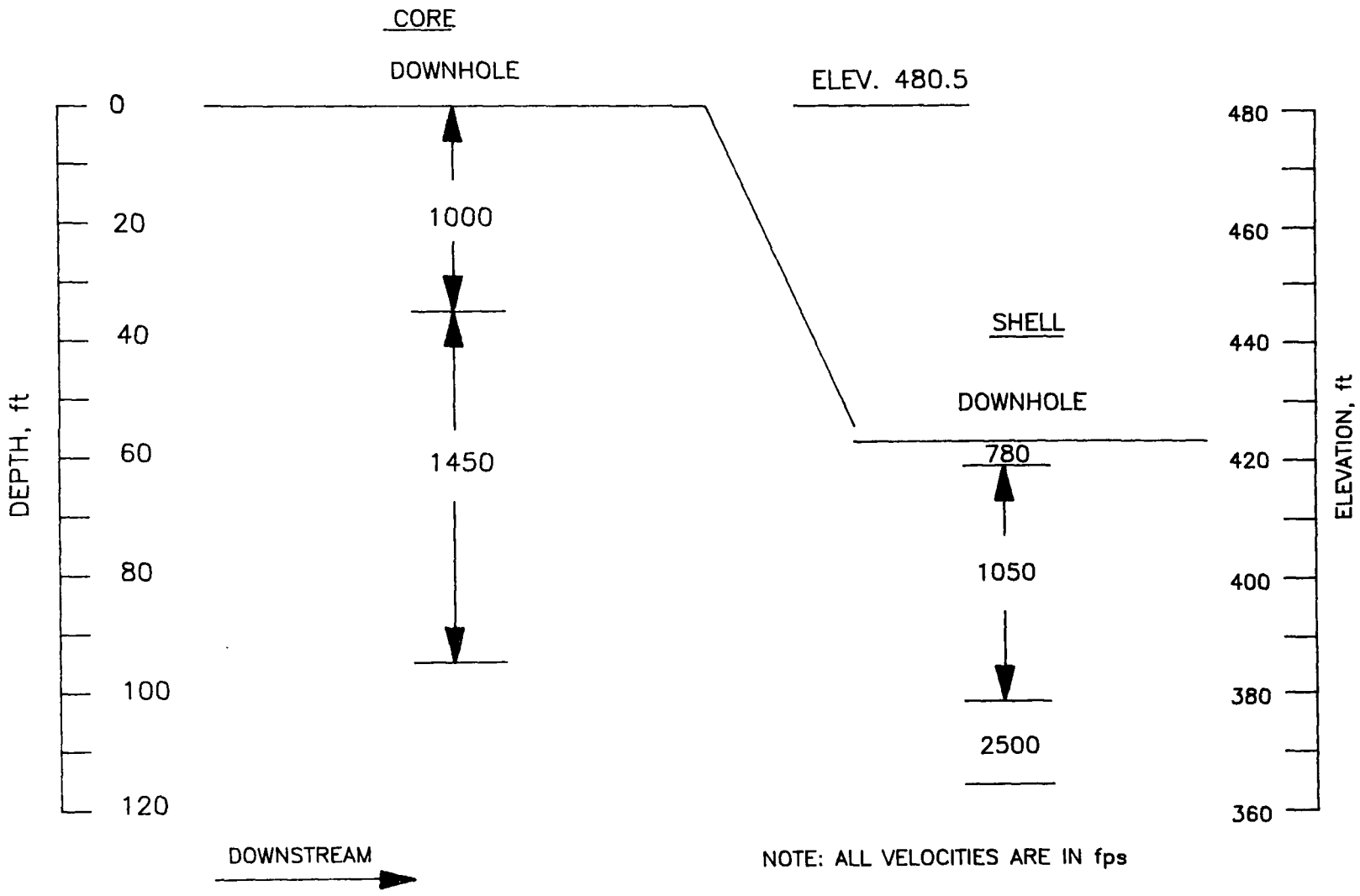

Figure 19. Interpreted S-wave profile from downhole testing, Dike 5

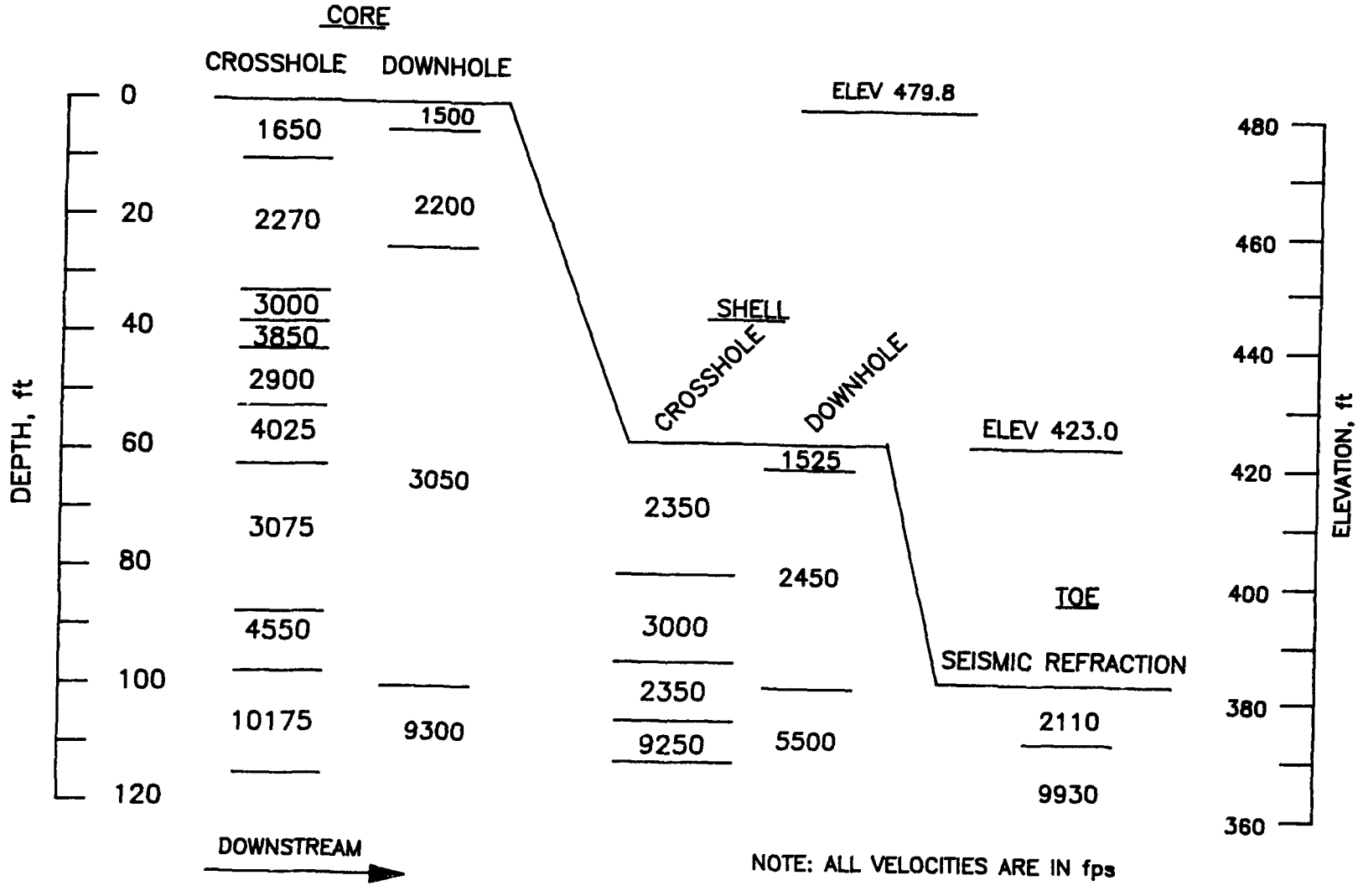

Figure 20. P-wave composite for cross section through approximate Station 180+50 - Dike 5

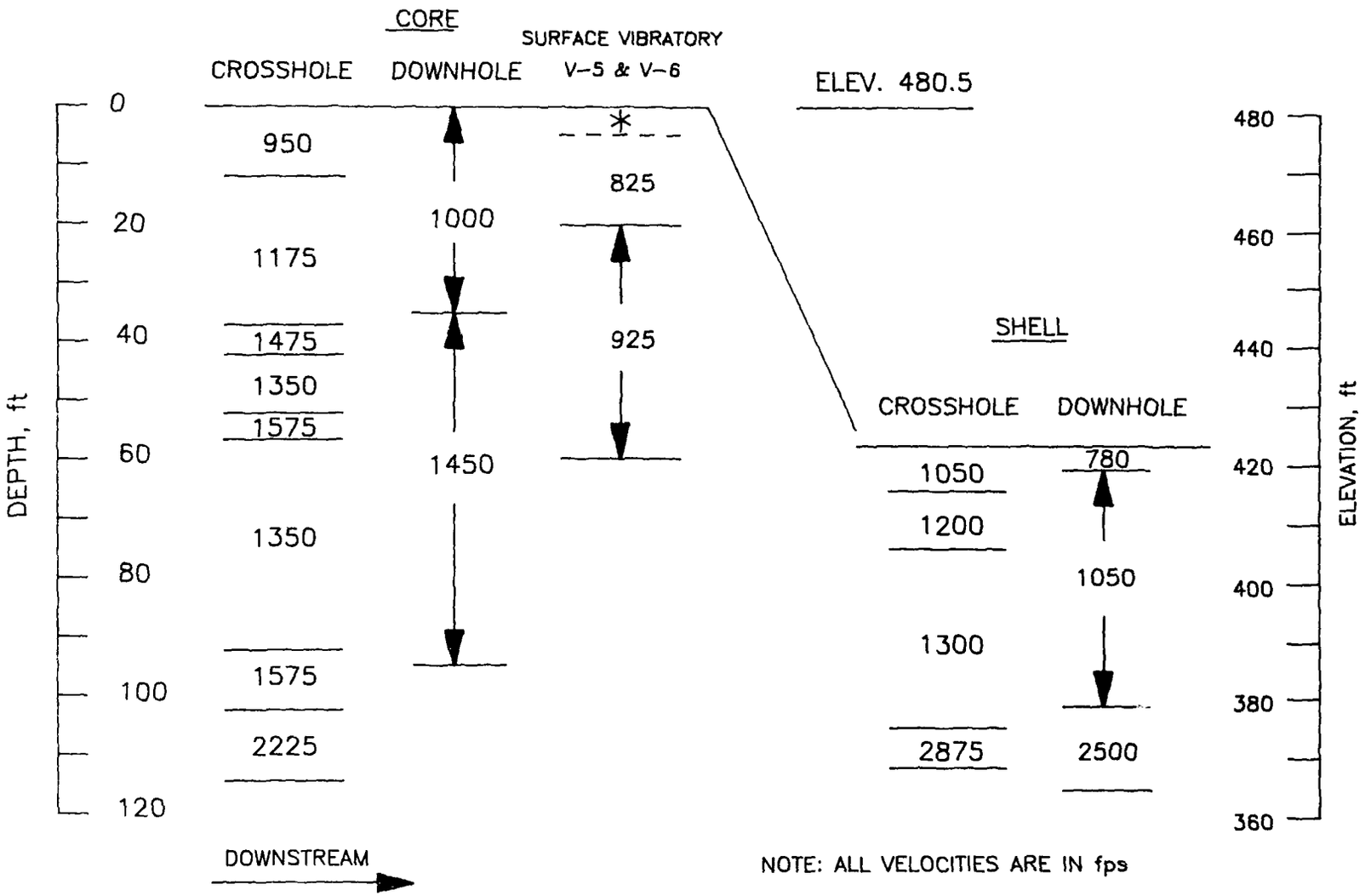

Figure 21. S-wave composite for cross section through approximate Station 180+50 - Dike 5

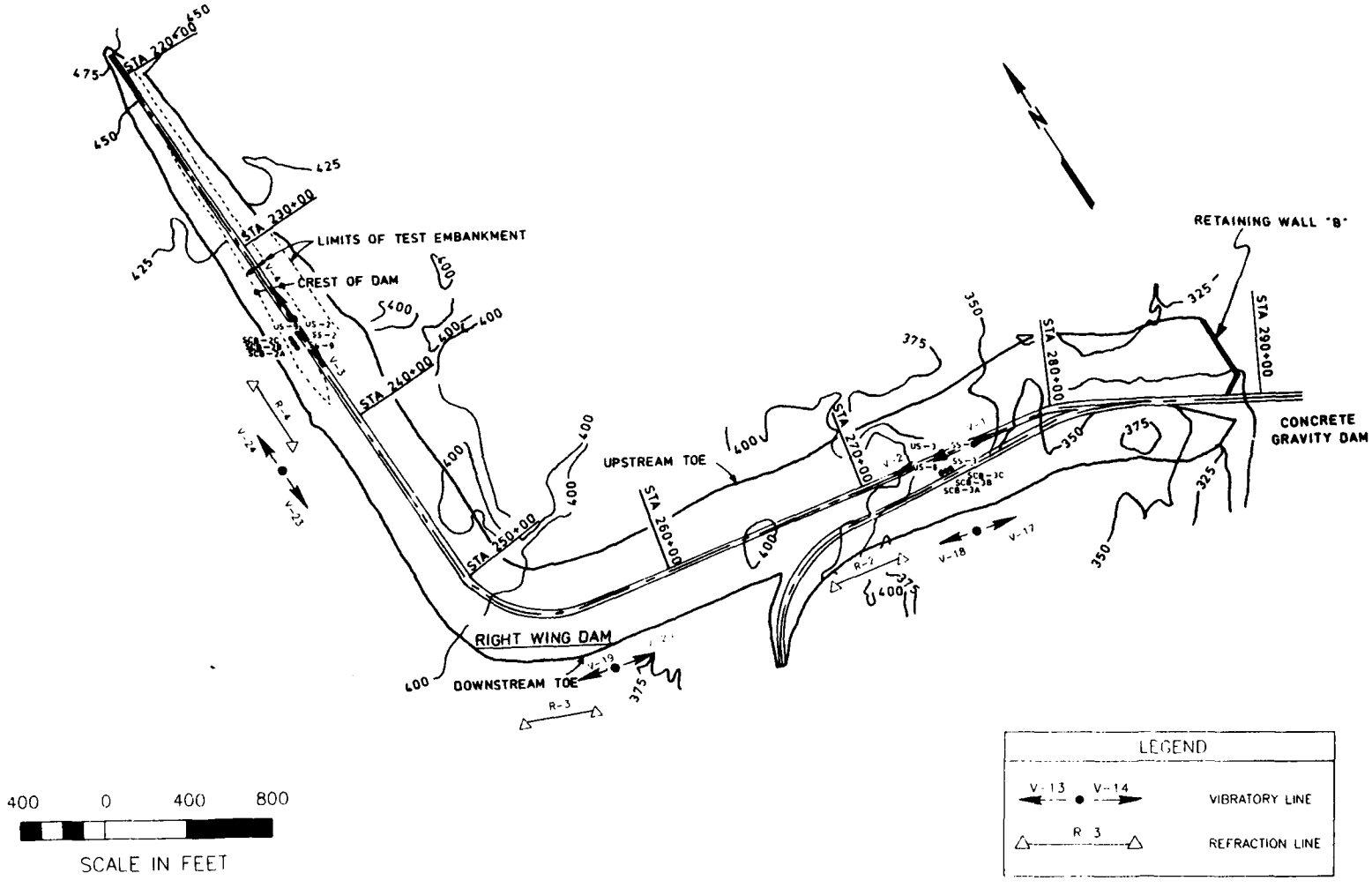

Figure 22. Plan view of Right and Left Wing Dams and test layout

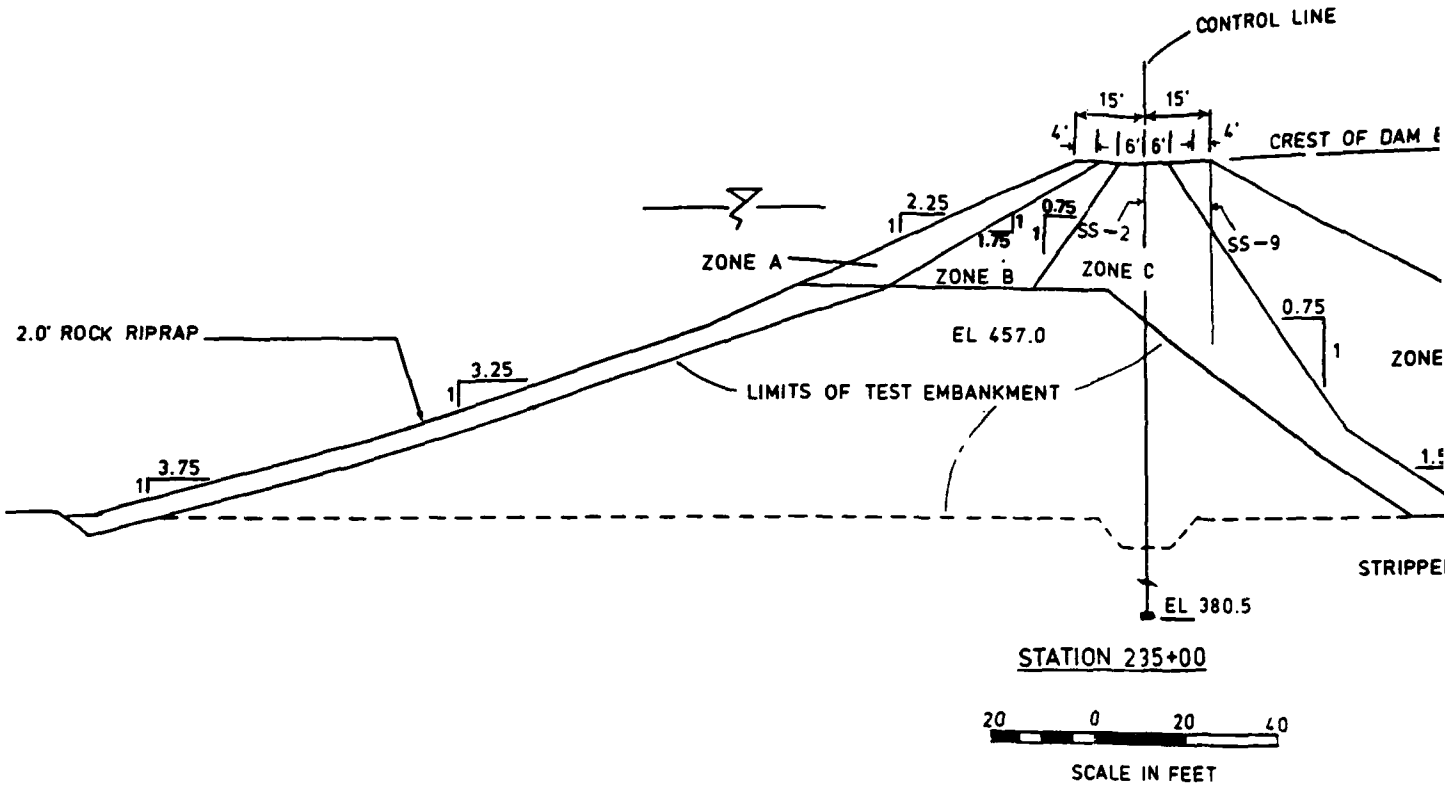

MATERIAL DESCRIPTIONS

ZONE A - ROCK FROM THE AMERICAN RIVER CHANNEL

ZONE B - UNPROCESSED SAND, GRAVEL, AND COBBLES FROM AMERICAN R
CHANNEL EXCAVATION

ZONE C - DECOMPOSED GRANITE FROM BORROW AREA NO. 2 AND SUITABL
RIVER CHANNEL EXCAVATION

Figure 23. Cross section of Right Wing Dam, approximate S

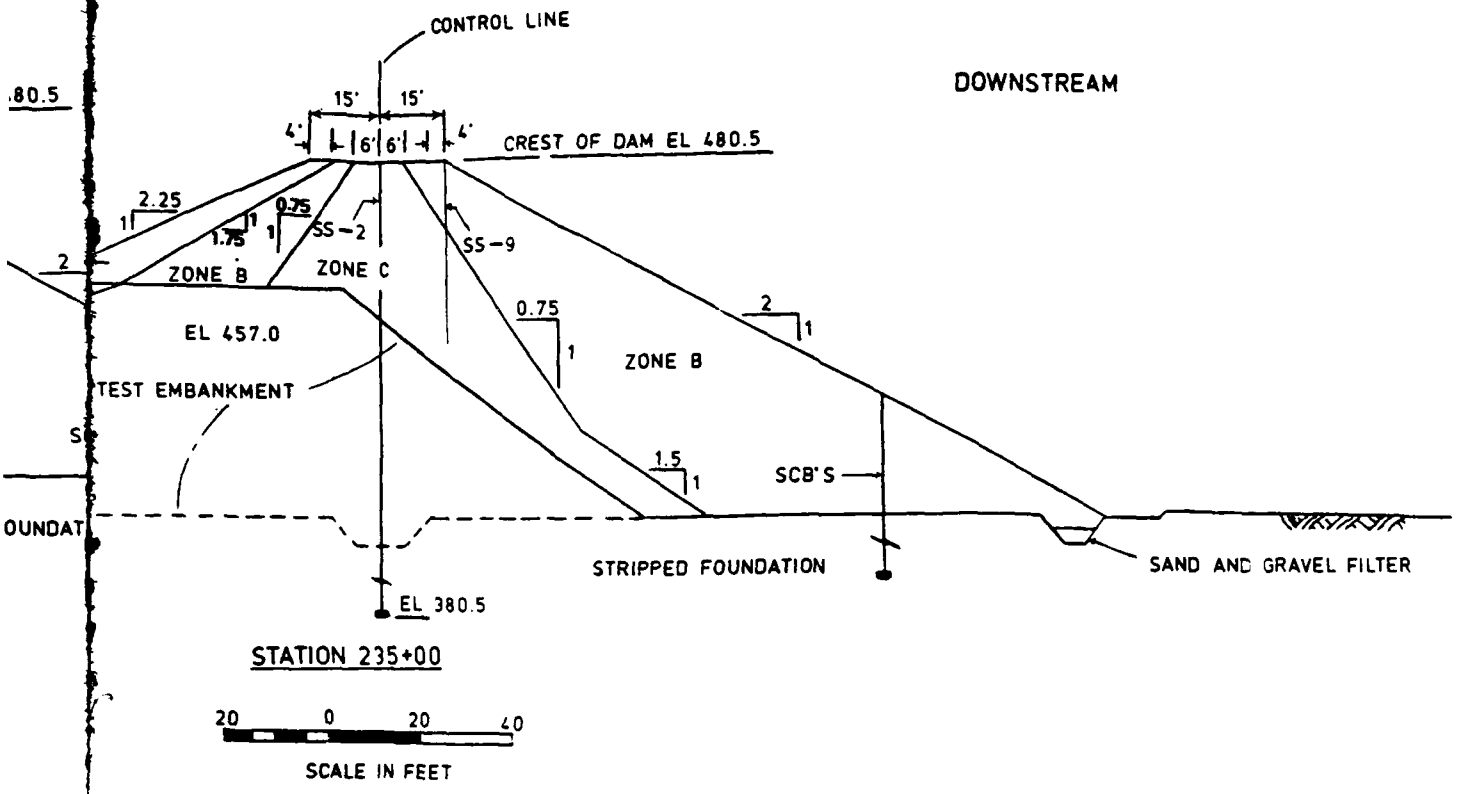

STATION 235+00

20 0 20 40

SCALE IN FEET

MATERIAL DESCRIPTIONS

E AMERICAN RIVER CHANNEL

SAND, GRAVEL, AND COBBLES FROM AMERICAN RIVER
VATION

RANITE FROM BORROW AREA NO. 2 AND SUITABLE FINE-GRAINED
L EXCAVATION

section of Right Wing Dam, approximate Station 235+00

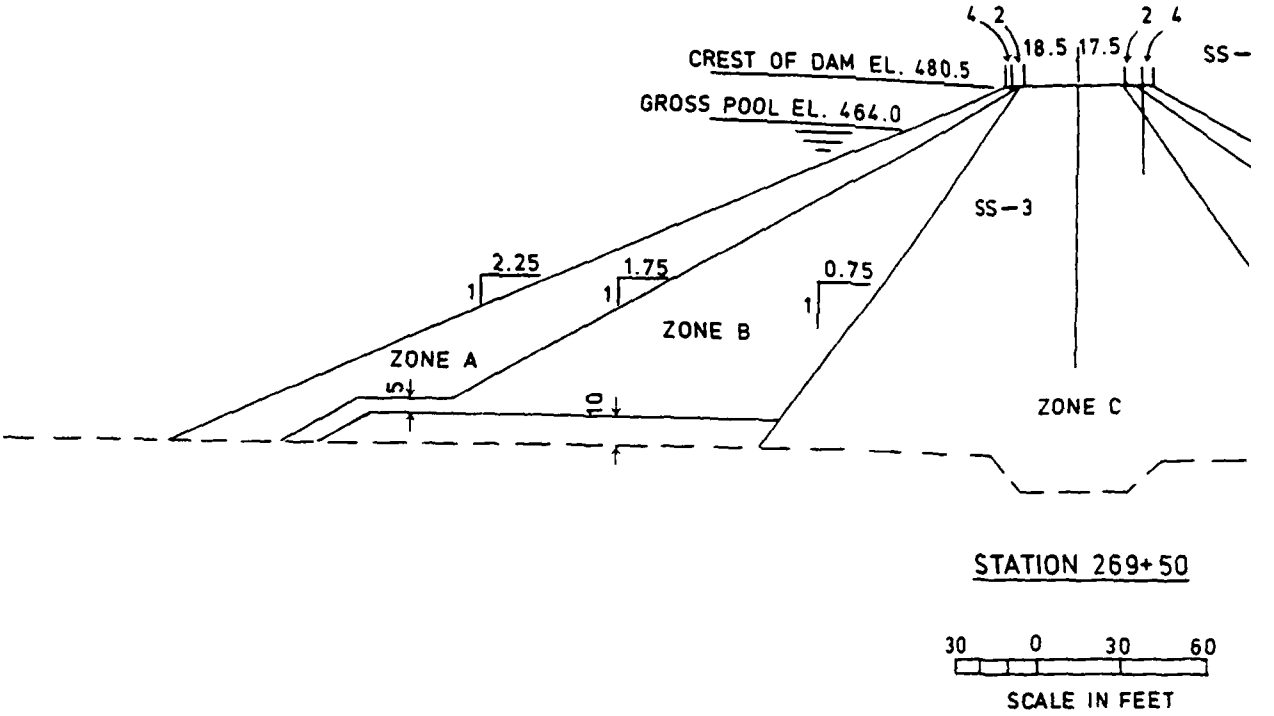

STATION 269+50

30 0 30 60

SCALE IN FEET

MATERIAL DESCRIPTION

ZONE A - ROCK FROM THE AMERICAN RIVER CHANNEL

ZONE B - UNPROCESSED SAND, GRAVEL, AND COBBLES FI
CHANNEL EXCAVATION

ZONE C - DECOMPOSED GRANITE FROM BORROW AREA NO.
RIVER CHANNEL EXCAVATION

Figure 24. Cross section of Right Wing Dam, a

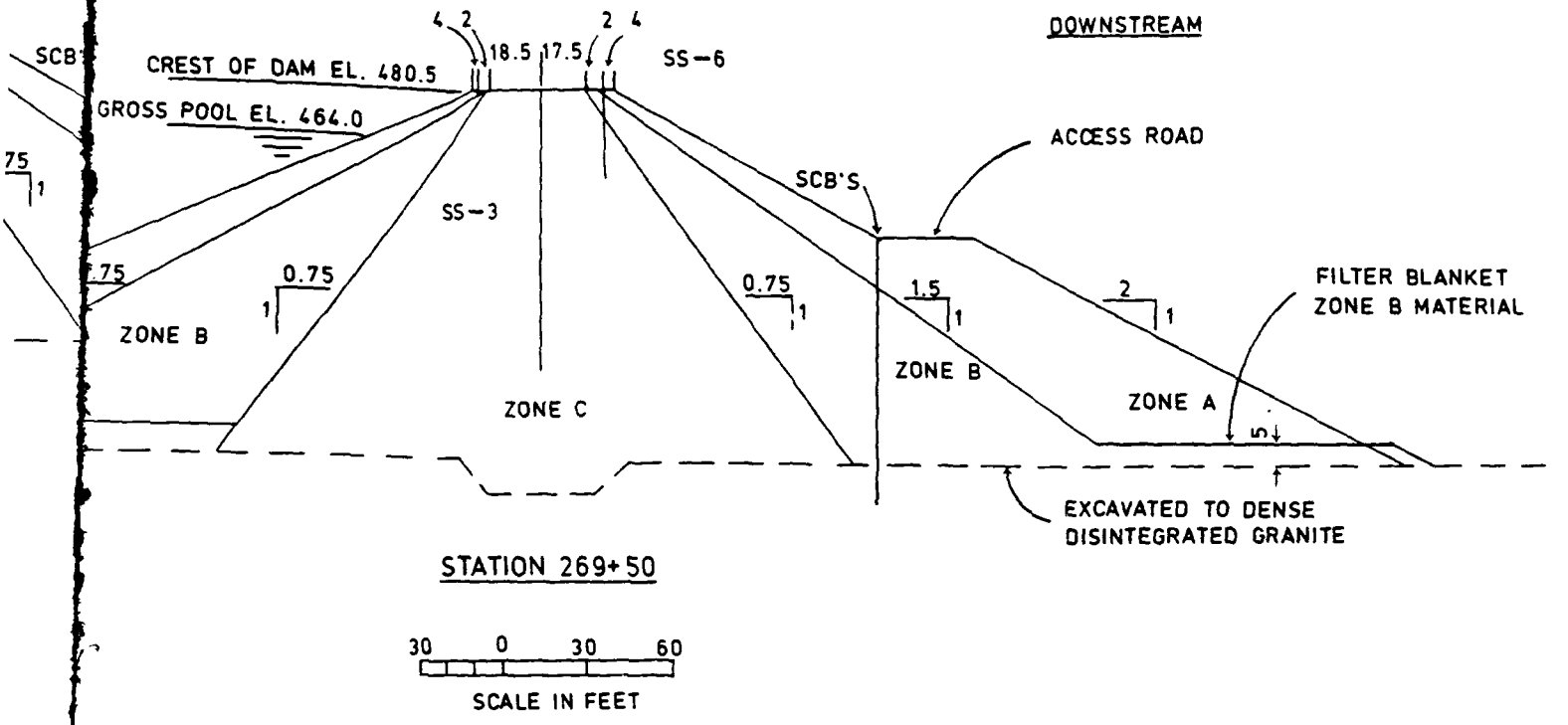

STATION 269+50

30 0 30 60

SCALE IN FEET

MATERIAL DESCRIPTIONS

OCK FROM THE AMERICAN RIVER CHANNEL

NPROCESSED SAND, GRAVEL, AND COBBLES FROM AMERICAN RIVER
HANNEL EXCAVATION

ECOMPOSED GRANITE FROM BORROW AREA NO. 2 AND SUITABLE FINE-GRAINED
IVER CHANNEL EXCAVATION

e 24. Cross section of Right Wing Dam, approximate Station 269+50

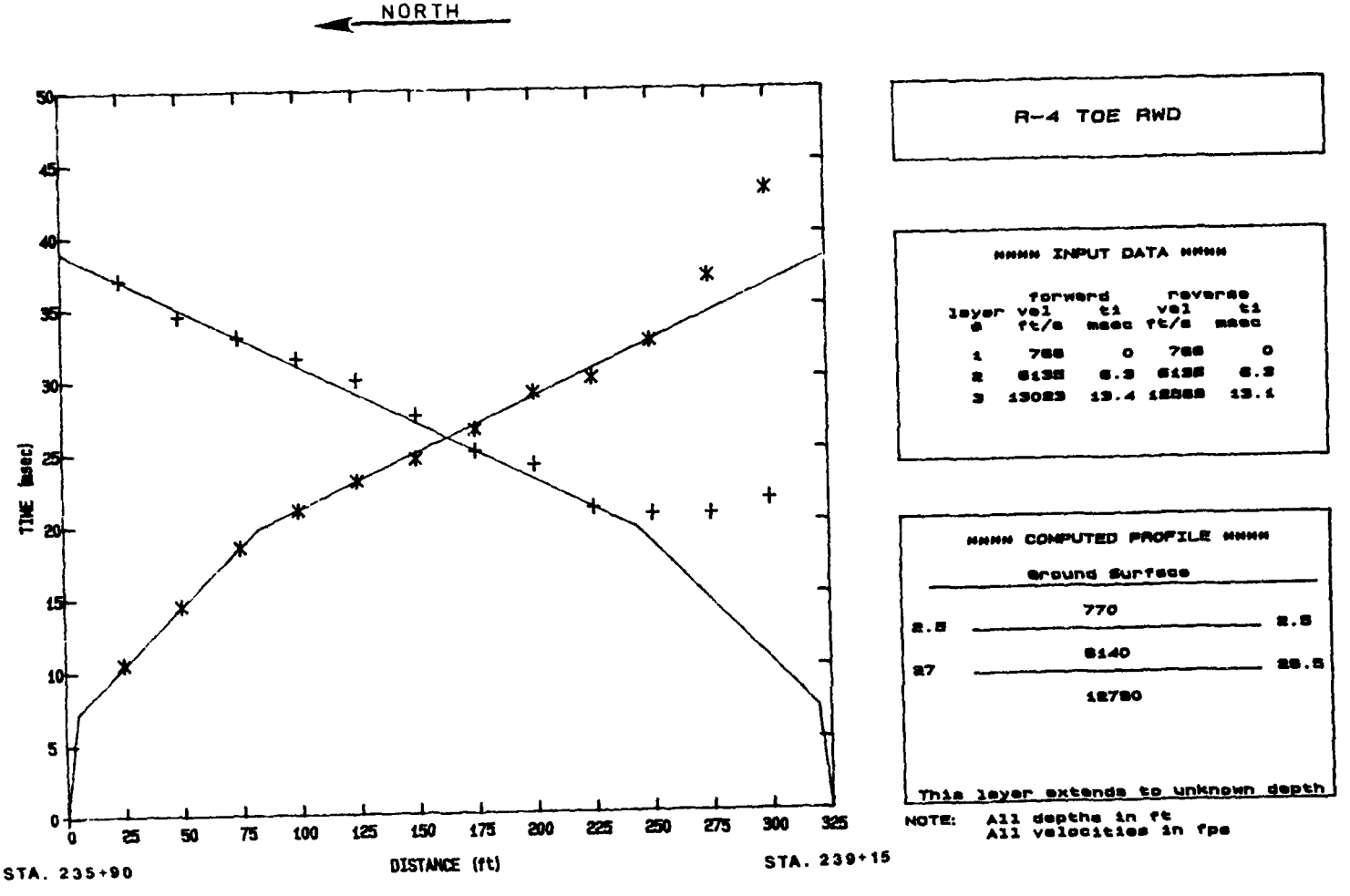

Figure 25. Seismic refraction line R-4, downstream toe of Right Wing Dam

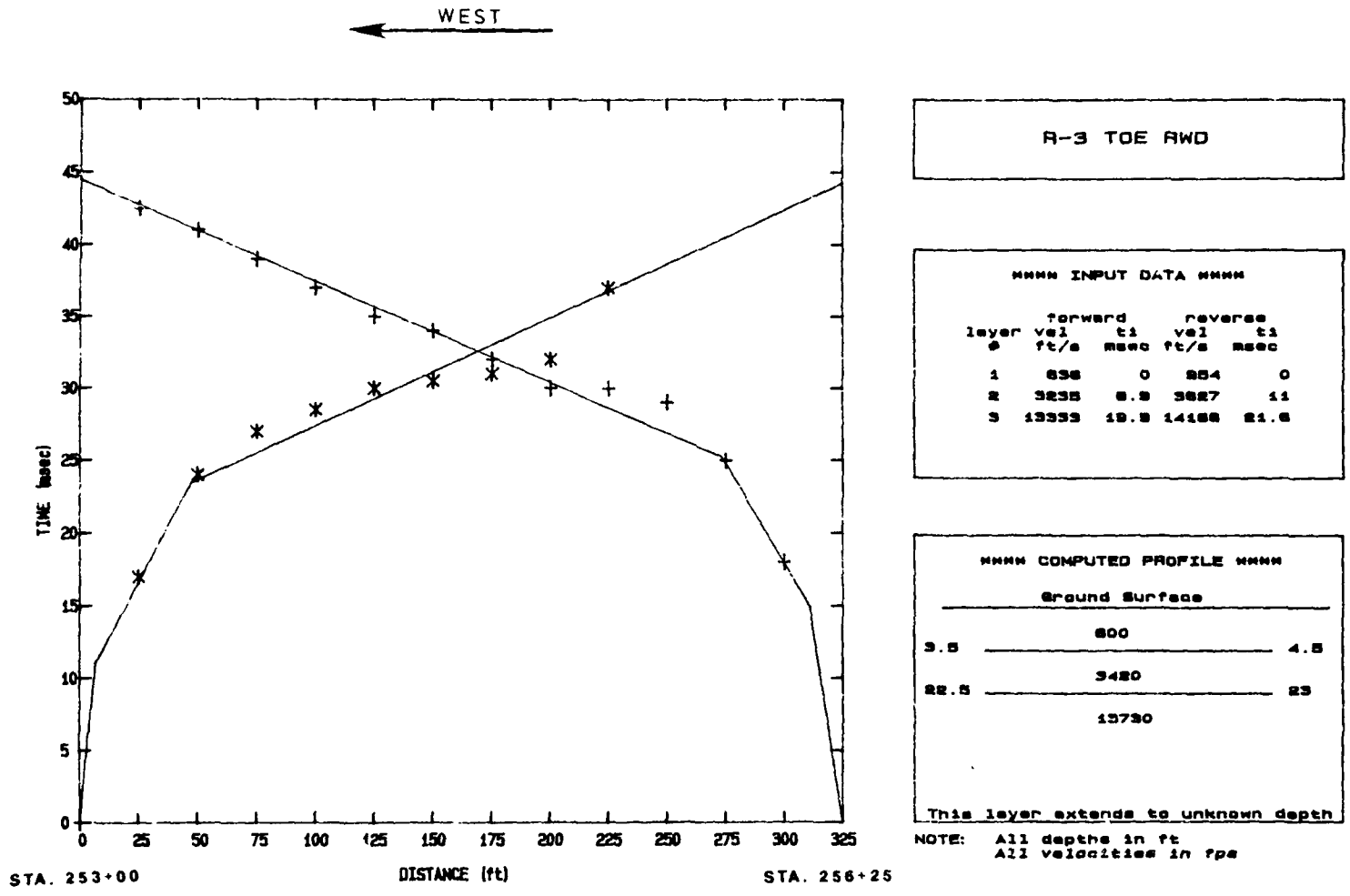

Figure 26. Seismic refraction line R-3, downstream toe of Right Wing Dam

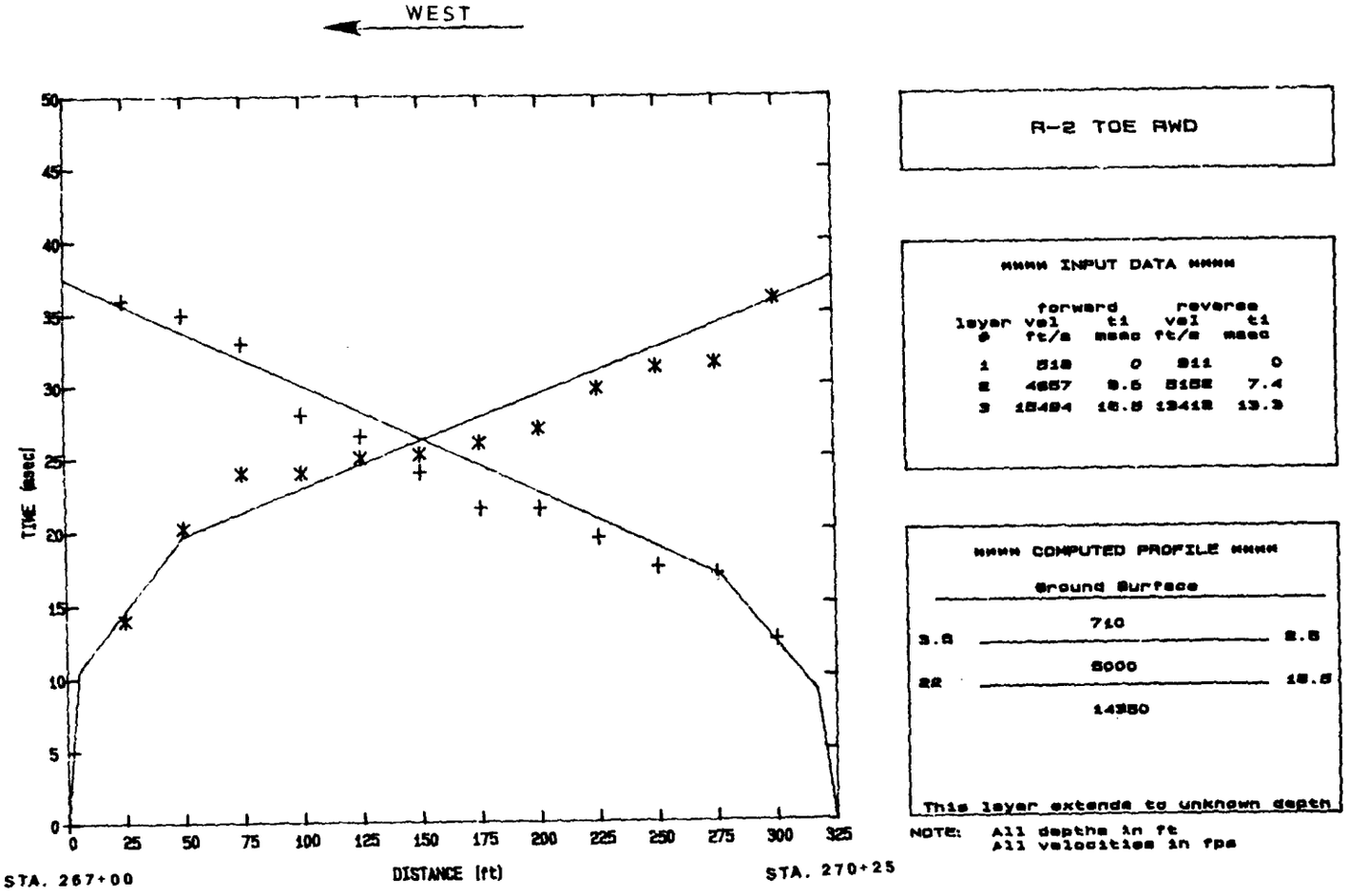

Figure 27. Seismic refraction line R-2, downstream toe of Right Wing Dam

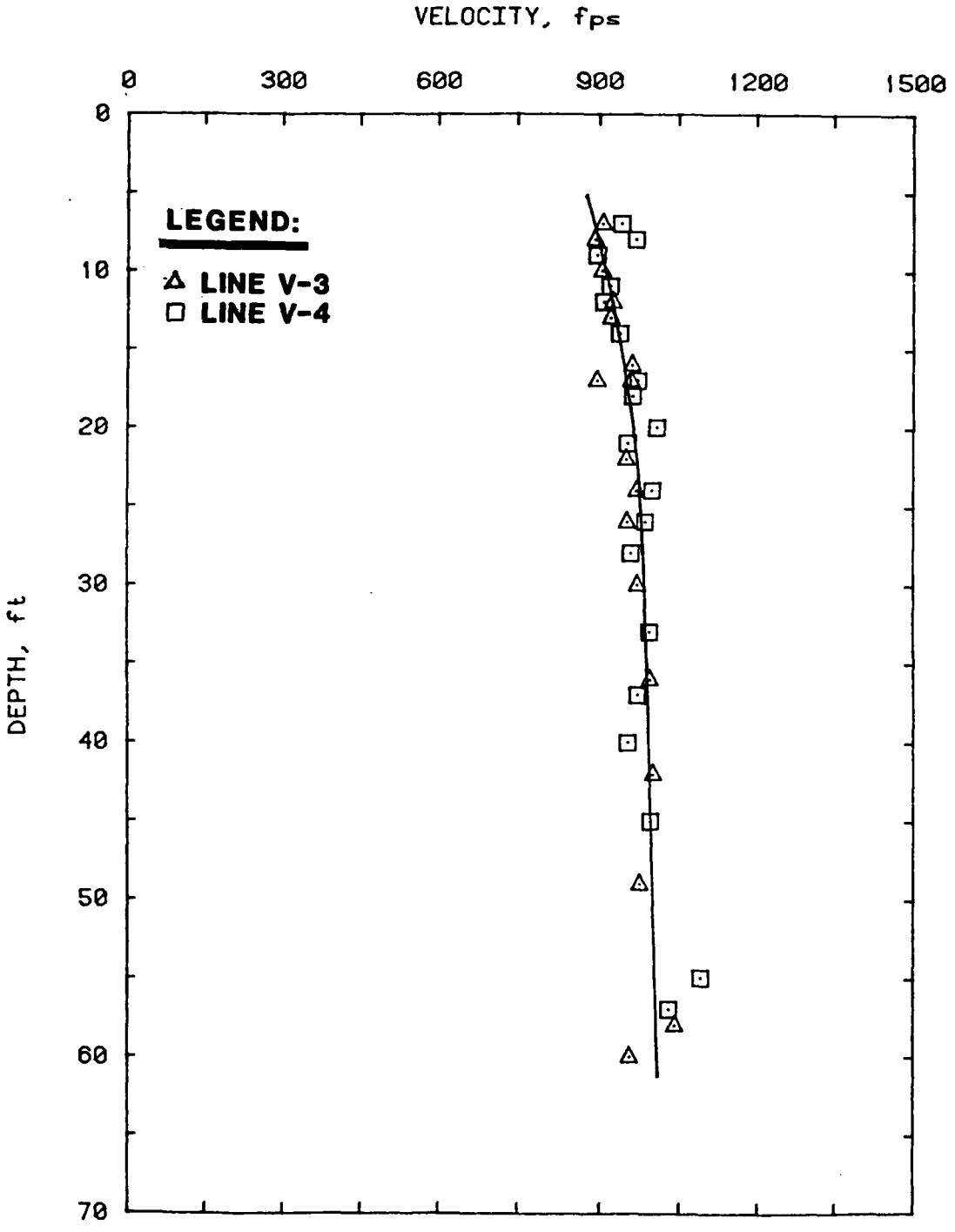

Figure 28. R-wave velocity versus depth for lines V-3 and V-4, crest of Right Wing Dam, approximate Station 235+00

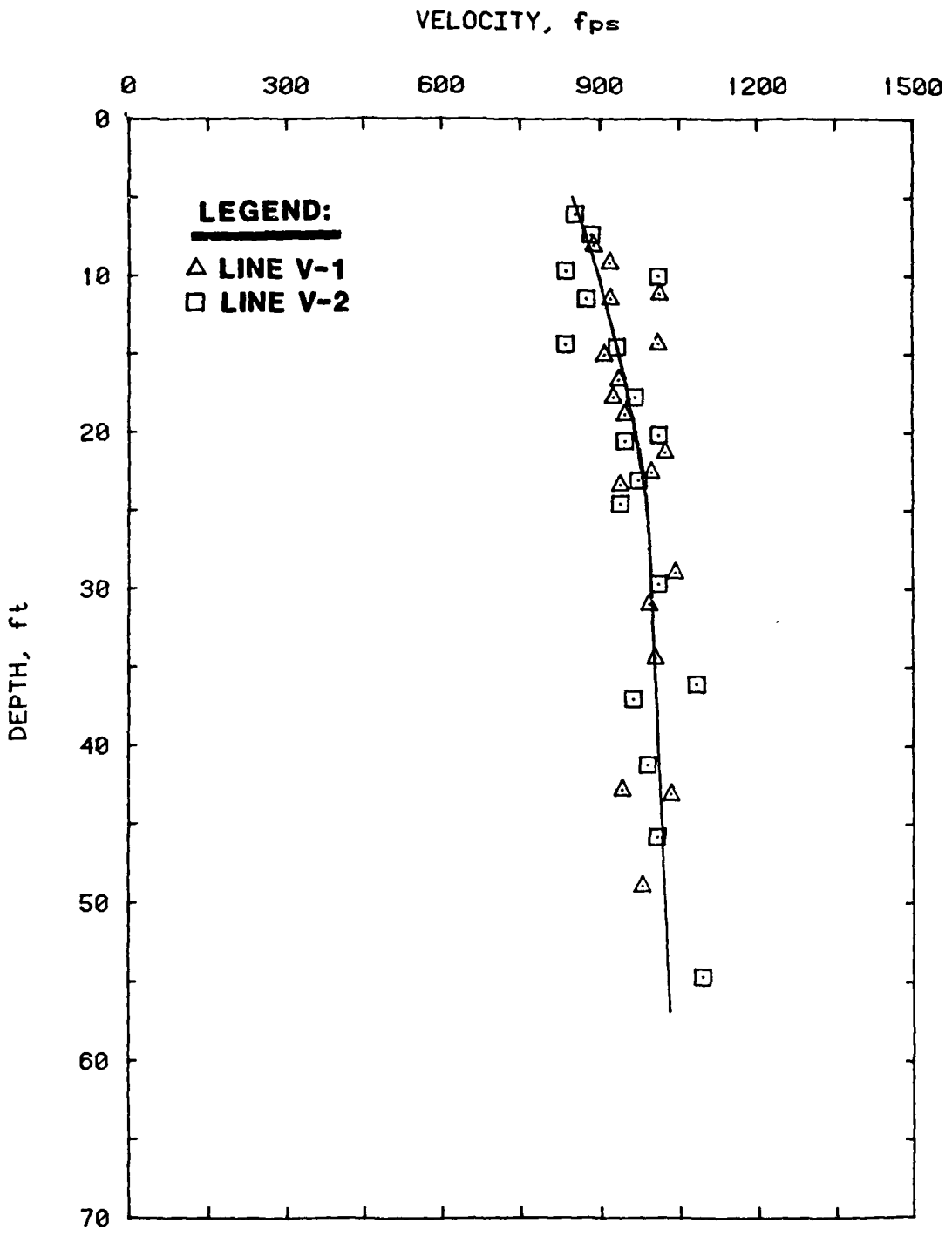

Figure 29. R-wave velocity versus depth for lines V-1 and V-2, crest of Right Wing Dam, approximate Station 269+50

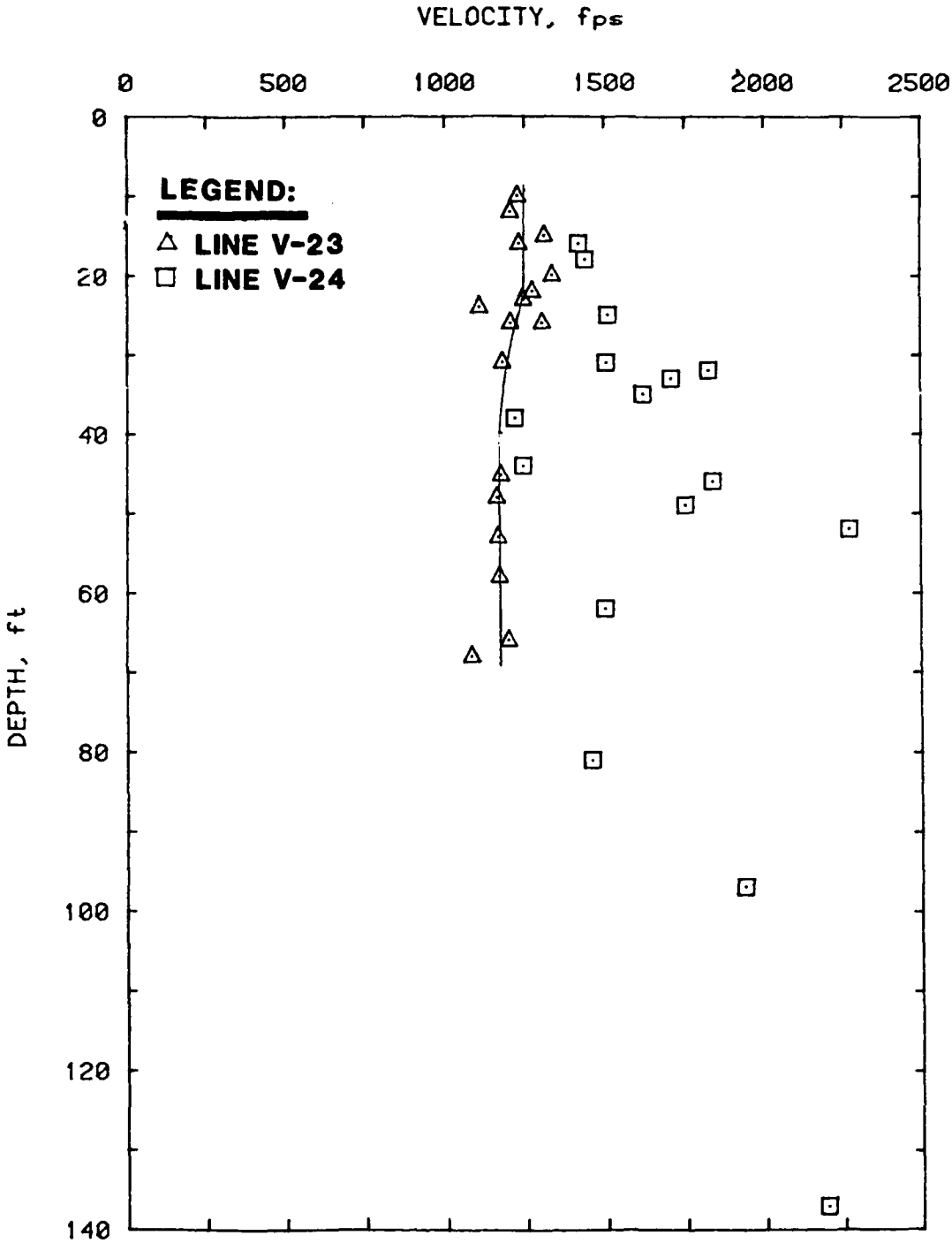

Figure 30. R-wave velocity versus depth for lines V-23 and V-24, toe of Right Wing Dam, approximate Station 240+75

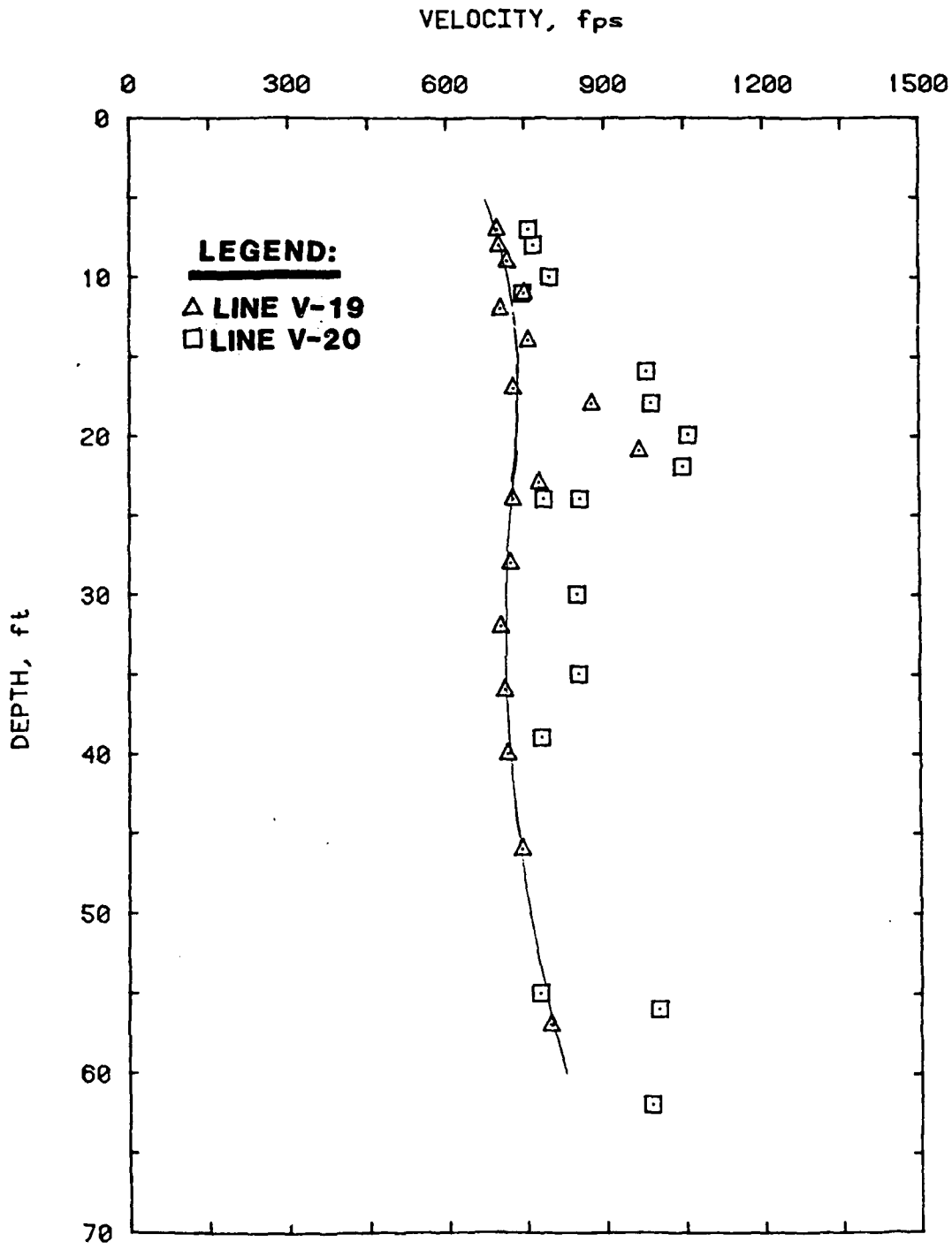

Figure 31. R-wave velocity versus depth for lines V-19 and V-20, toe of Right Wing Dam, approximate Station 253+50

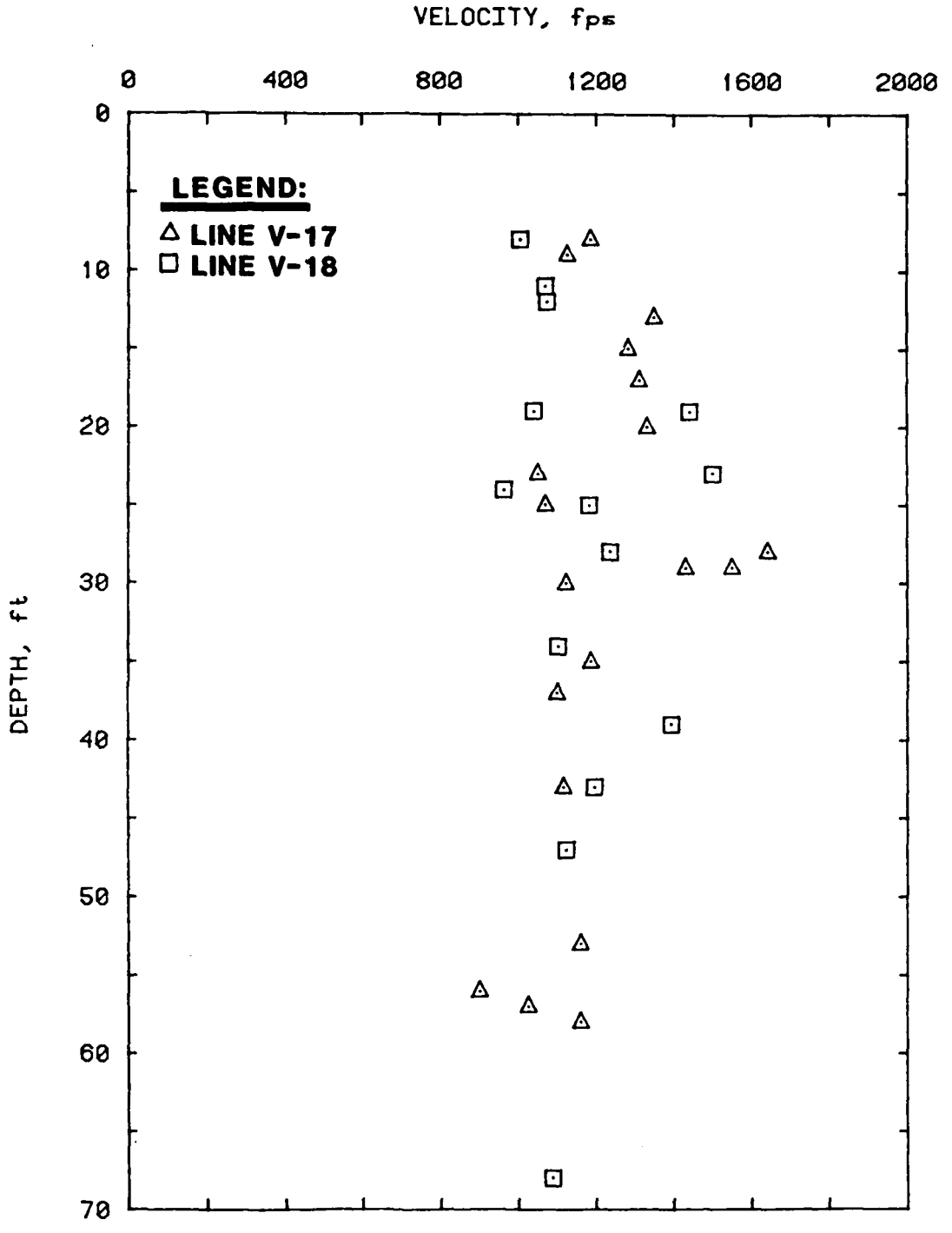

Figure 32. R-wave velocity versus depth for lines V-17 and V-18, toe of Right Wing Dam, approximate Station 273+00

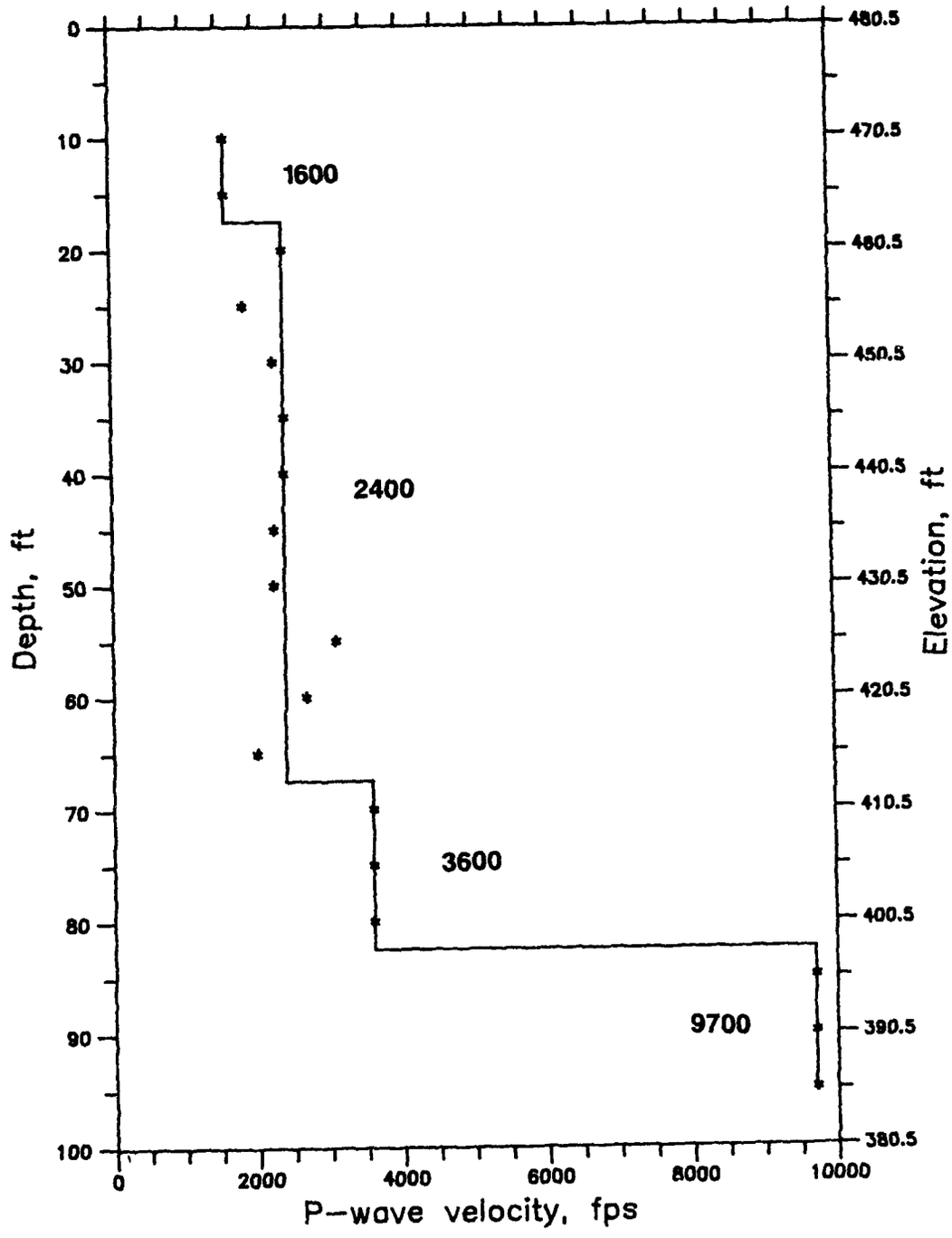

Figure 33. Crosshole P-wave results, centerline Right Wing Dam, Station 235+00

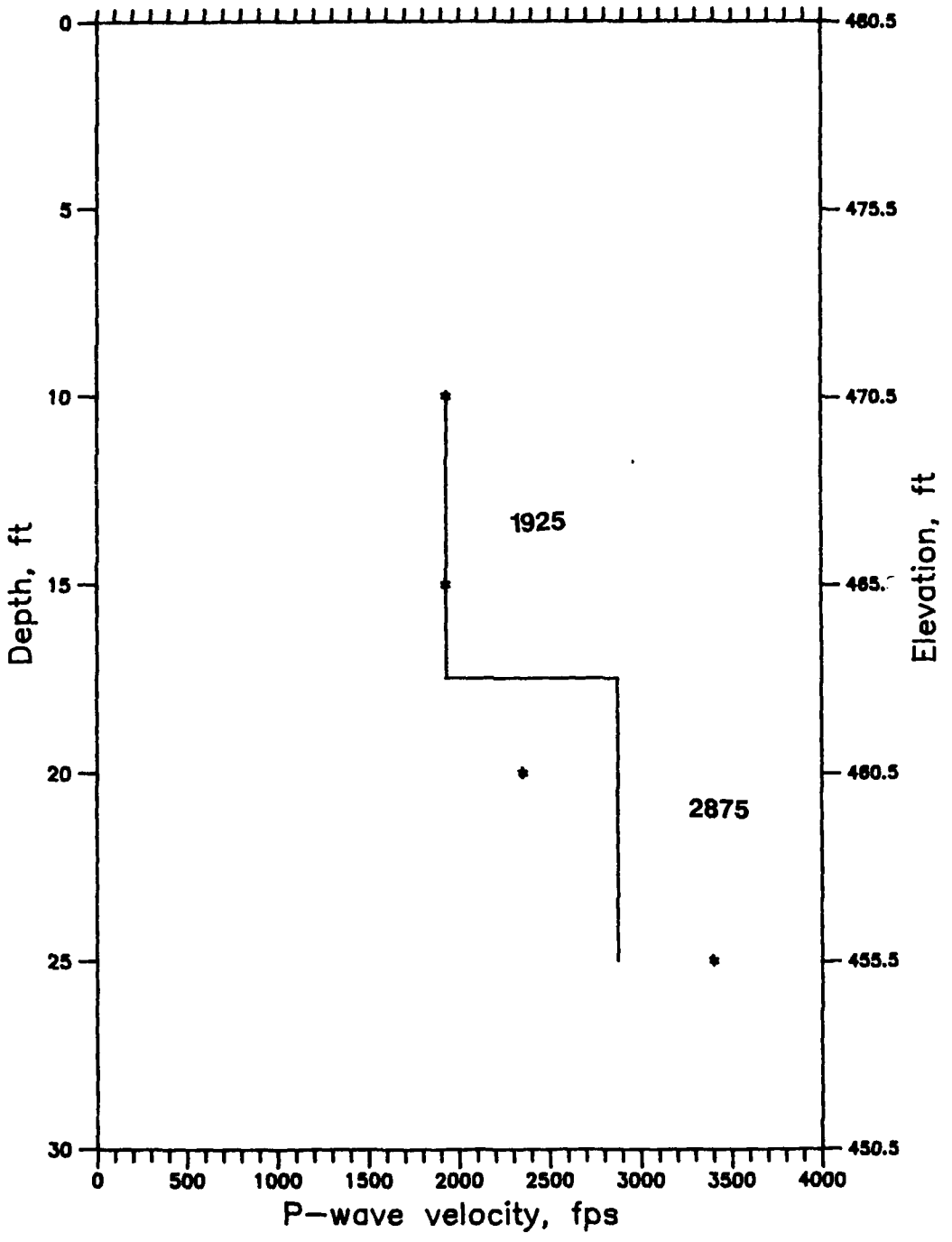

Figure 34. Crosshole P-wave results, downstream shoulder, Right Wing Dam, Station 235+00

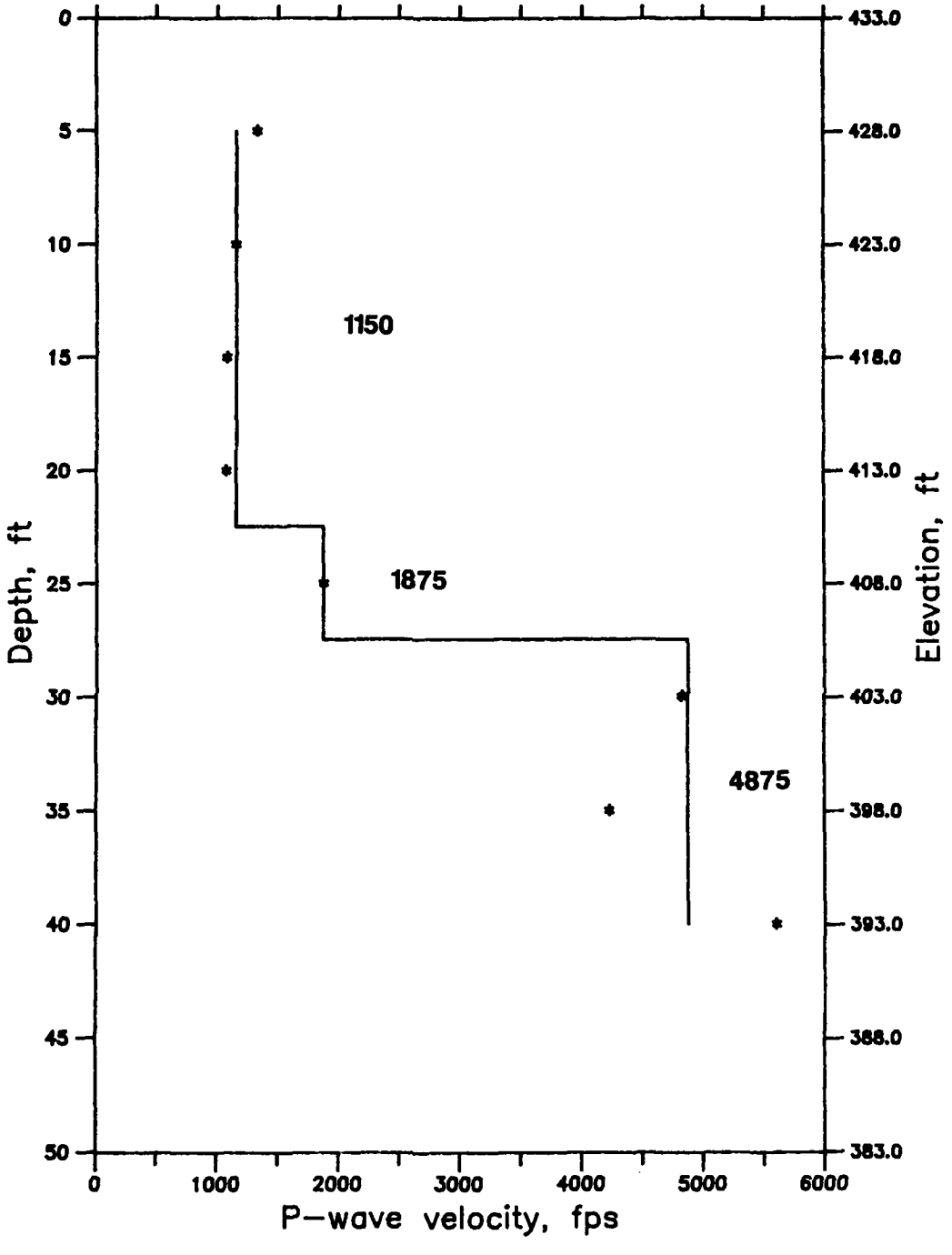

Figure 35. Crosshole P-wave results, downstream slope, Right Wing Dam, Station 235+00

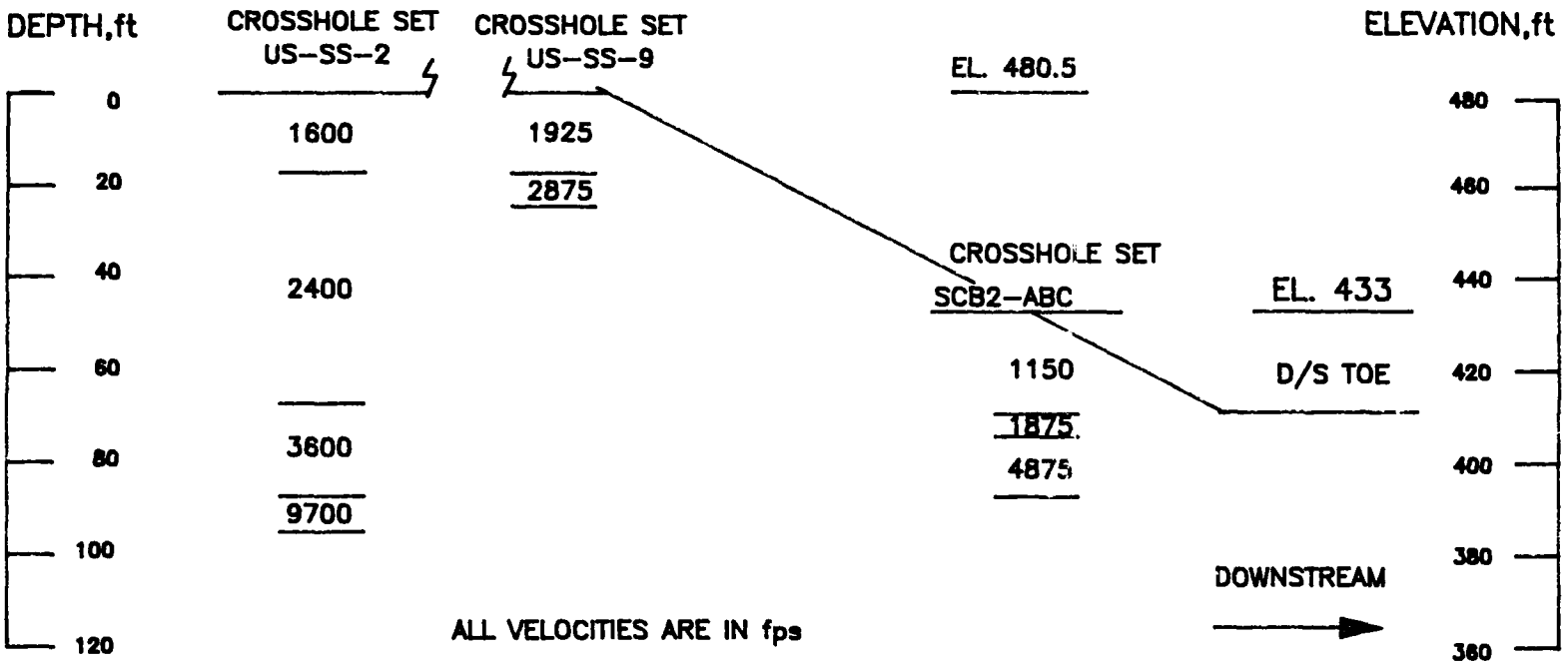

Figure 36. Interpreted P-wave profile from crosshole testing, Station 235+00

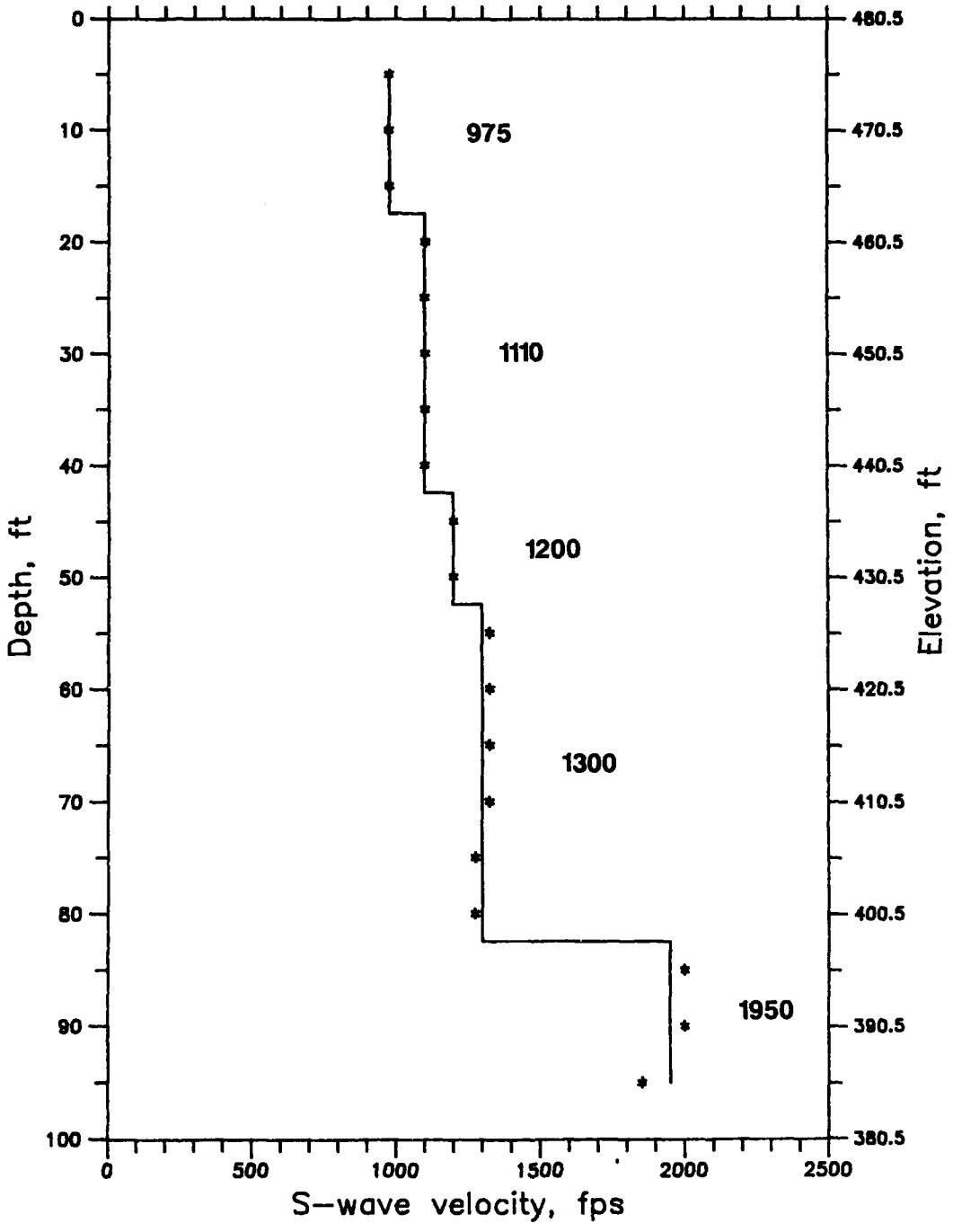

Figure 37. Crosshole S-wave results, centerline Right Wing Dam, Station 235+00

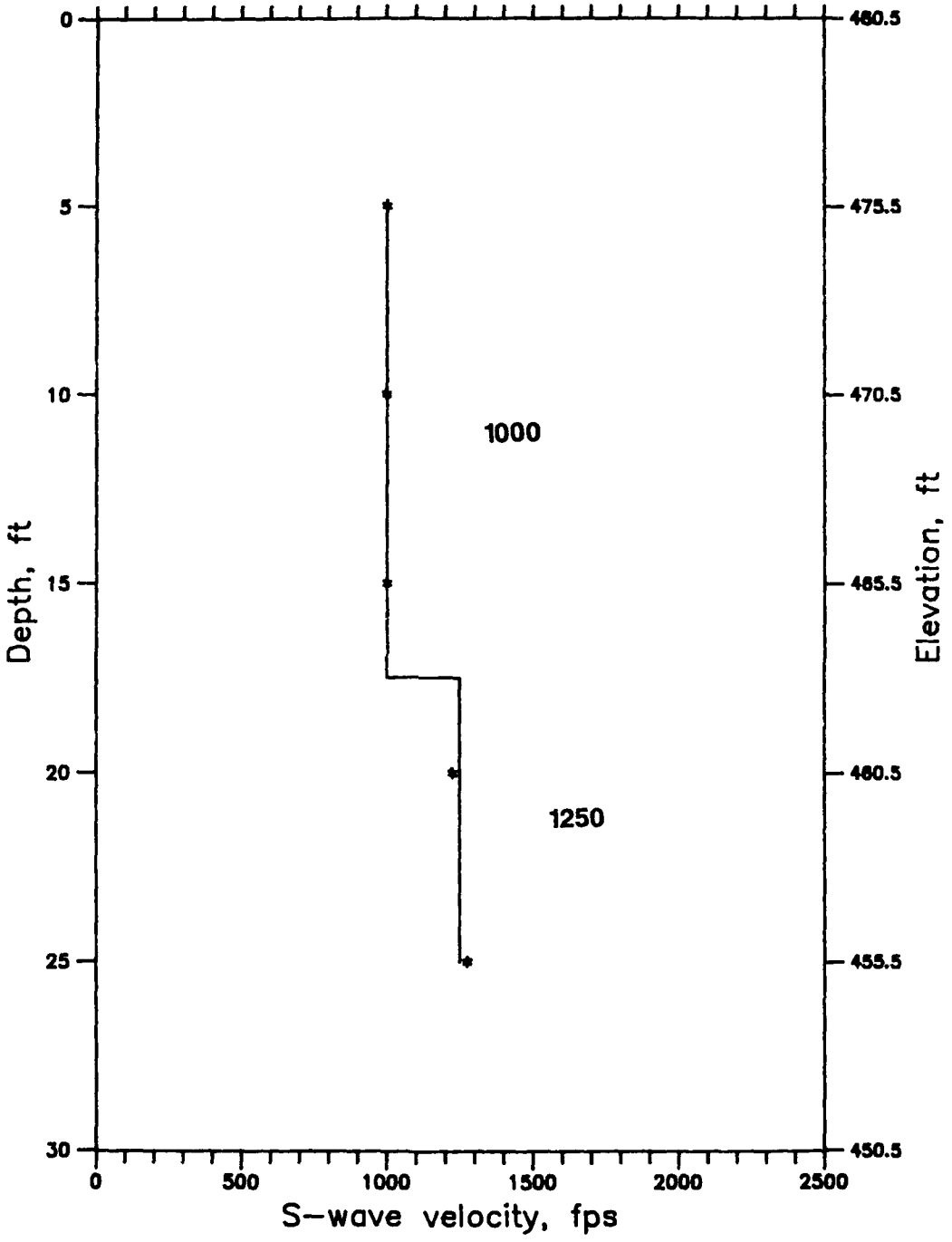

Figure 38. Crosshole S-wave results, downstream shoulder, Right Wing Dam, Station 235+00

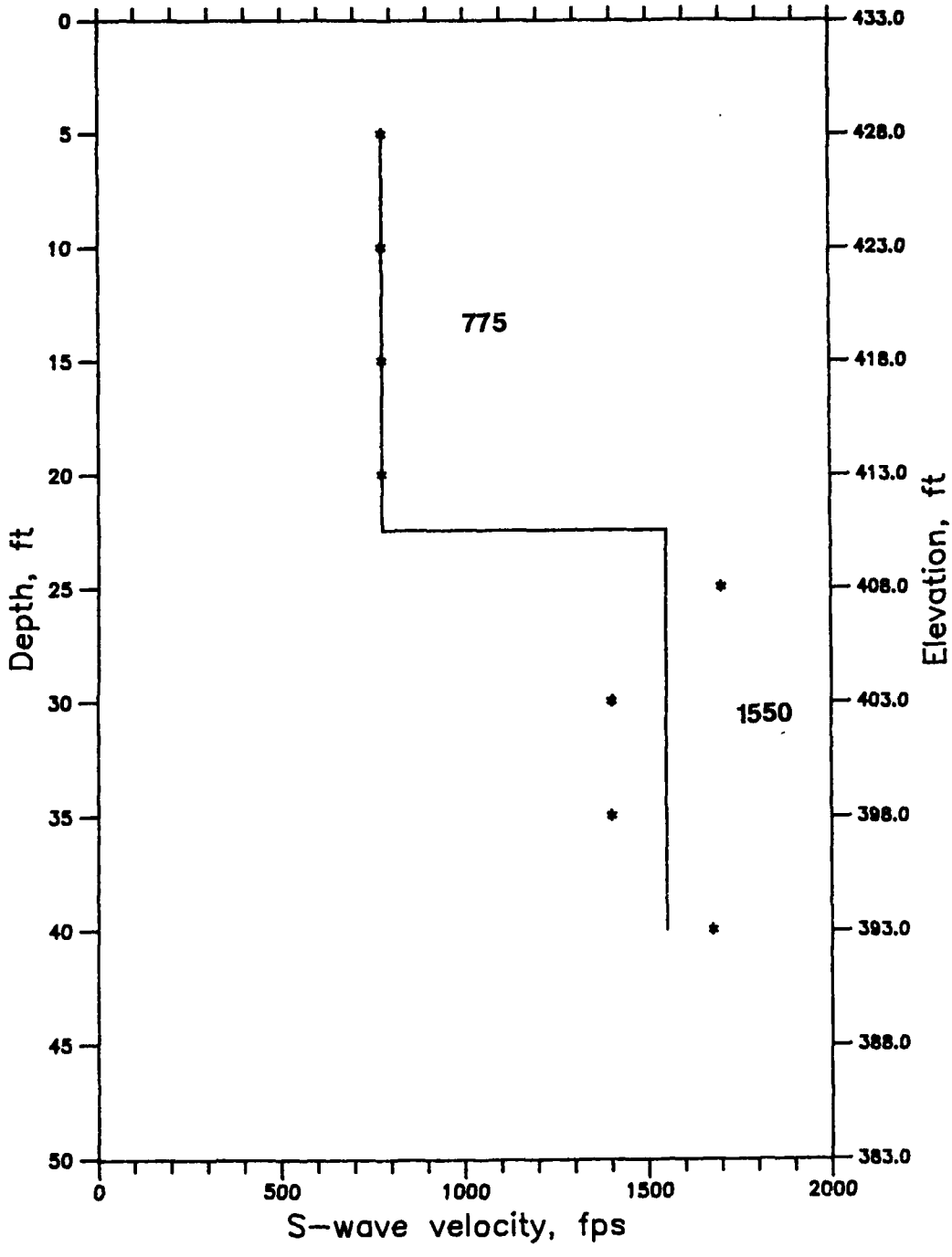

Figure 39. Crosshole S-wave results, downstream slope, Right Wing Dam, Station 235+00

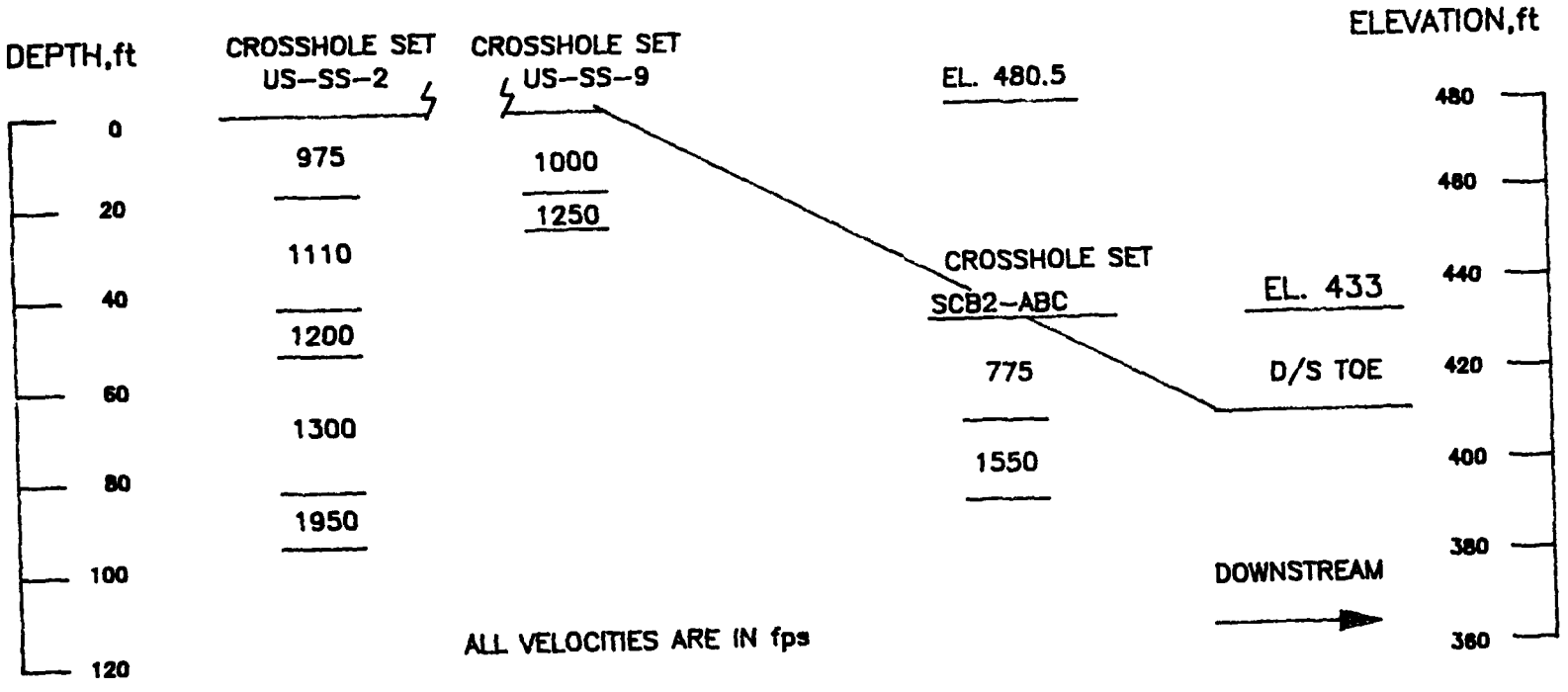

Figure 40. Interpreted S-wave profile from crosshole testing, Station 235+00

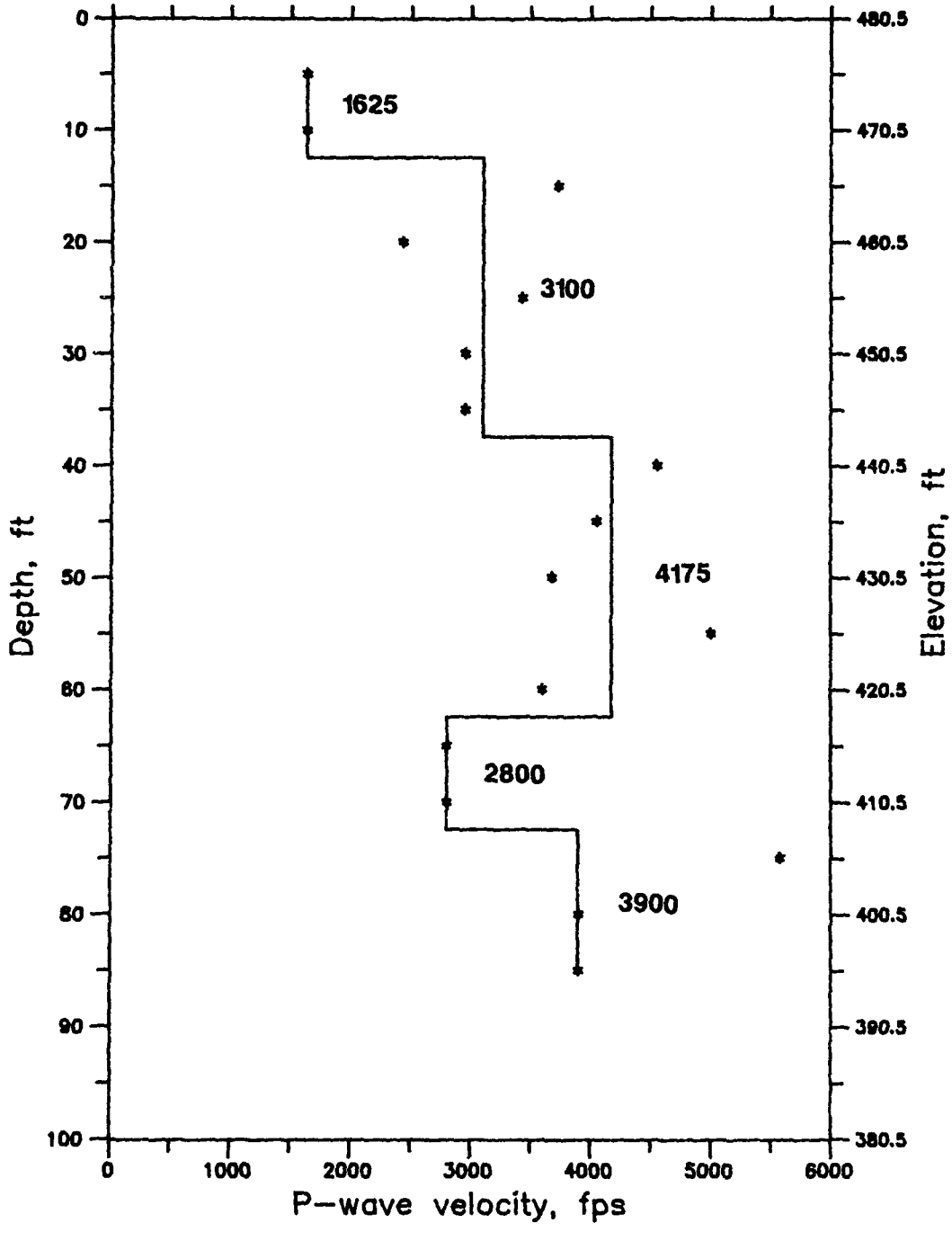

Figure 41. Crosshole P-wave results, centerline Right Wing Dam, Station 269+50

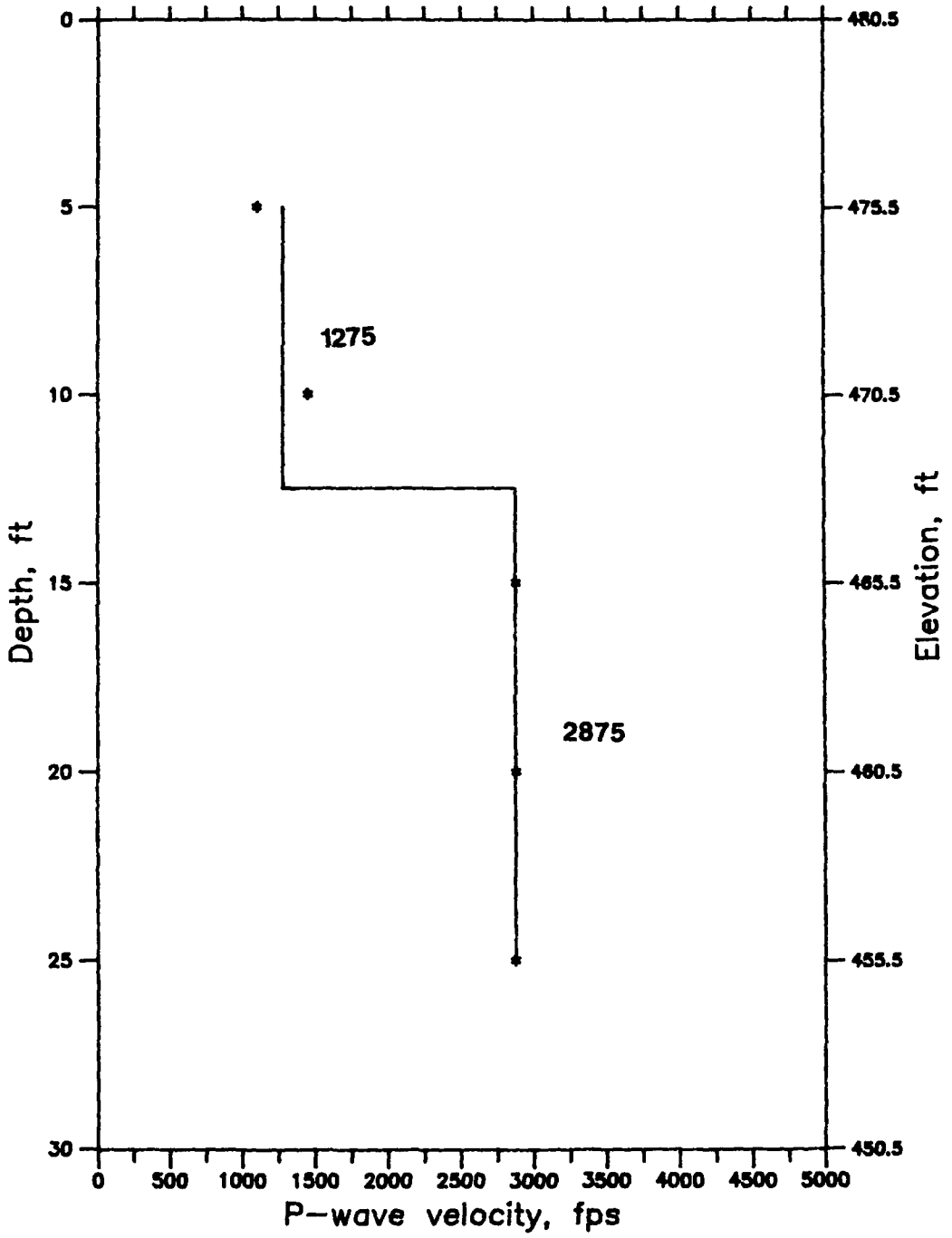

Figure 42. Crosshole P-wave results, downstream shoulder, Right Wing Dam, Station 269+50

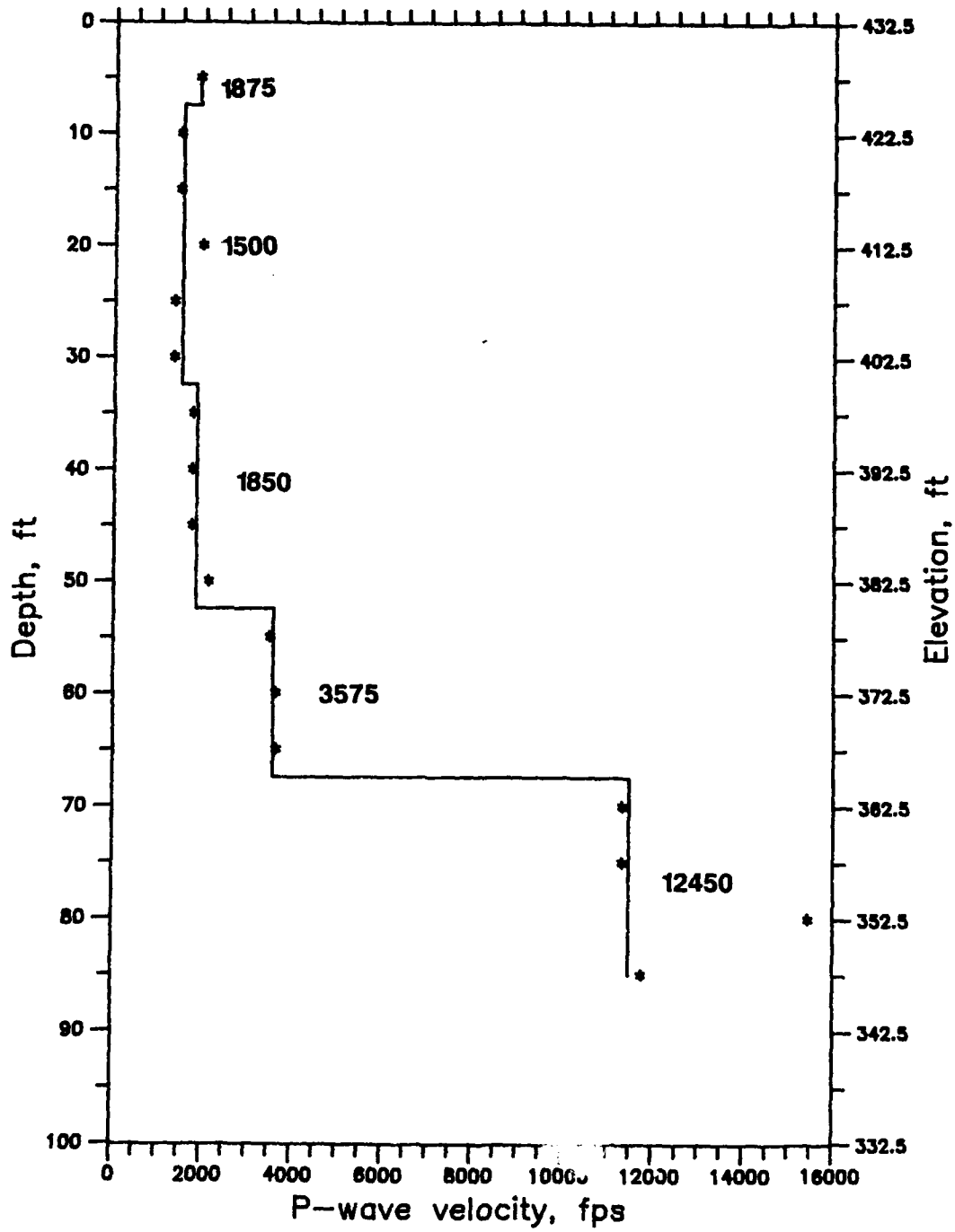

Figure 43. Crosshole P-wave results, downstream slope, Right Wing Dam, Station 269+50

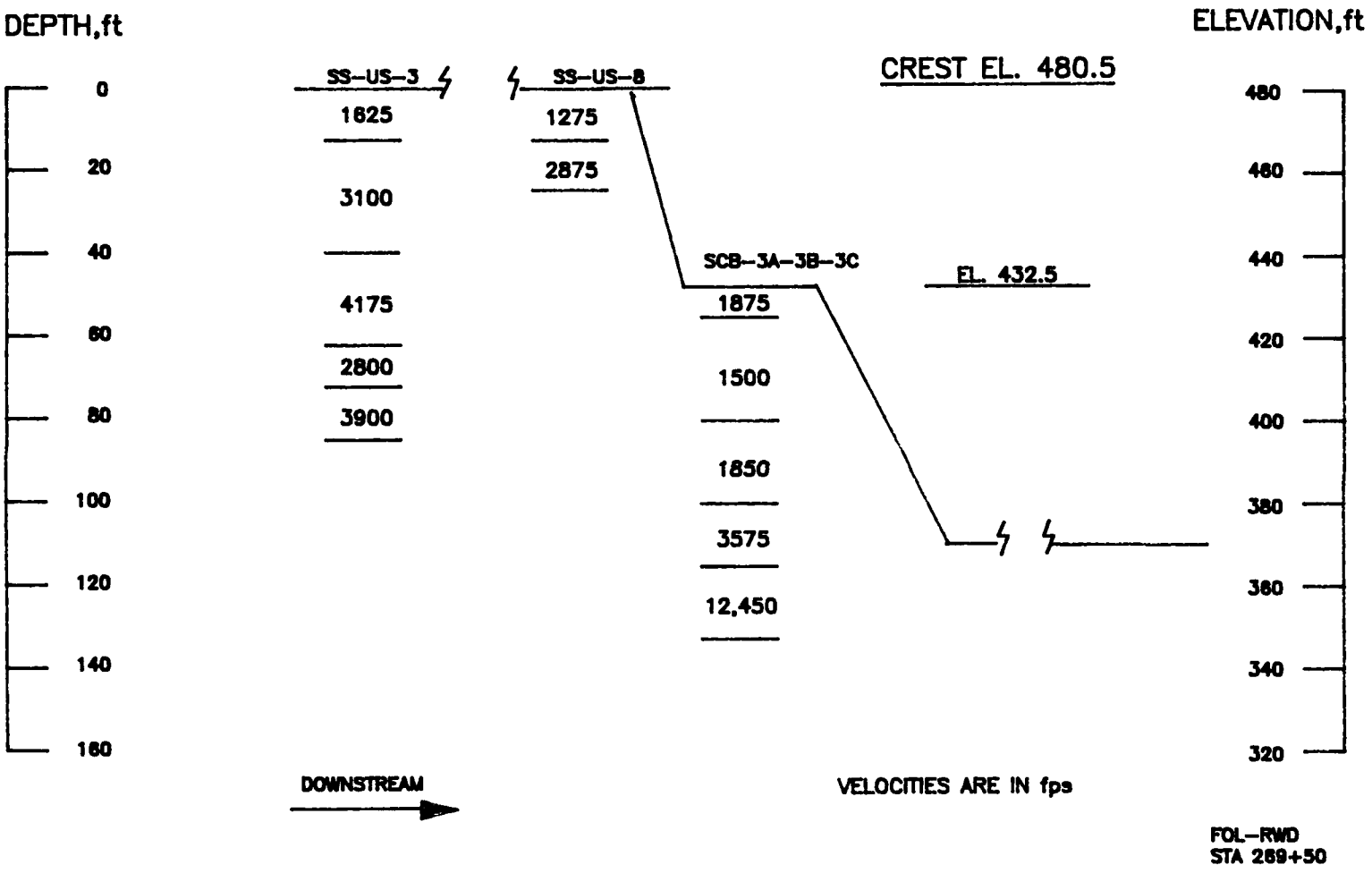

Figure 44. Interpreted P-wave profile from crosshole testing, Station 269+50

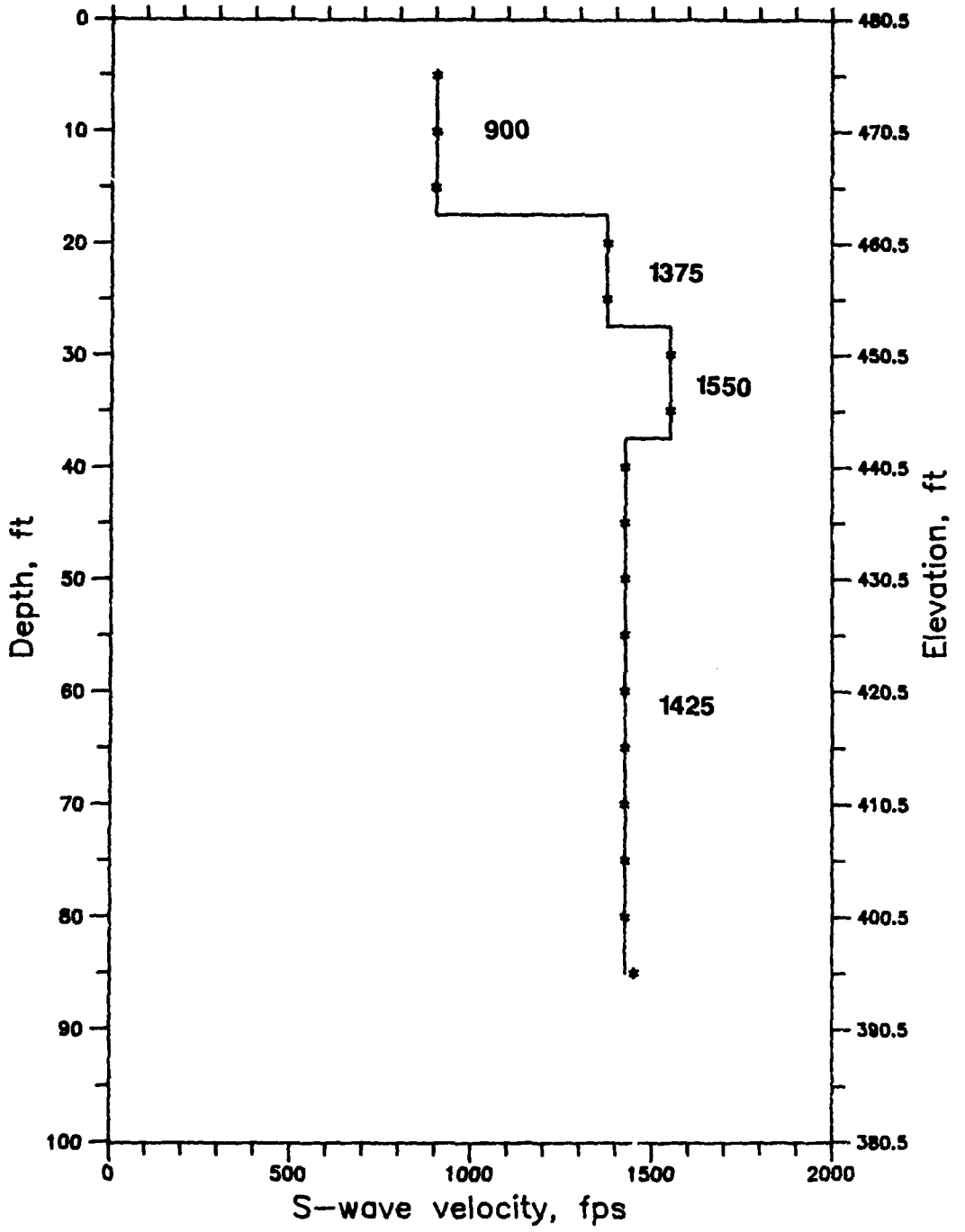

Figure 45. Crosshole S-wave results, centerline Right Wing Dam, Station 269+50

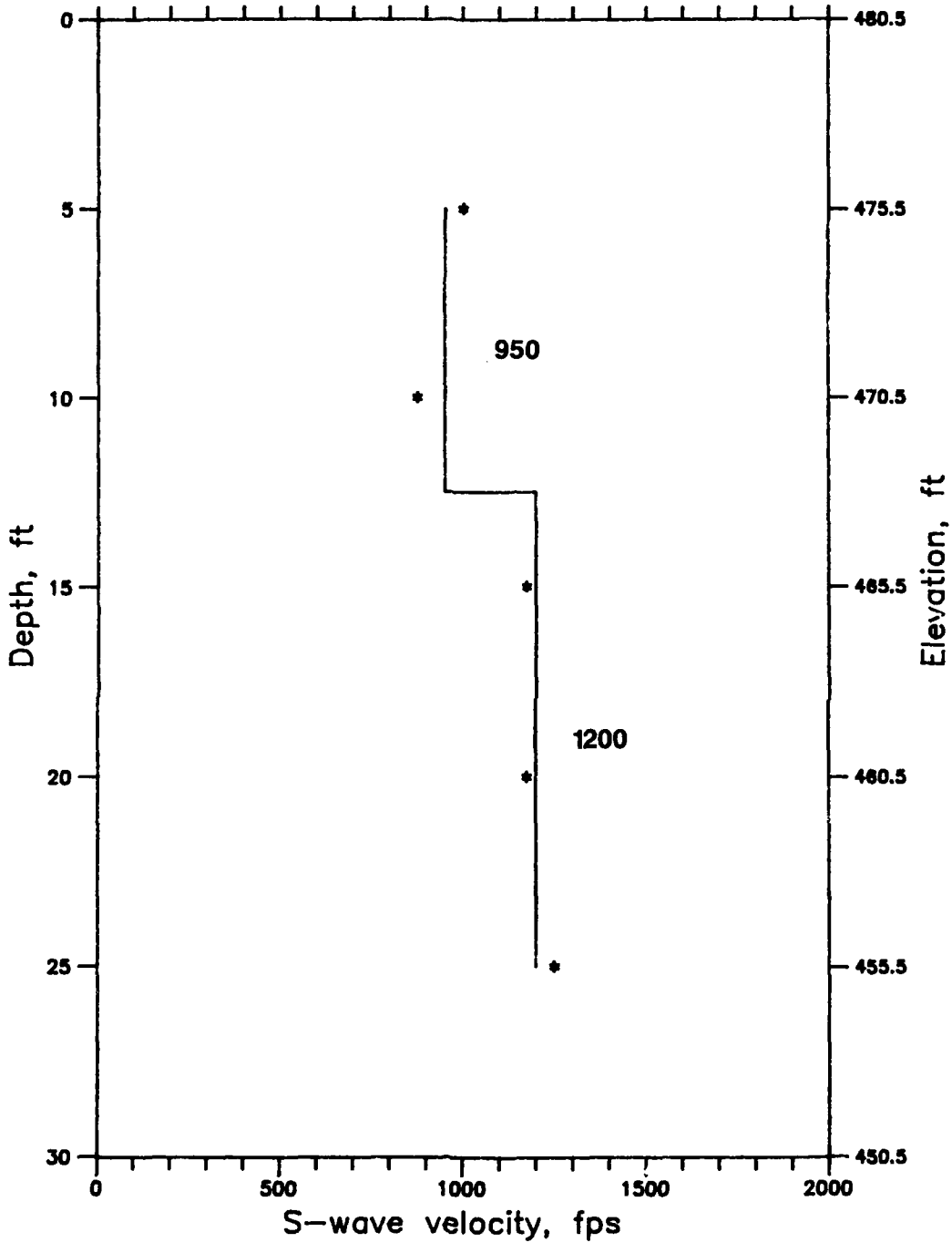

Figure 46. Crosshole S-wave results, downstream shoulder, Right Wing Dam, Station 269+50

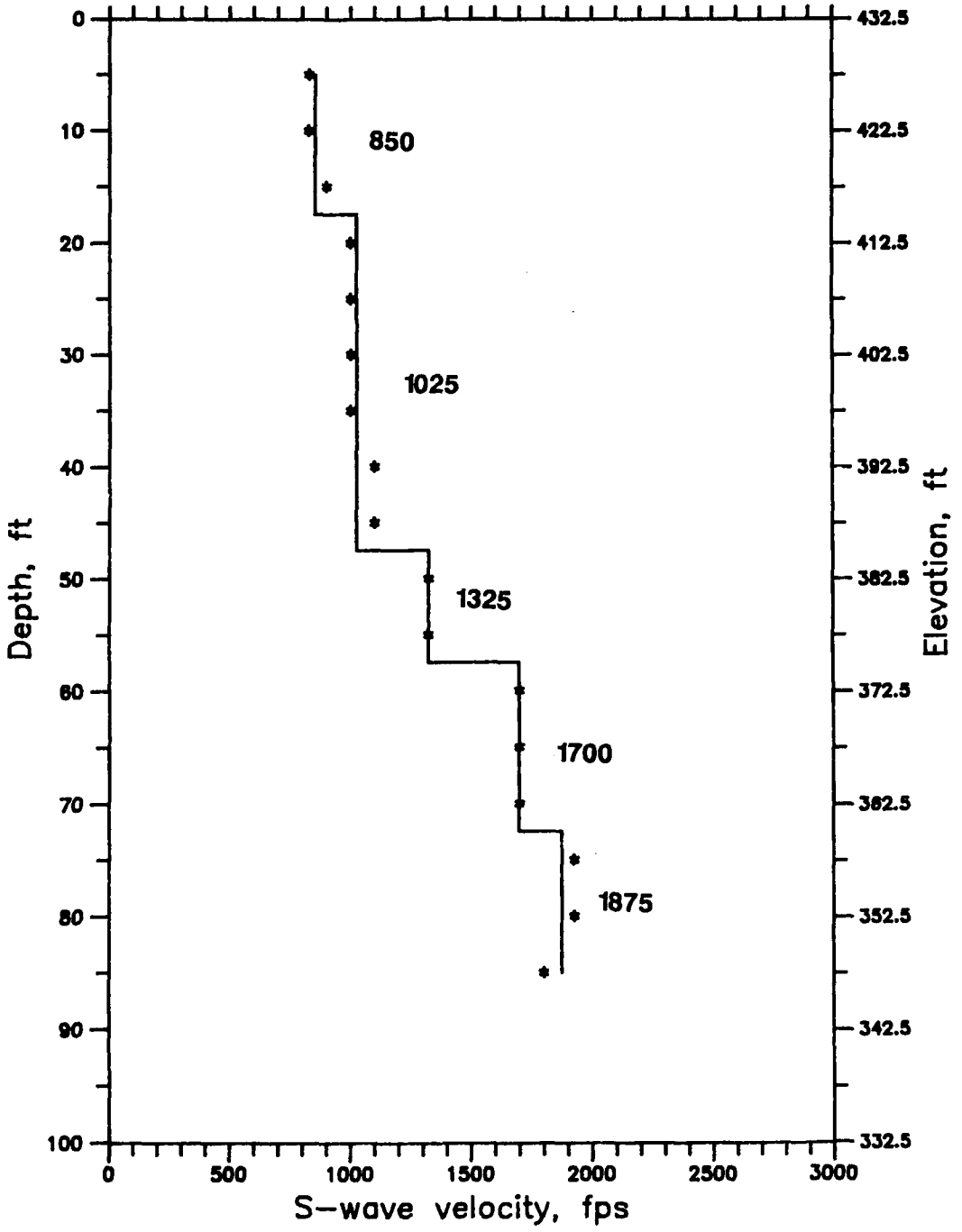

Figure 47. Crosshole S-wave results, downstream slope, Right Wing Dam, Station 269+50

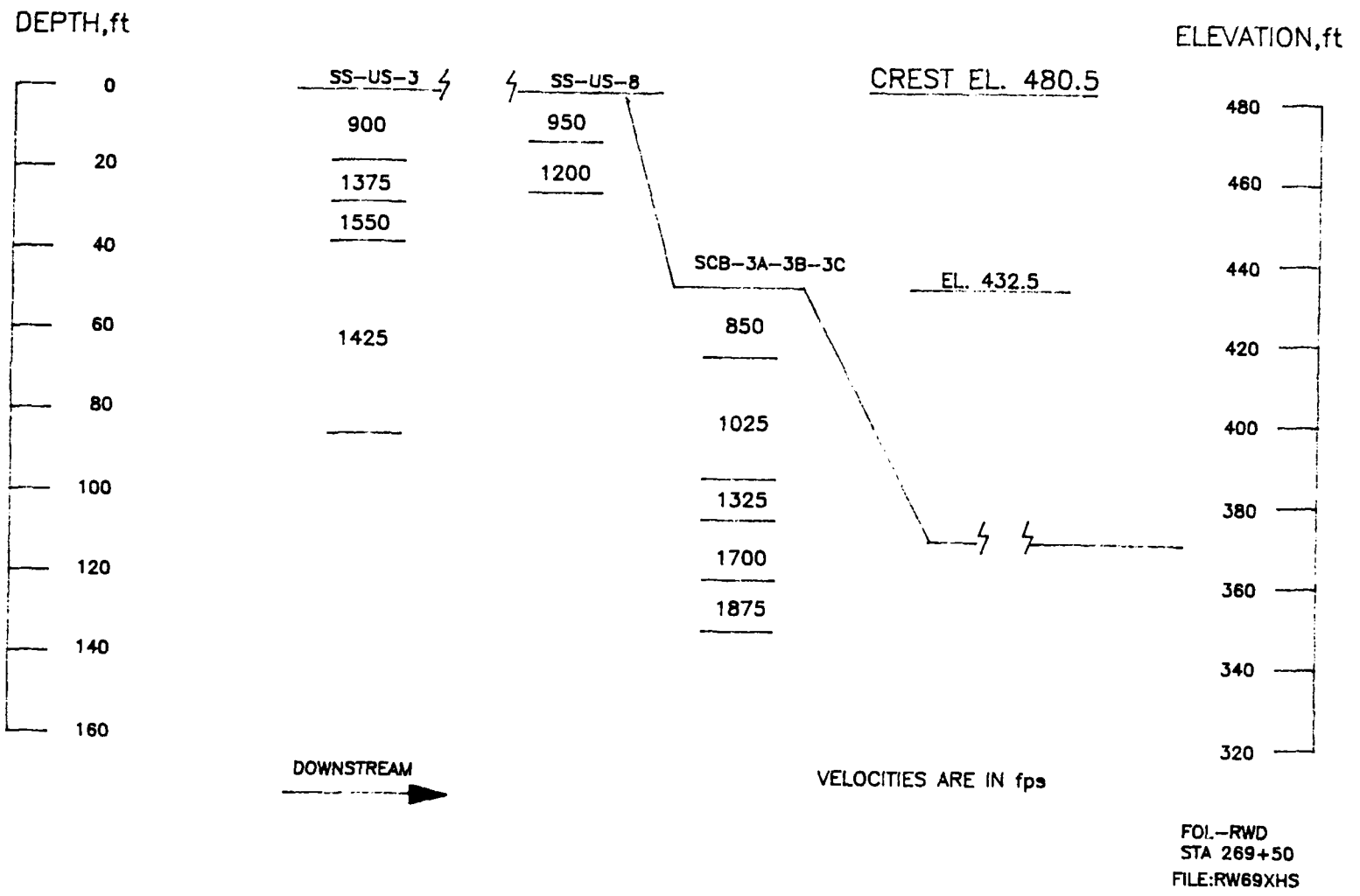

Figure 48. Interpreted S-wave profile from crosshole testing, Station 269+50

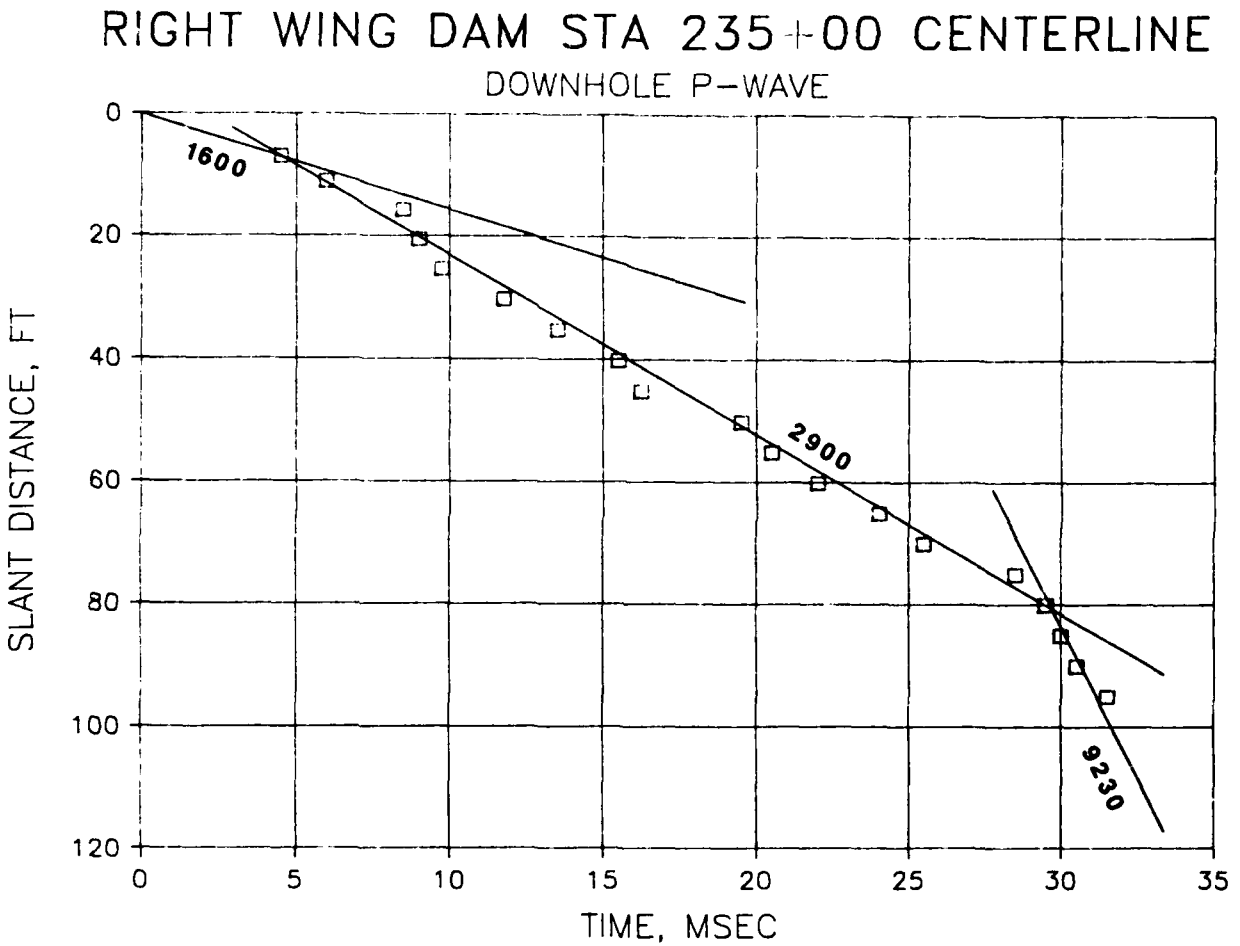

Figure 49. Downhole P-wave results, centerline Right Wing Dam Station 235+00

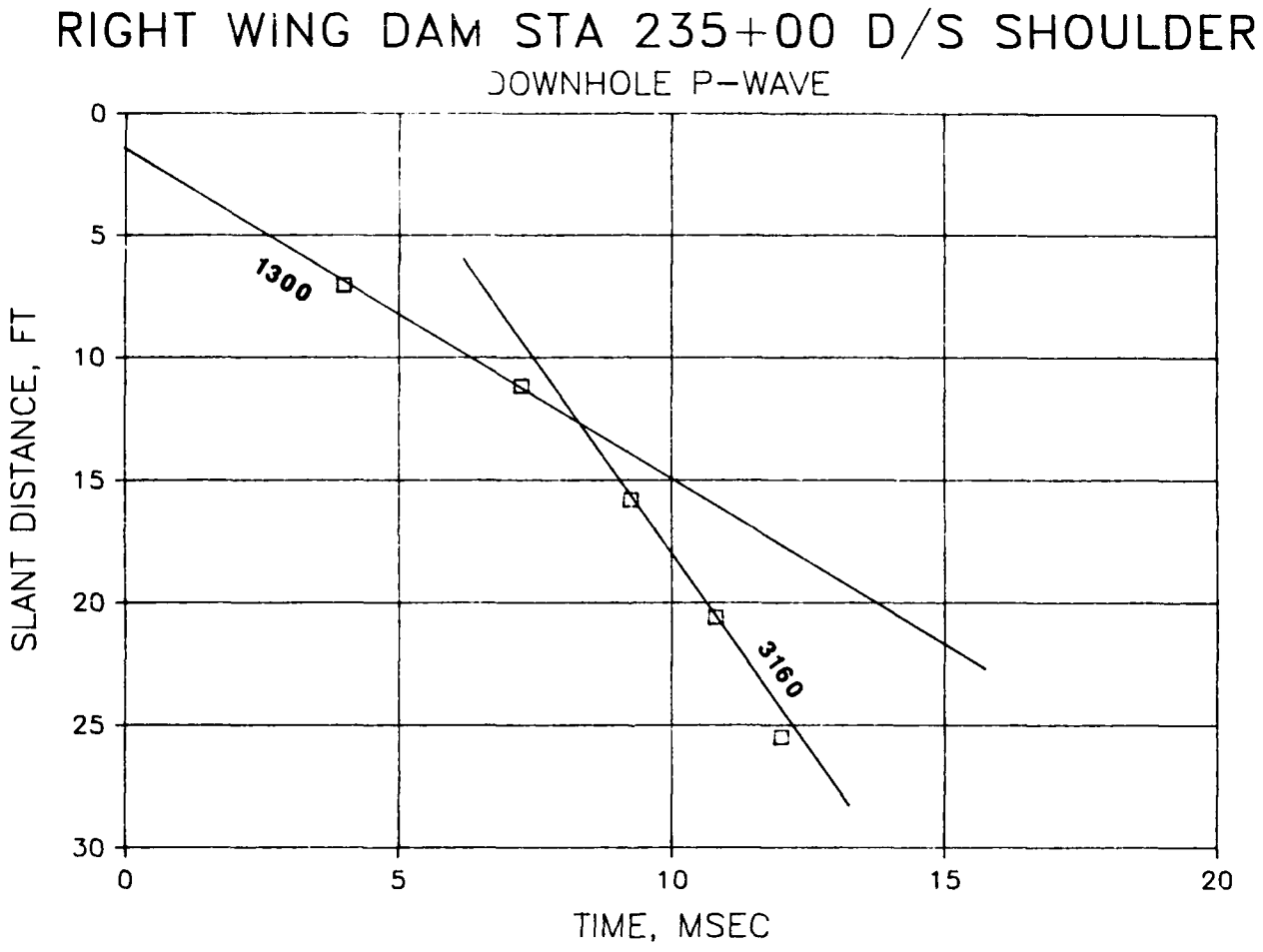

Figure 50. Downhole P-wave results, downstream shoulder Right Wing Dam Station 235+00

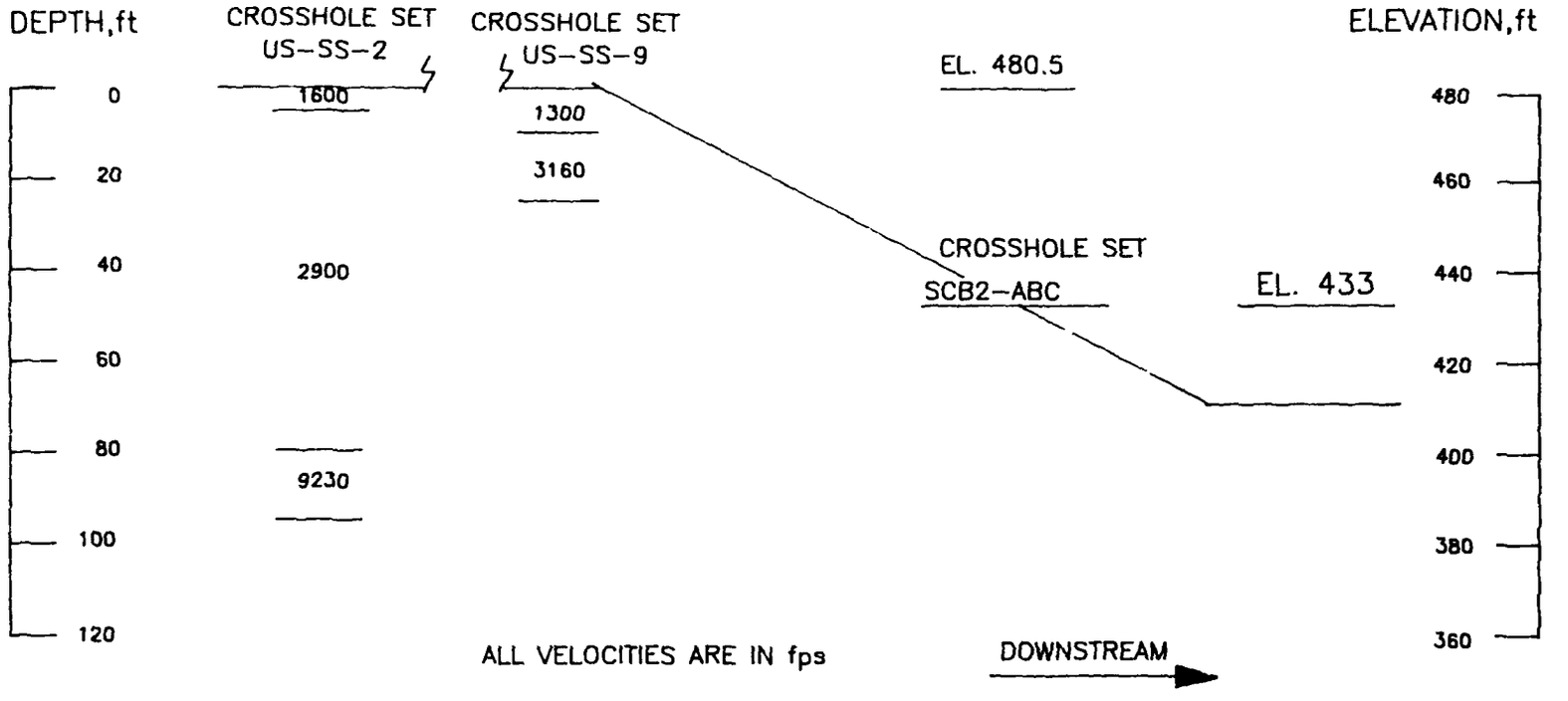

Figure 51. Interpreted P-wave profile from downhole testing, Right Wing Dam Station 235+00

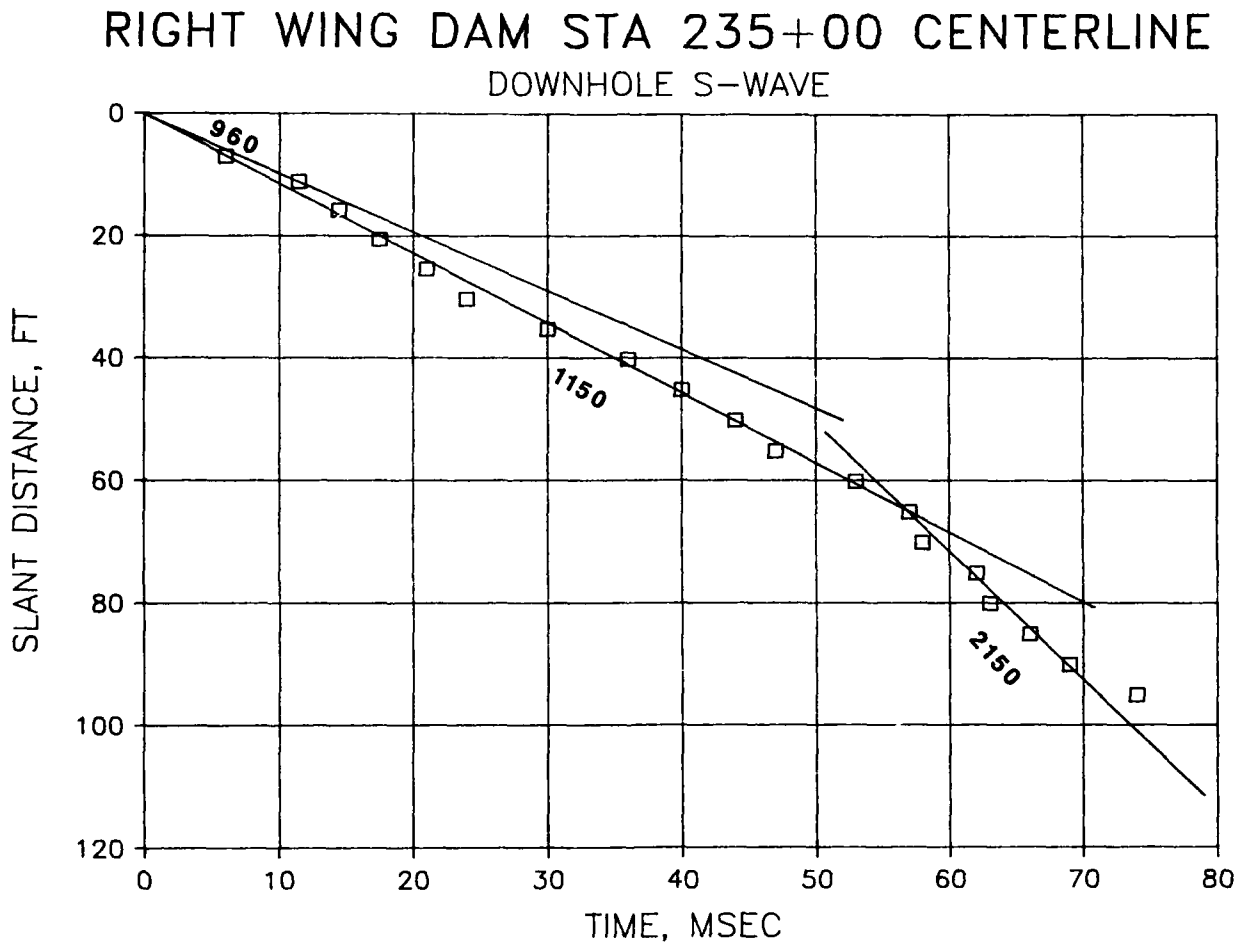

Figure 52. Downhole S-wave results, centerline Right Wing Dam Station 235+00

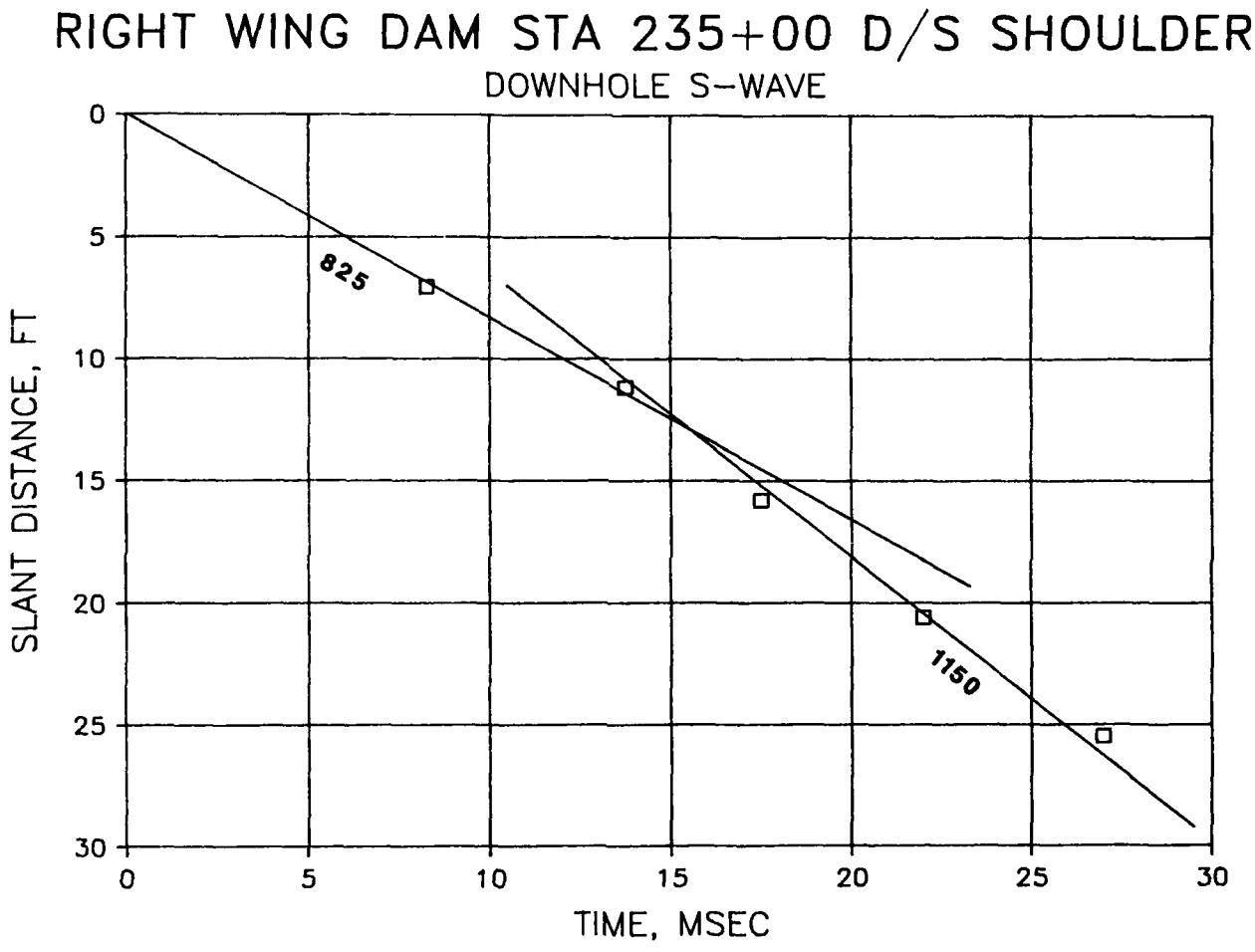

Figure 53. Downhole S-wave results, downstream shoulder Right Wing Dam Station 235+00

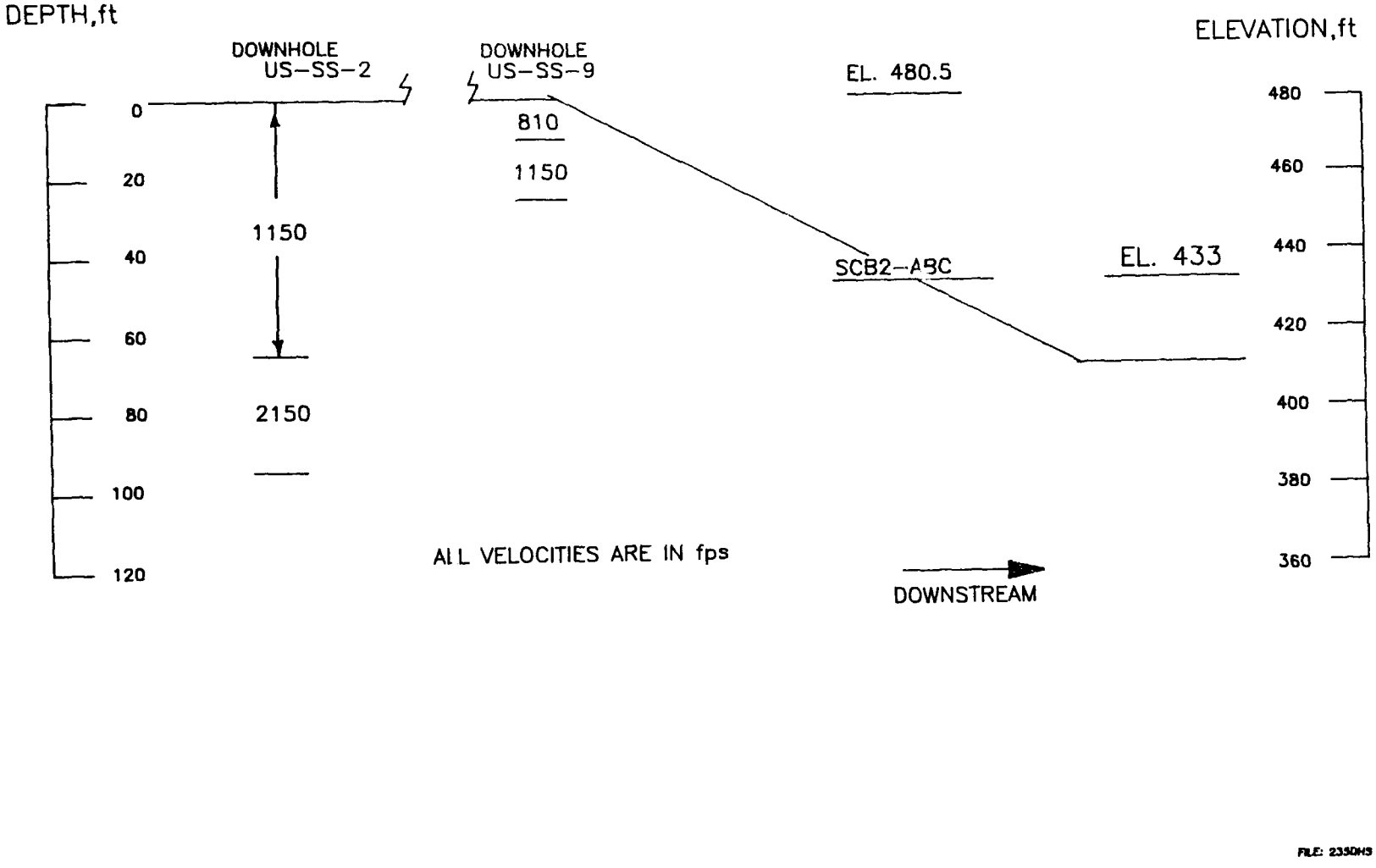

Figure 54. Interpreted S-wave profile from downhole testing, Right Wing Dam Station 235+00

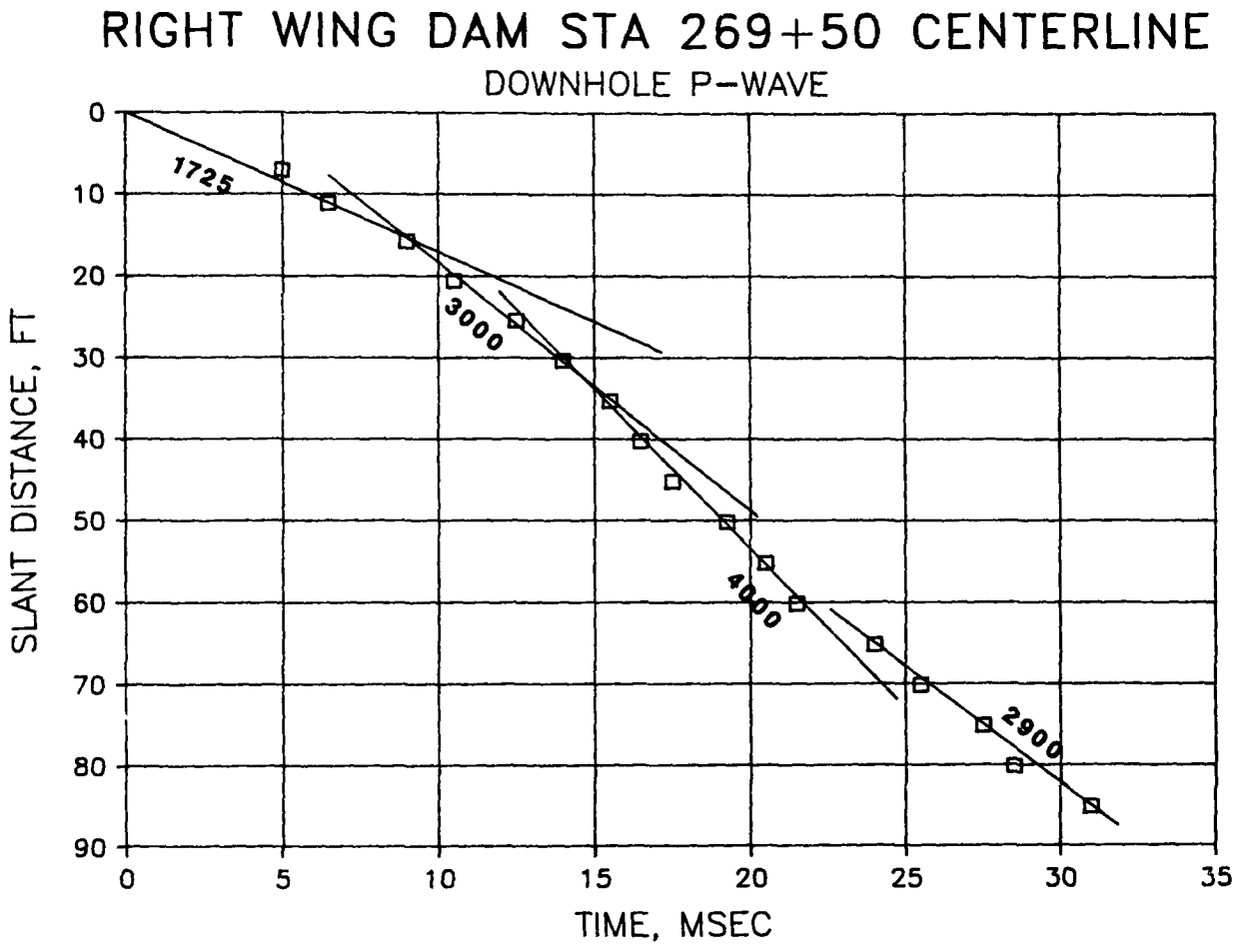

Figure 55. Downhole P-wave results, centerline Right Wing Dam Station 269+50

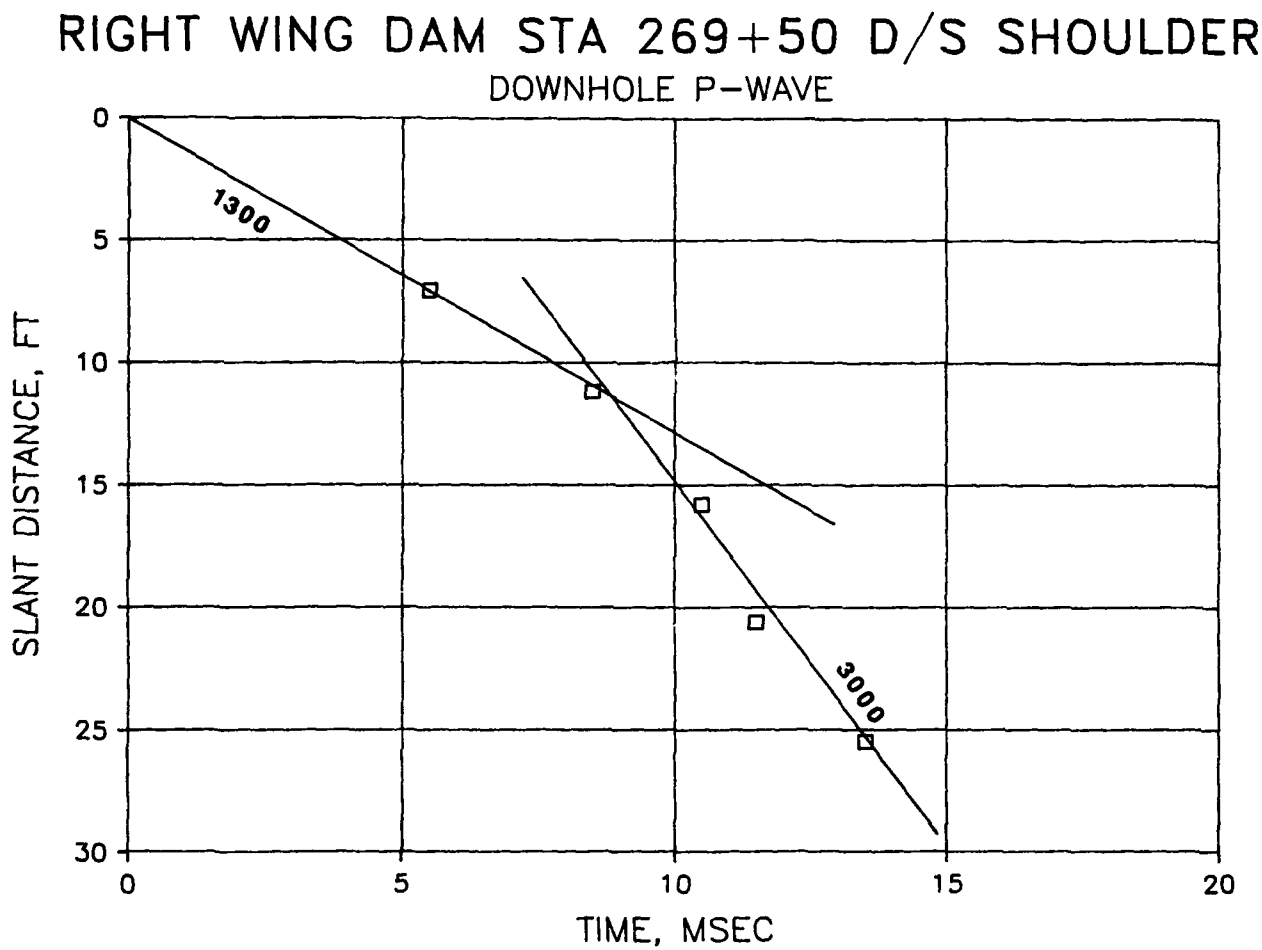

Figure 56. Downhole P-wave results, downstream shoulder
Right Wing Dam Station 269+50

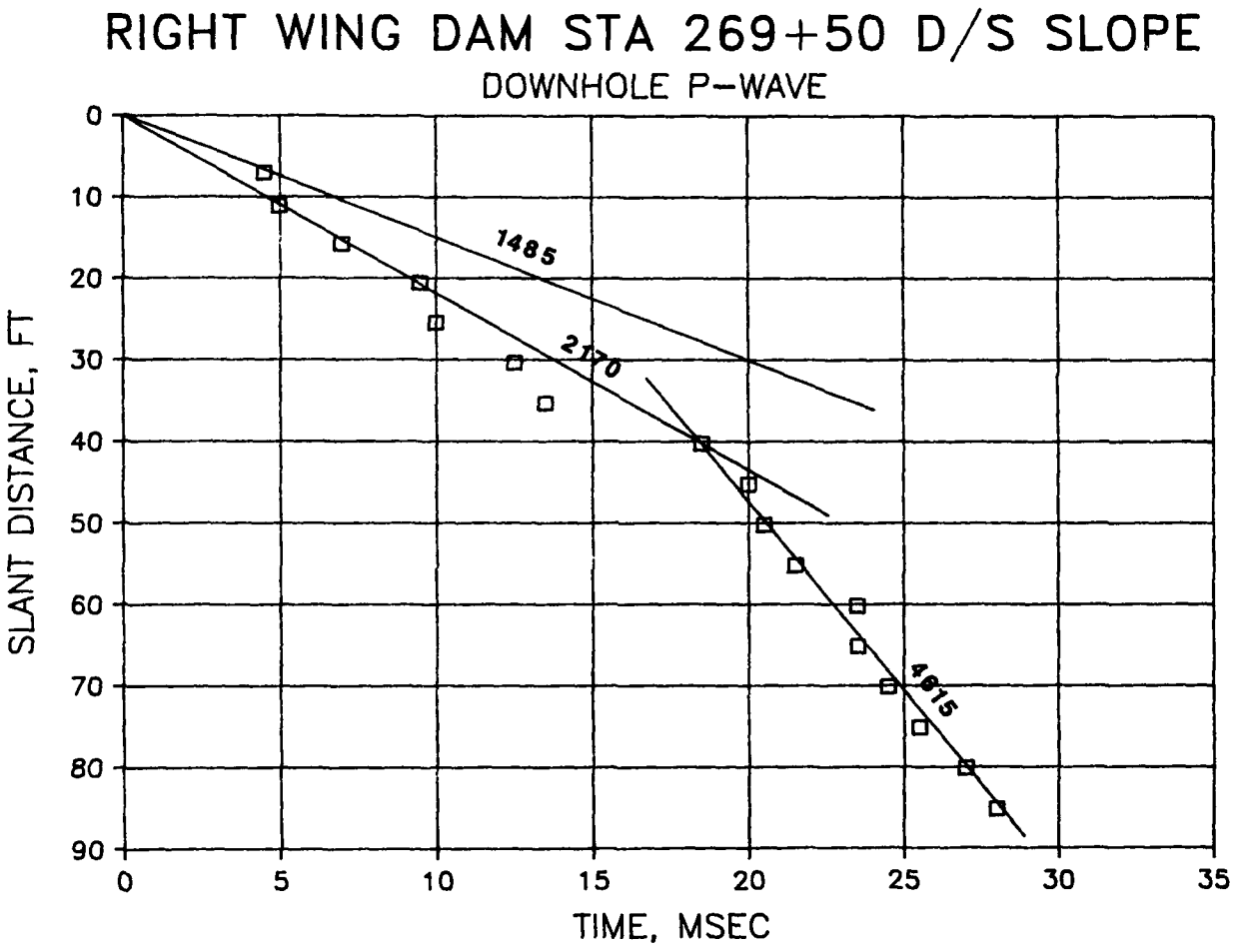

Figure 57. Downhole P-wave results, downstream slope Right Wing Dam Station 269+50

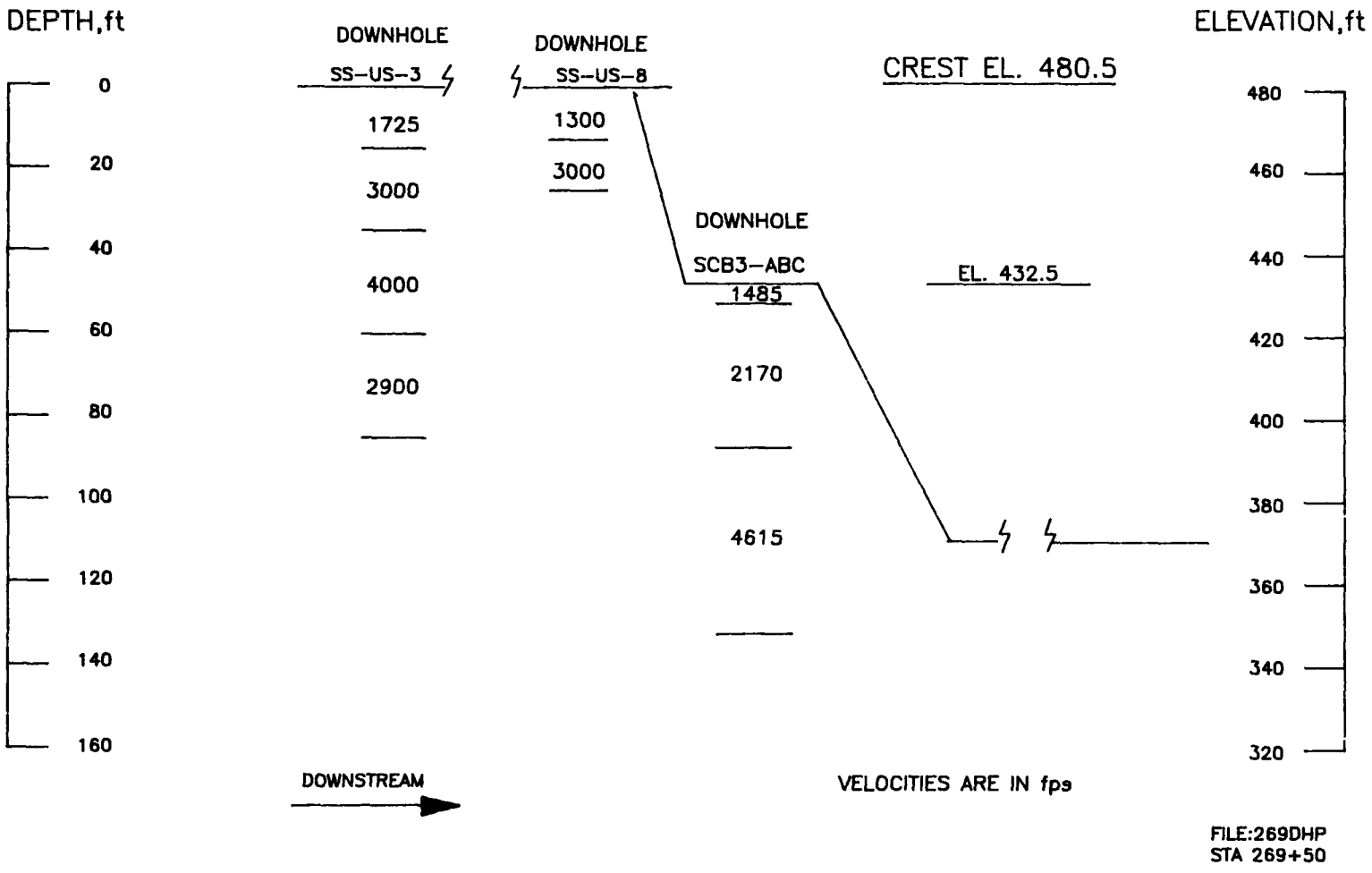

Figure 58. Interpreted P-wave profile from downhole testing, Right Wing Dam Station 269+50

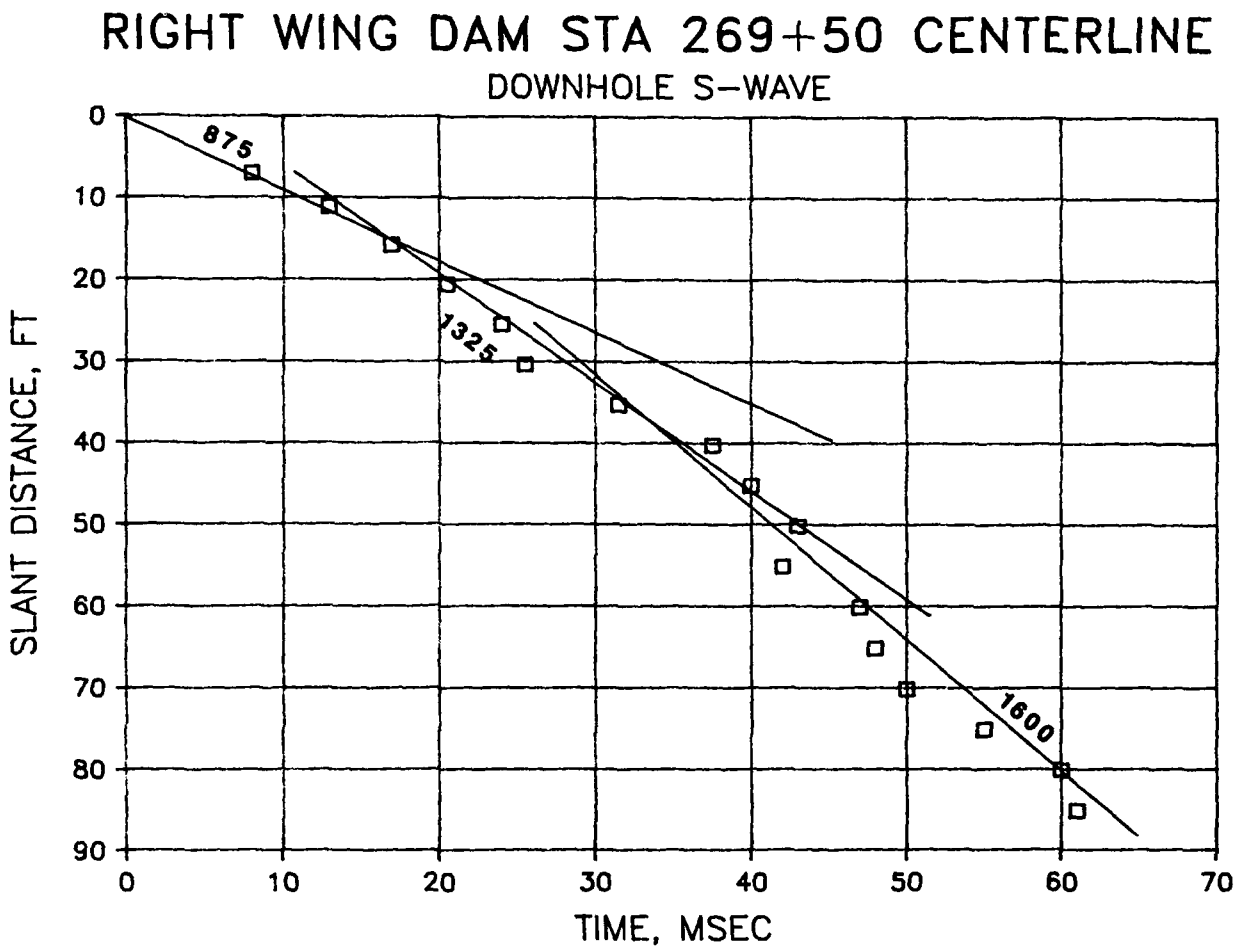

Figure 59. Downhole S-wave results, centerline Right Wing Dam Station 269+50

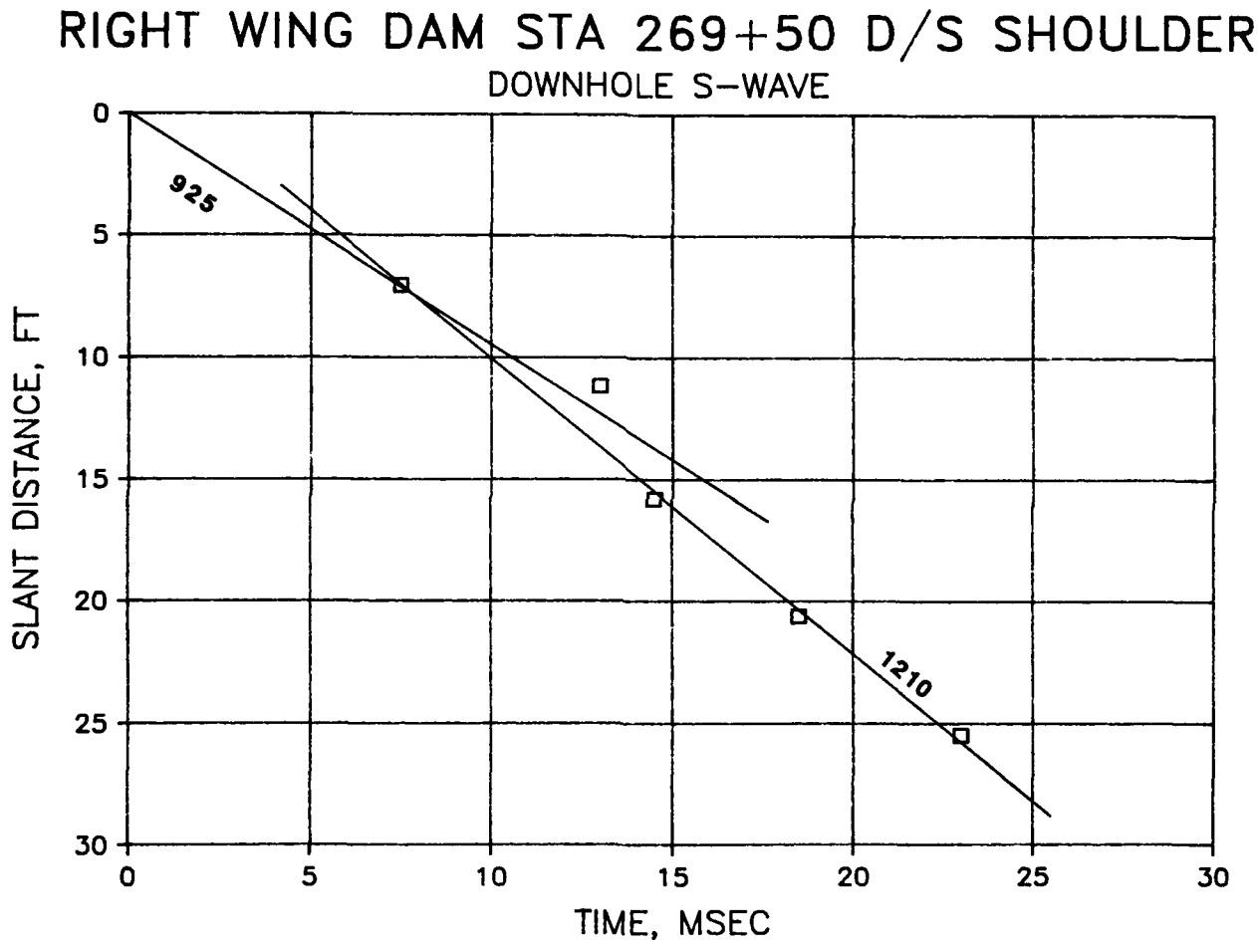

Figure 60. Downhole S-wave results, downstream shoulder
Right Wing Dam Station 269+50

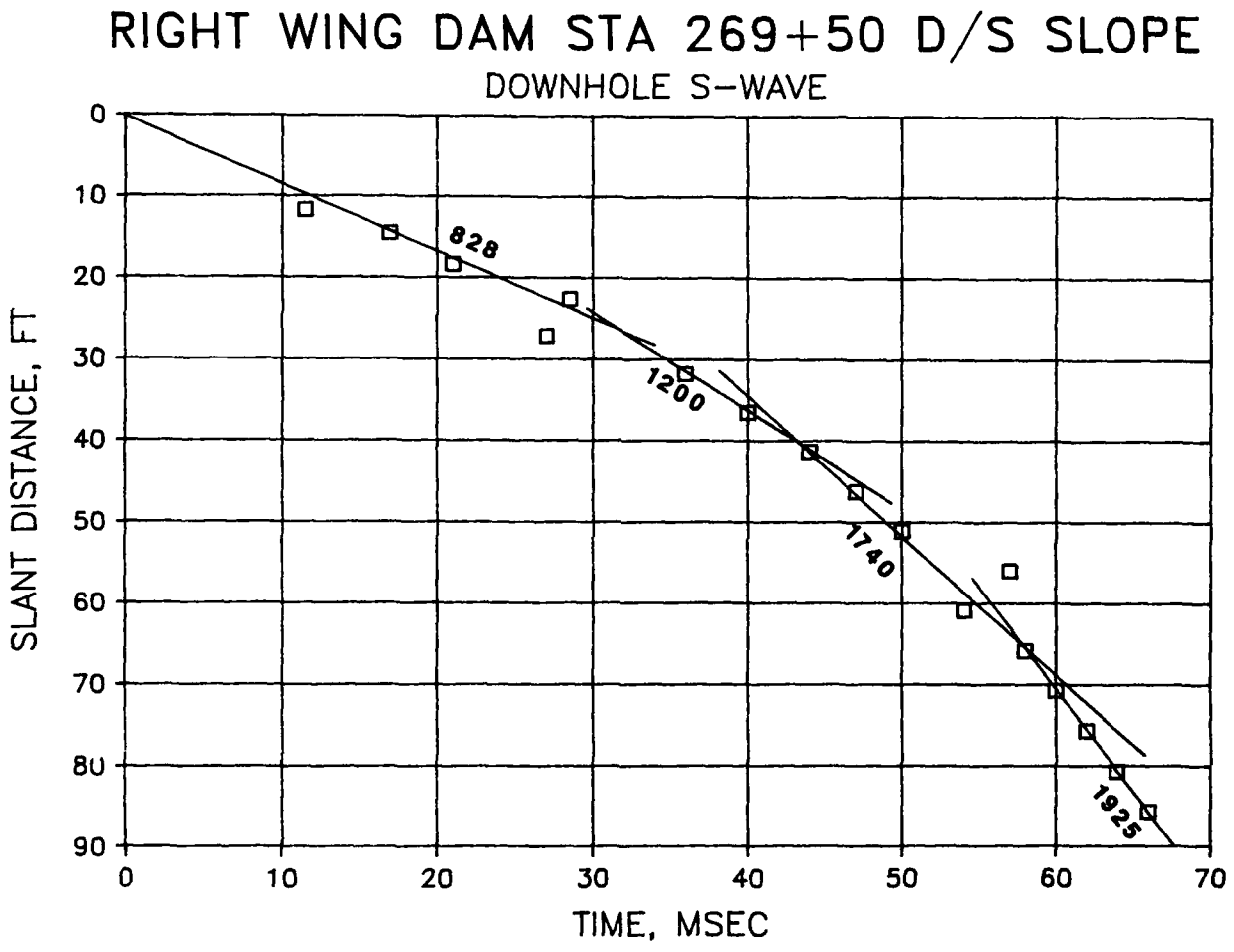

Figure 61. Downhole S-wave results, downstream slope
Right Wing Dam Station 269+50

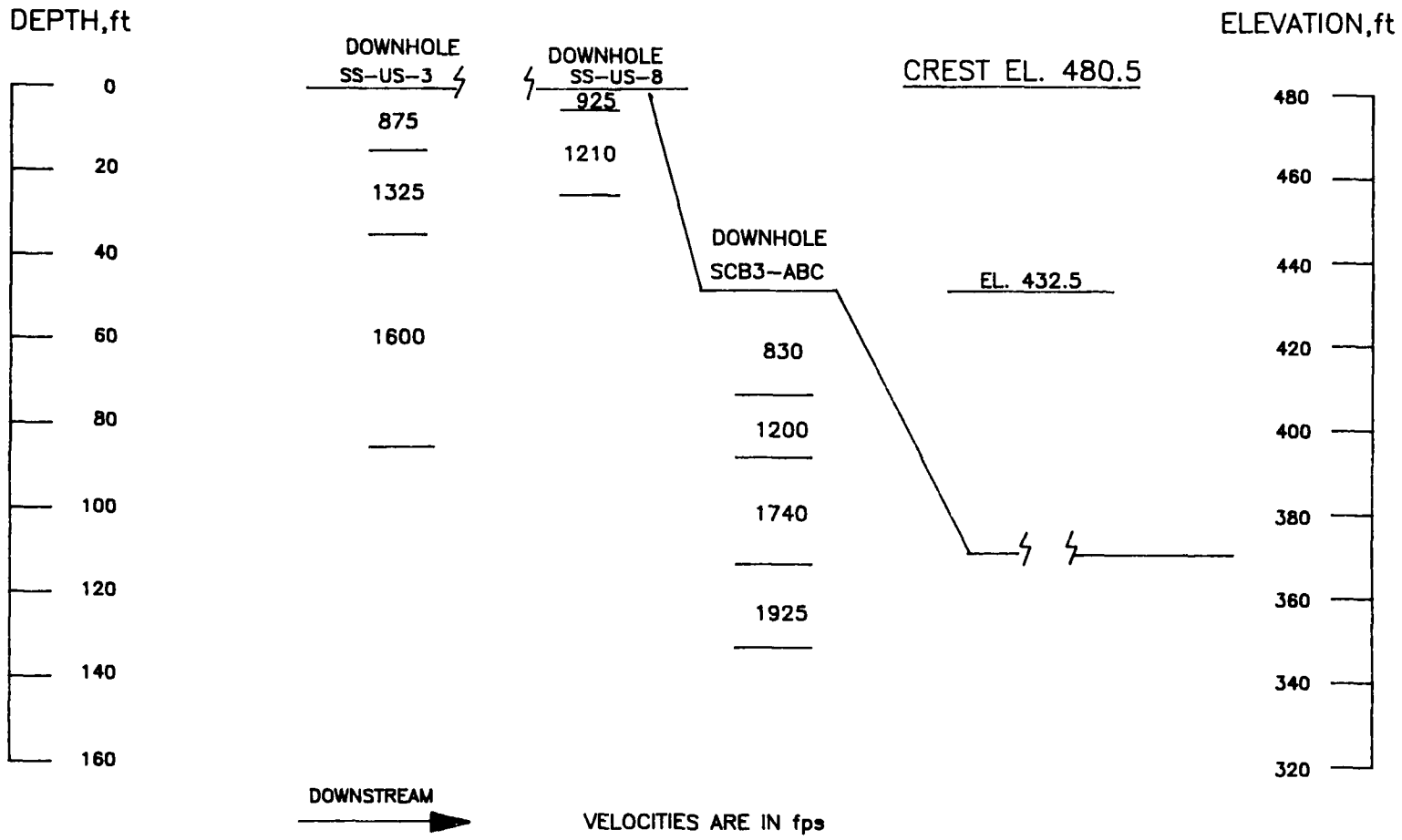

Figure 62. Interpreted S-wave profile from downhole testing, Right Wing Dam Station 269+50

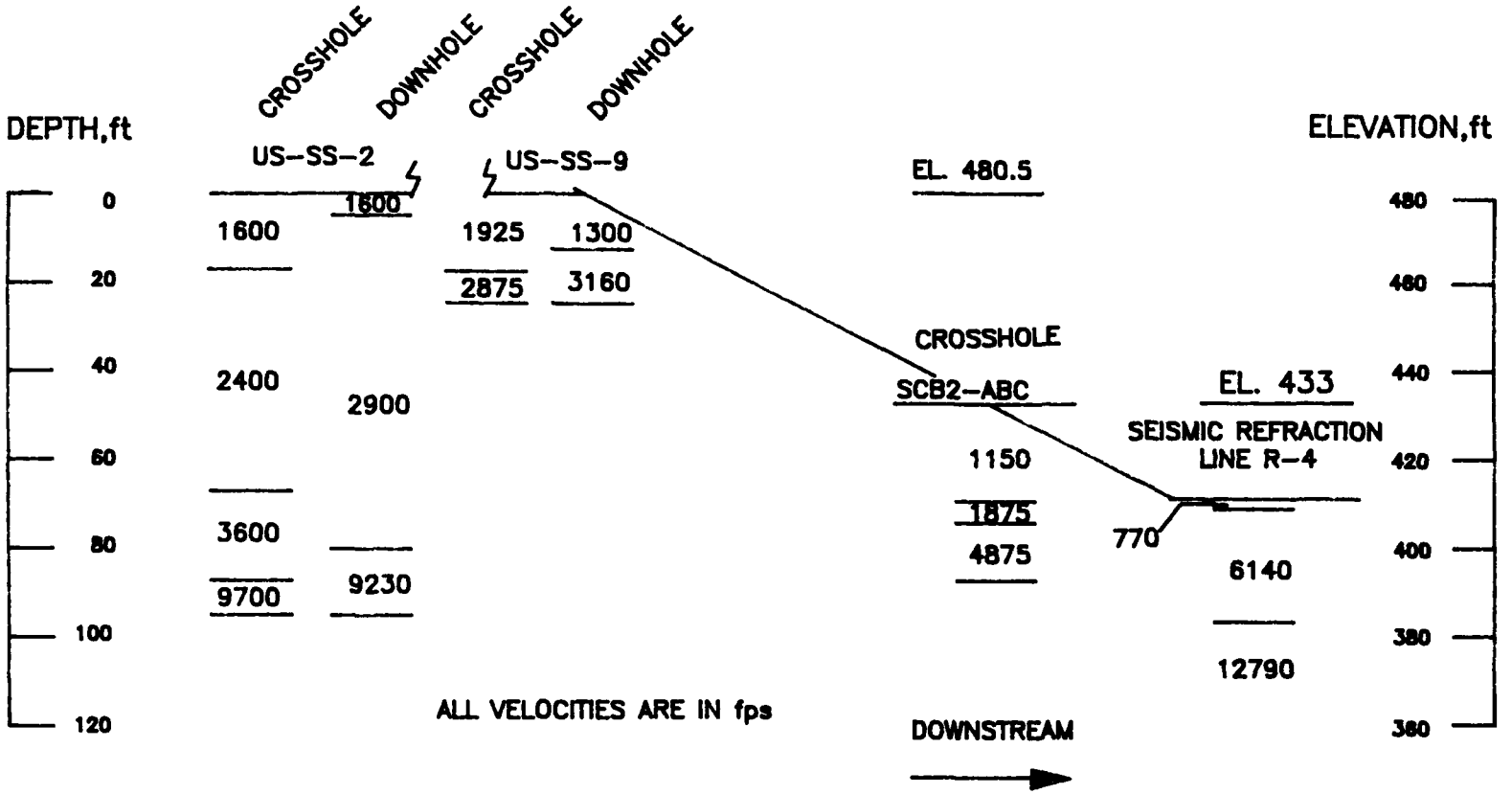

Figure 63. P-wave composite for cross section through Station 235+00 Right Wing Dam

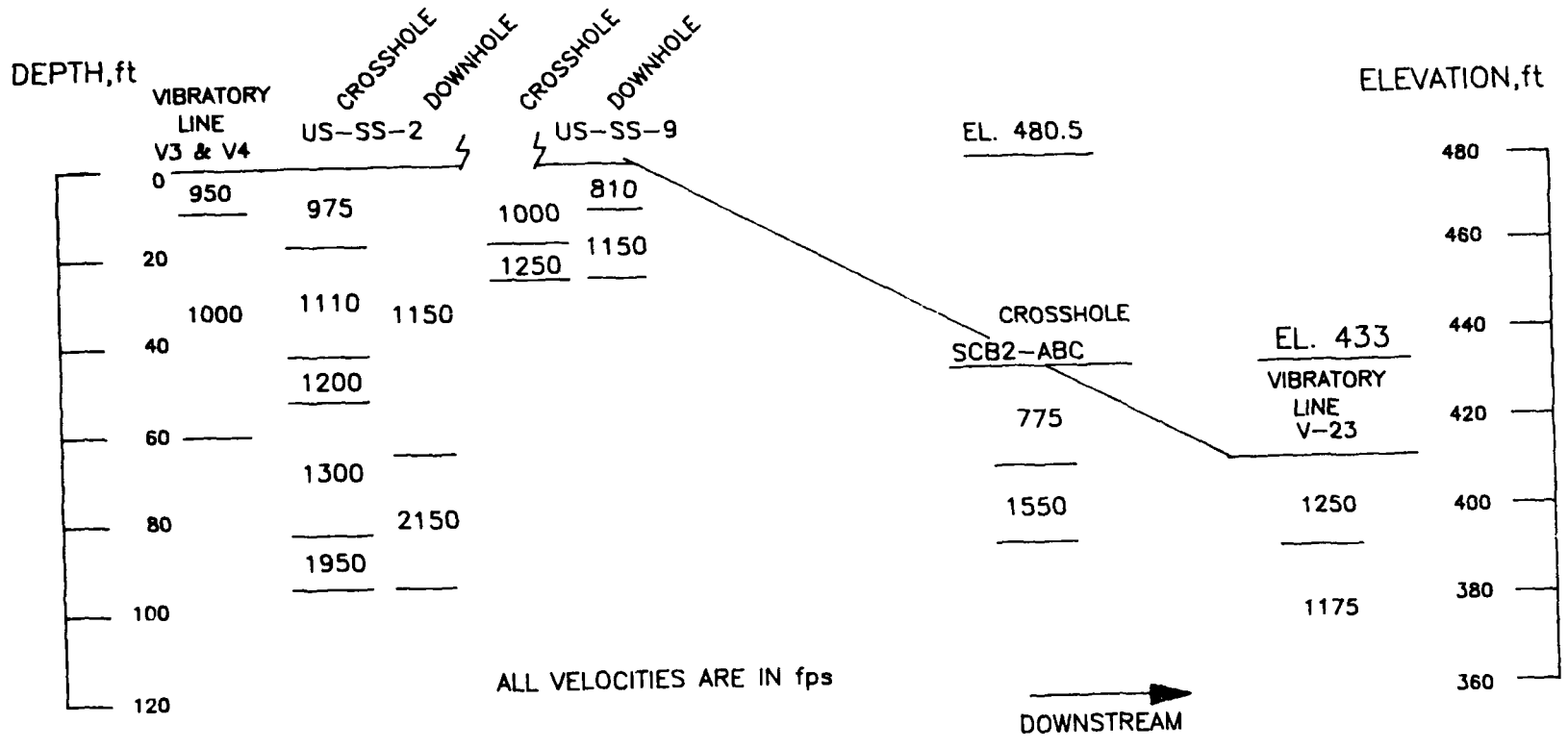

Figure 64. S-wave composite for cross section through Station 235+00 Right Wing Dam

FILE:RWD2335

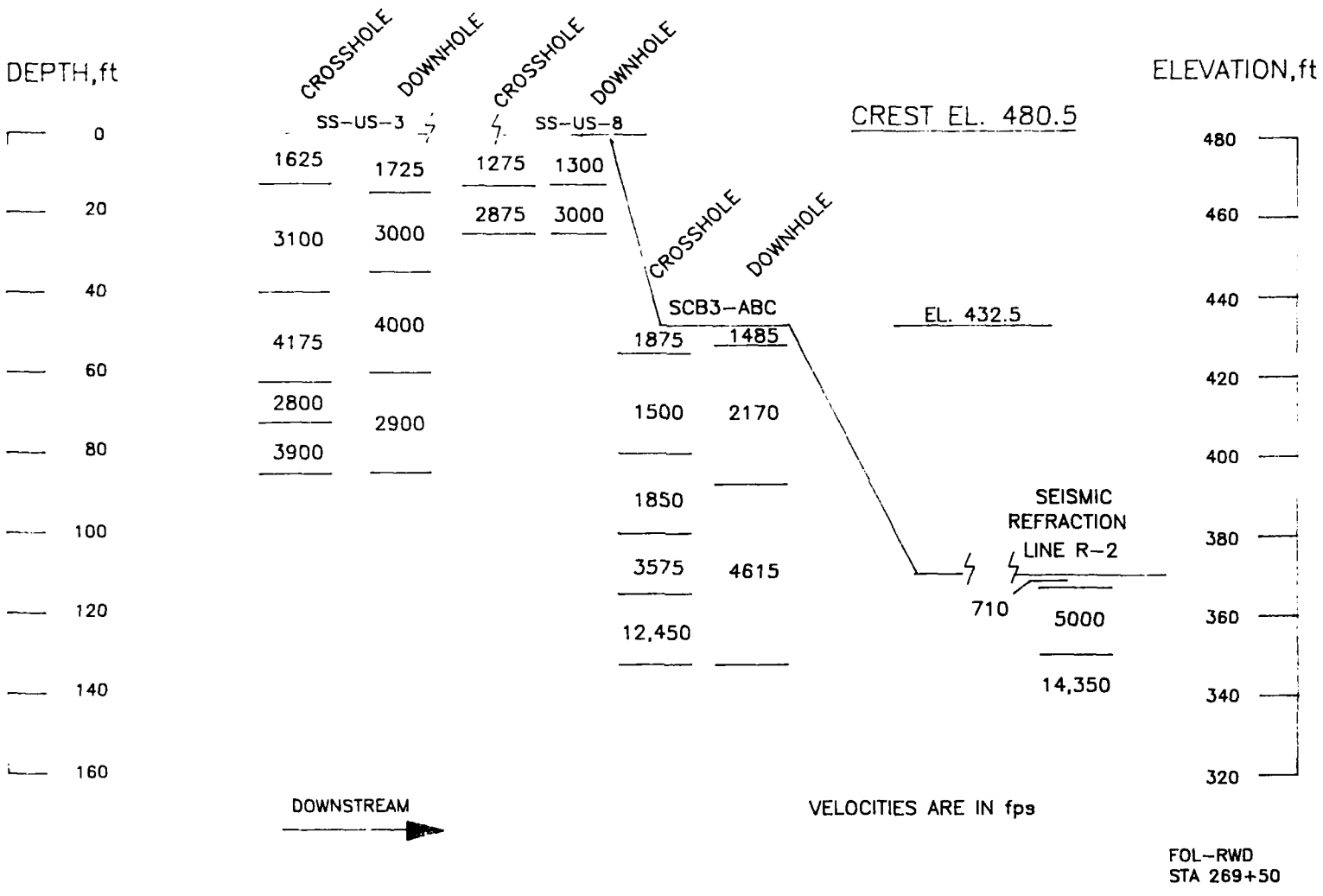

Figure 65. P-wave composite for cross section through Station 269+50 Right Wing Dam

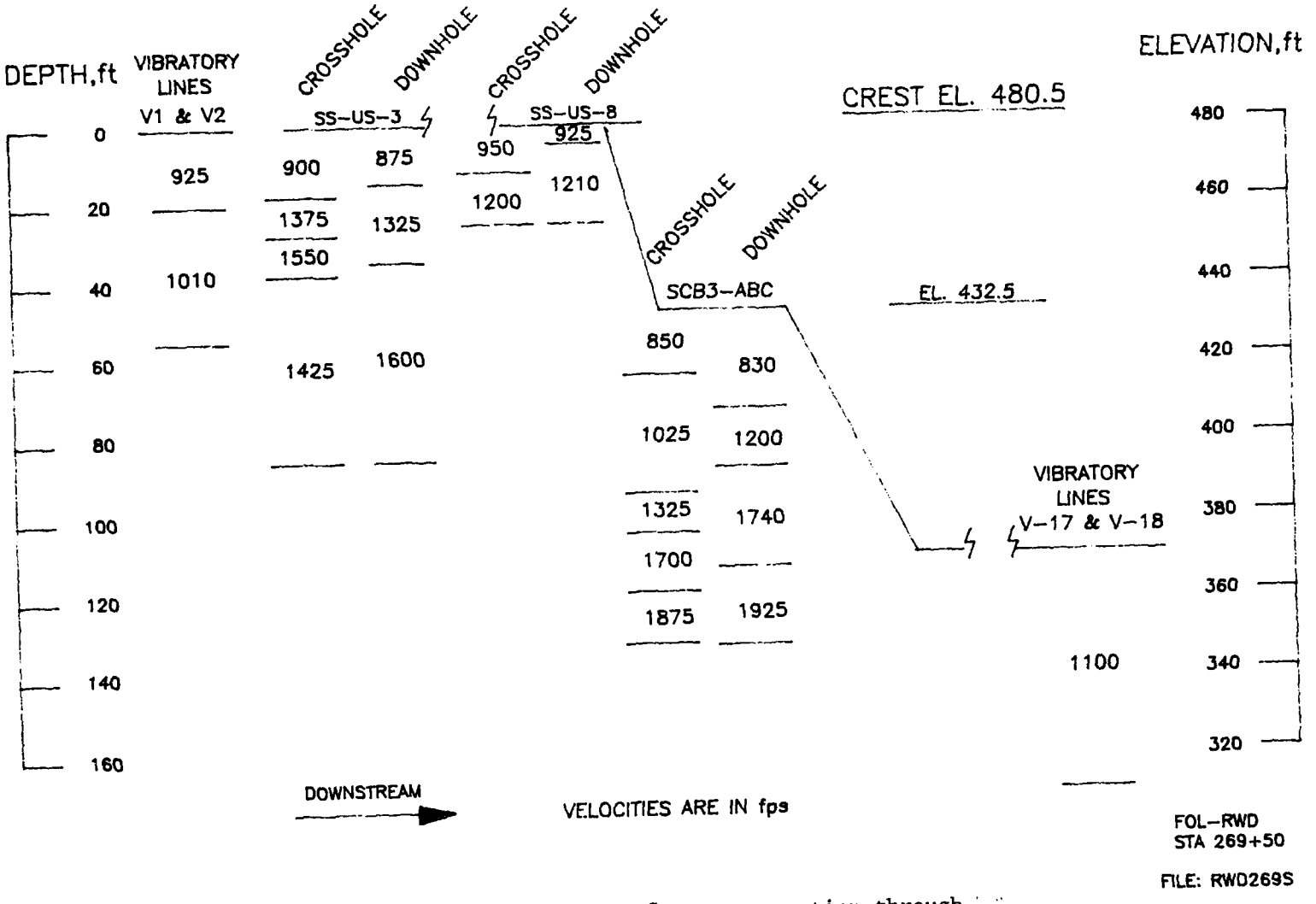

Figure 66. S-wave composite for cross section through Station 269+50 Right Wing Dam

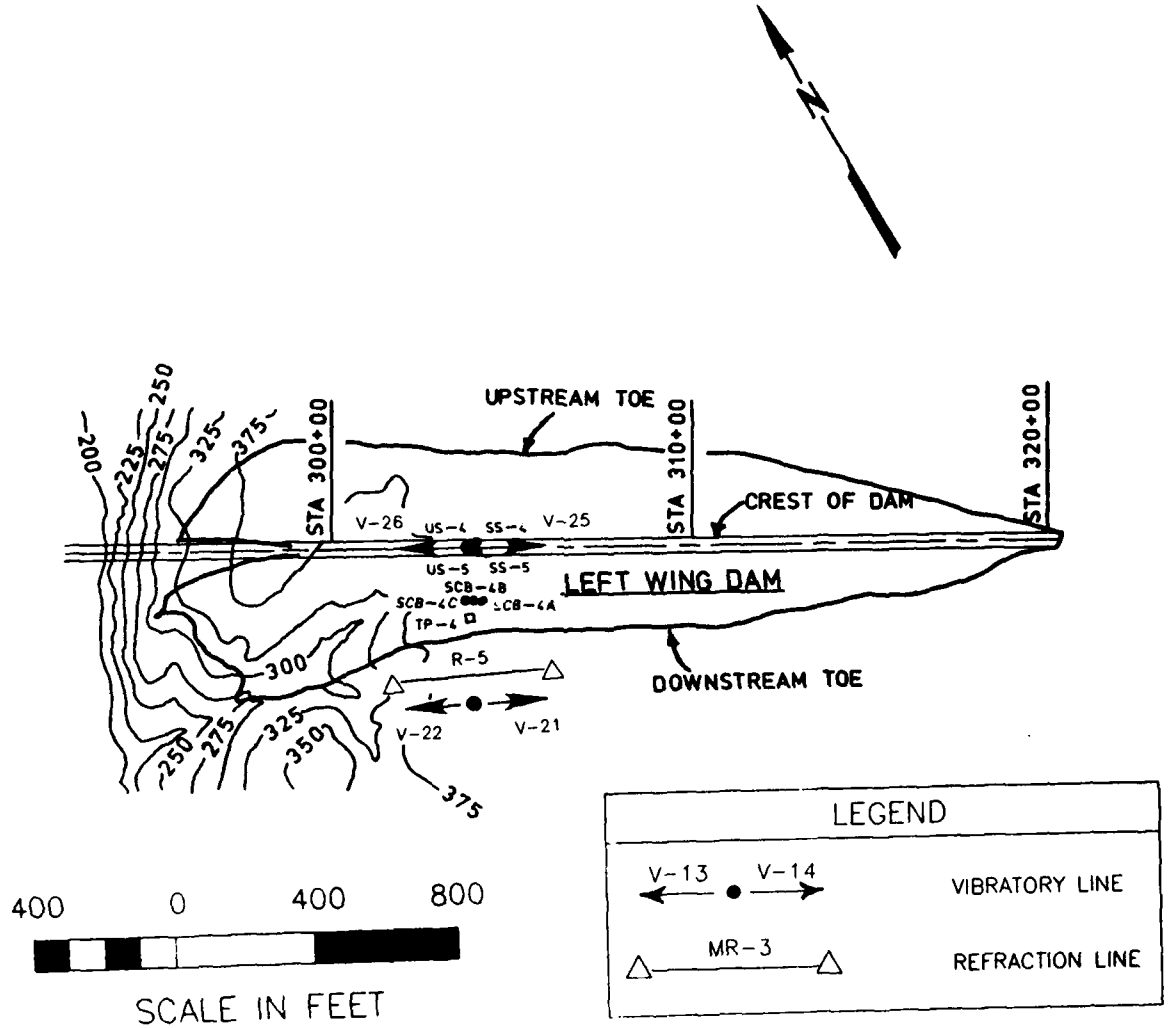

Figure 67. Plan view and test layout for the Left Wing Dam

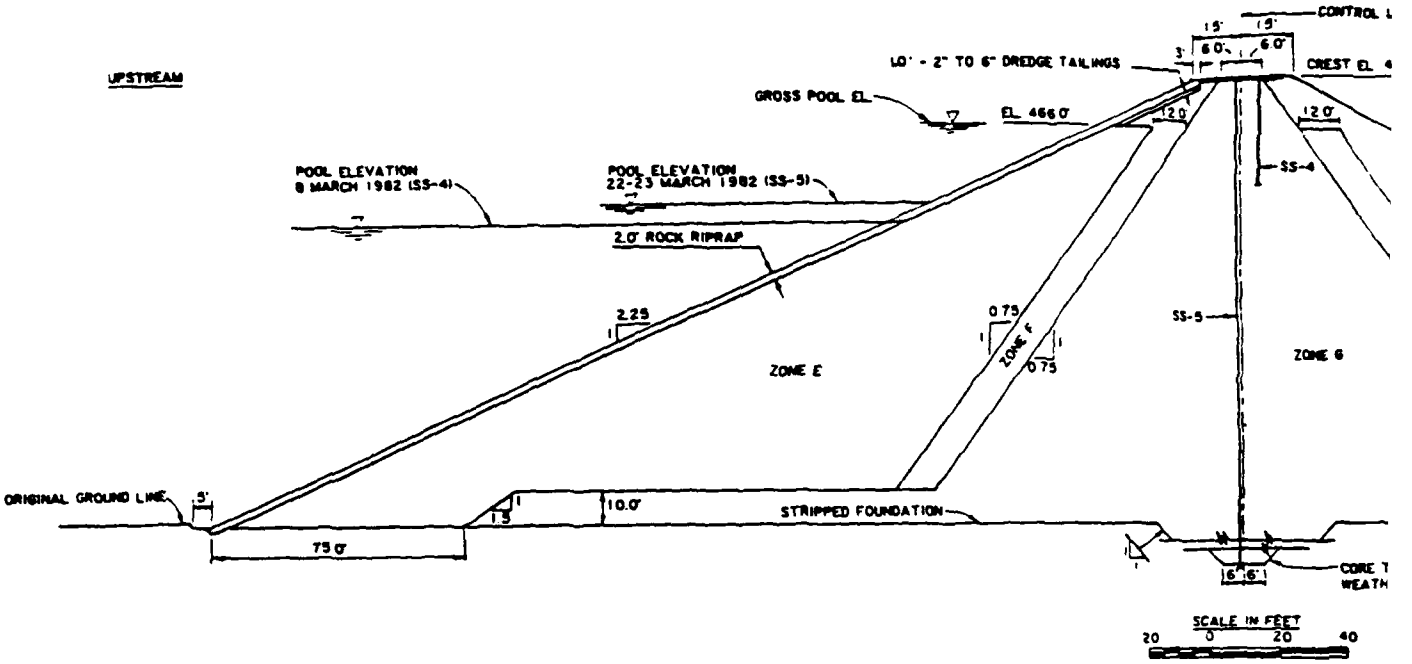

STATION 303+90

ZONE E - UNPROCESSED COARSE DREDGE TAILINGS

ZONE F - MINUS 2" COARSE DREDGE TAILINGS FR

ZONE G - COMPACTED DECOMPOSED GRANITE OBTAI

Figure 68. Cross section of the L

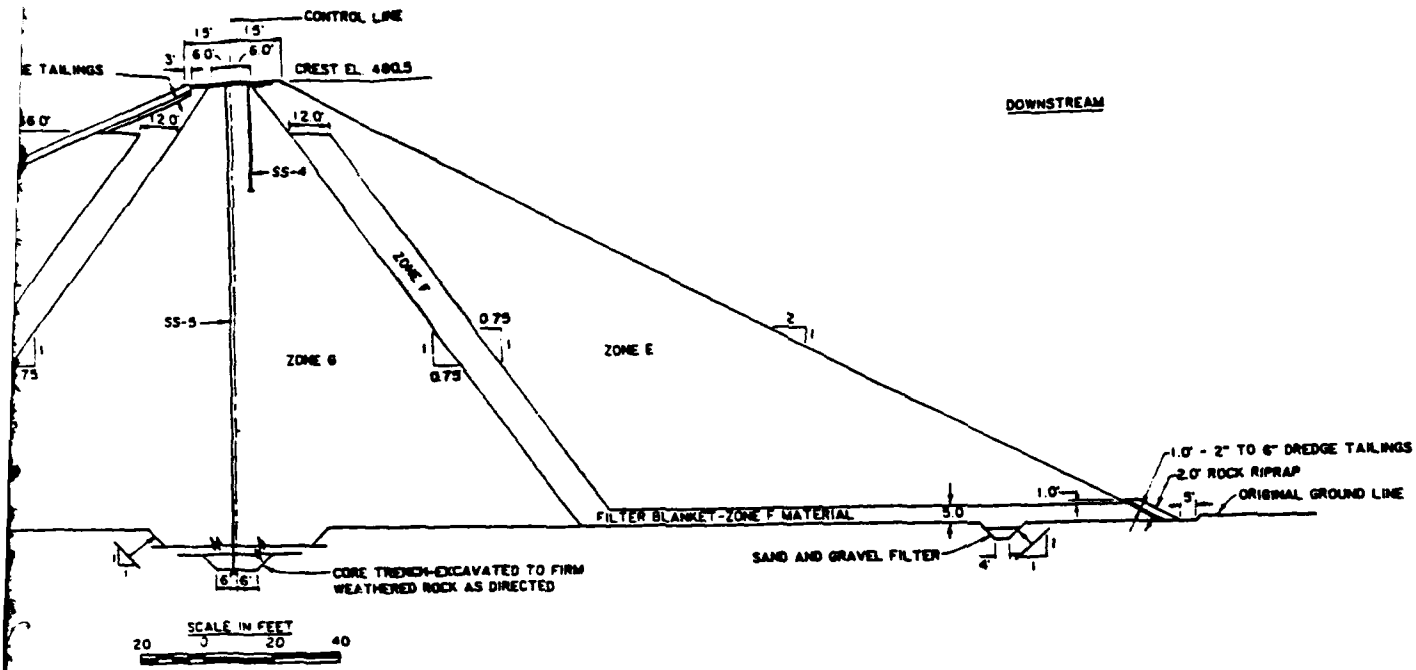

STATION 303+90

ED COARSE DREDGE TAILINGS FROM BORROW AREA NO. 5

COARSE DREDGE TAILINGS FROM BORROW AREA NO. 5

DECOMPOSED GRANITE OBTAINED FROM BORROW AREA NO. 1

. Cross section of the Left Wing Dam

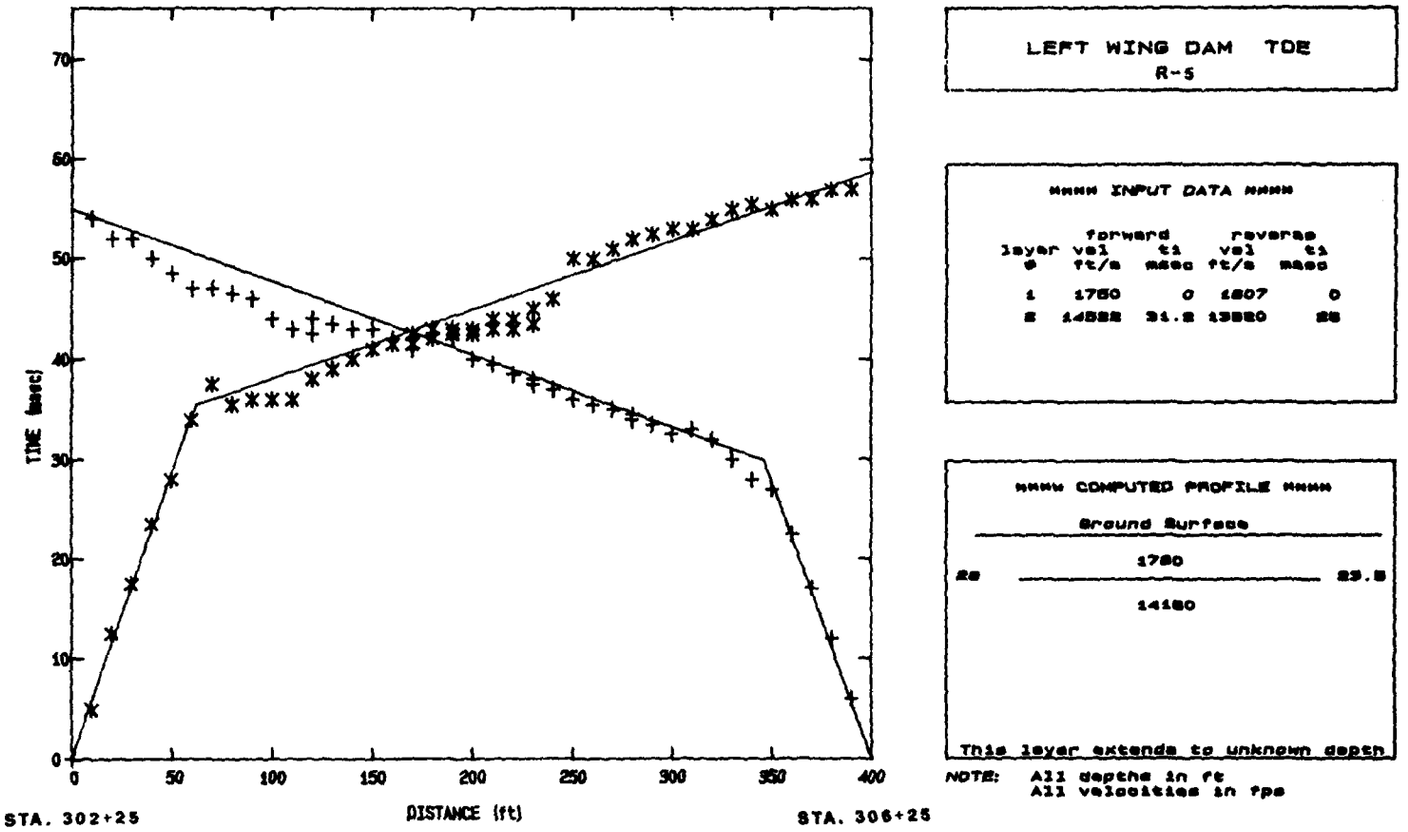

Figure 69. Seismic refraction line R-5, toe of Left Wing Dam

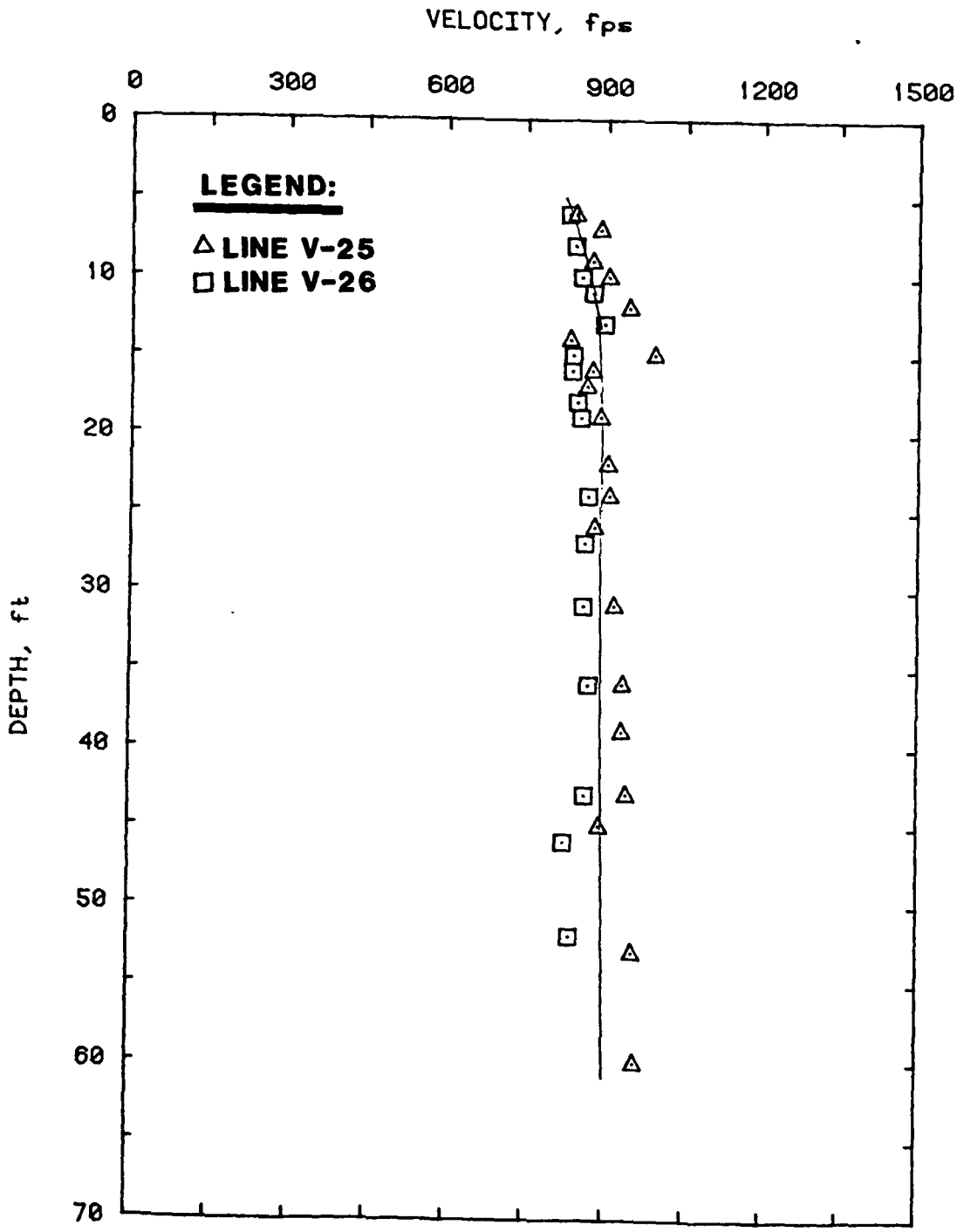

Figure 70. R-wave velocity versus depth for lines V-25 and V-26, centered on Station 303+90 crest of Left Wing Dam

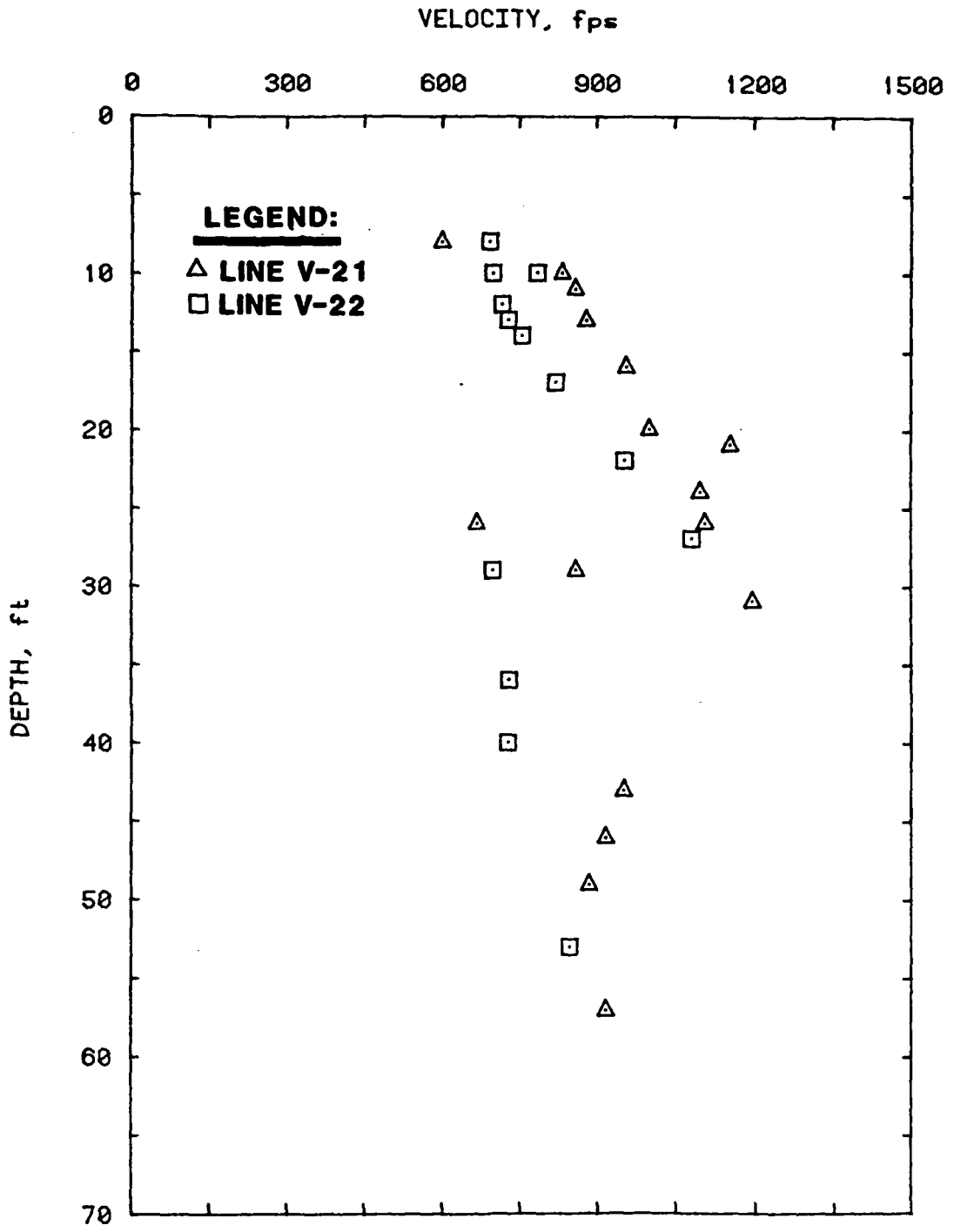

Figure 71. R-wave velocity versus depth for lines V-21 and V-22, centered on Station 303+90 toe of Left Wing Dam

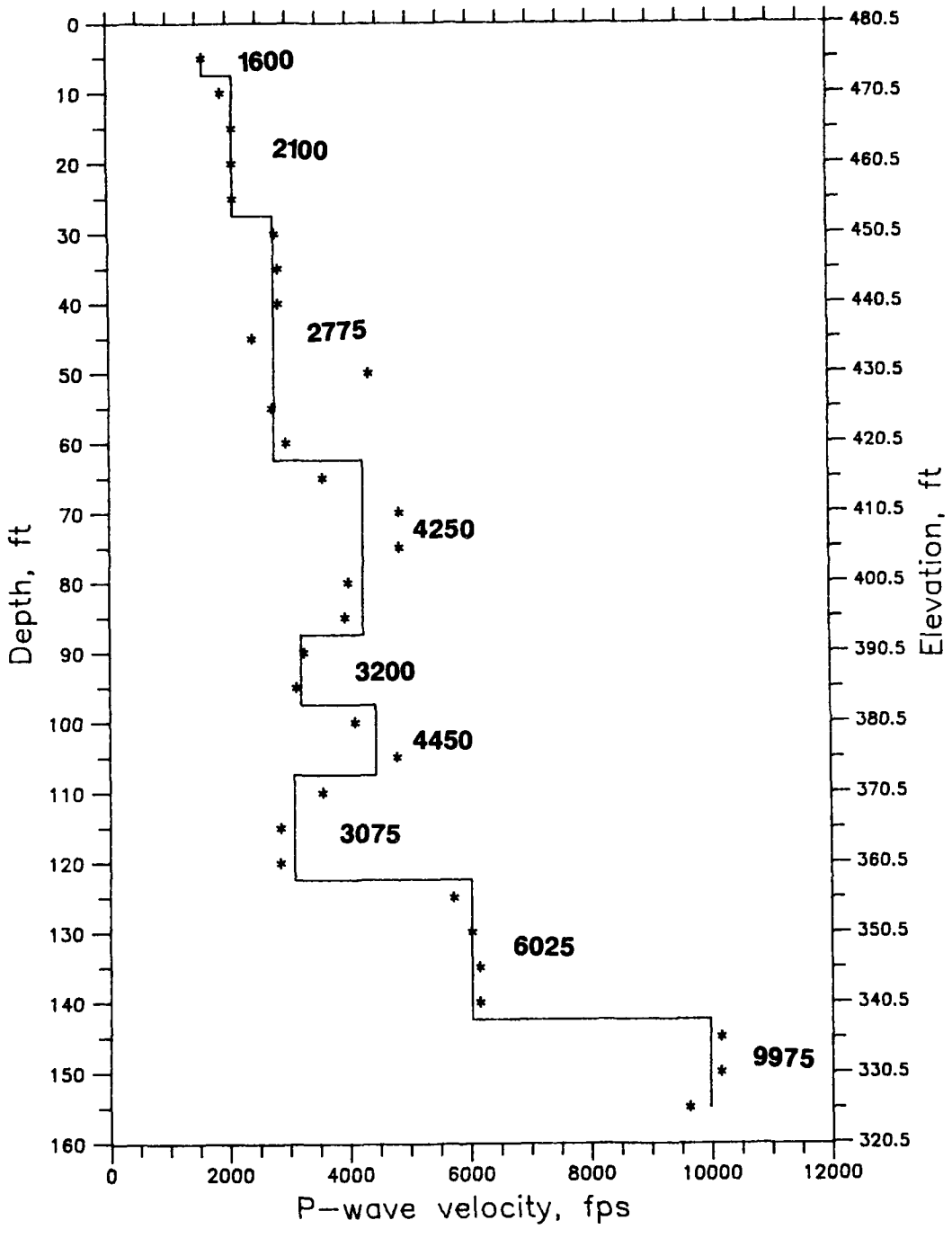

Figure 72. Crosshole P-wave results, centerline Left Wing Dam

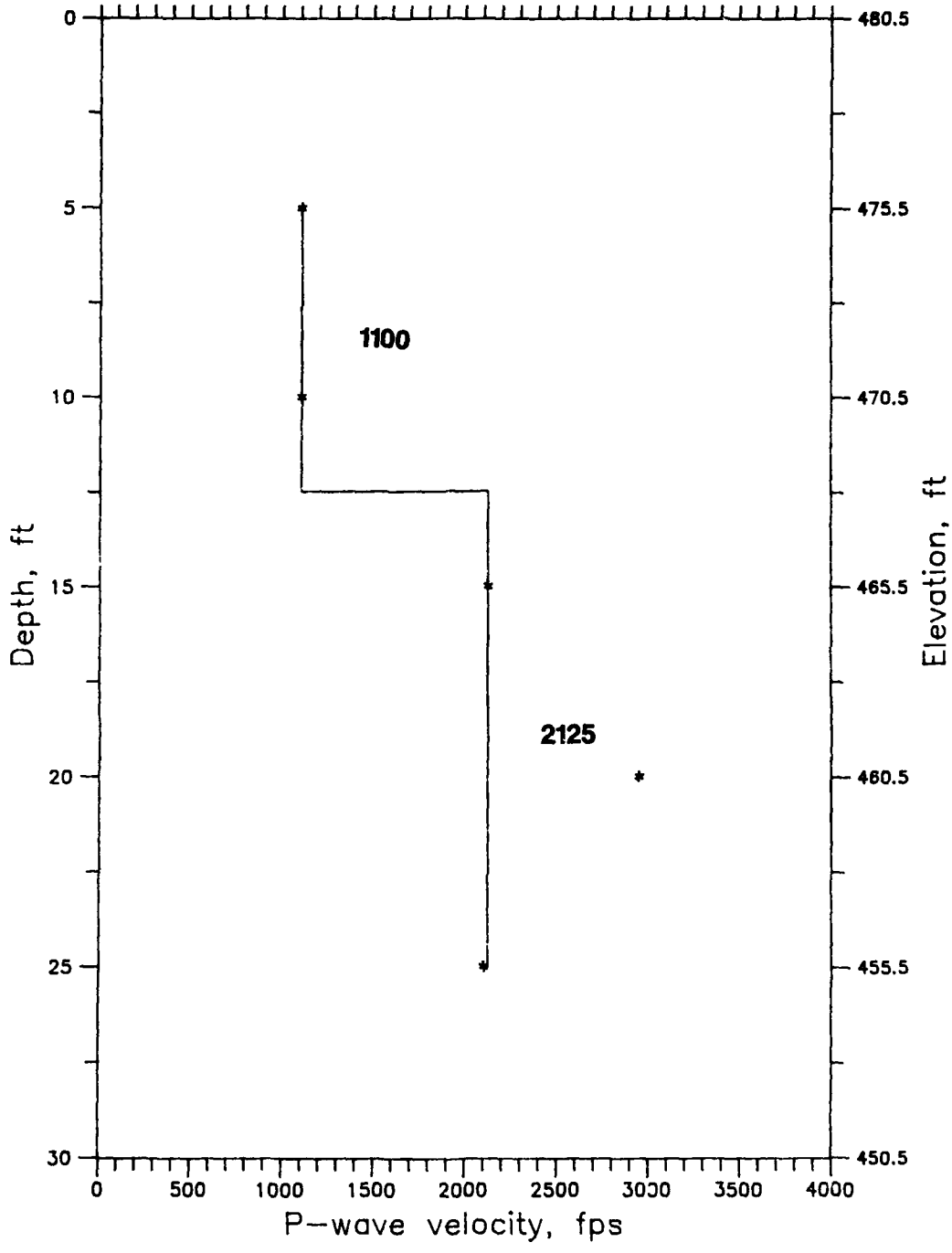

Figure 73. Crosshole P-wave results, downstream shoulder Left Wing Dam

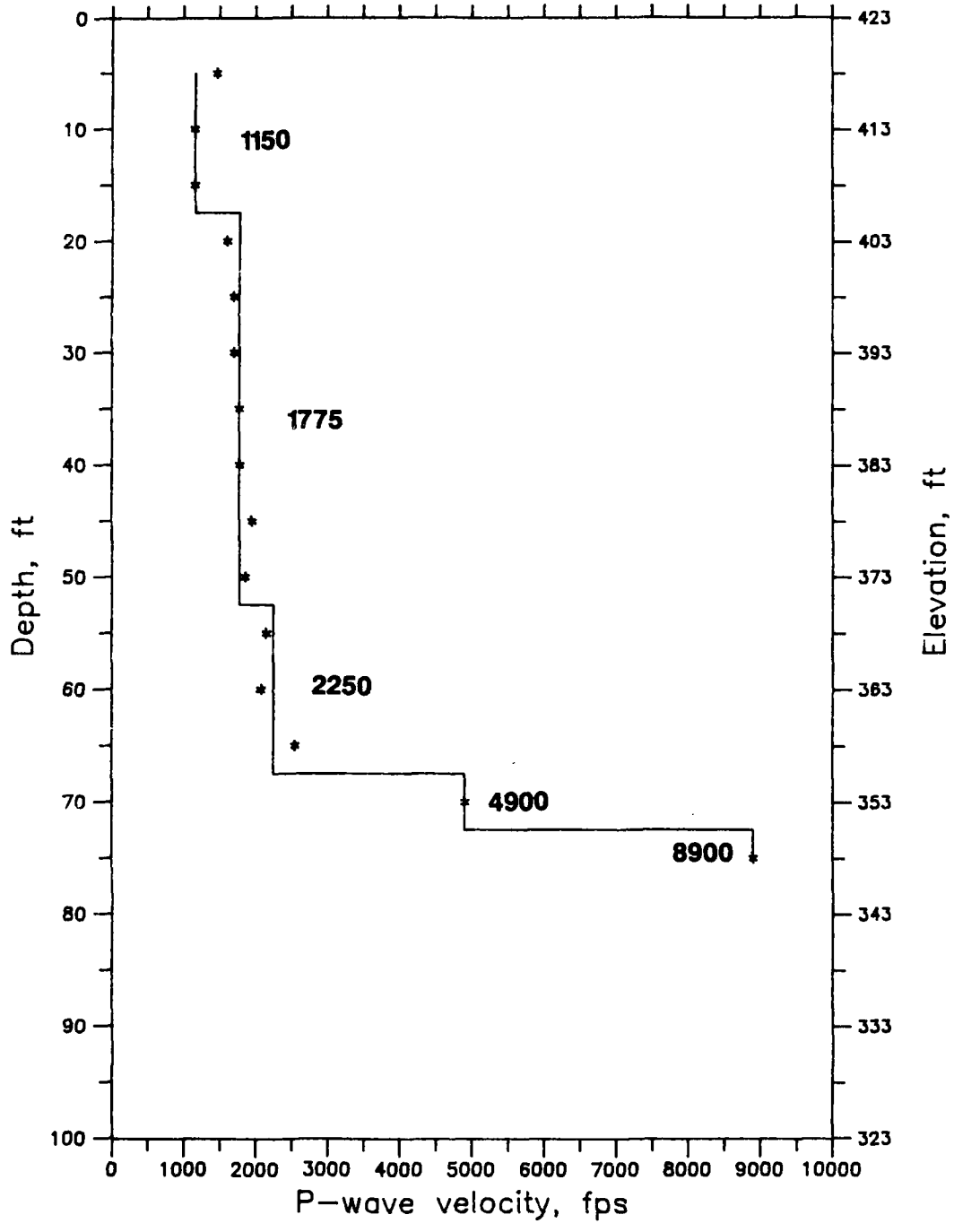

Figure 74. Crosshole P-wave results, downstream slope
Left Wing Dam

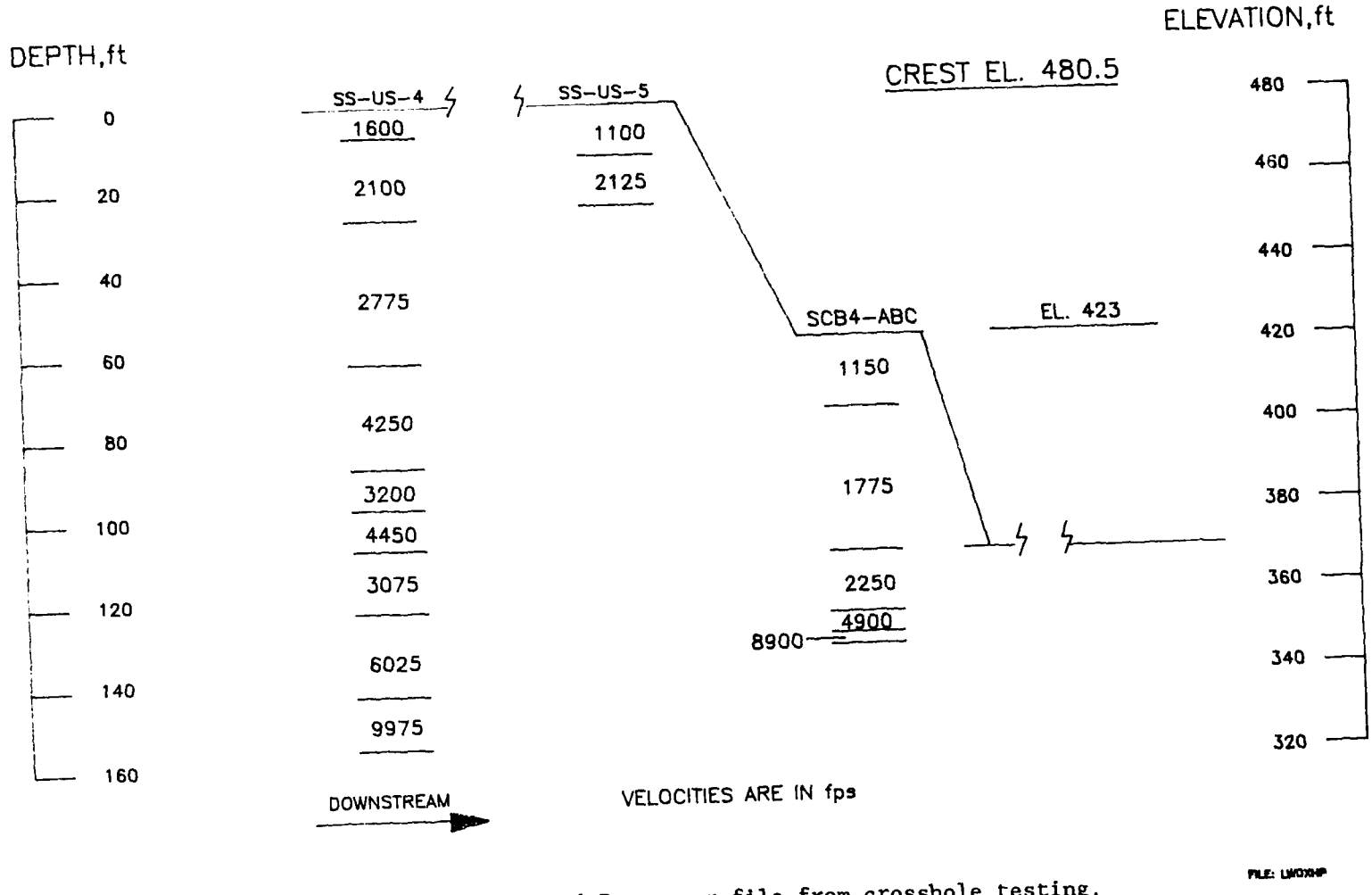

Figure 75. Interpreted P-wave profile from crosshole testing, Left Wing Dam

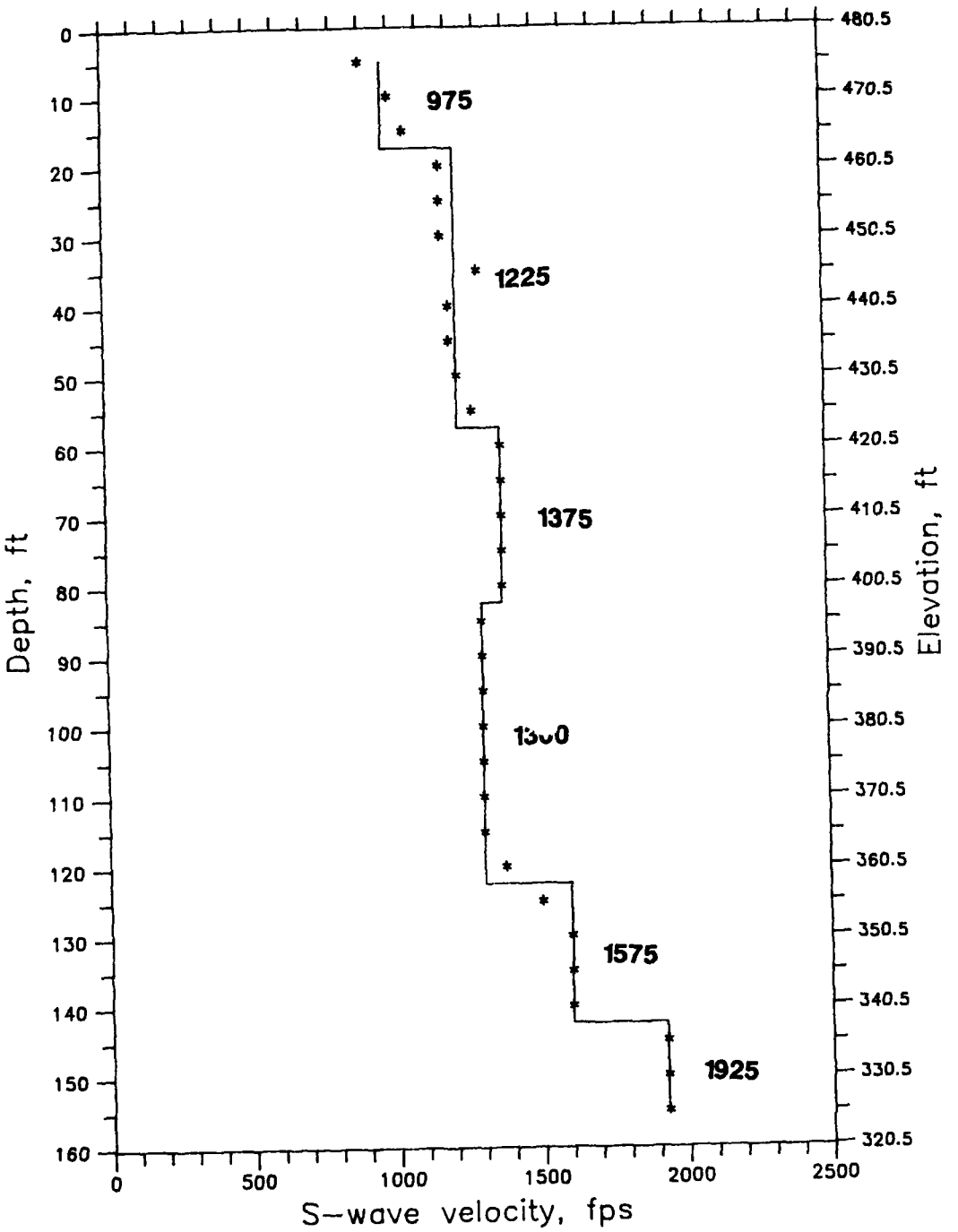

Figure 76. Crosshole S-wave results, centerline Left Wing Dam

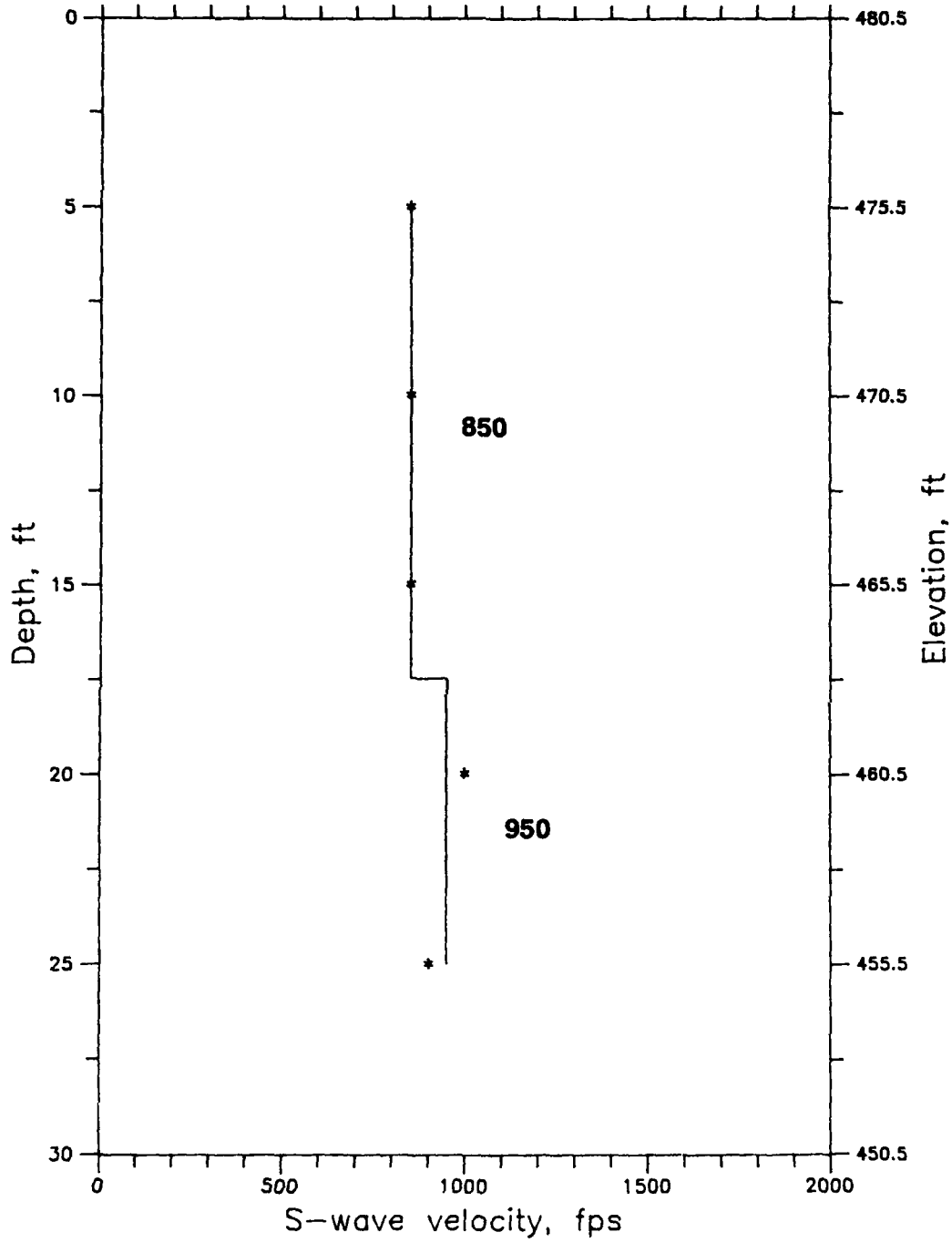

Figure 77. Crosshole S-wave results, downstream shoulder Left Wing Dam

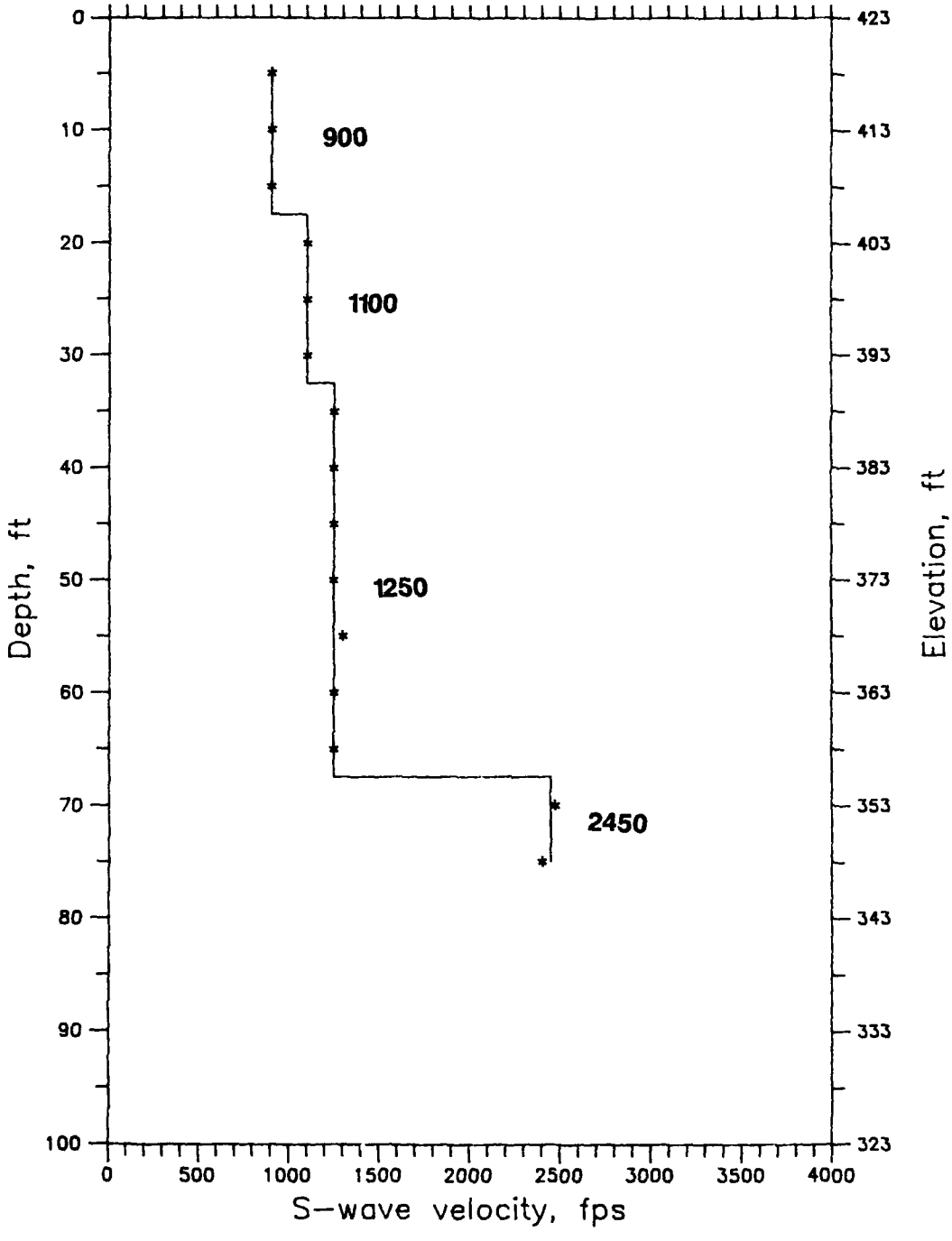

Figure 78. Crosshole S-wave results, downstream slope Left Wing Dam

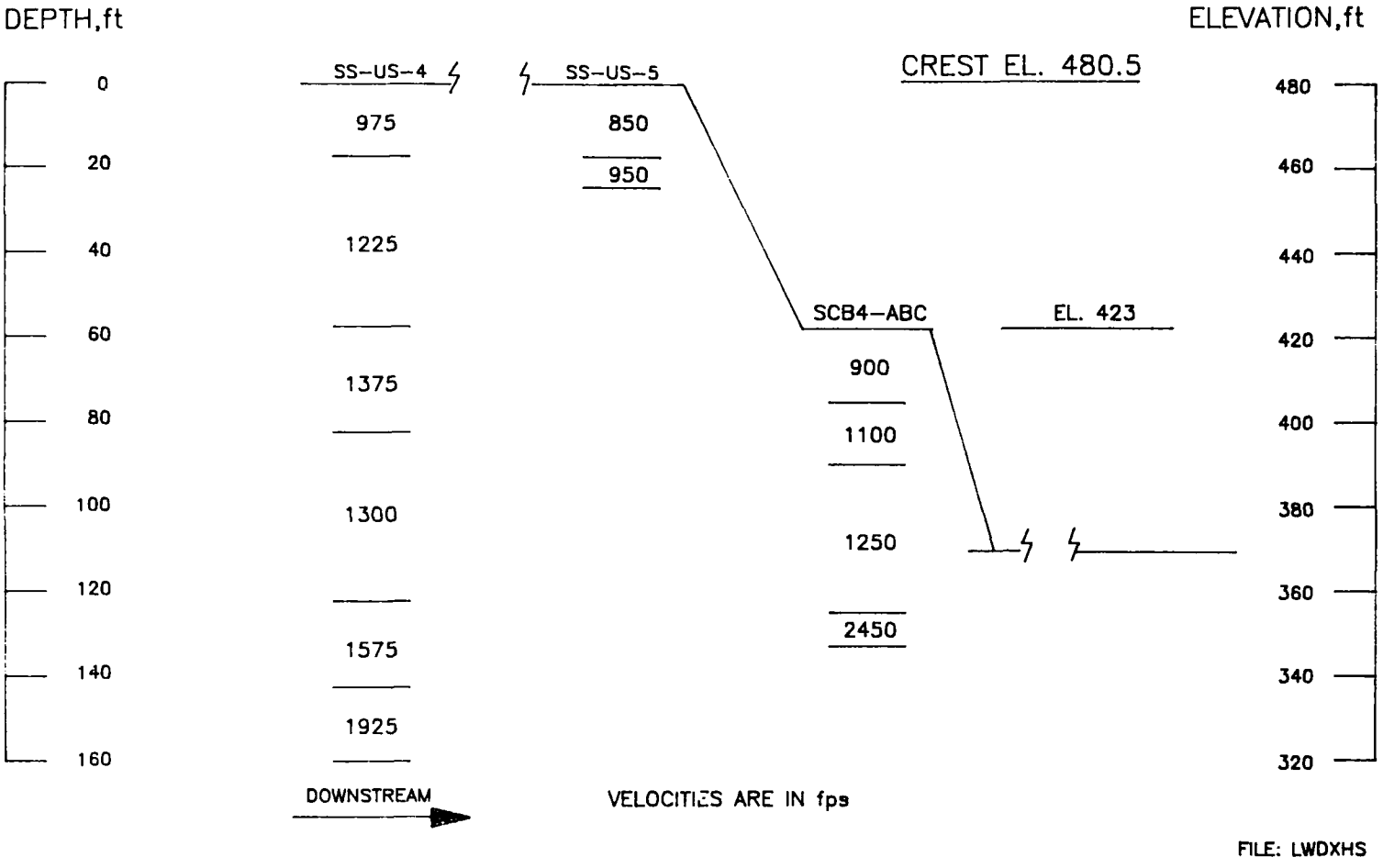

Figure 79. Interpreted S-wave profile from crosshole testing, Left Wing Dam

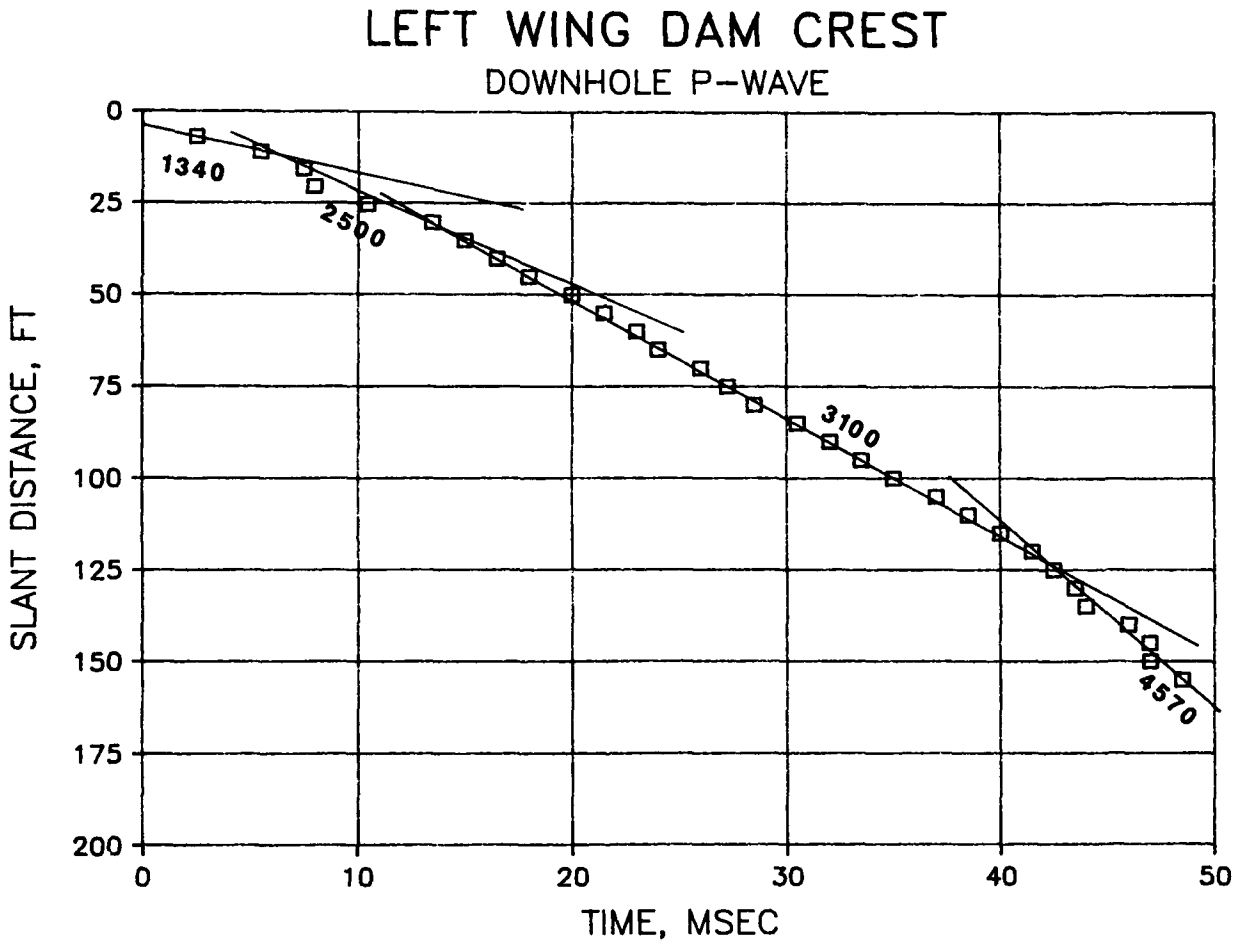

Figure 80. Downhole P-wave results, centerline Left Wing Dam

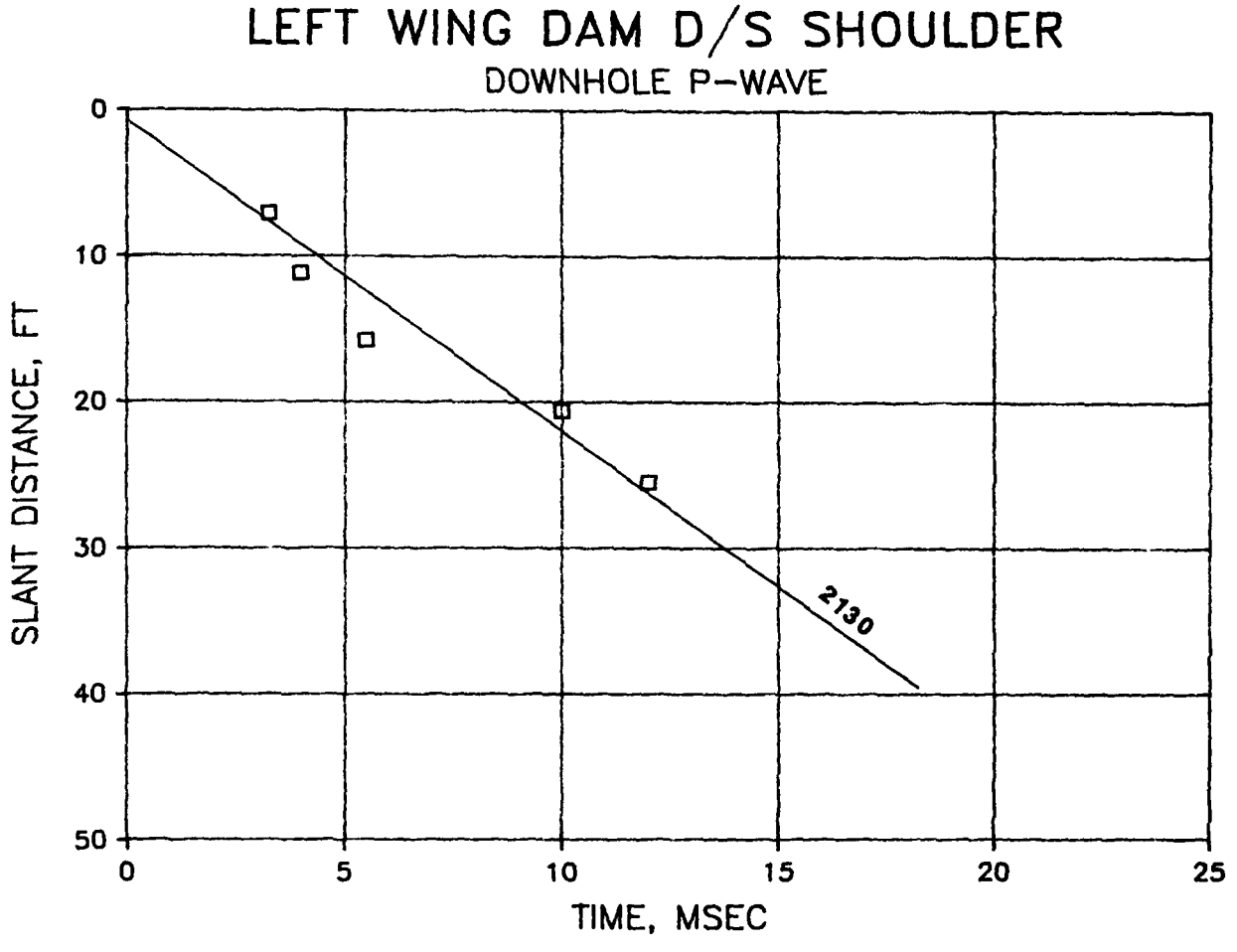

Figure 81. Downhole P-wave results, downstream shoulder Left Wing Dam

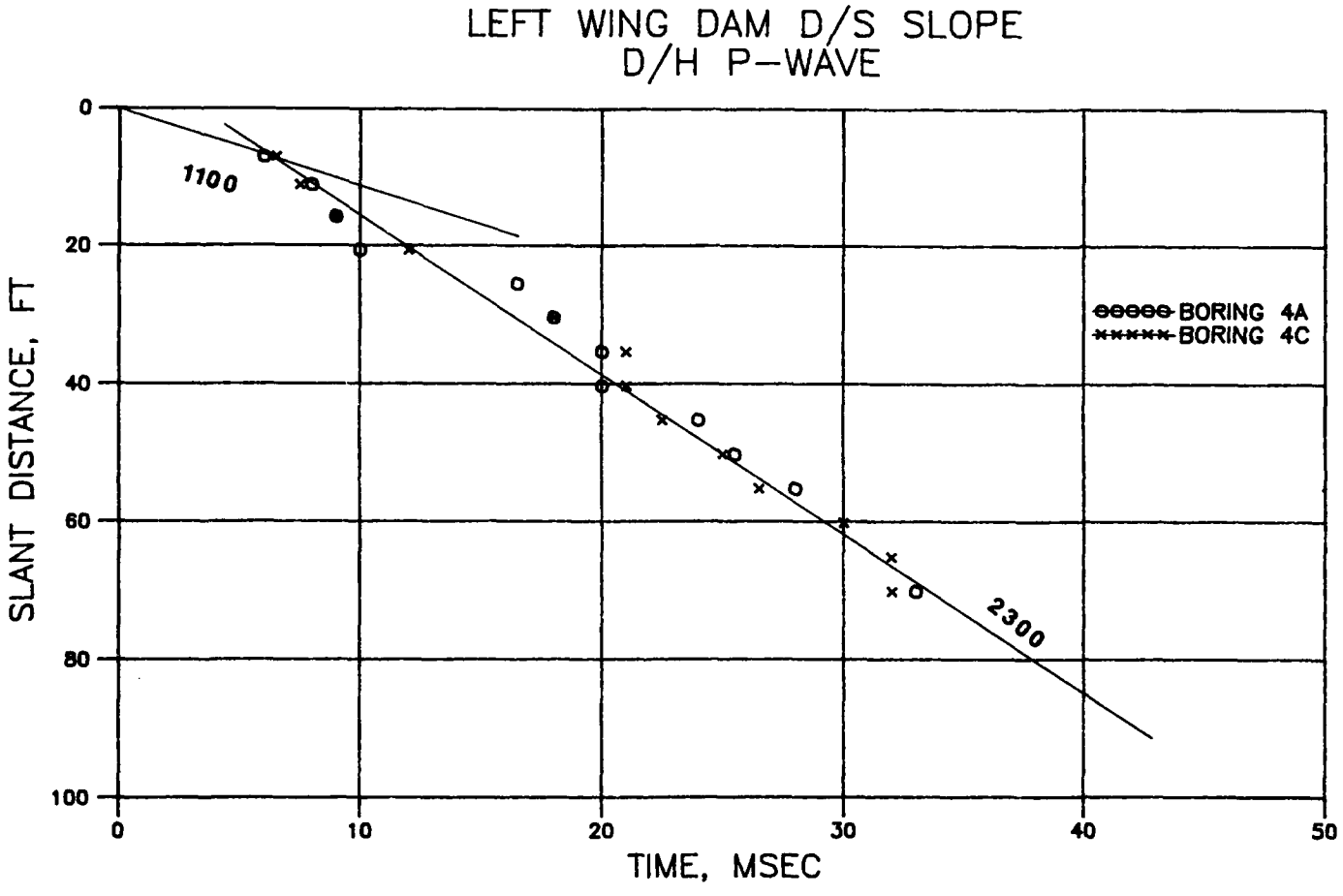

Figure 82. Downhole P-wave results, downstream slope Left Wing Dam, 5 ft

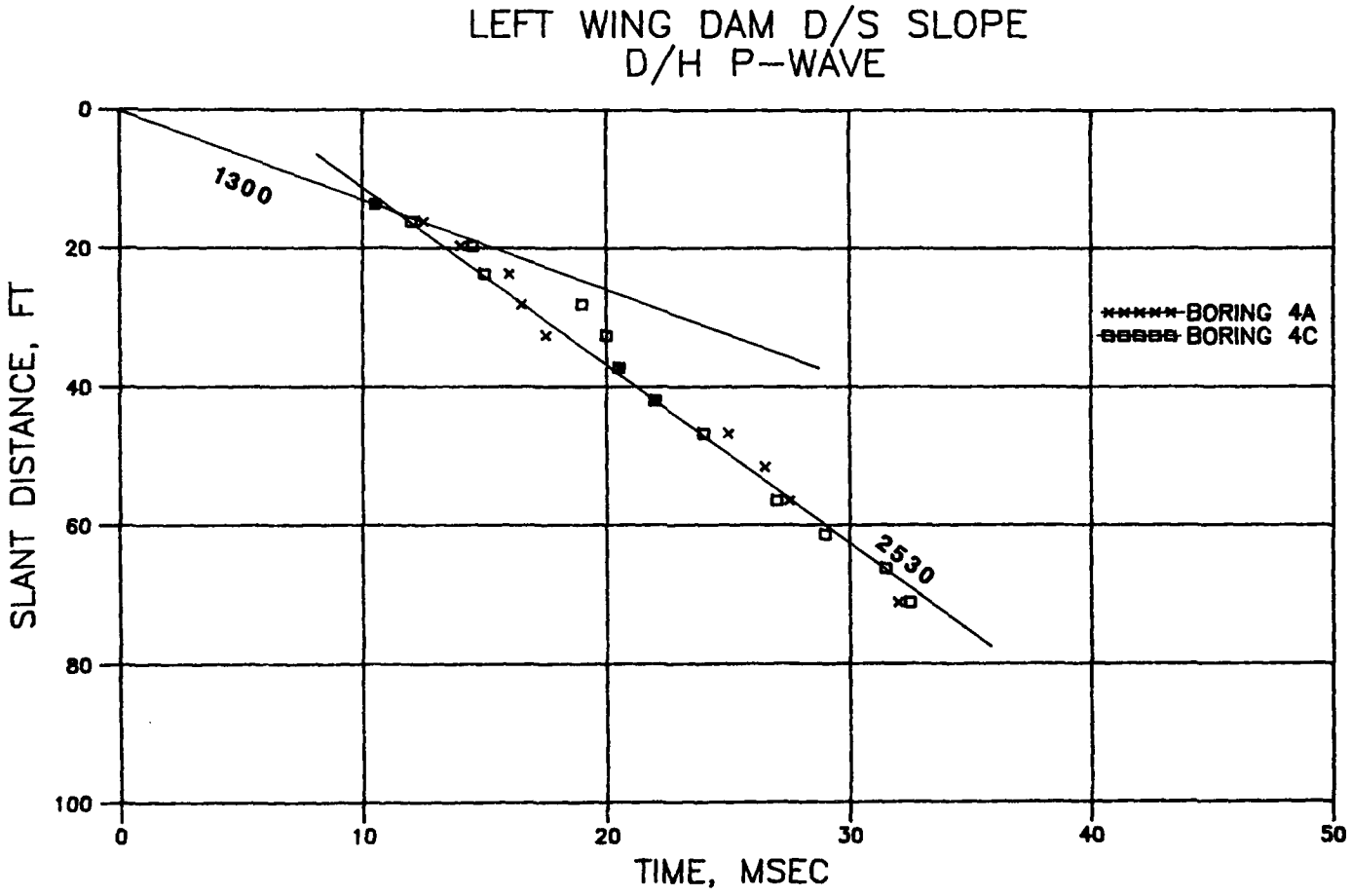

Figure 83. Downhole P-wave results, downstream slope Left Wing Dam, 12.7 ft

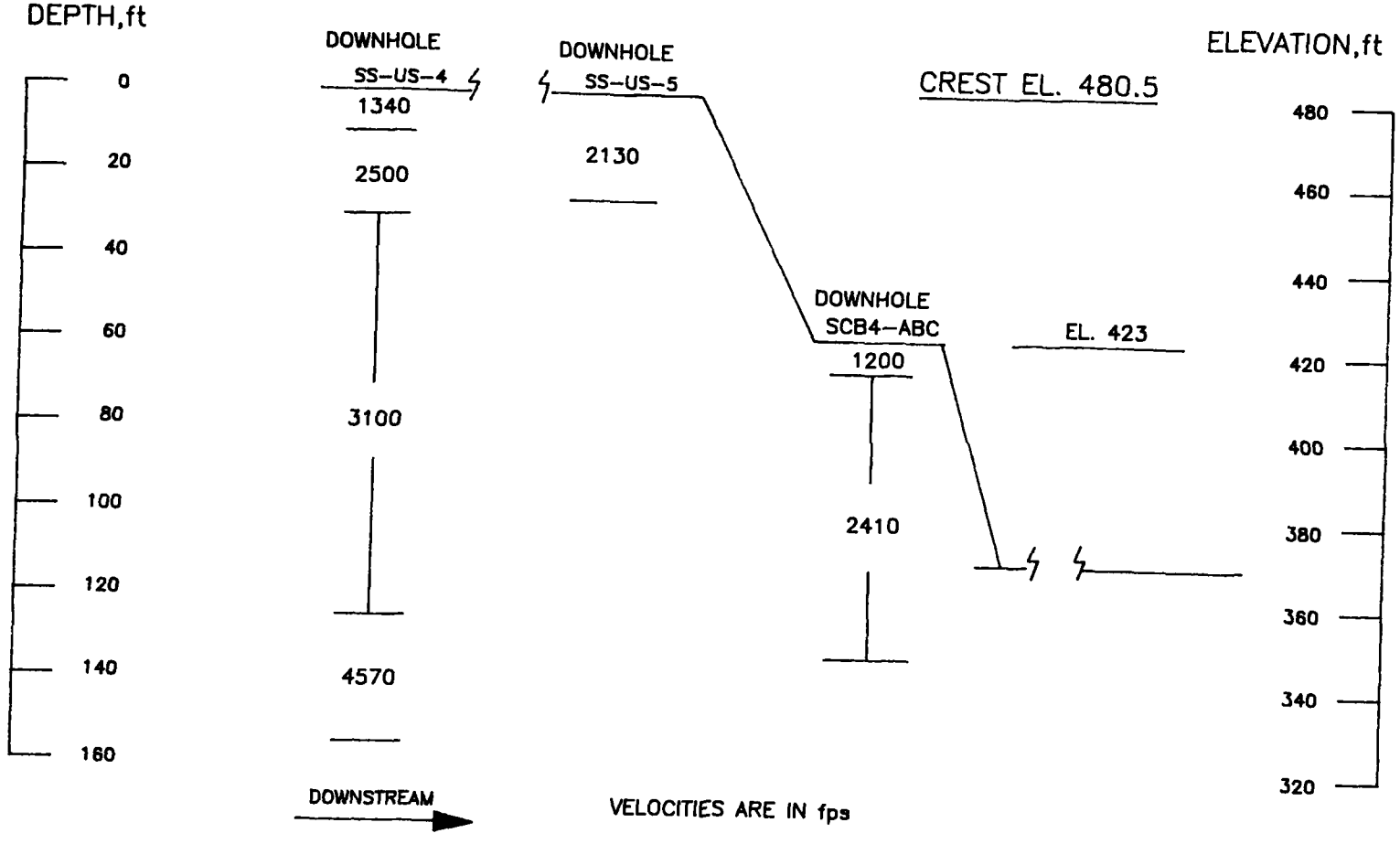

Figure 84. Interpreted P-wave profile from downhole testing, Left Wing Dam

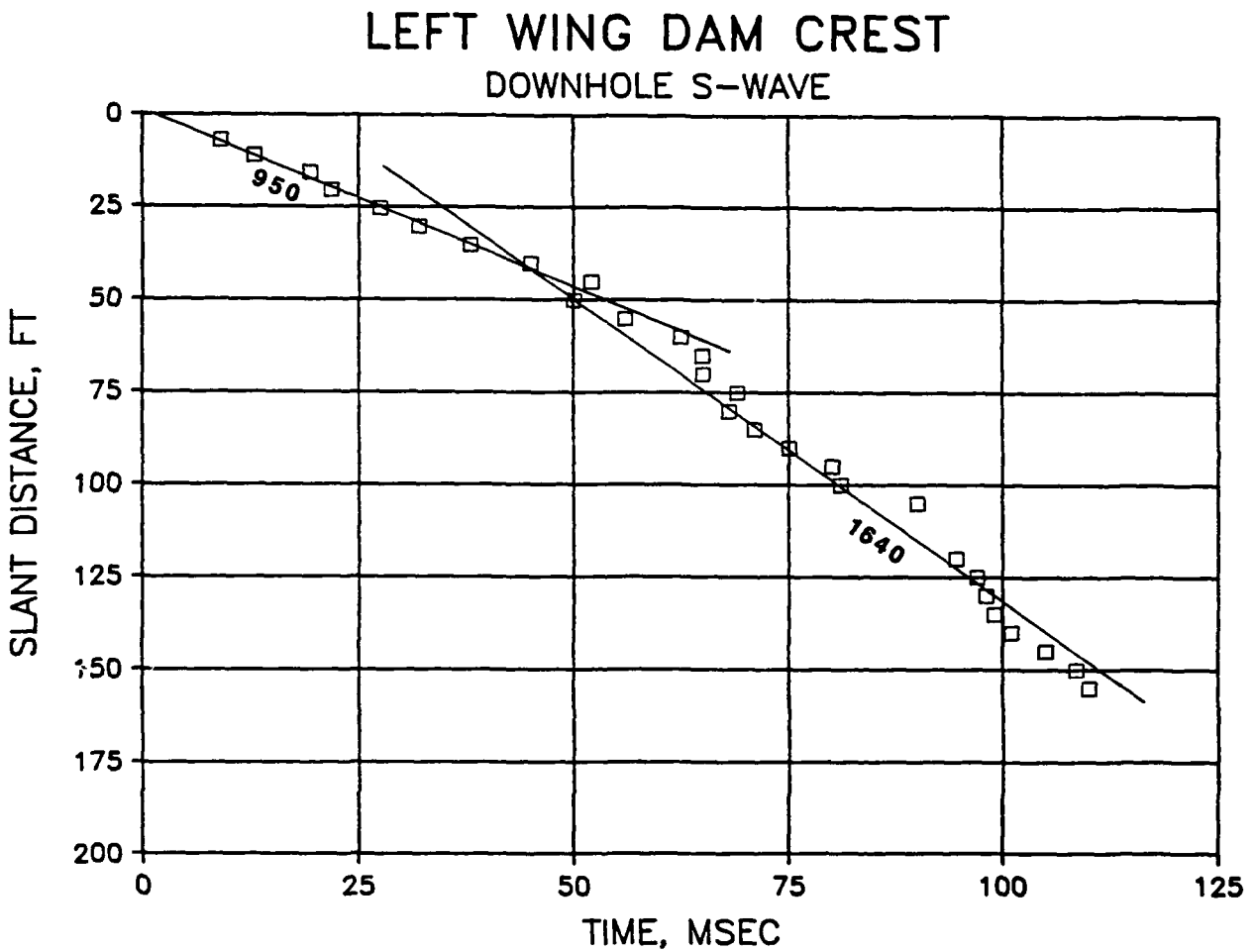

Figure 85. Downhole S-wave results, centerline Left Wing Dam

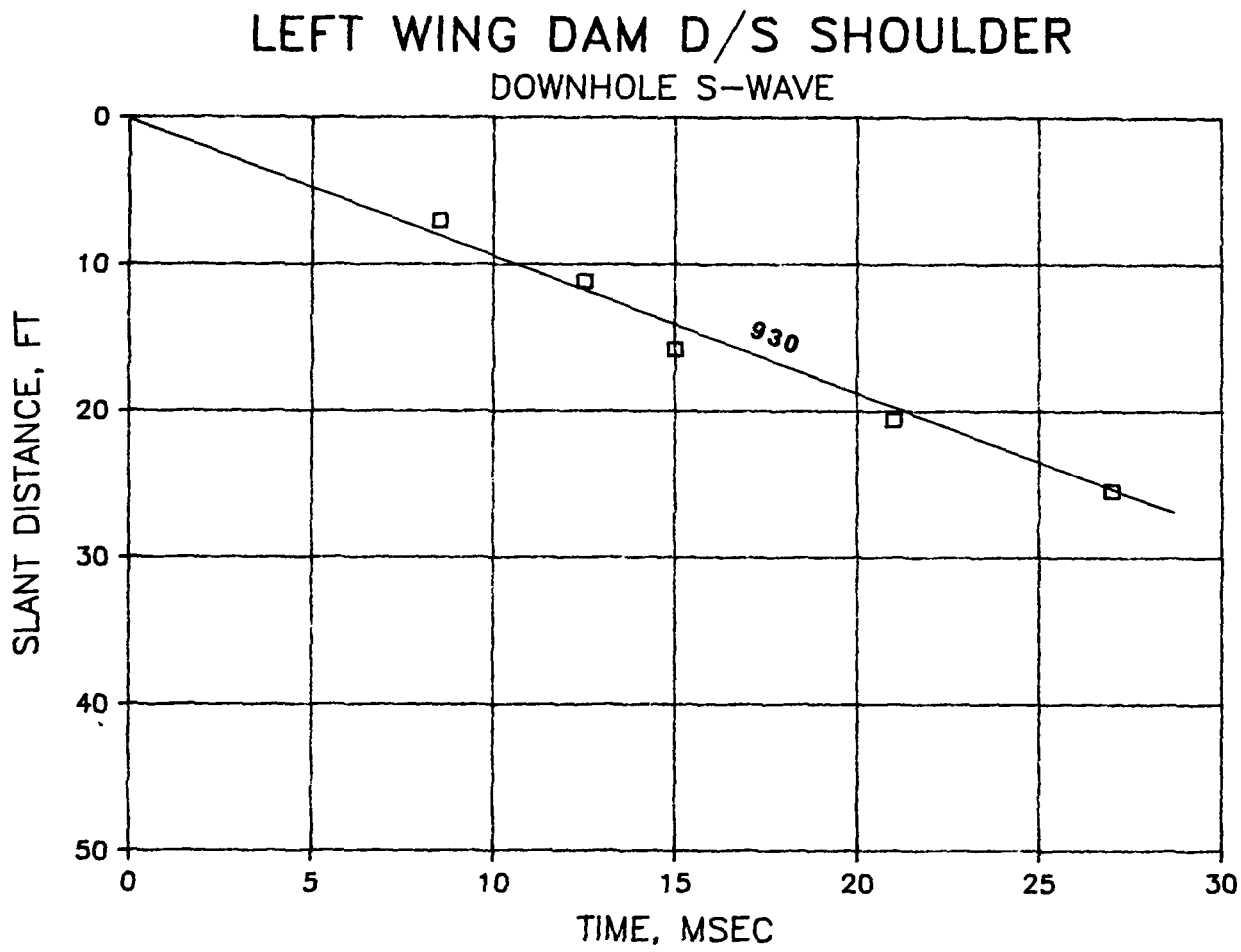

Figure 86. Downhole S-wave results, downstream shoulder Left Wing Dam

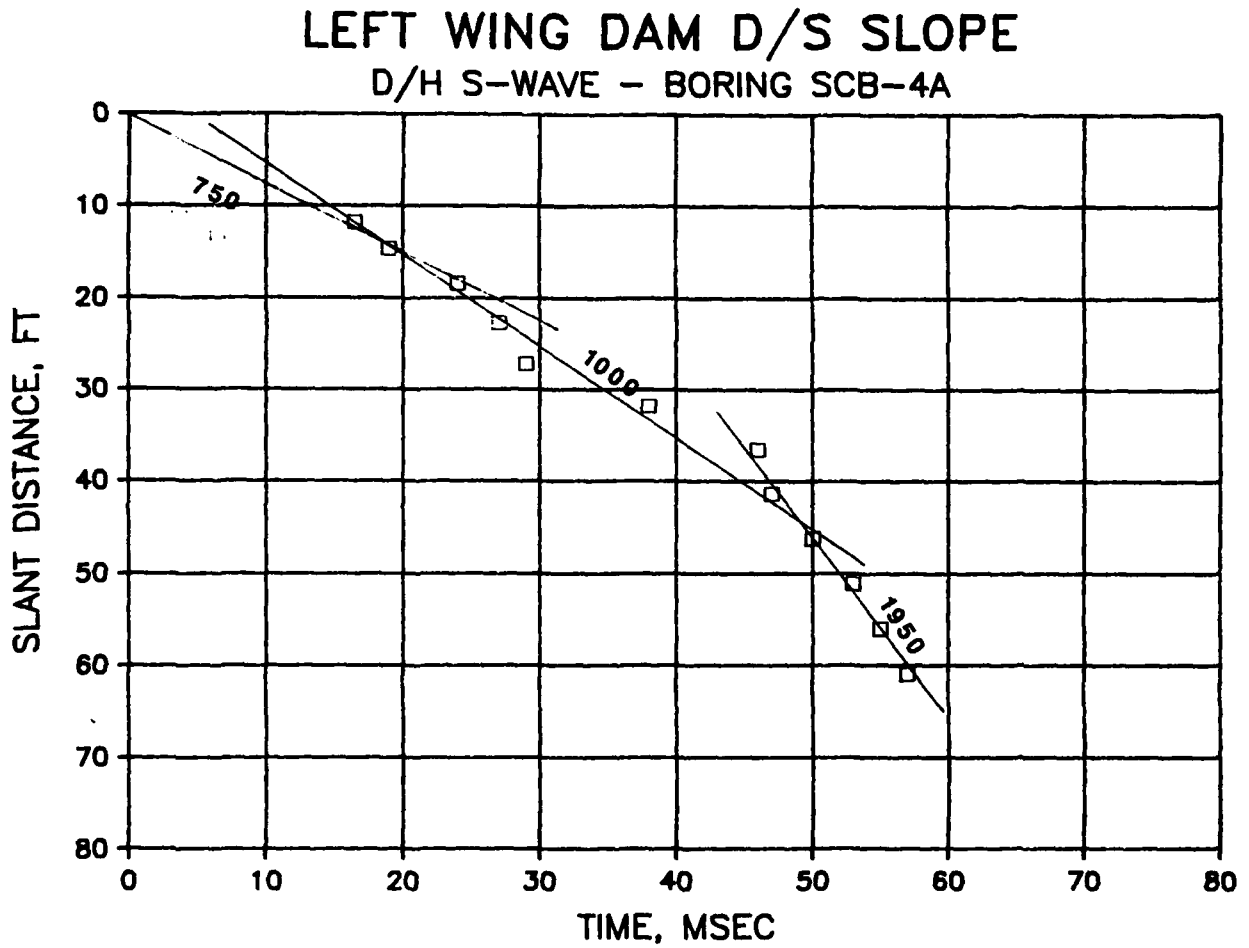

Figure 87. Downhole S-wave results, downstream slope Left Wing Dam

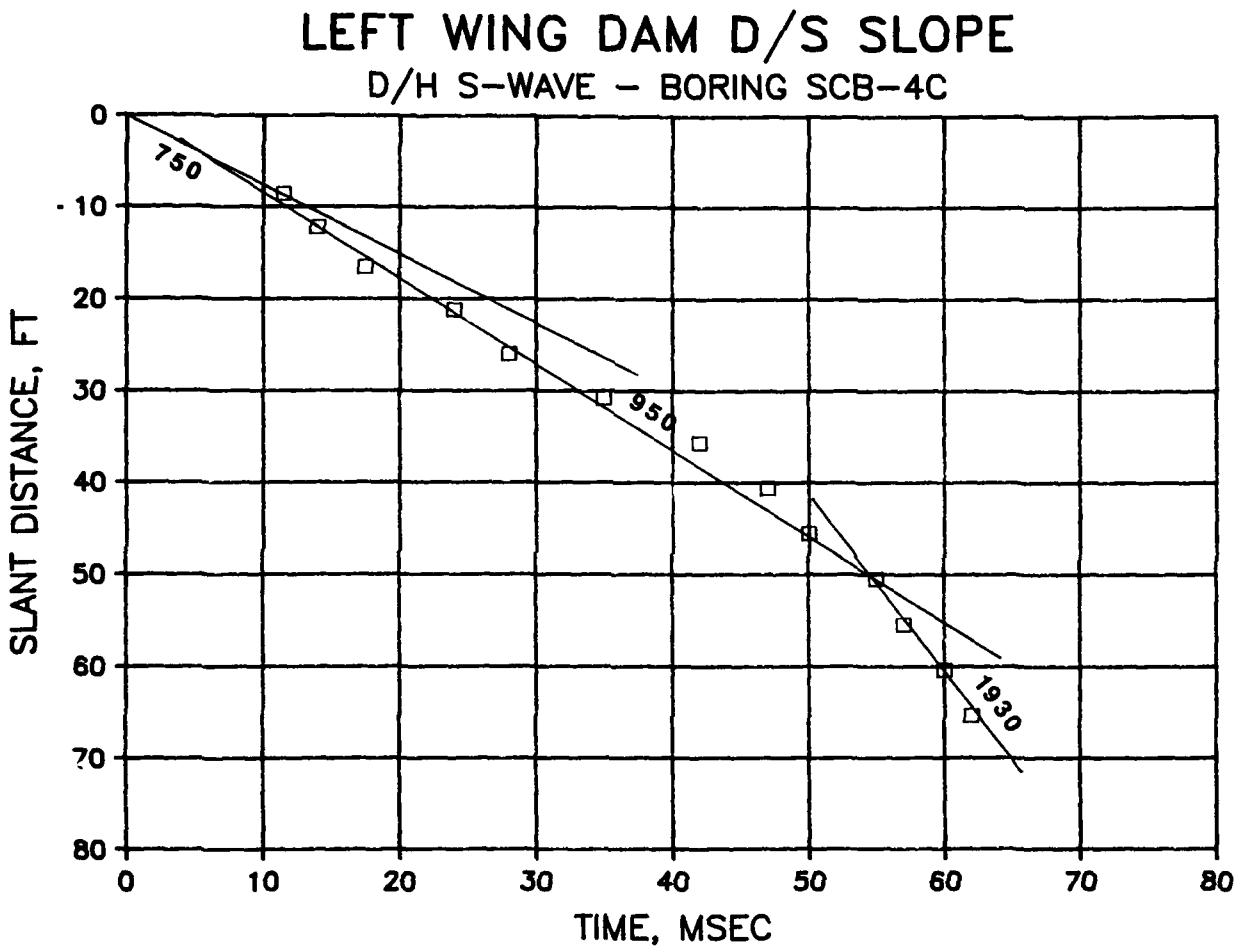

Figure 88. Downhole S-wave results, downstream slope Left Wing Dam

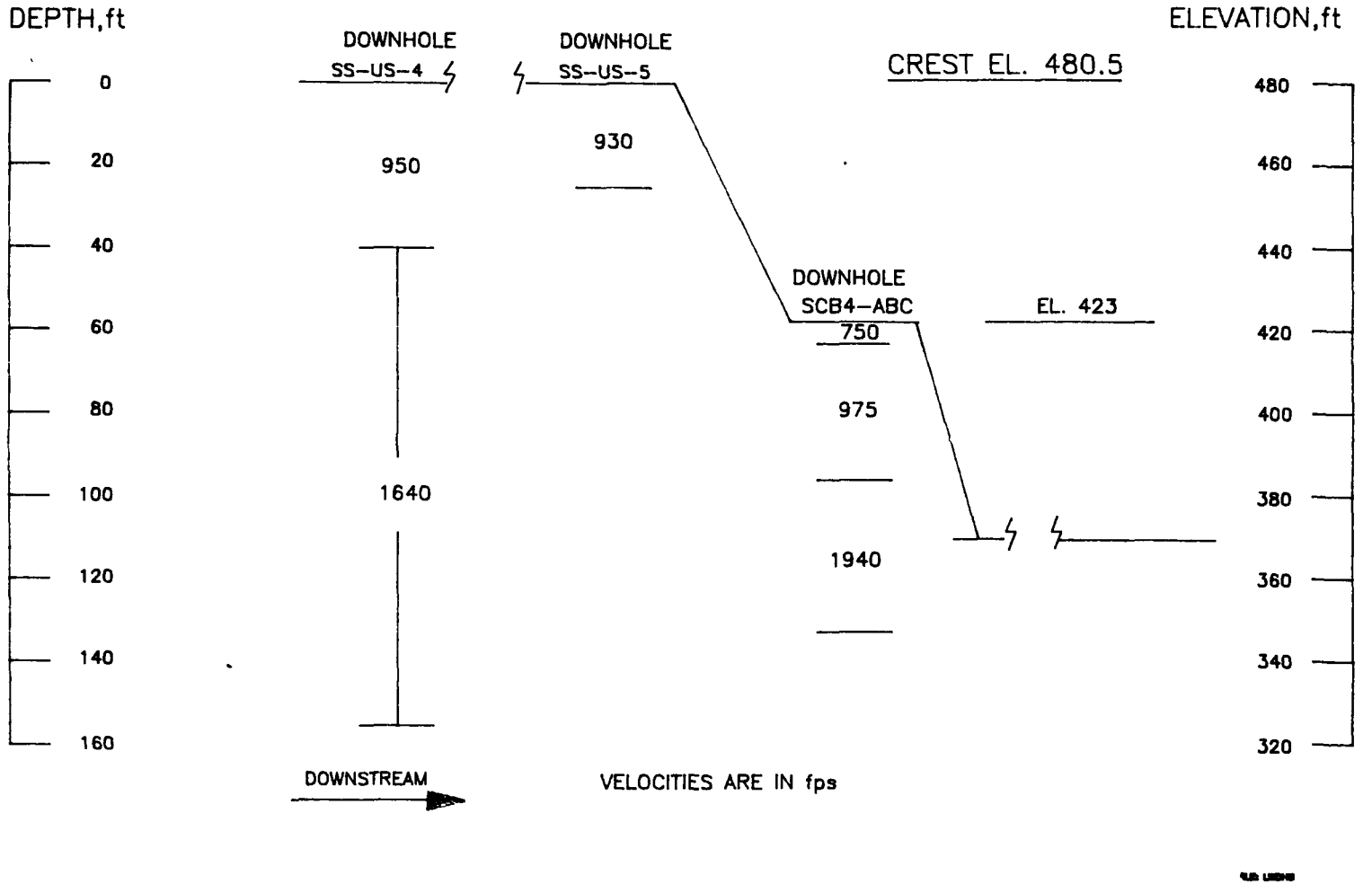

Figure 89. Interpreted S-wave profile from downhole testing, Left Wing Dam

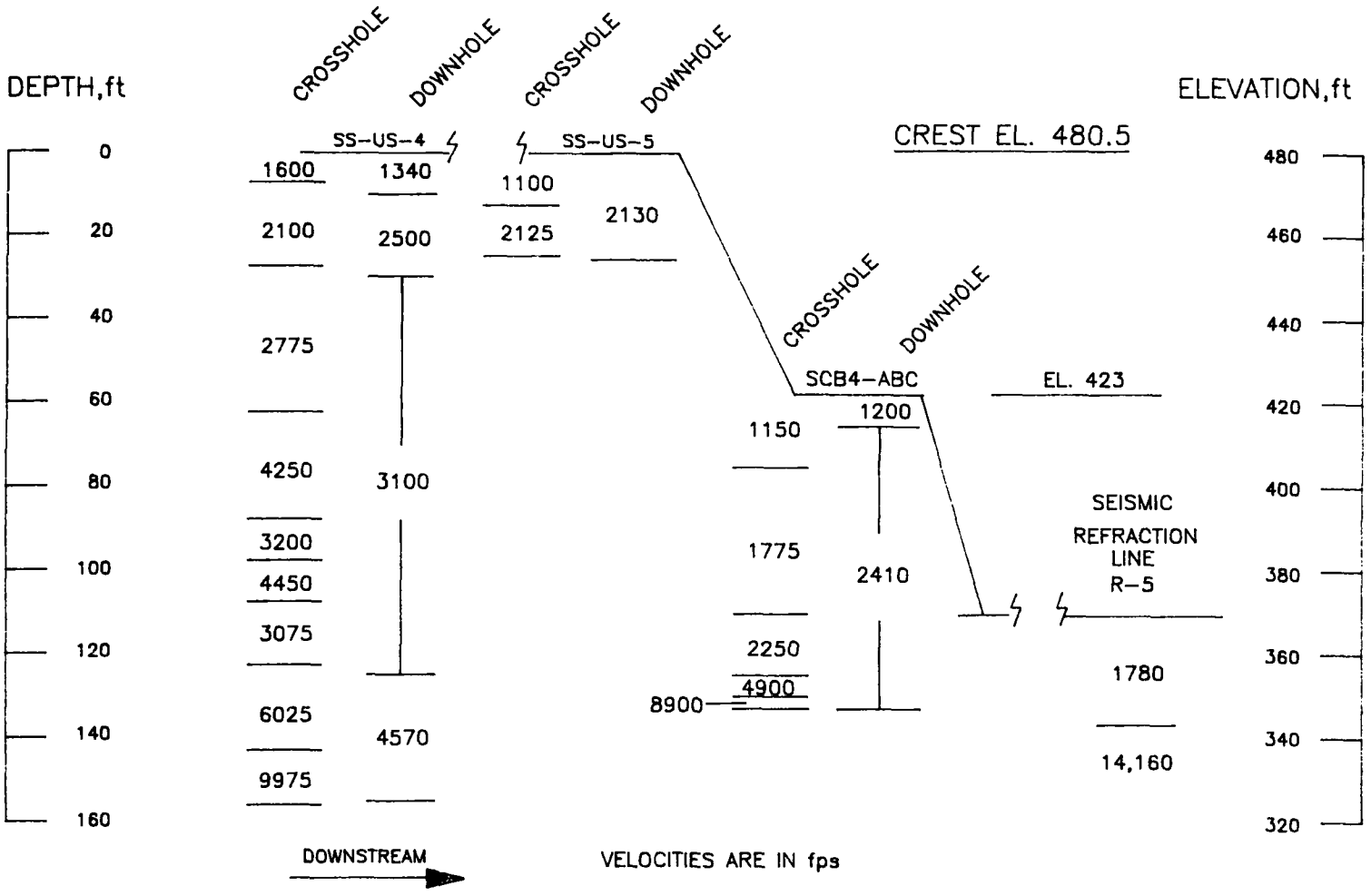

Figure 90. P-wave composite for cross section through Station 303+90 Left Wing Dam

FILE: LWDP

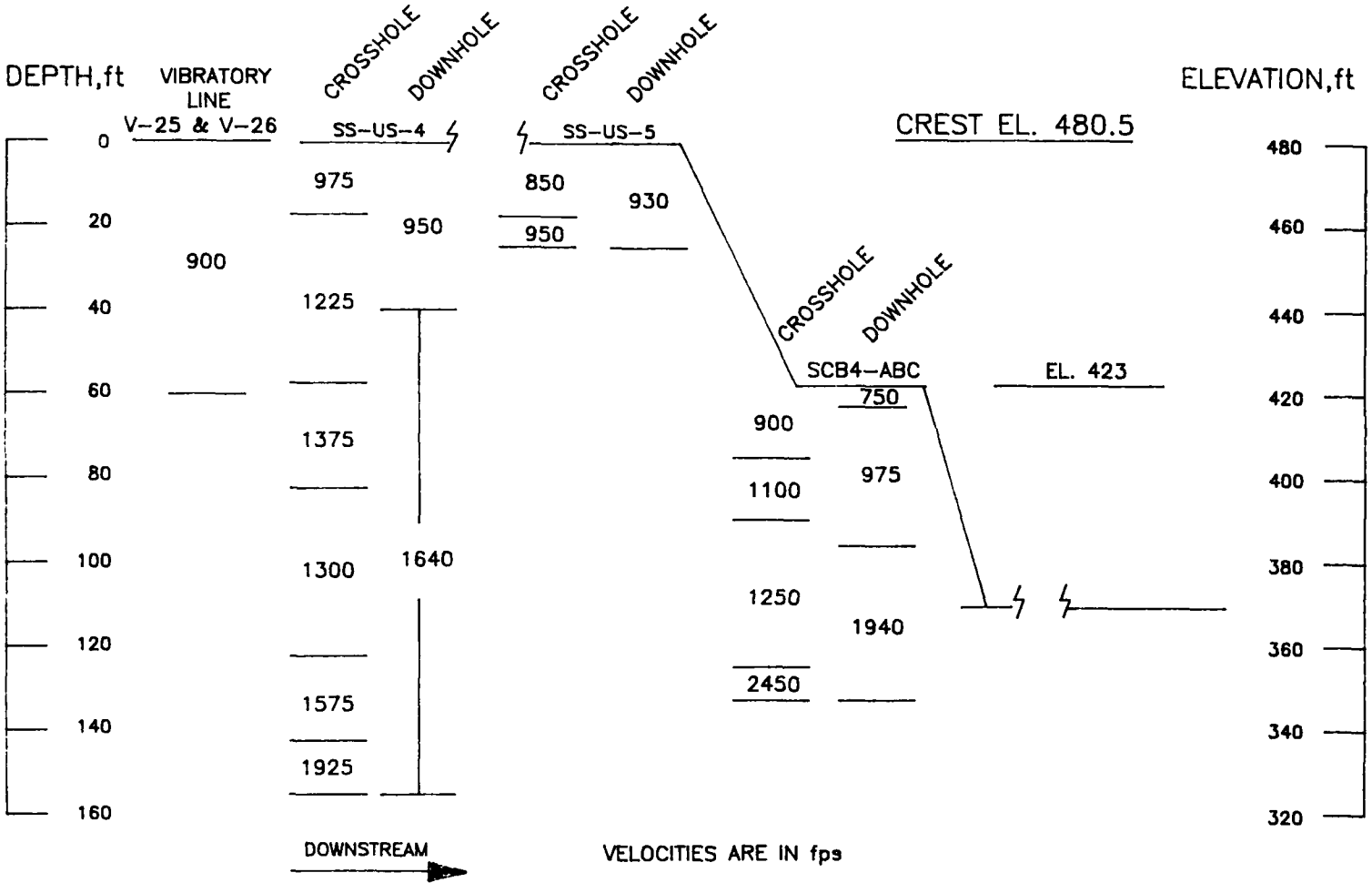

Figure 91. S-wave composite for cross section through Station 303+90 Left Wing Dam

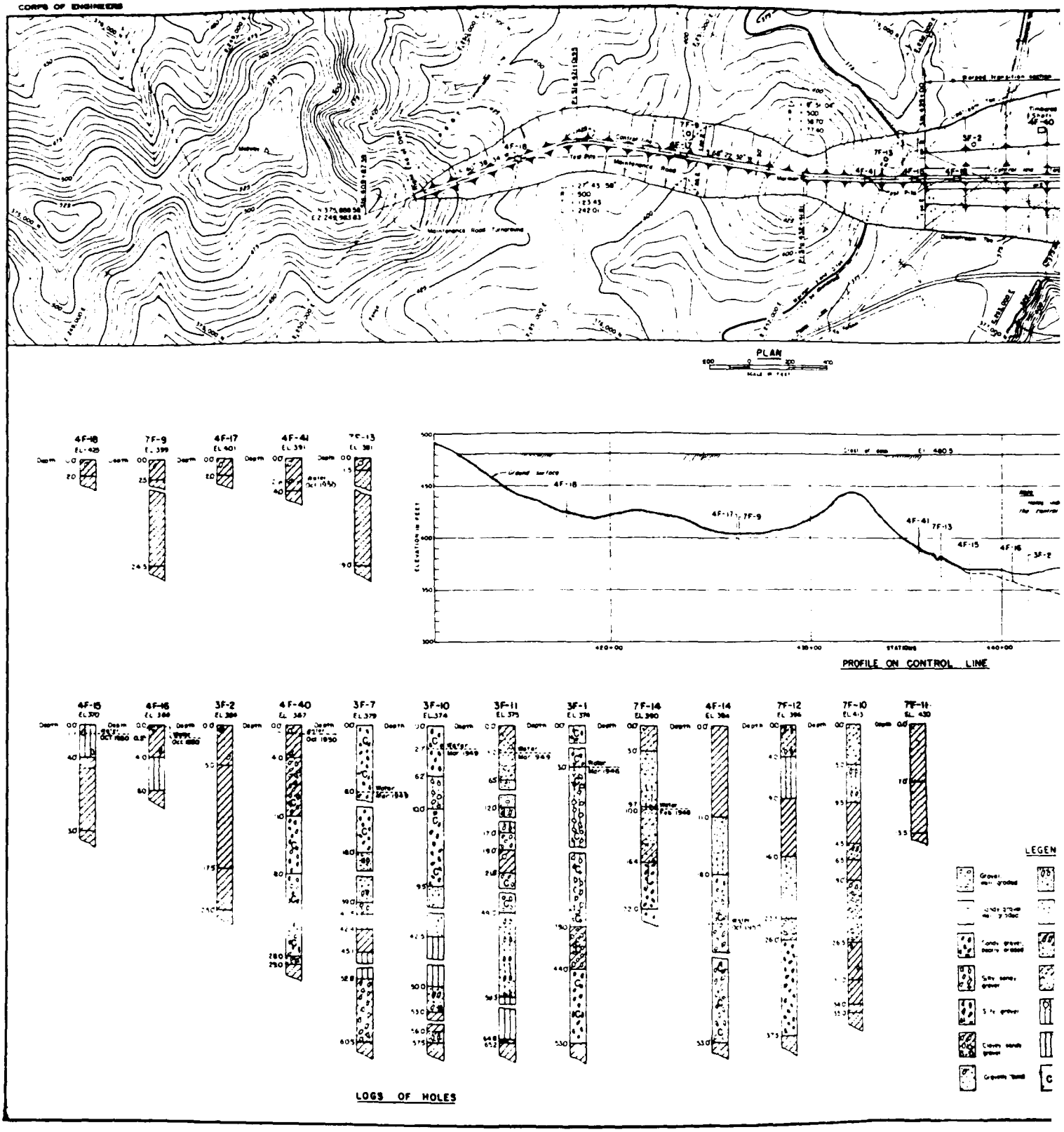

Figure 92. Plan and axial sections of Mormon Island Auxili

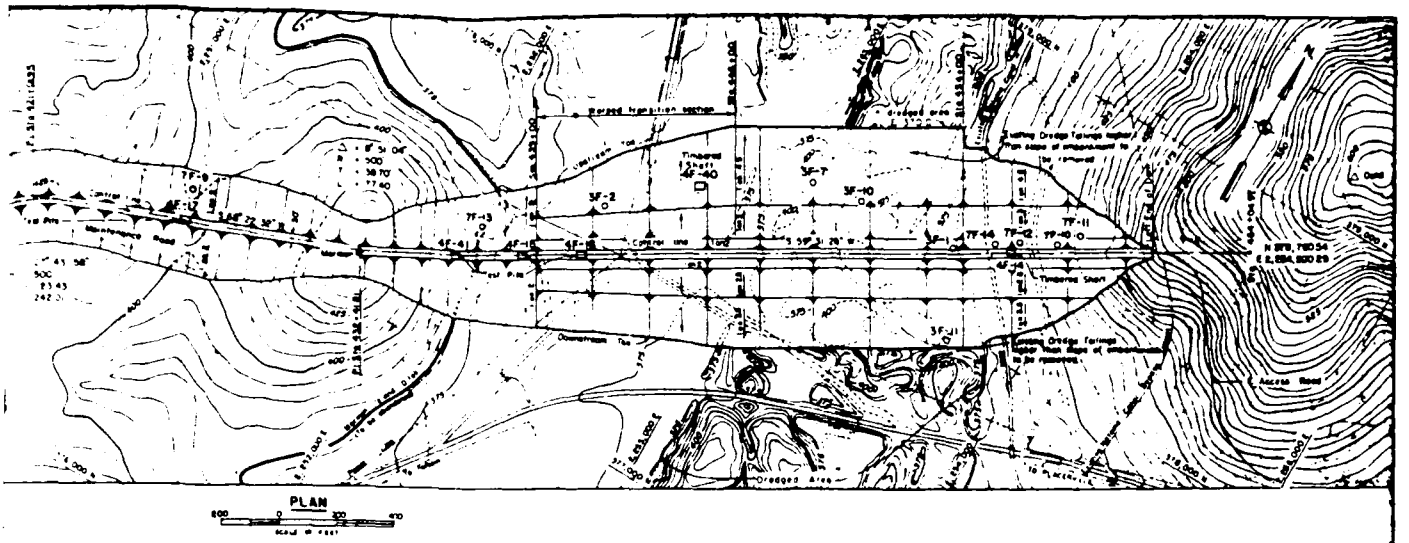

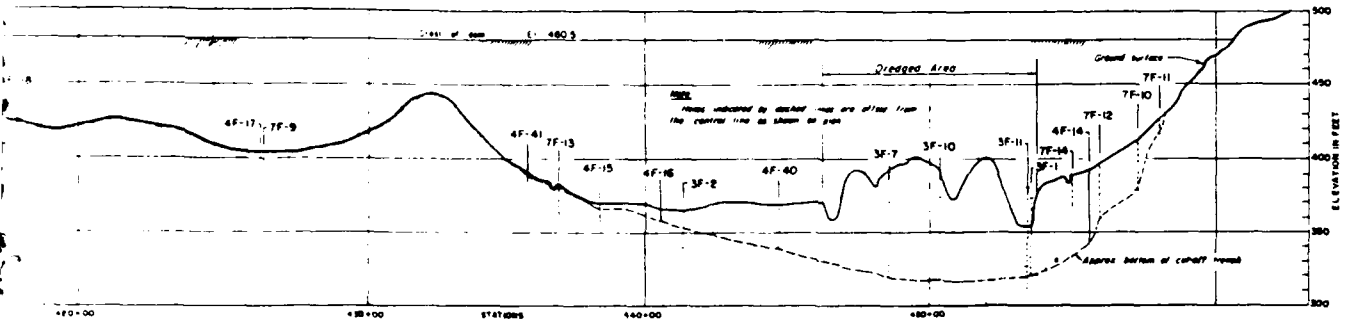

PROFILE ON CONTROL LINE

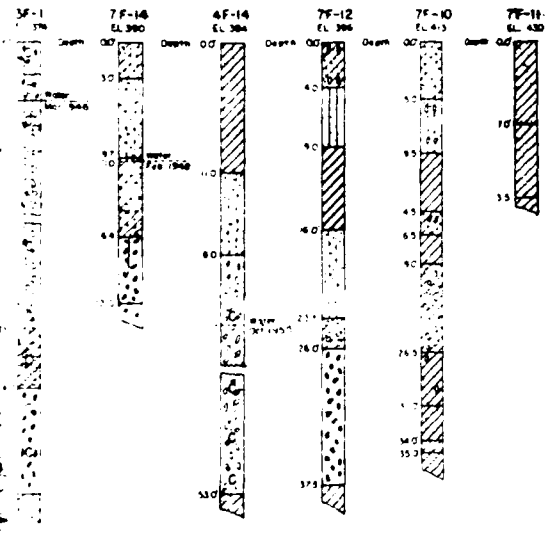

LEGEND

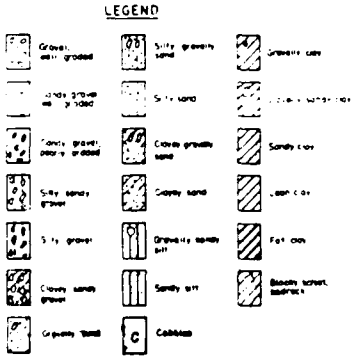

NOTES

1 Datum is Sea Level Datum of 1929.
2 Elevations shown on logs are ground surface elevations.
3 Laboratory classification shown for all materials, according to the Corps of Engineers' Uniform Soils Classification, except those shown in logs of holes 3F-1, 3F-2, 7F-13 and 7F-14, which are field classifications.
4 Holes 3F-1 and 3F-2 were drilled with a 12" churn drill. Holes 3F-7, 3F-10 and 3F-11 were drilled with a 10" churn drill. Samples were taken with a power auger and push tube sampler, where possible.
5 All 4F holes are open pits or shafts.
6 All 7F holes were drilled with a Failing drill rig using a 7" diameter rotary core drill.
7 Typical embankment sections shown on Sheet No. 357/7.
8 Limit of contractors work areas including waste areas are shown on drawing Sheet No. 357/2.
9 Slopes of warped transition vary uniformly from Station 439+00 to 446+00.
10 The term gravel, under the classification system used for this drawing, applies to grain sizes larger than the No. 10 sieve.
11 The term cobbles includes material from 3" to 18" in size and the presence of some is indicated by the letter "C" in the logs.
12 This drawing was taken from As-Constructed sheet no. 357/3, File No. AM-1-9-357.

AMERICAN RIVER BASIN DEVELOPMENT, CALIFORNIA
FOLSOM RESERVOIR PROJECT
AMERICAN RIVER
MORMON ISLAND AUXILIARY DAM
FOUNDATION EXPLORATION
PLAN, PROFILE AND LOGS OF HOLES

357/5

lan and axial sections of Mormon Island Auxiliary Dam

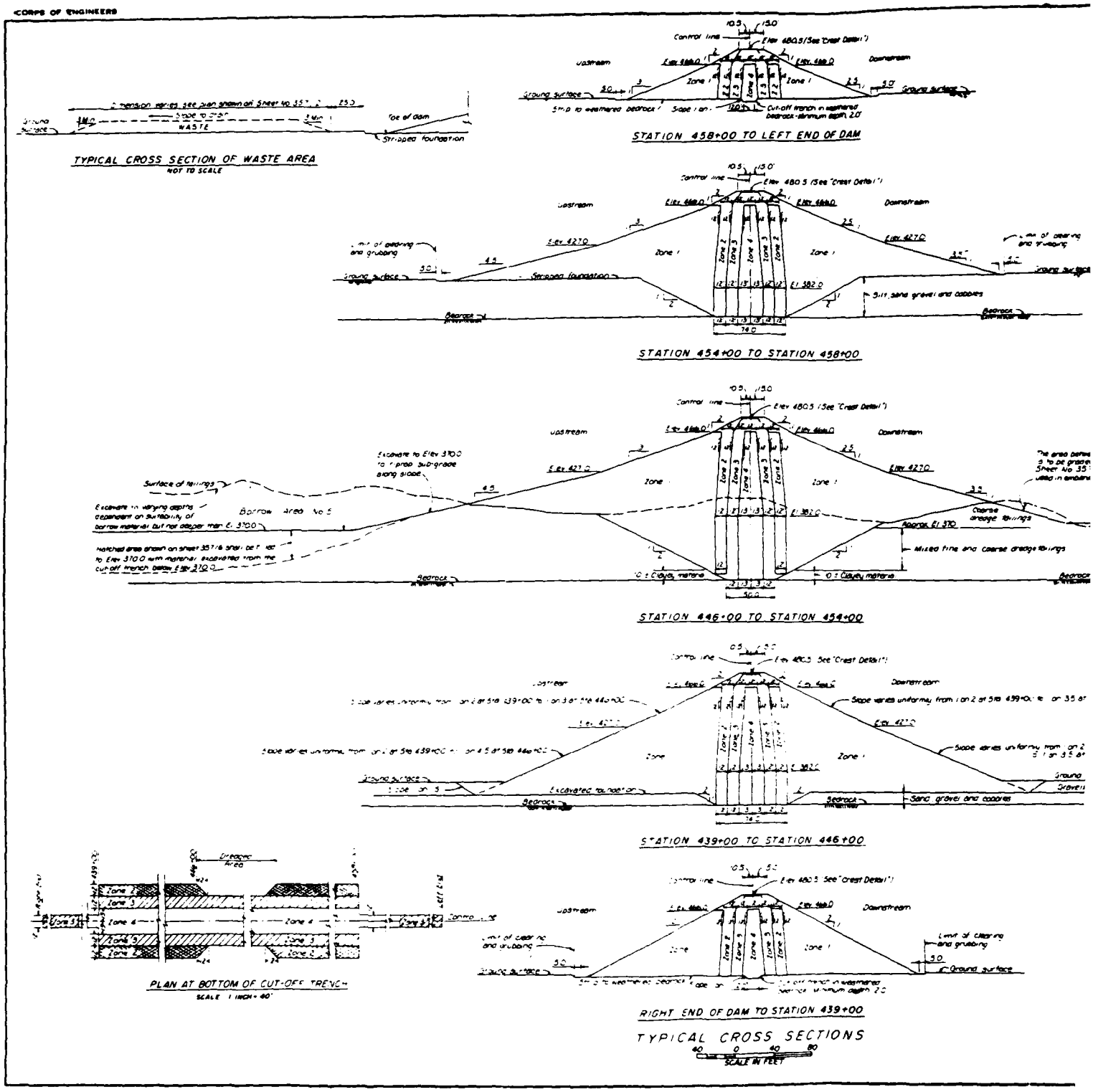

Figure 93. Typical embankment sections of Mormon Island Auxiliary

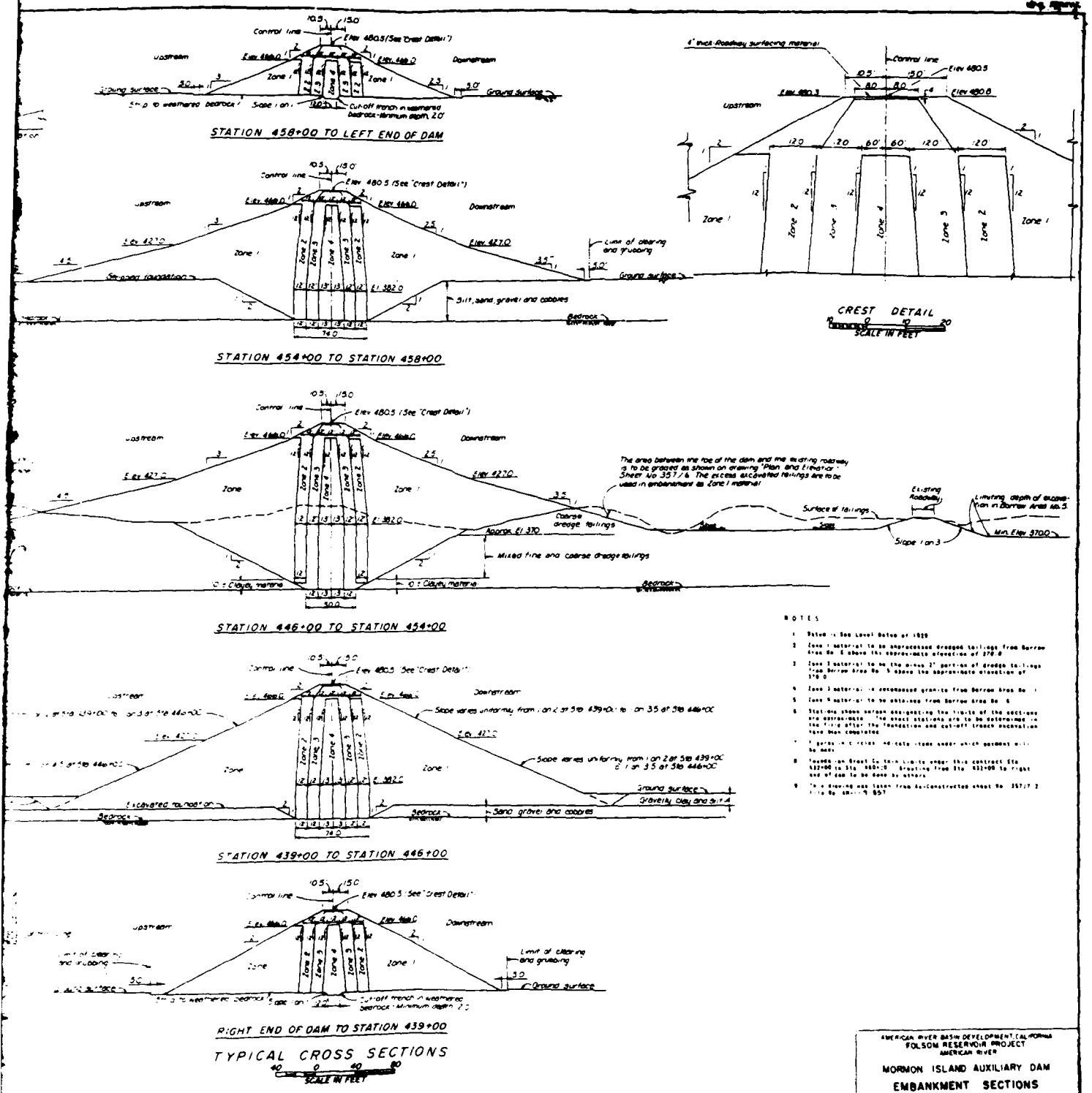

93. Typical embankment sections of Mormon Island Auxiliary Dam

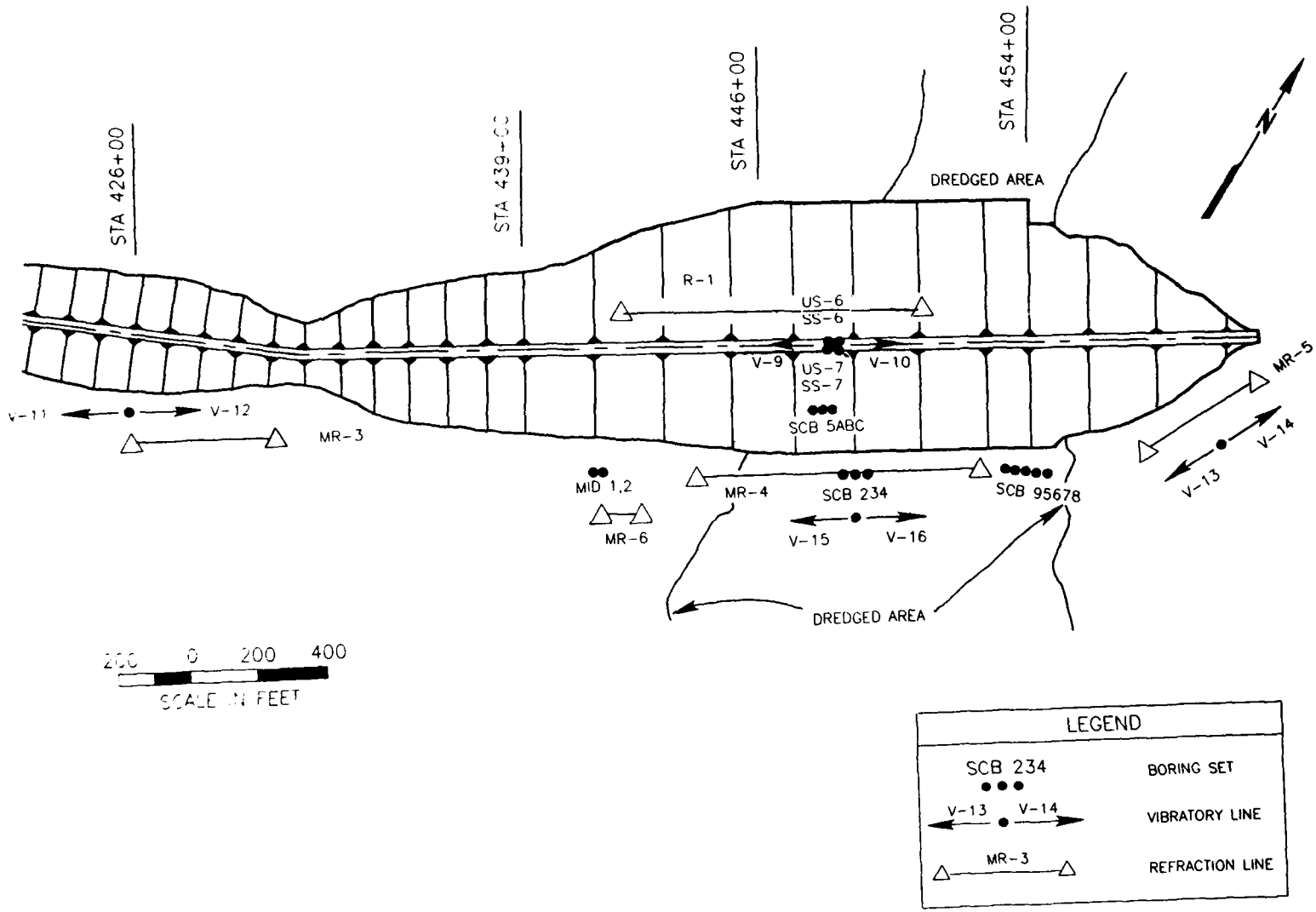

Figure 94. Test layout for Mormon Island Auxiliary Dam

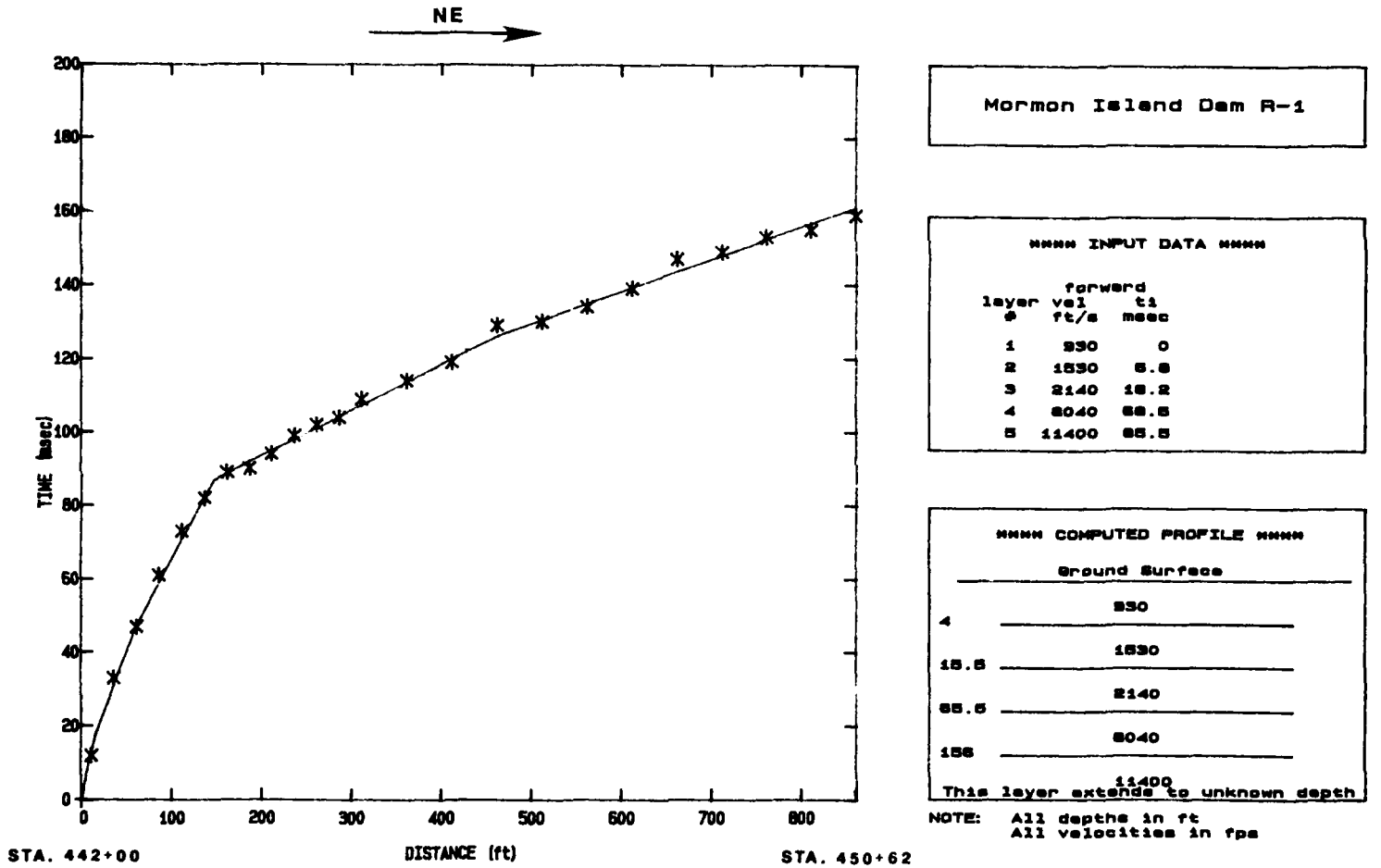

Figure 95. Seismic refraction line R-1, crest

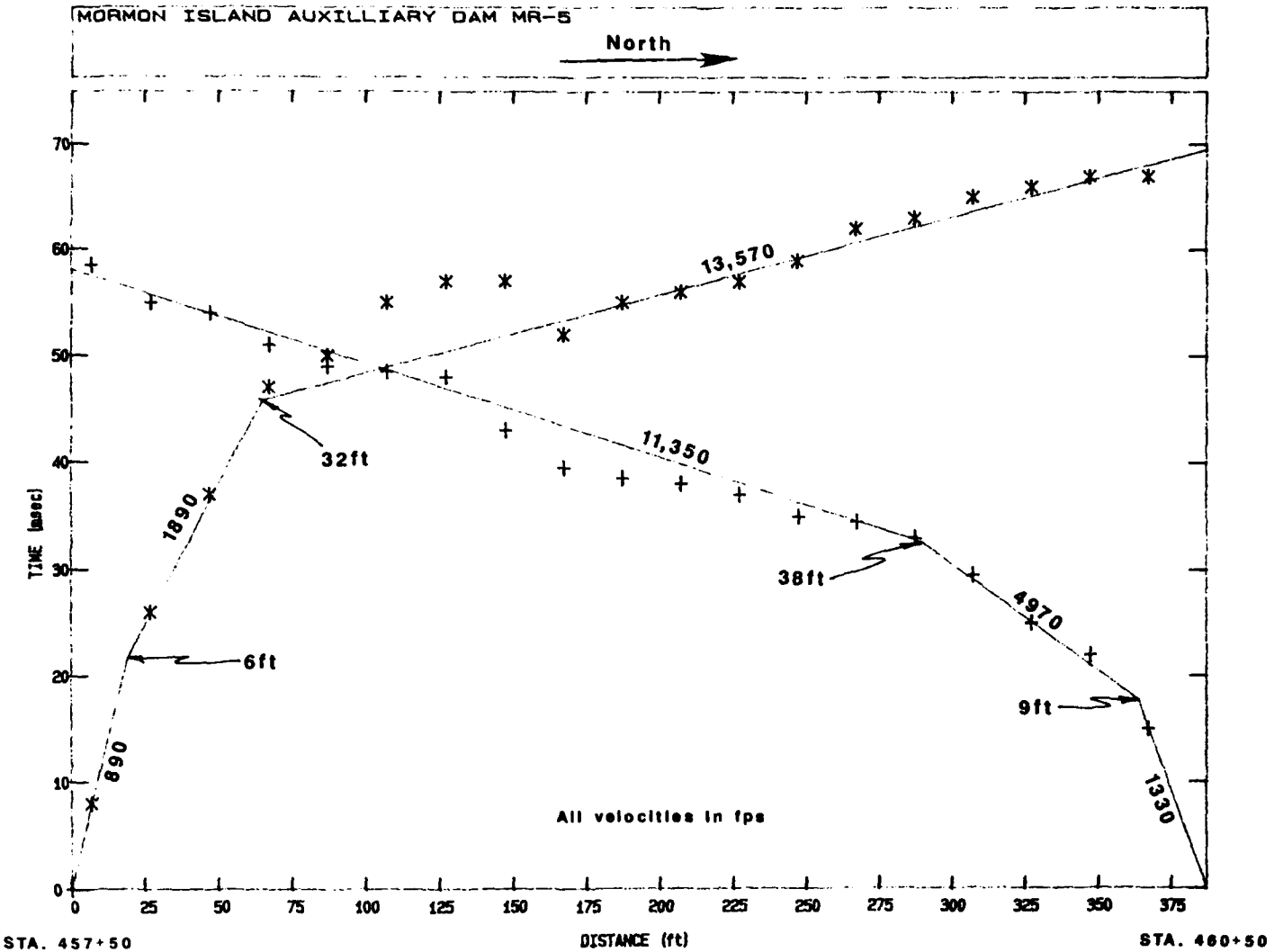

Figure 96. Seismic refraction line MR-5, toe left abutment

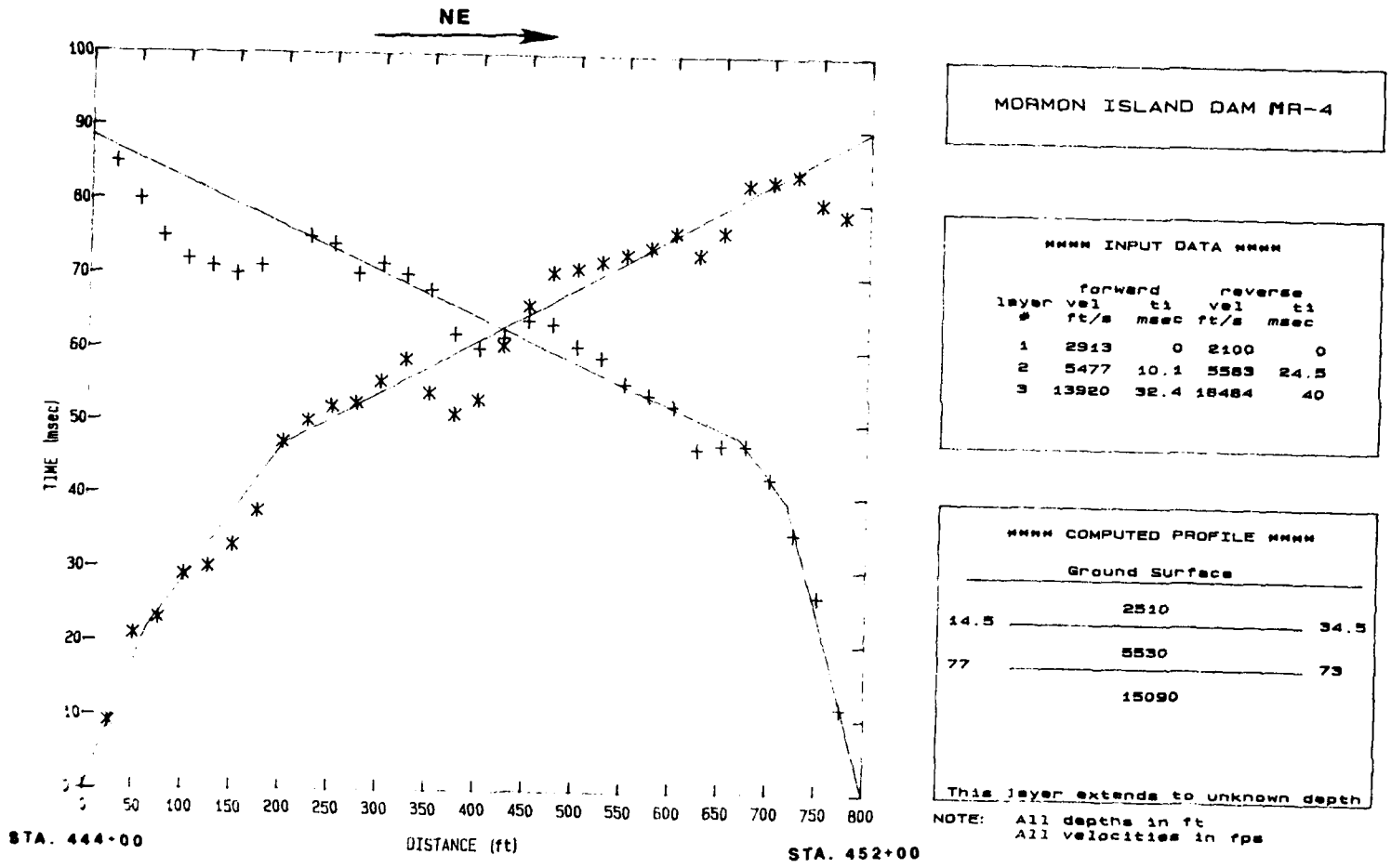

Figure 97. Seismic refraction line MR-4, toe

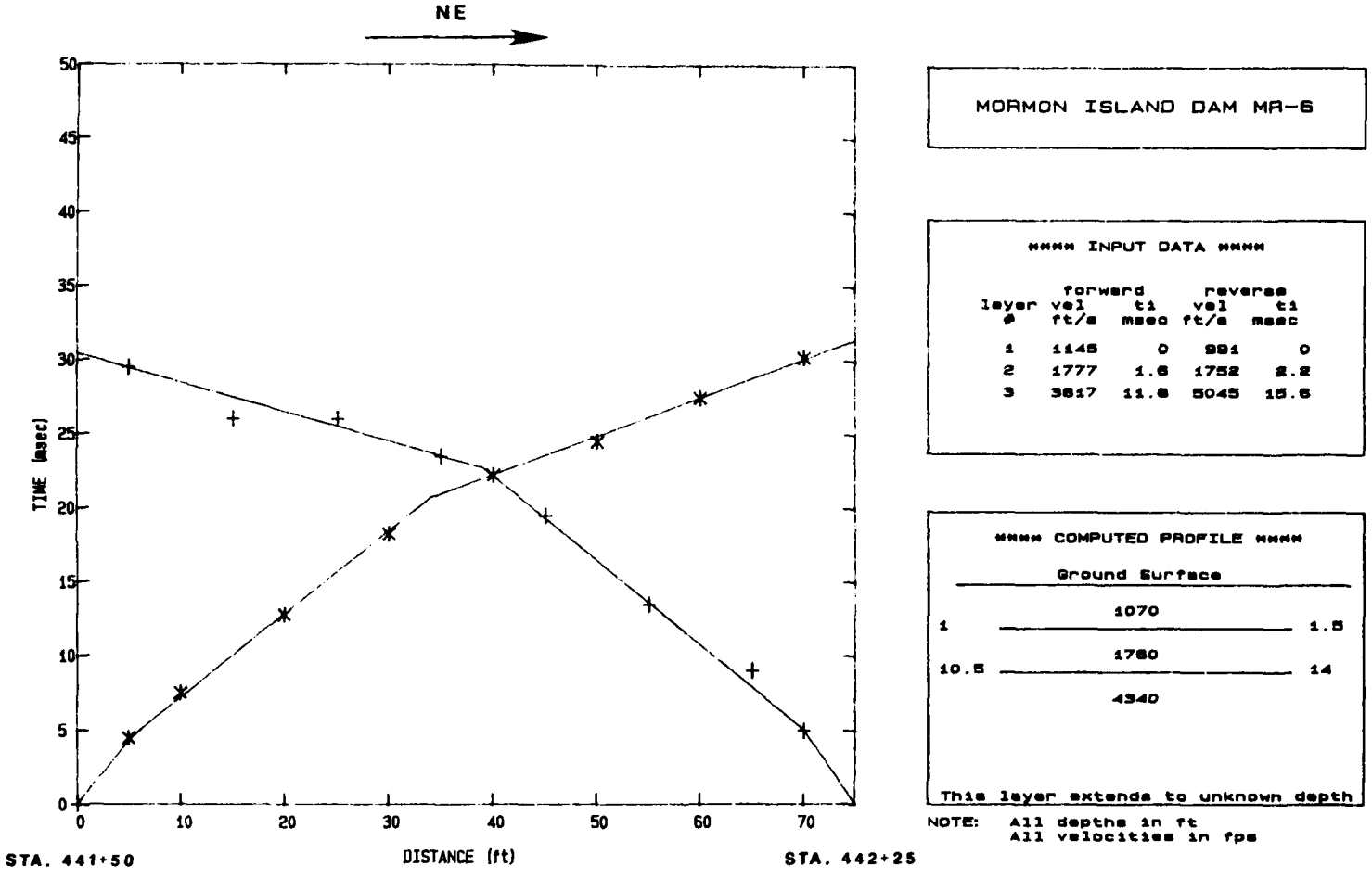

Figure 98. Seismic refraction line MR-6, toe

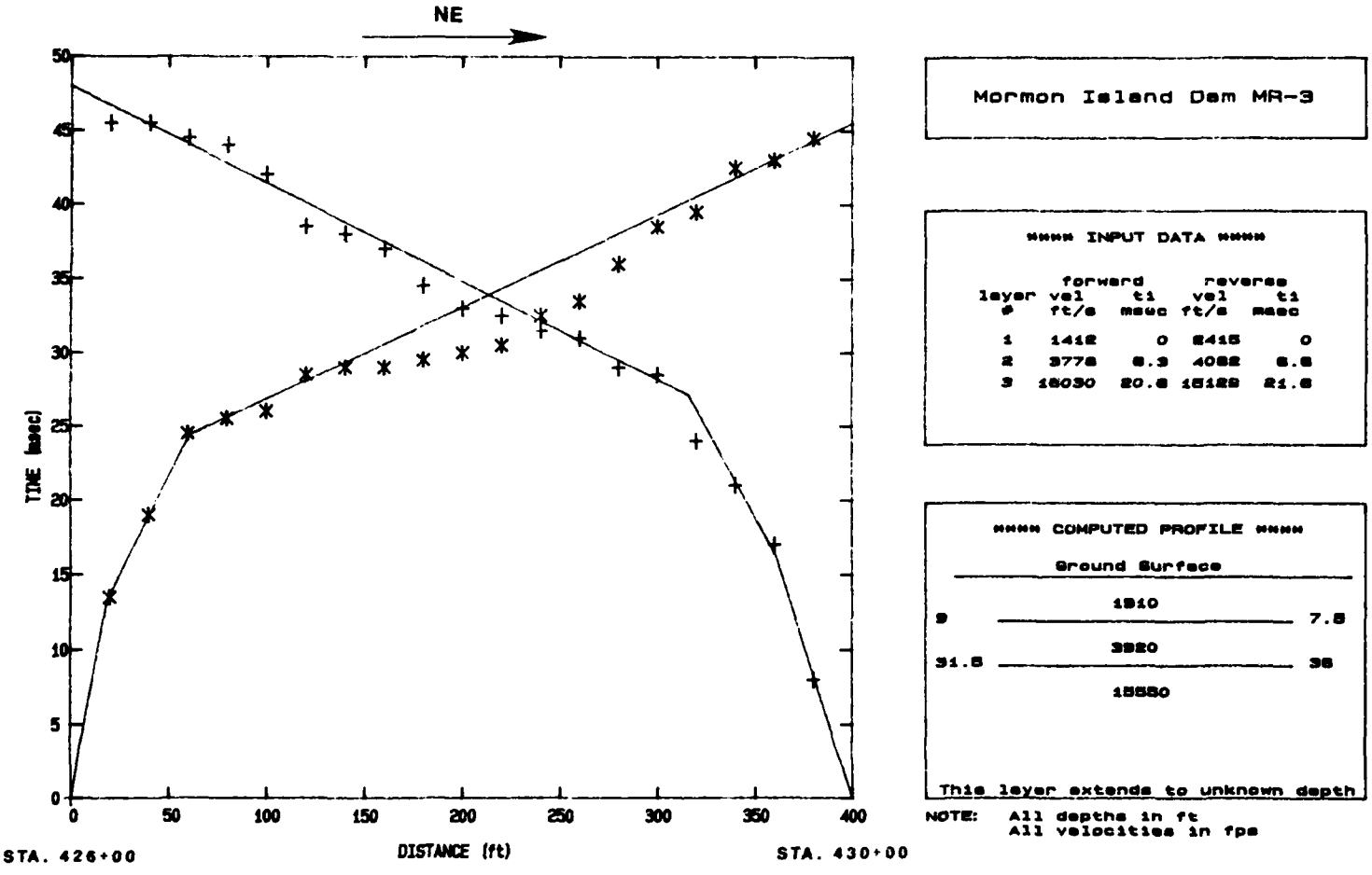

Figure 99. Seismic refraction line MR-3, toe

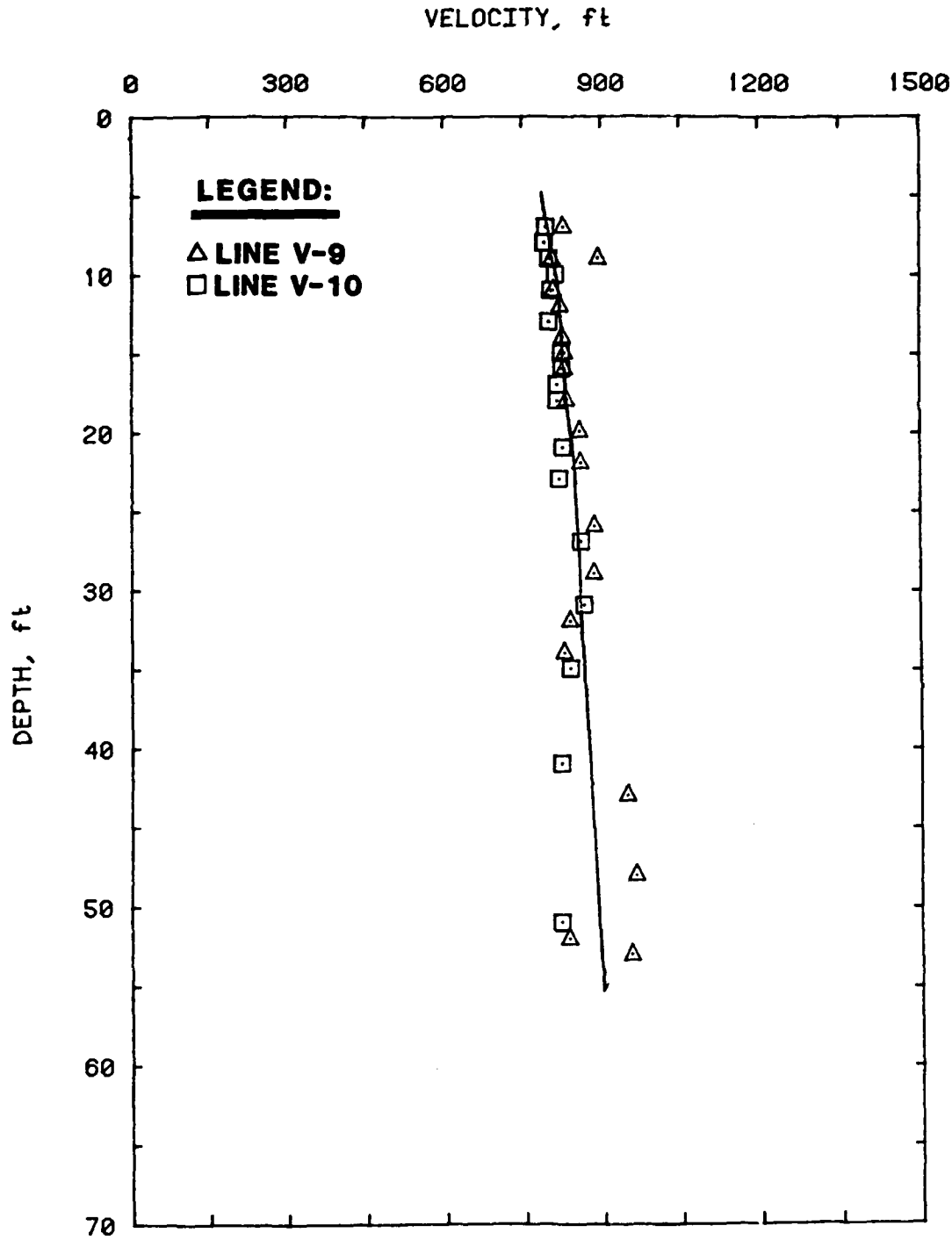

Figure 100. R-wave velocity versus depth for lines V-9 and V-10, crest, approximate Station 450+00

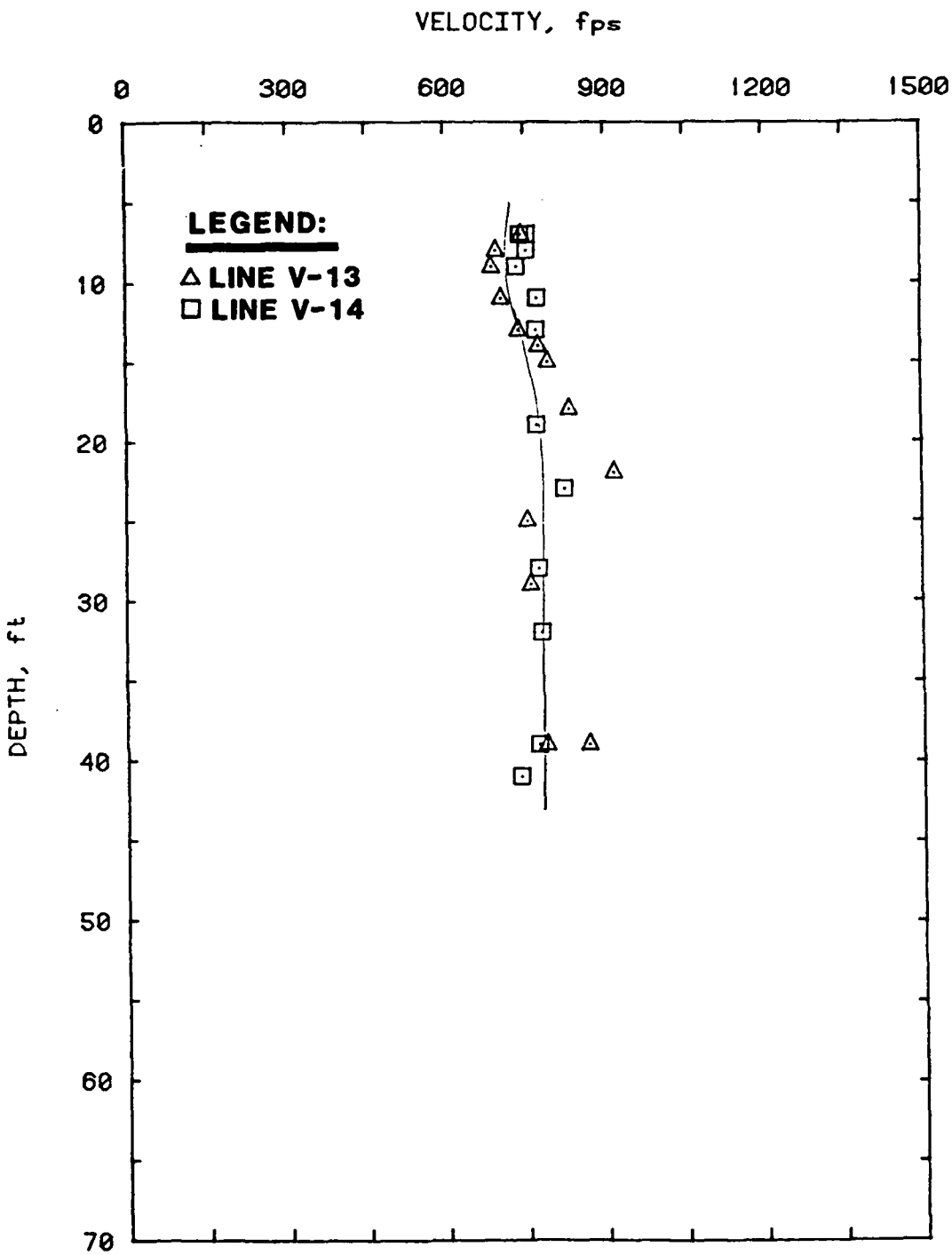

Figure 101. R-wave velocity versus depth for lines V-13 and V-14, toe of right abutment, approximate Station 459+50

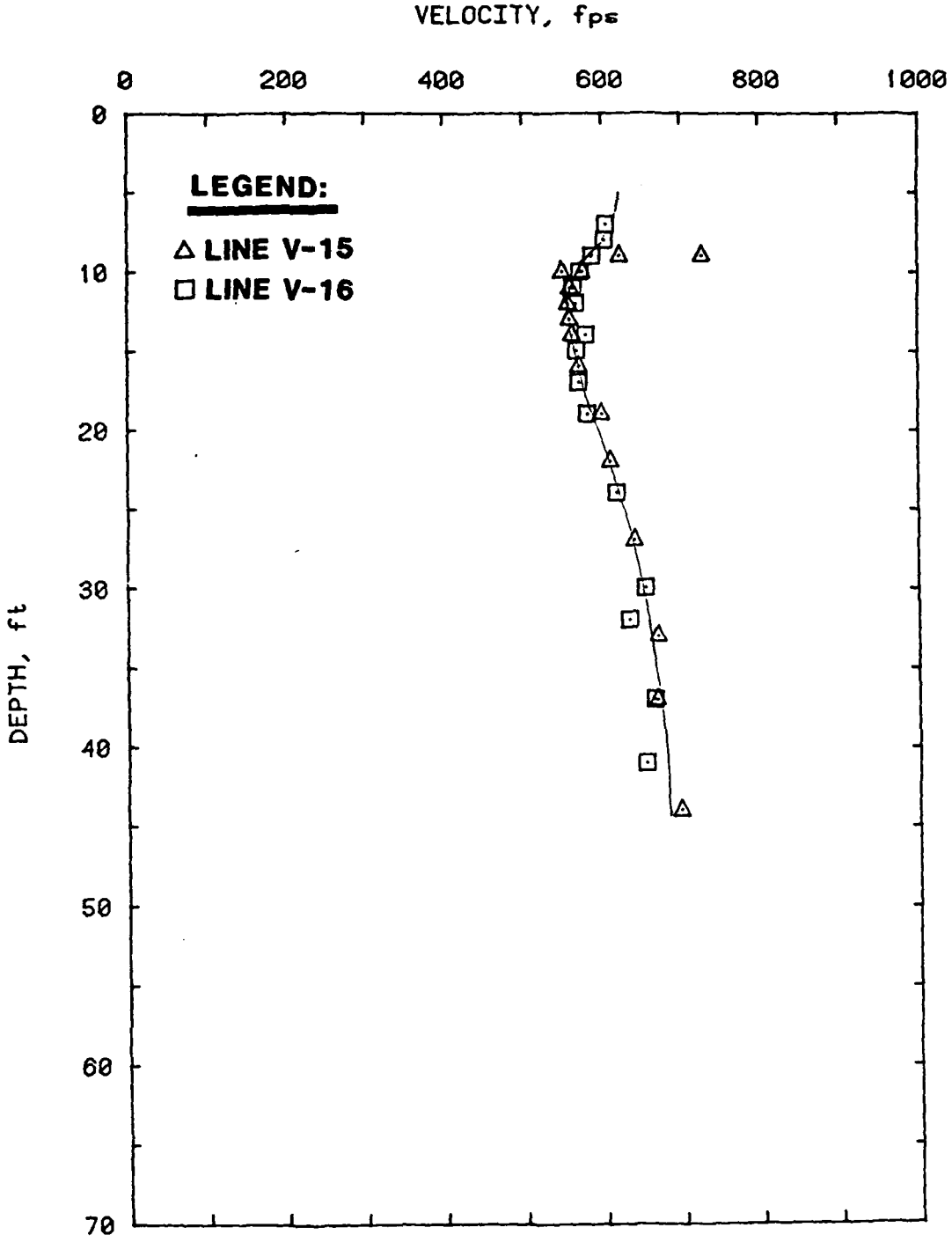

Figure 102. R-wave velocity versus depth for lines V-15 and V-16, toe, approximate Station 448+50

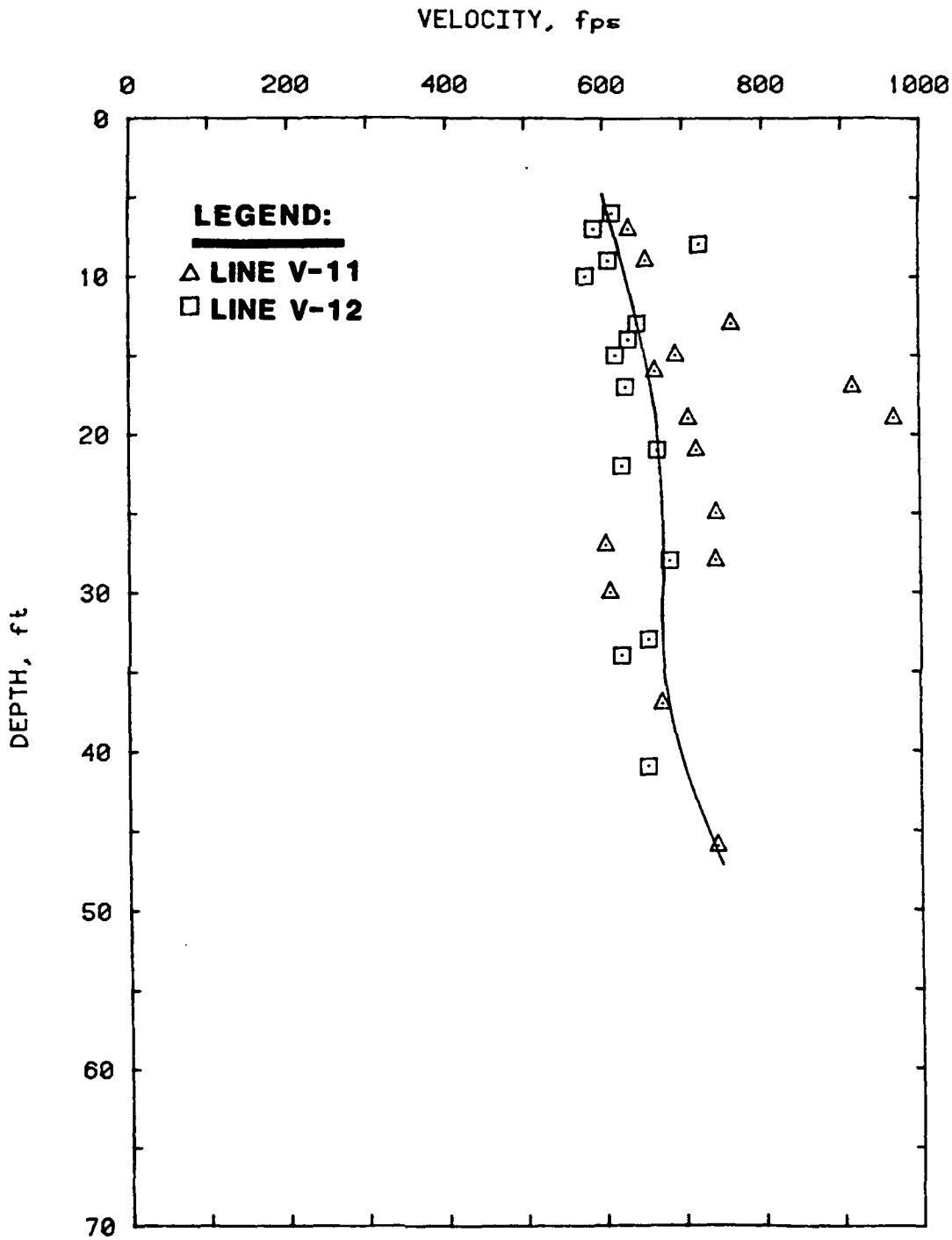

Figure 103. R-wave velocity versus depth for lines V-11 and V-12, toe, approximate Station 425+80

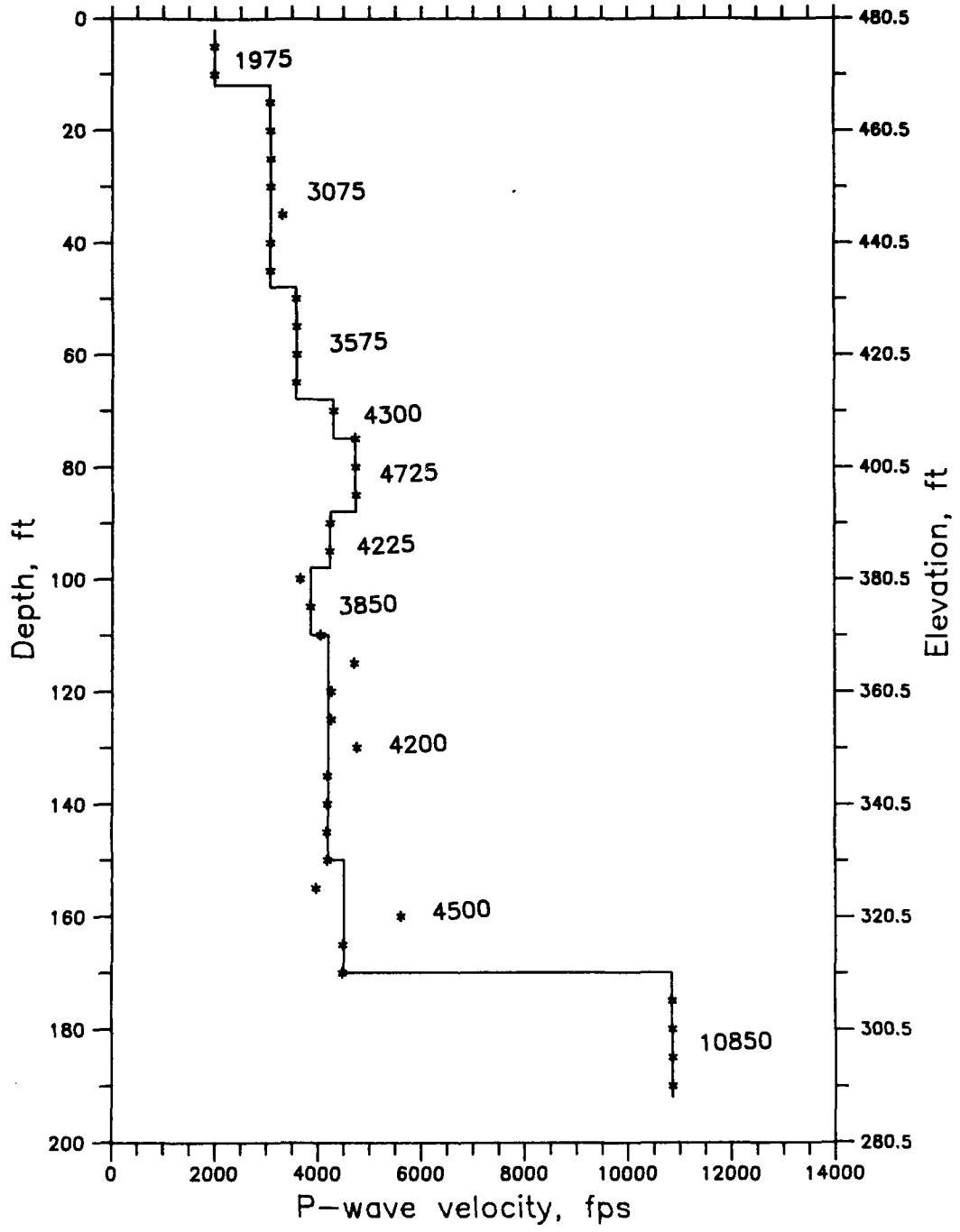

Figure 104. Crosshole P-wave results, centerline

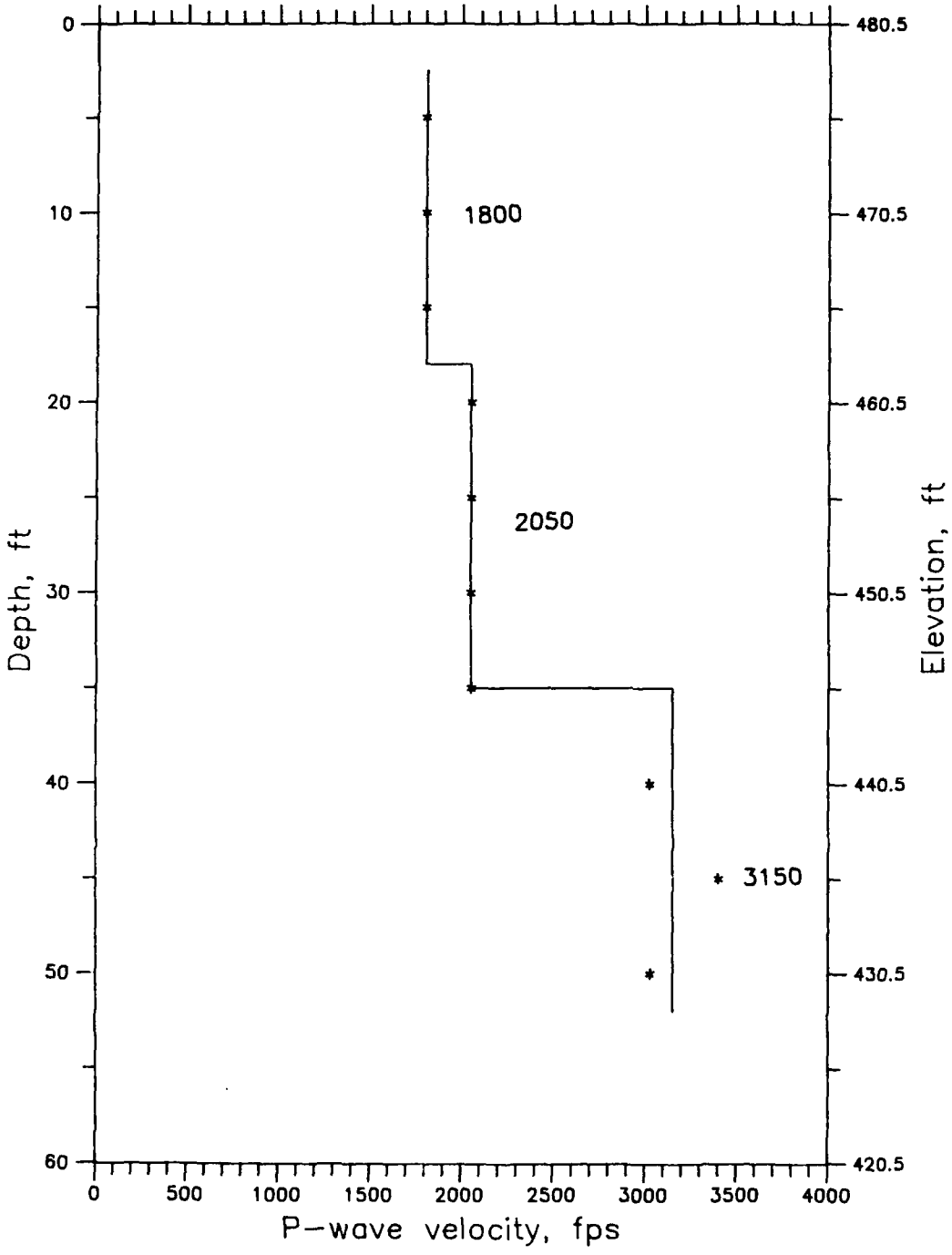

Figure 105. Crosshole P-wave results, downstream shoulder

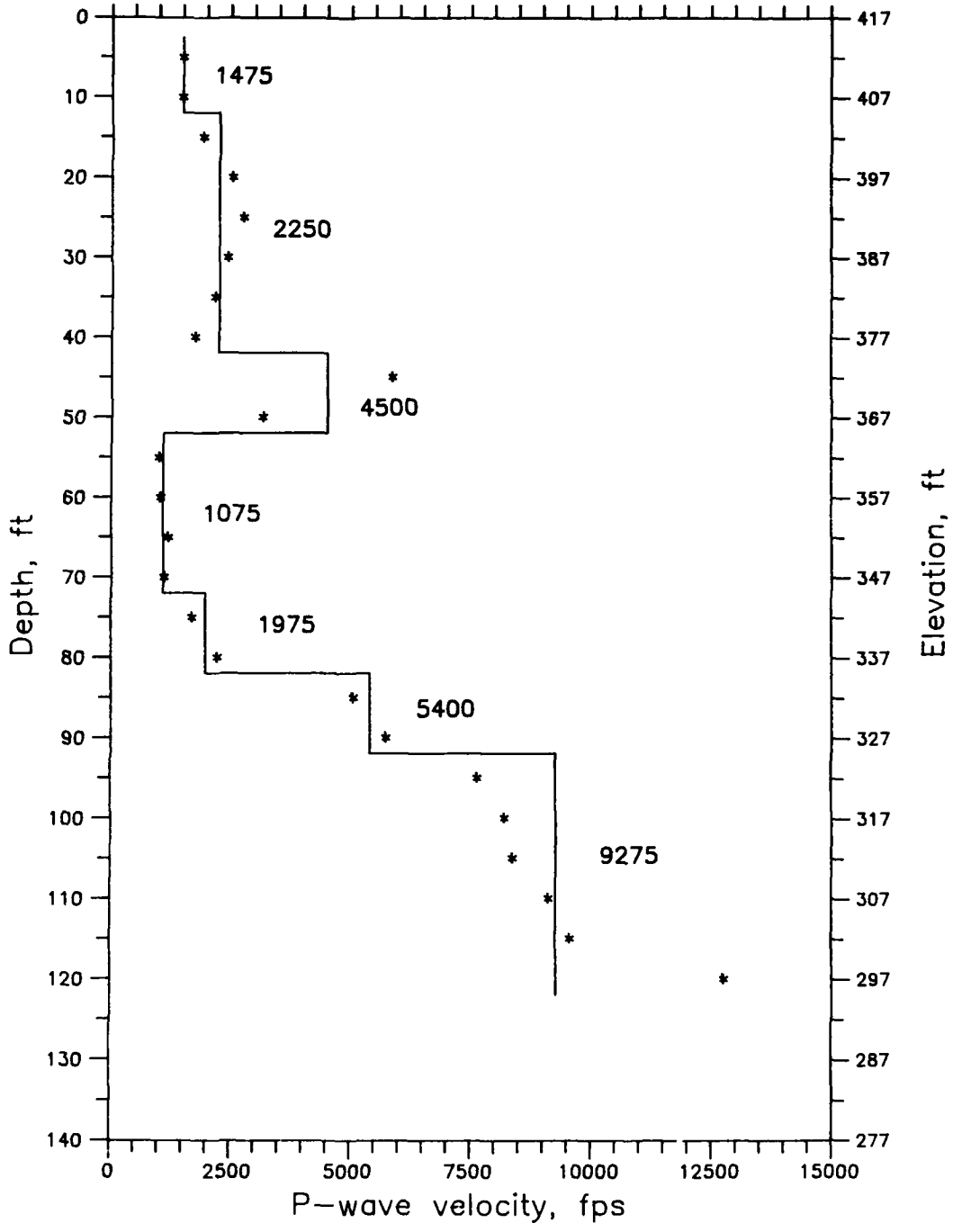

Figure 106. Crosshole P-wave results, downstream slope

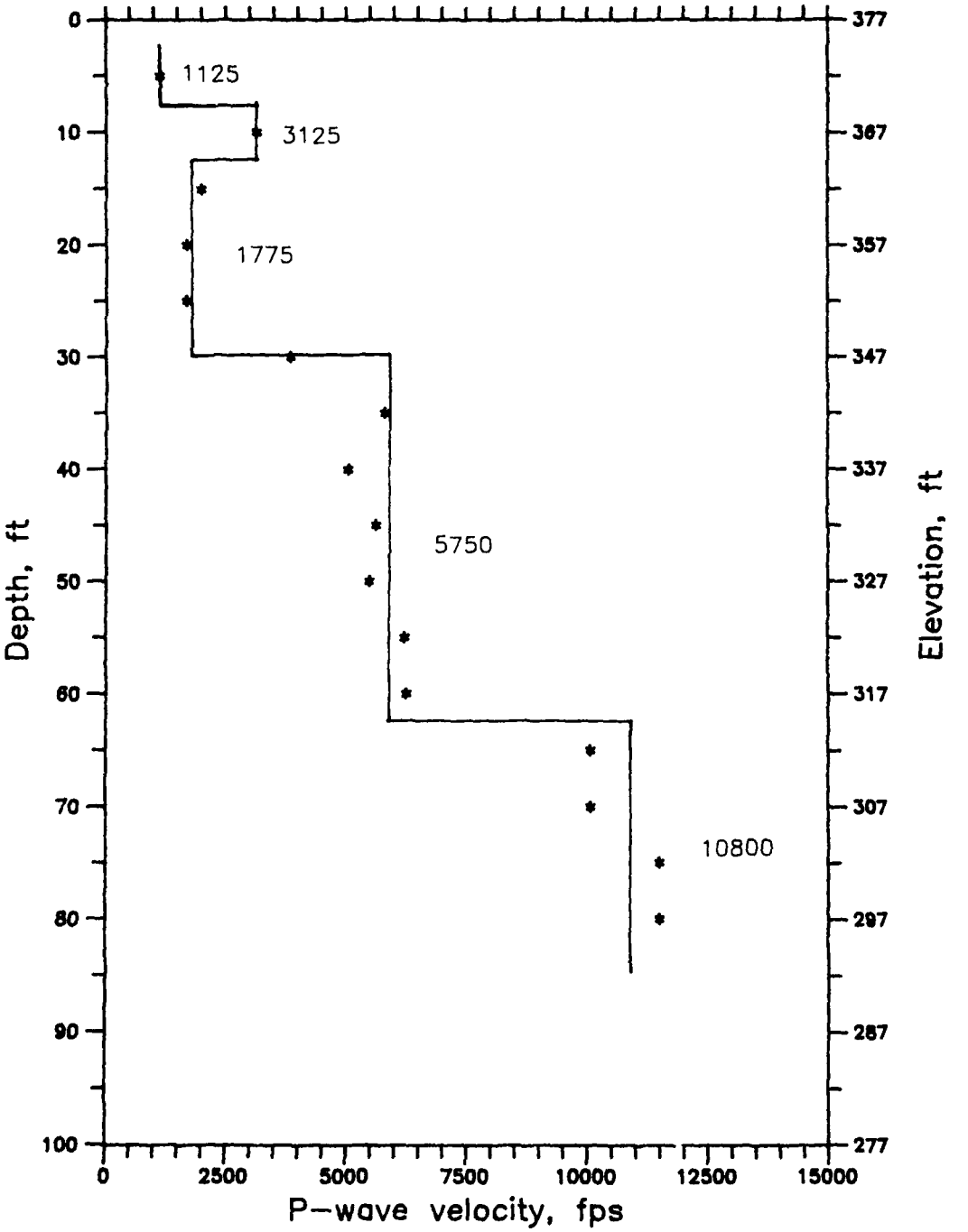

Figure 107. Crosshole P-wave results, SCB-9,5,6,7,8, toe

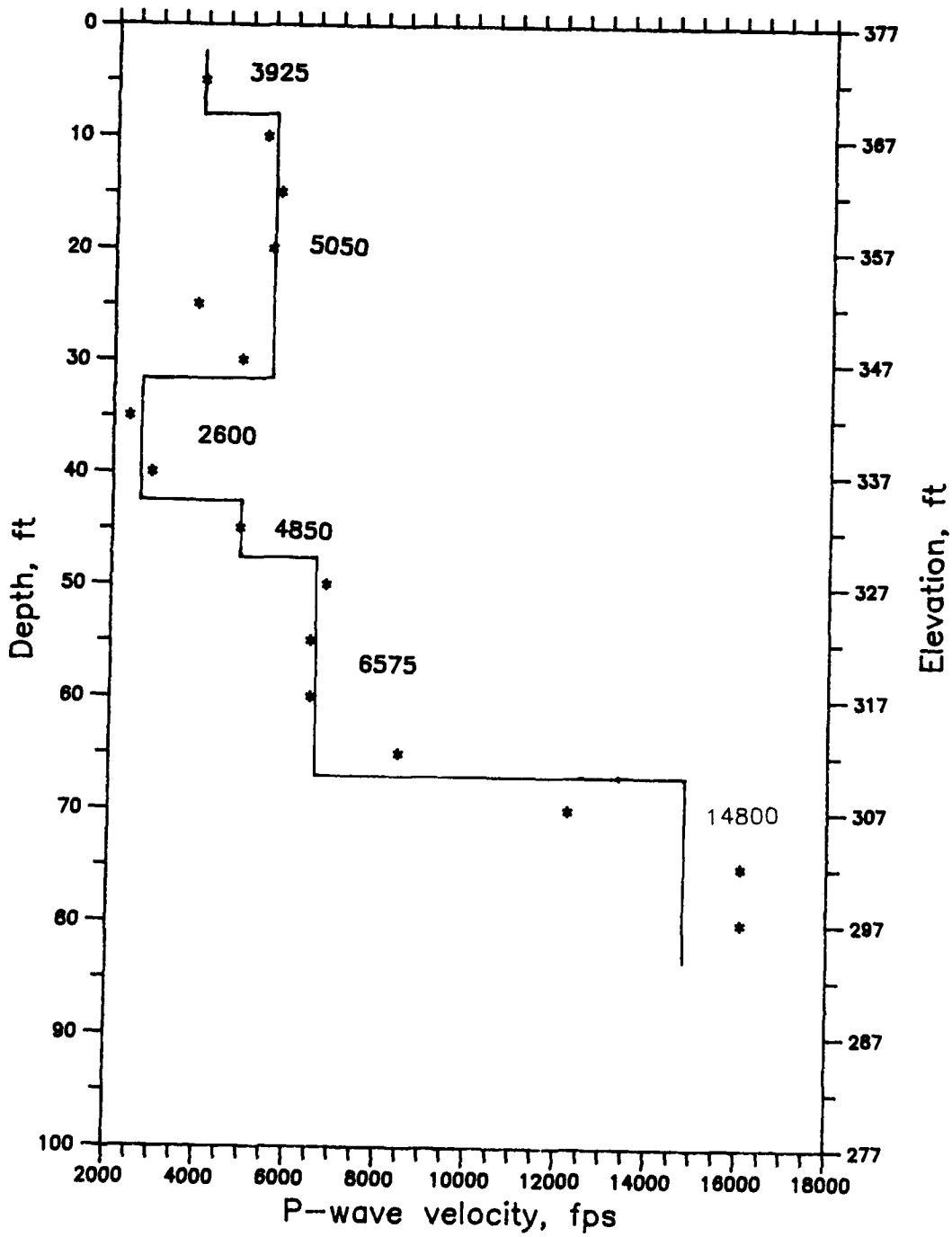

Figure 108. Crosshole P-wave results, SCB-2,3,4, toe

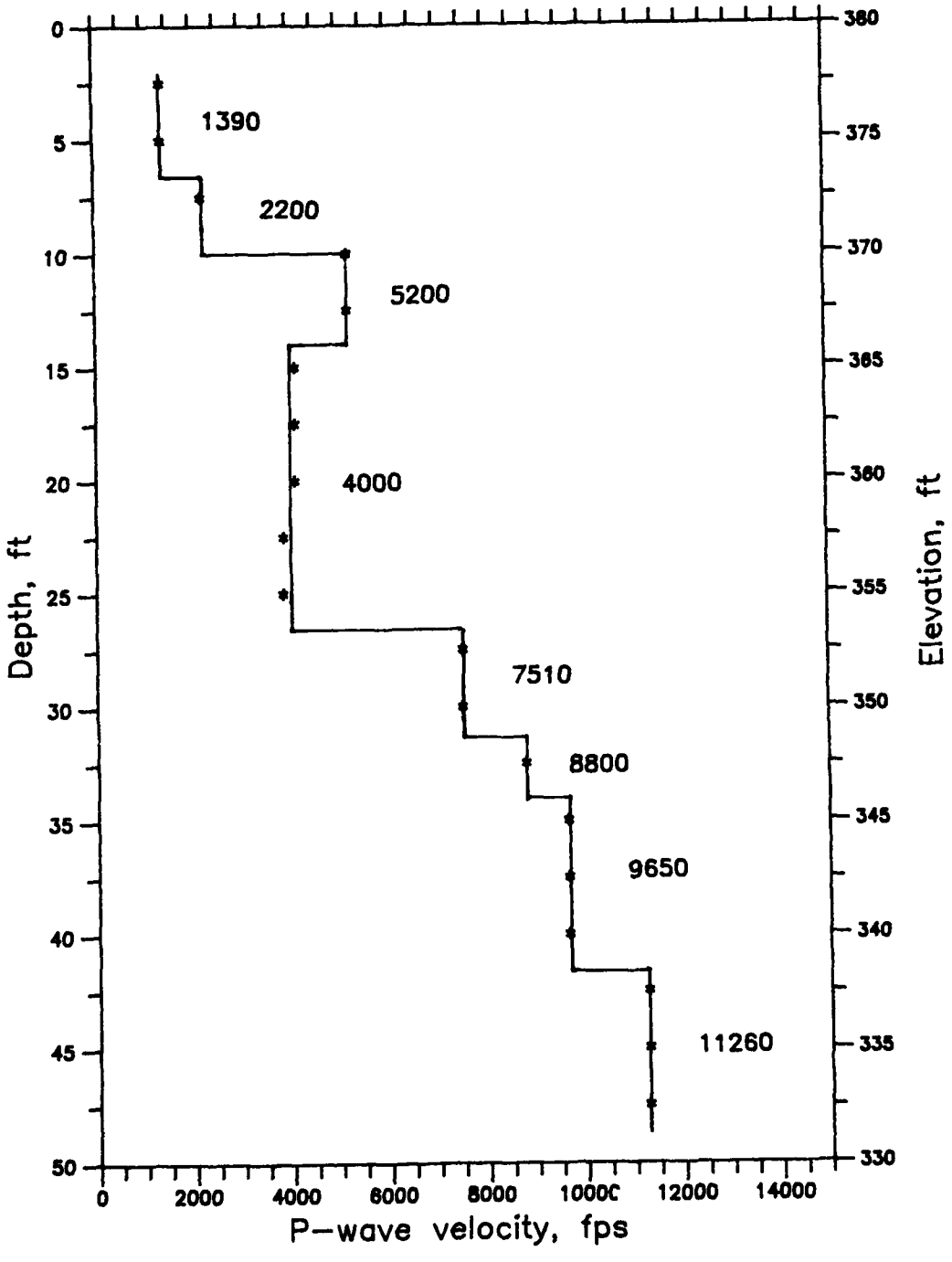

Figure 109. Crosshole P-wave results, MID-1,2, toe

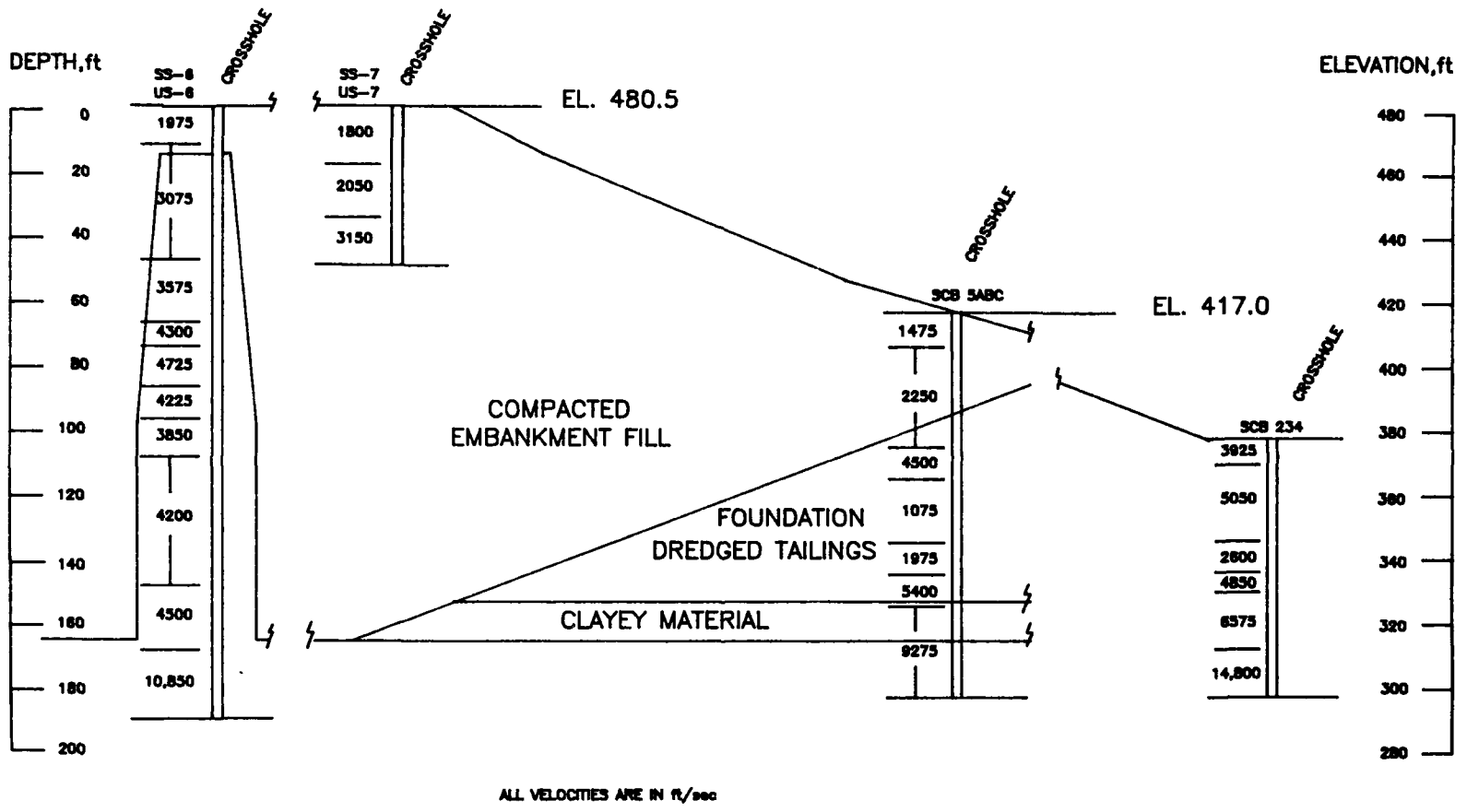

Figure 110. Interpreted P-wave profile from crosshole testing for the section through Station 448+00, Mormon Island Auxiliary Dam

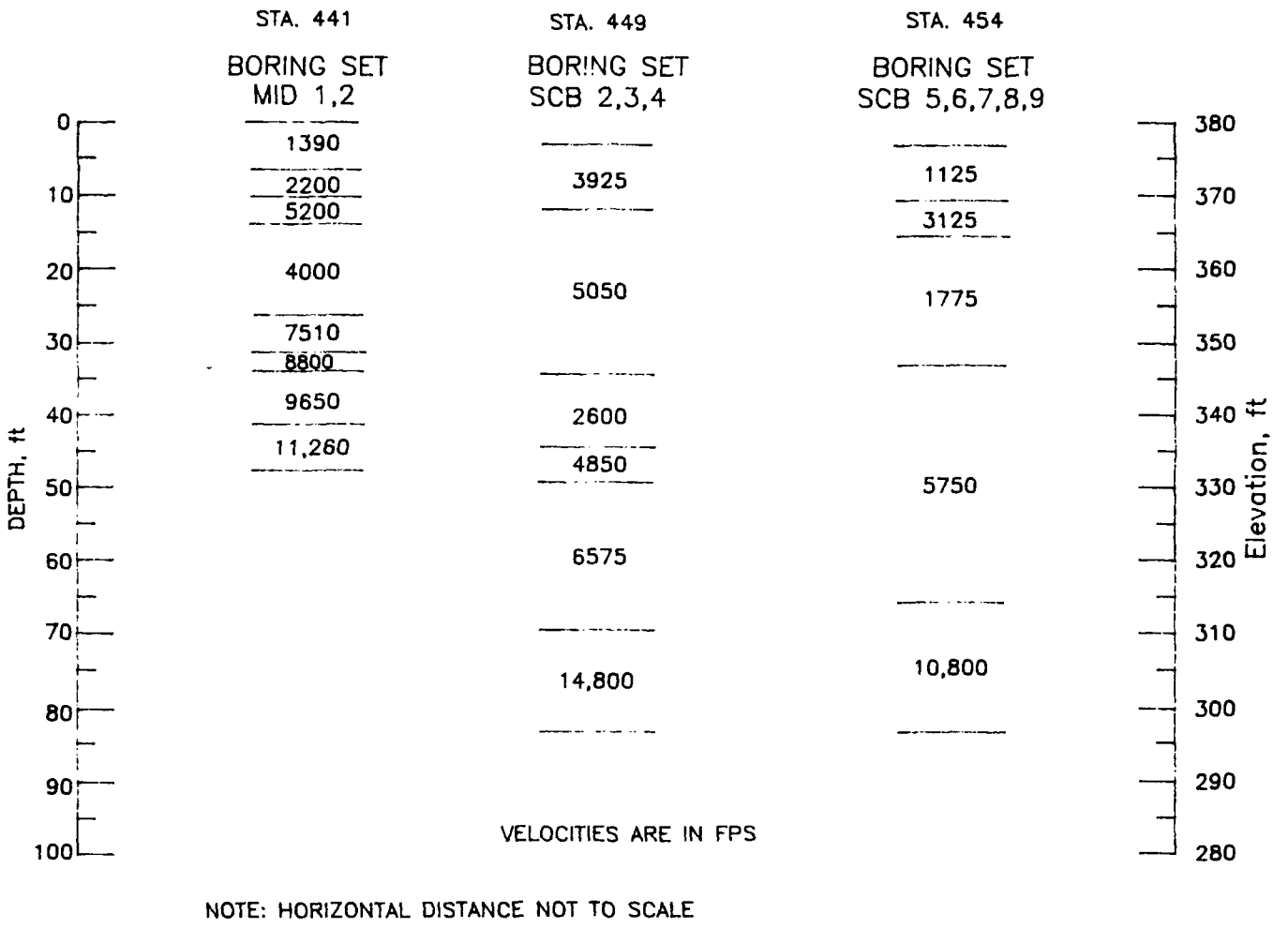

Figure 111. Interpreted P-wave profile from crosshole testing along the downstream toe of Mormon Island Auxiliary Dam

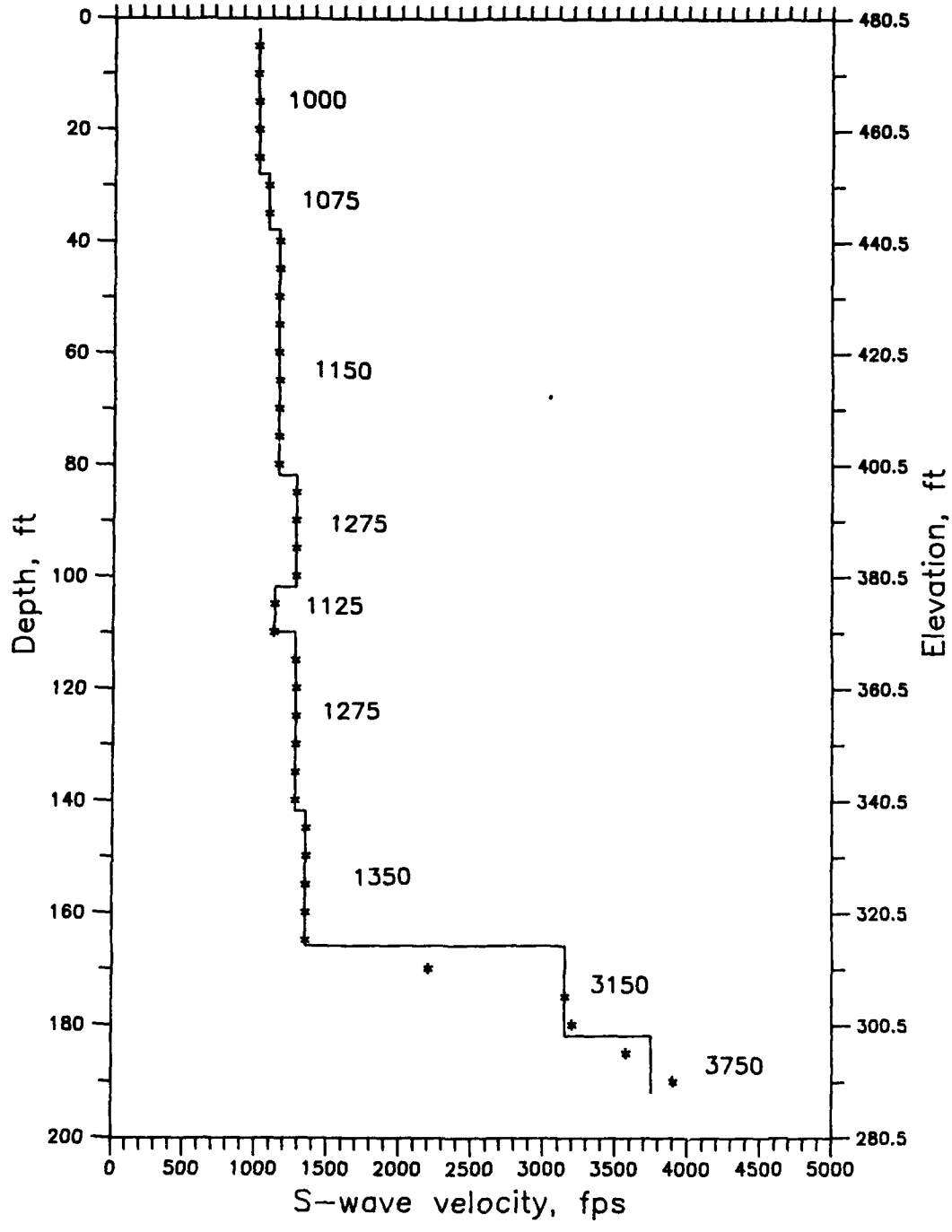

Figure 112. Crosshole S-wave results, centerline

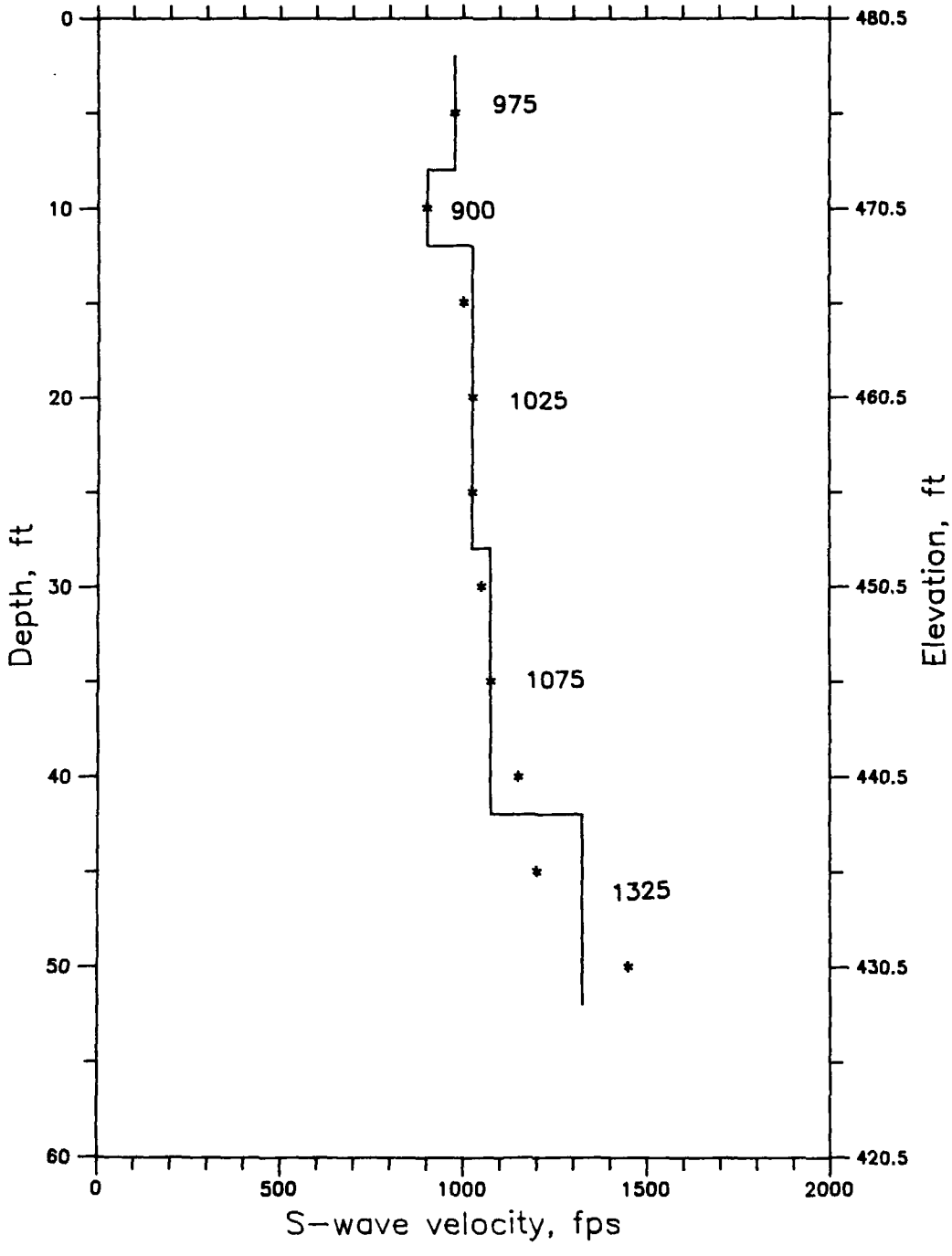

Figure 113. Crosshole S-wave results, downstream shoulder

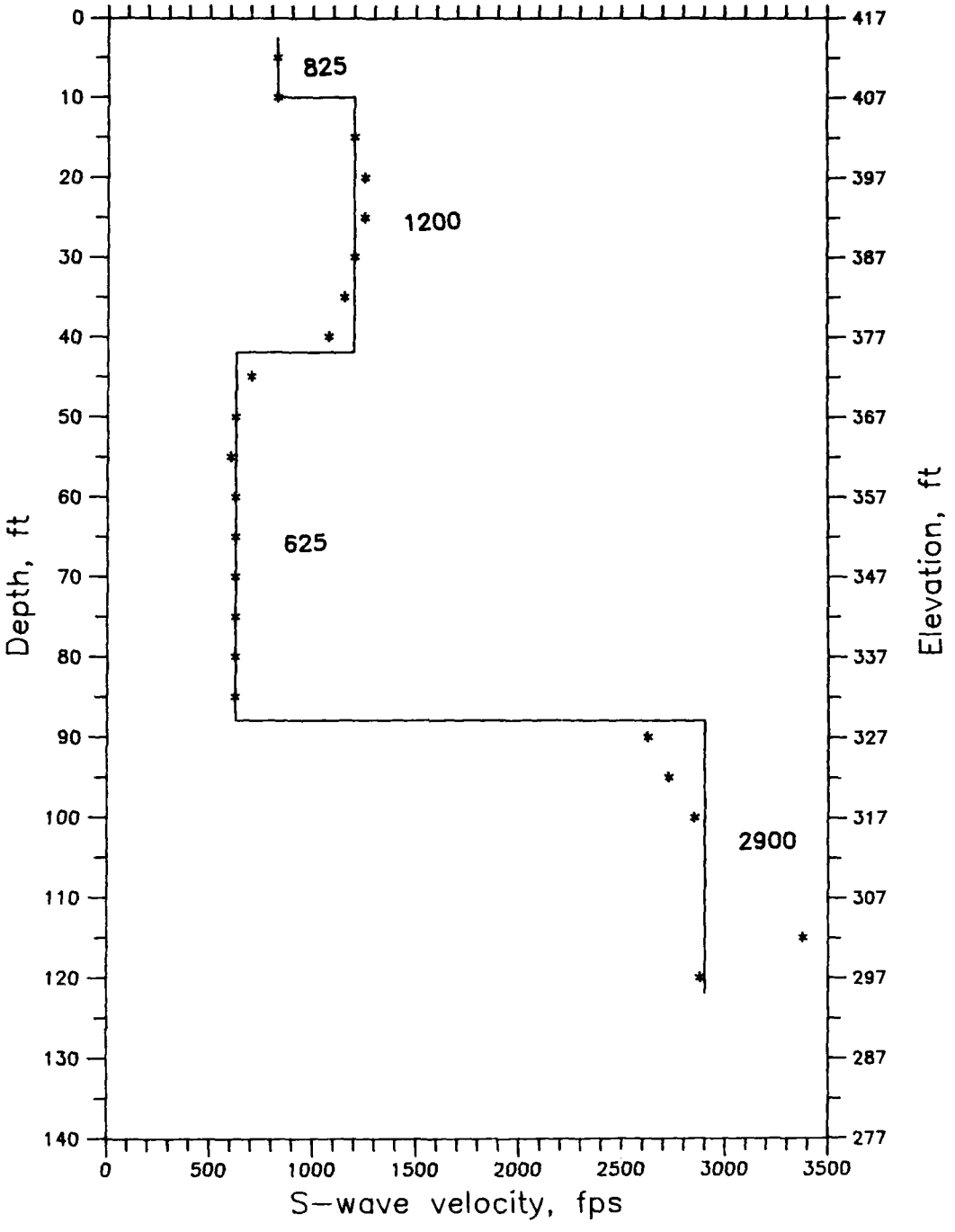

Figure 114. Crosshole S-wave results, downstream slope

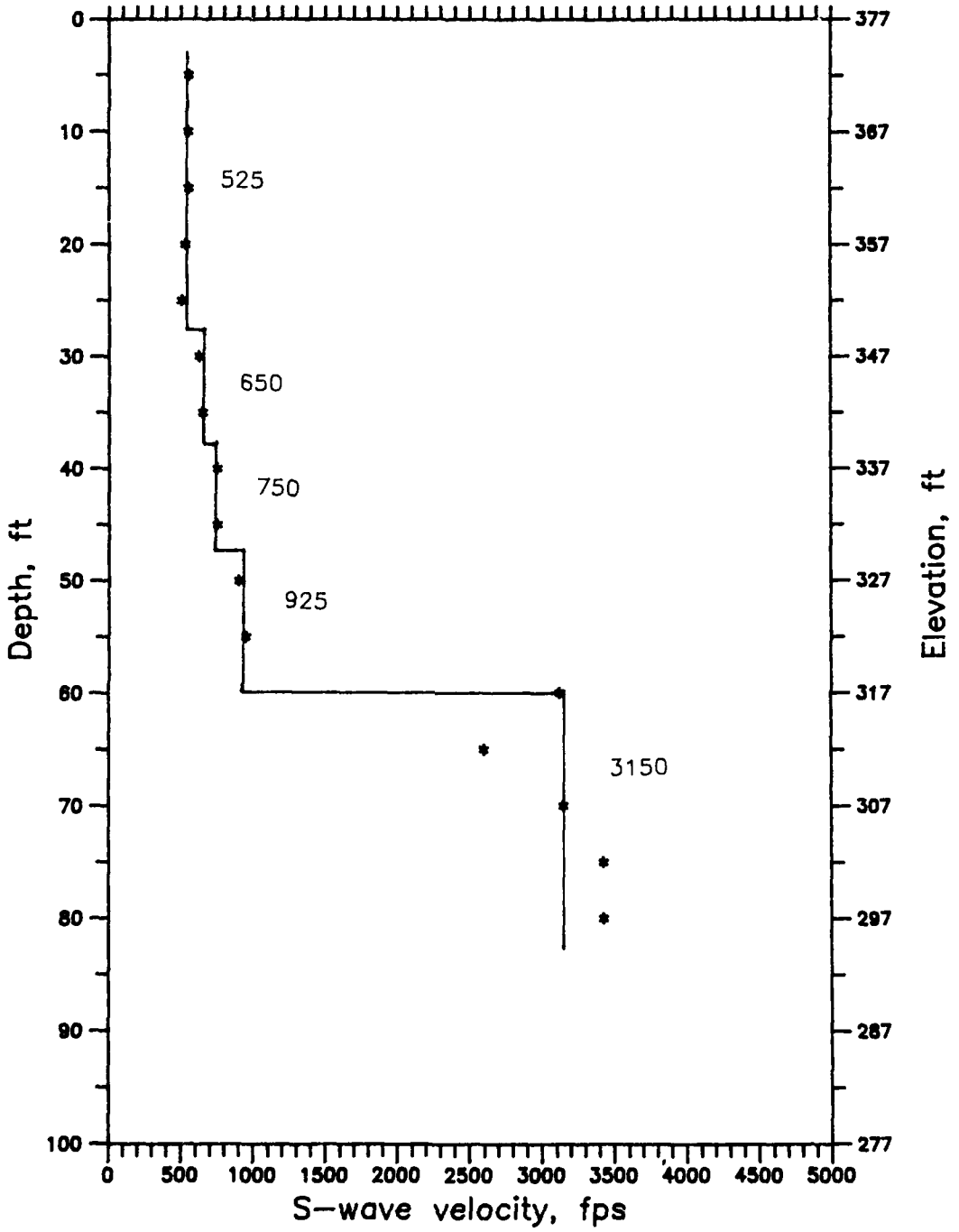

Figure 115. Crosshole S-wave results, SCB-9,5,6,7,8, toe

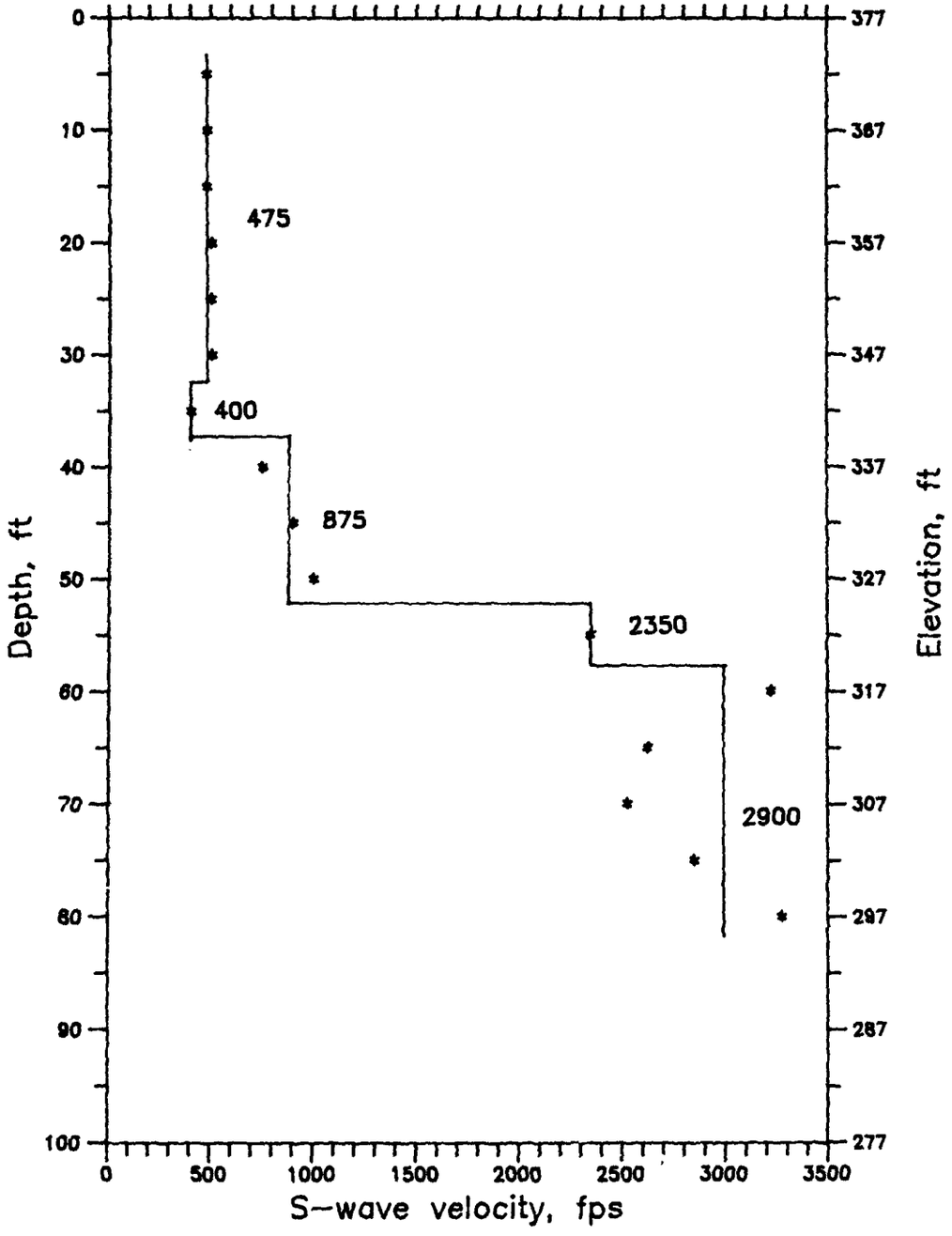

Figure 116. Crosshole S-wave results, SCB-2,3,4, toe

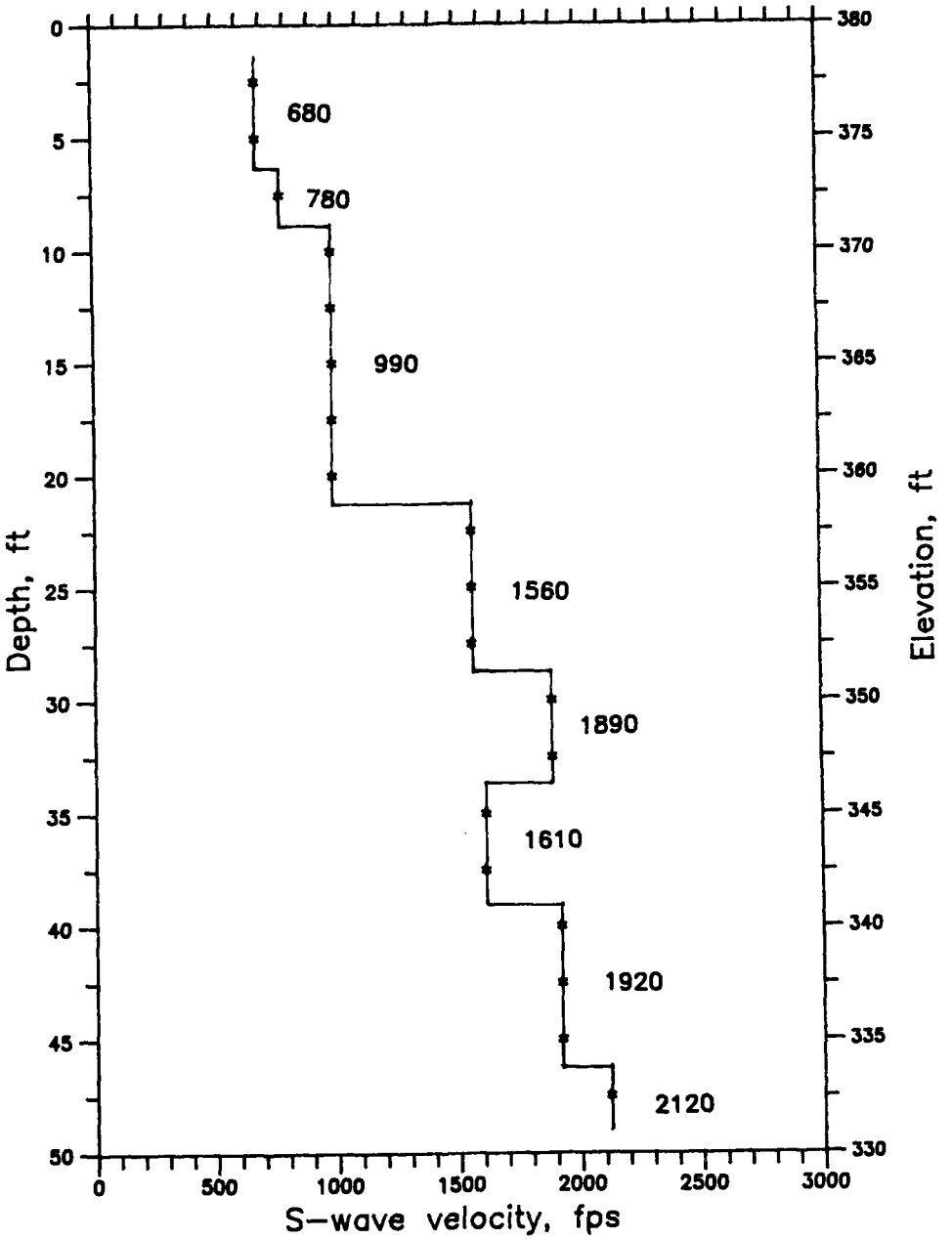

Figure 117. Crosshole S-wave results, MID-1,2, toe

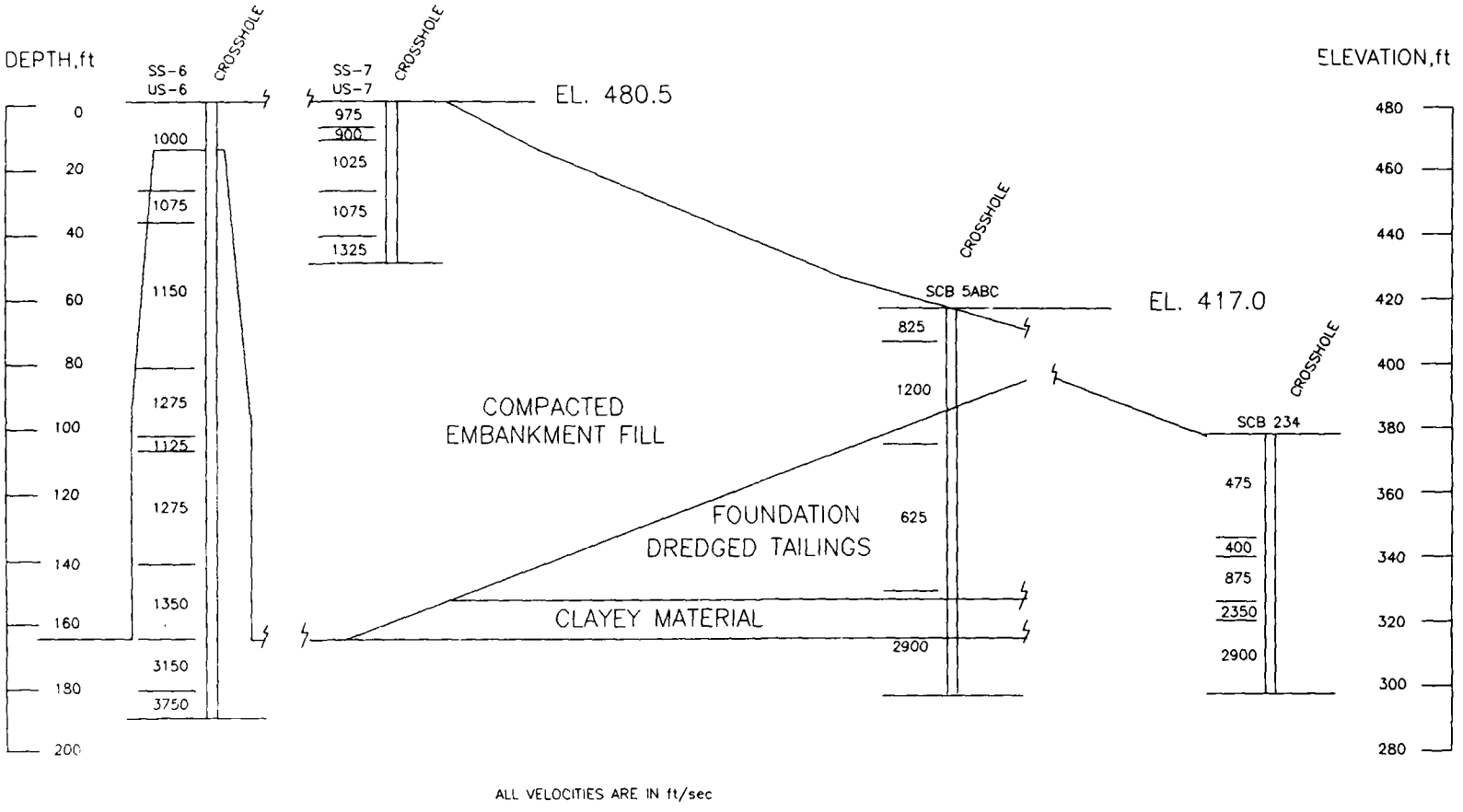

Figure 118. Interpreted S-wave profile from crosshole testing for the section through Station 448+00, Mormon Island Auxiliary Dam

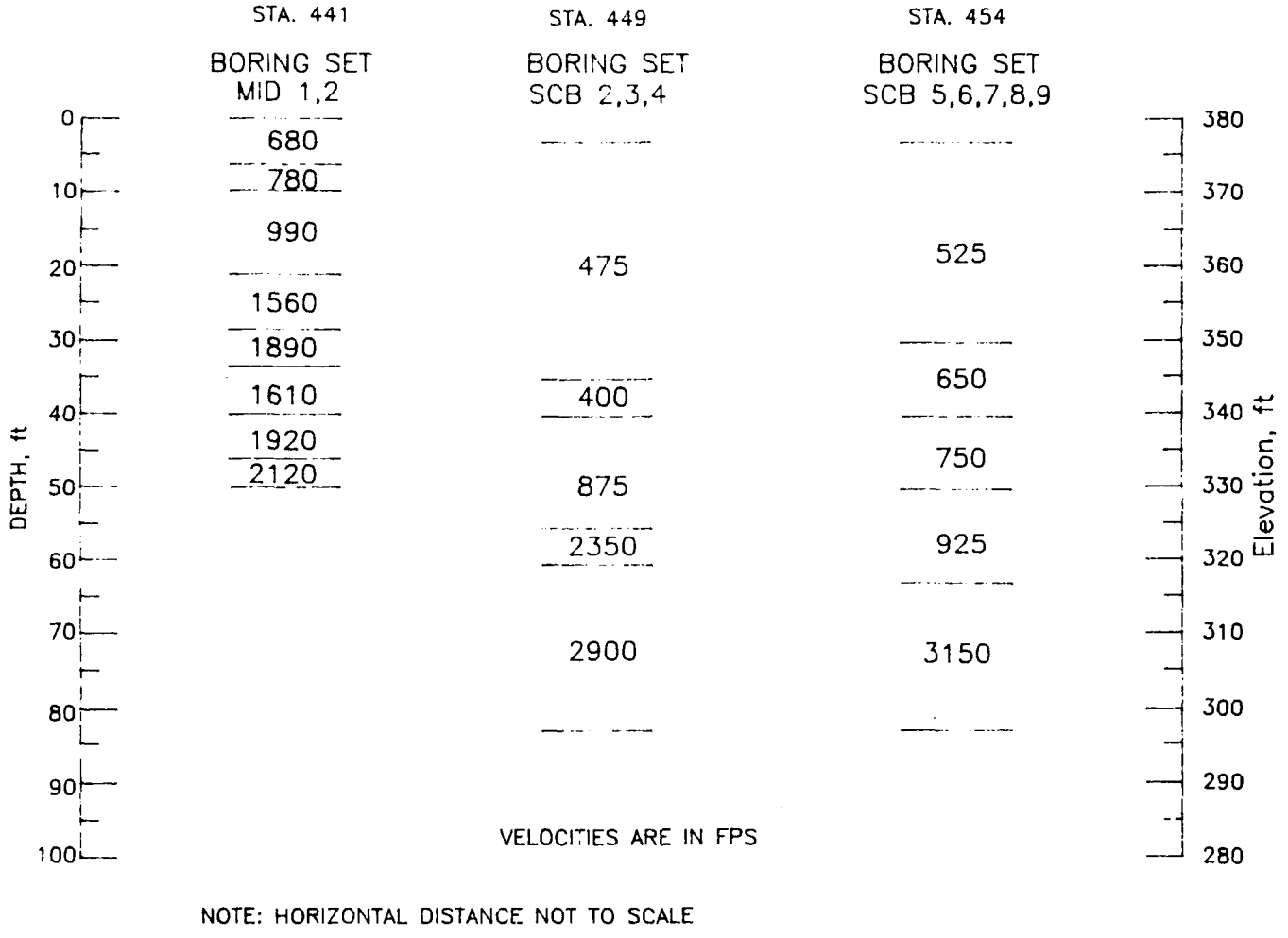

Figure 119. Interpreted S-wave profile from crosshole testing along the downstream toe of Mormon Island Auxiliary Dam

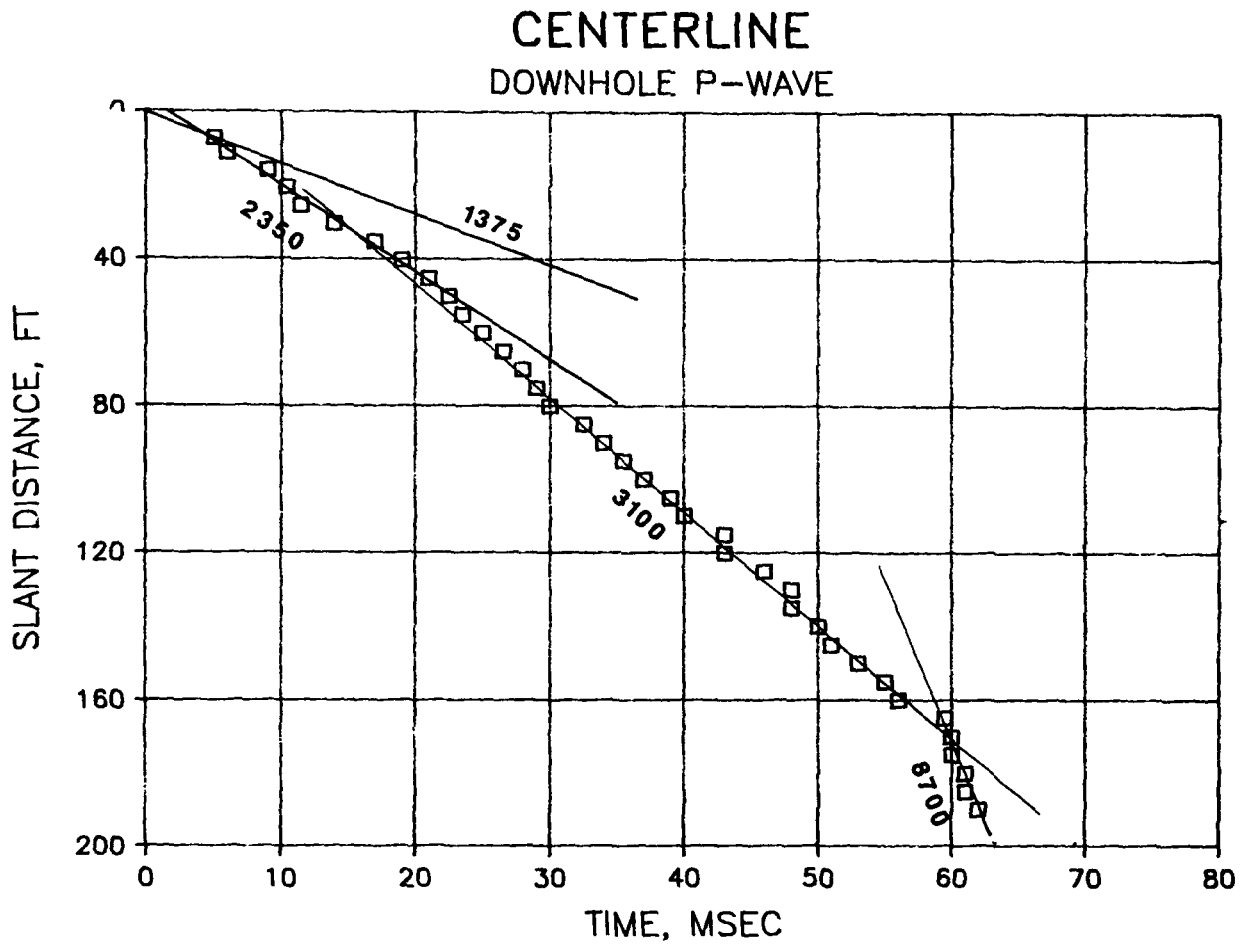

Figure 120. Downhole P-wave results, centerline

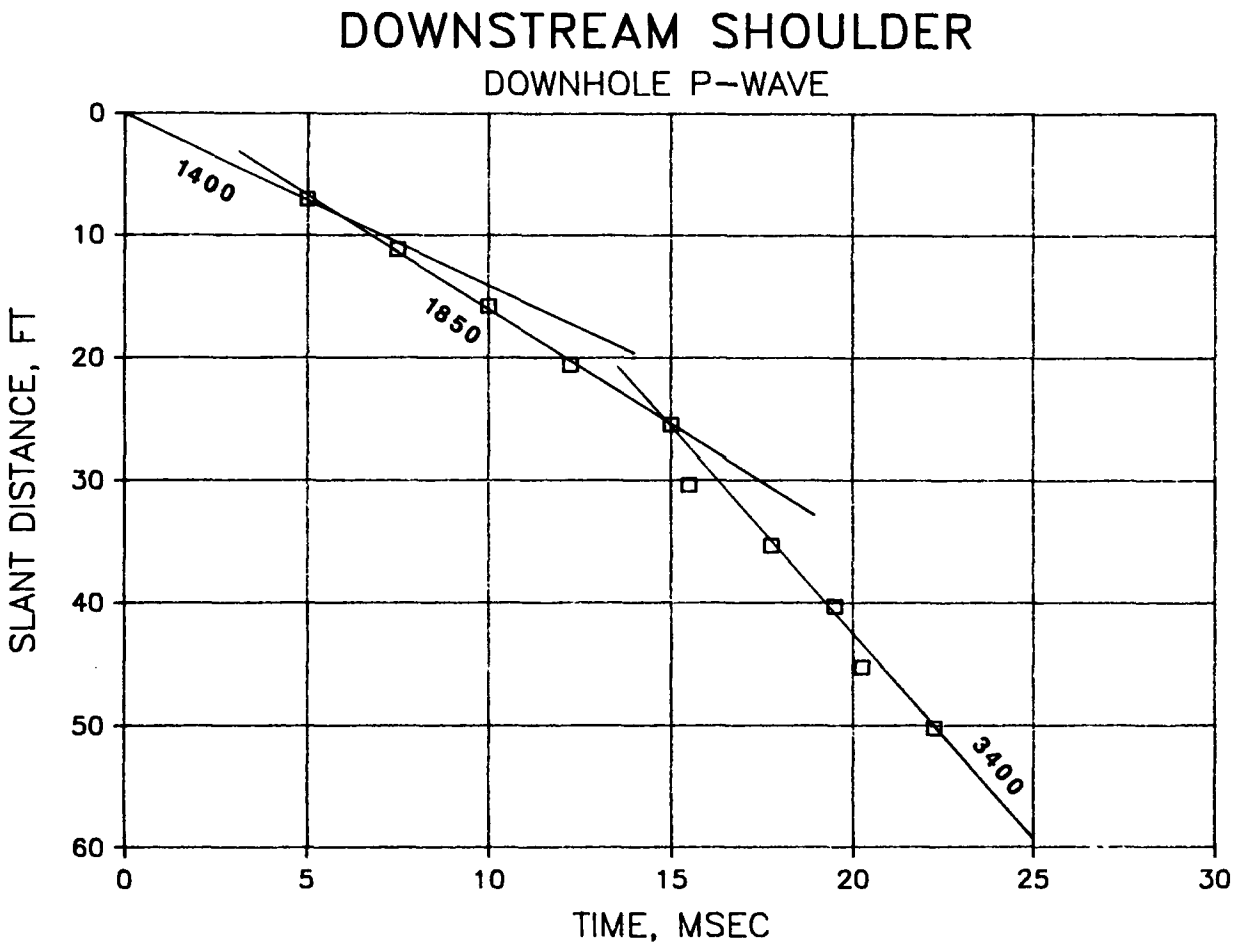

Figure 121. Downhole P-wave results, downstream shoulder

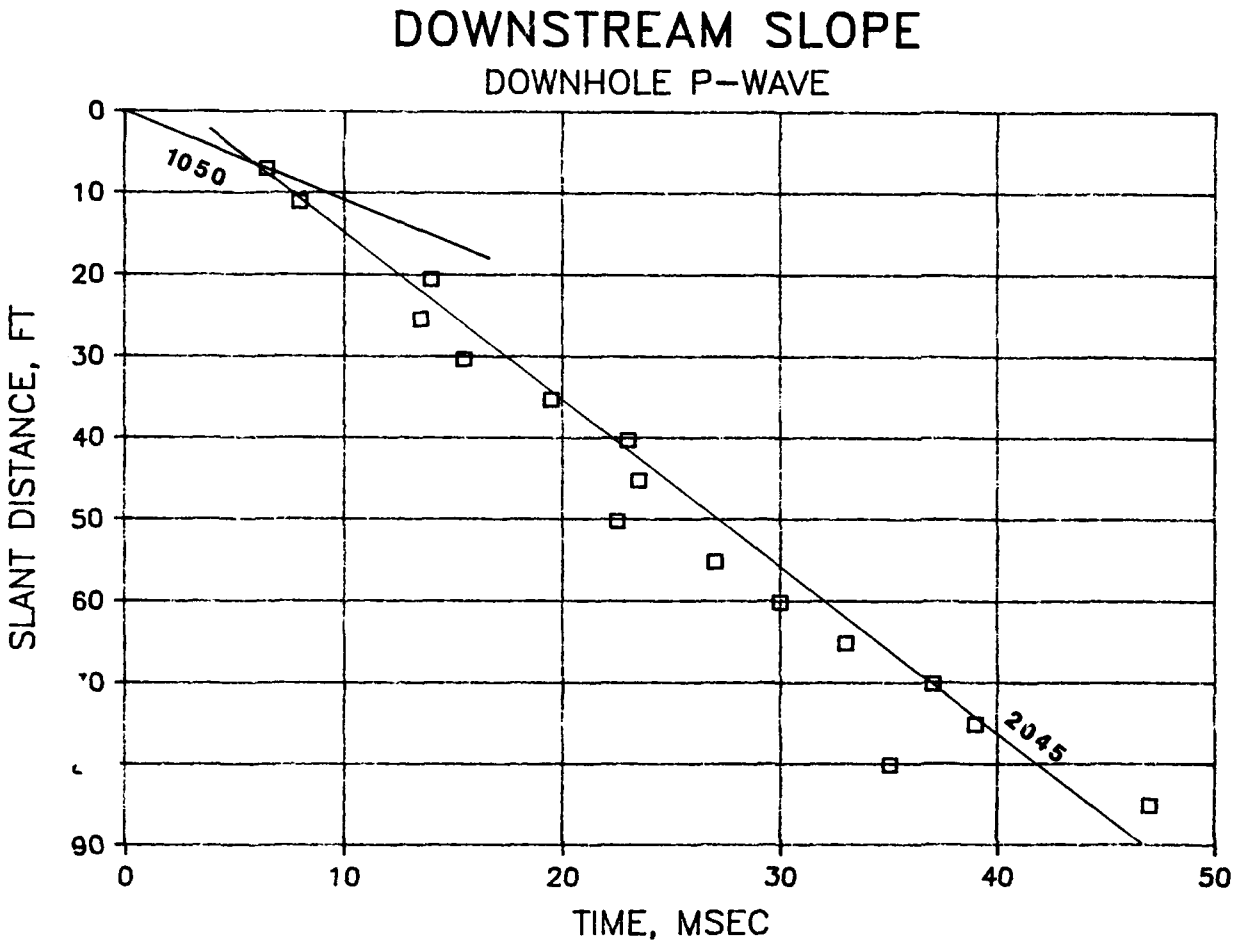

Figure 122. Downhole P-wave results, downstream slope, receiver in SCB5-A, shotpoint SP-A

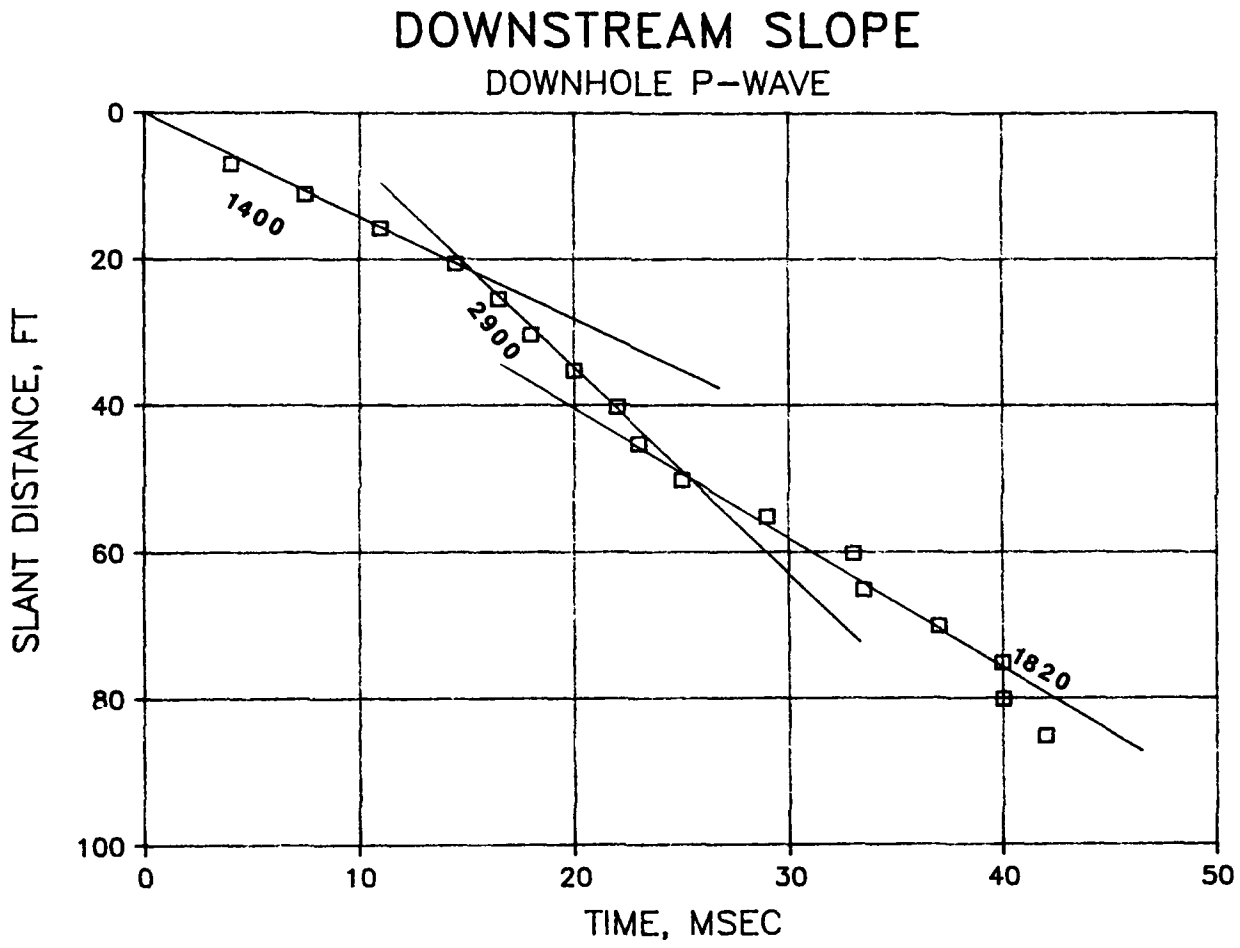

Figure 123. Downhole P-wave results, downstream slope, receiver in SCB5-C, shotpoint SP-B

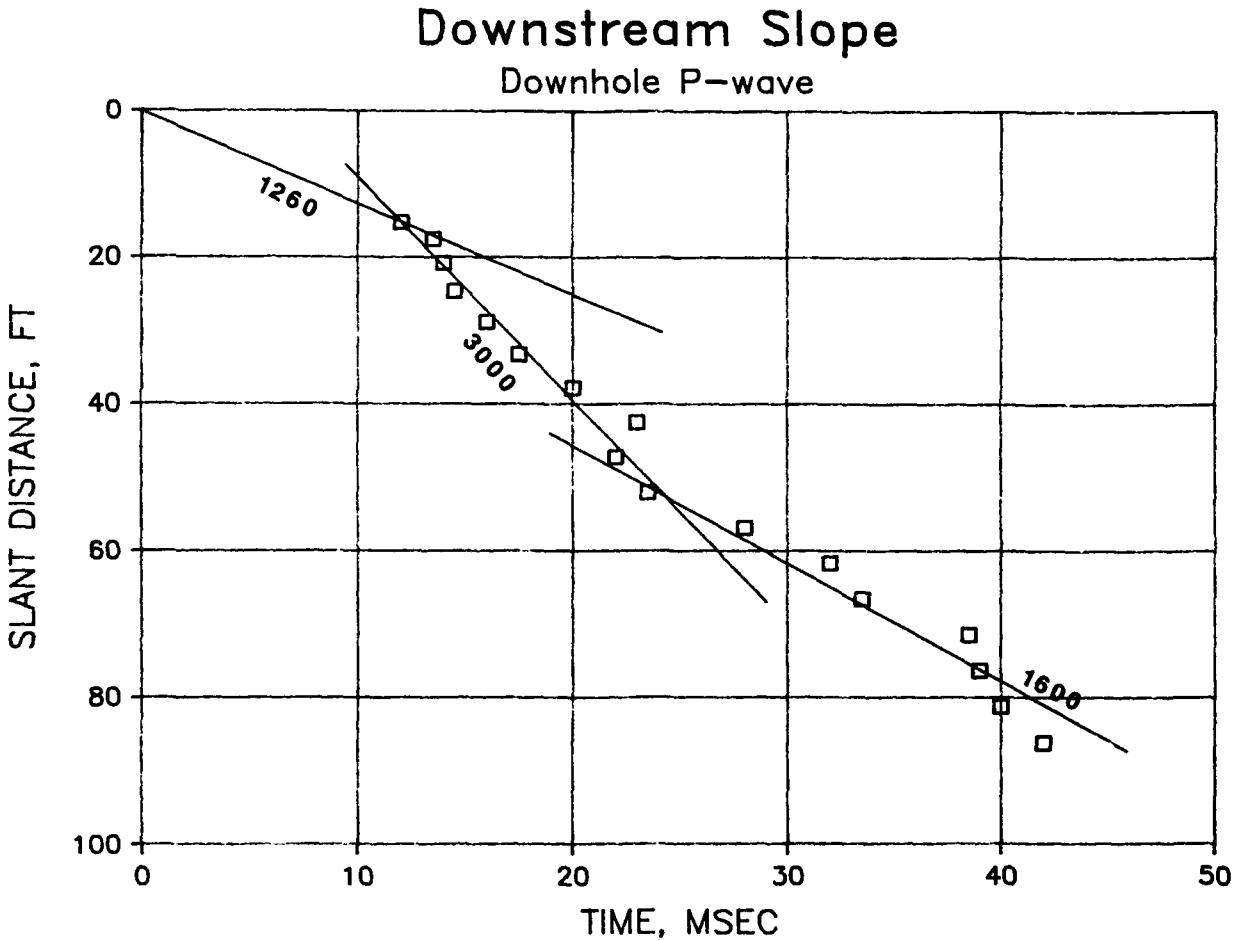

Figure 124. Downhole P-wave results, downstream slope, receiver in SCB5-A, shotpoint SP-B

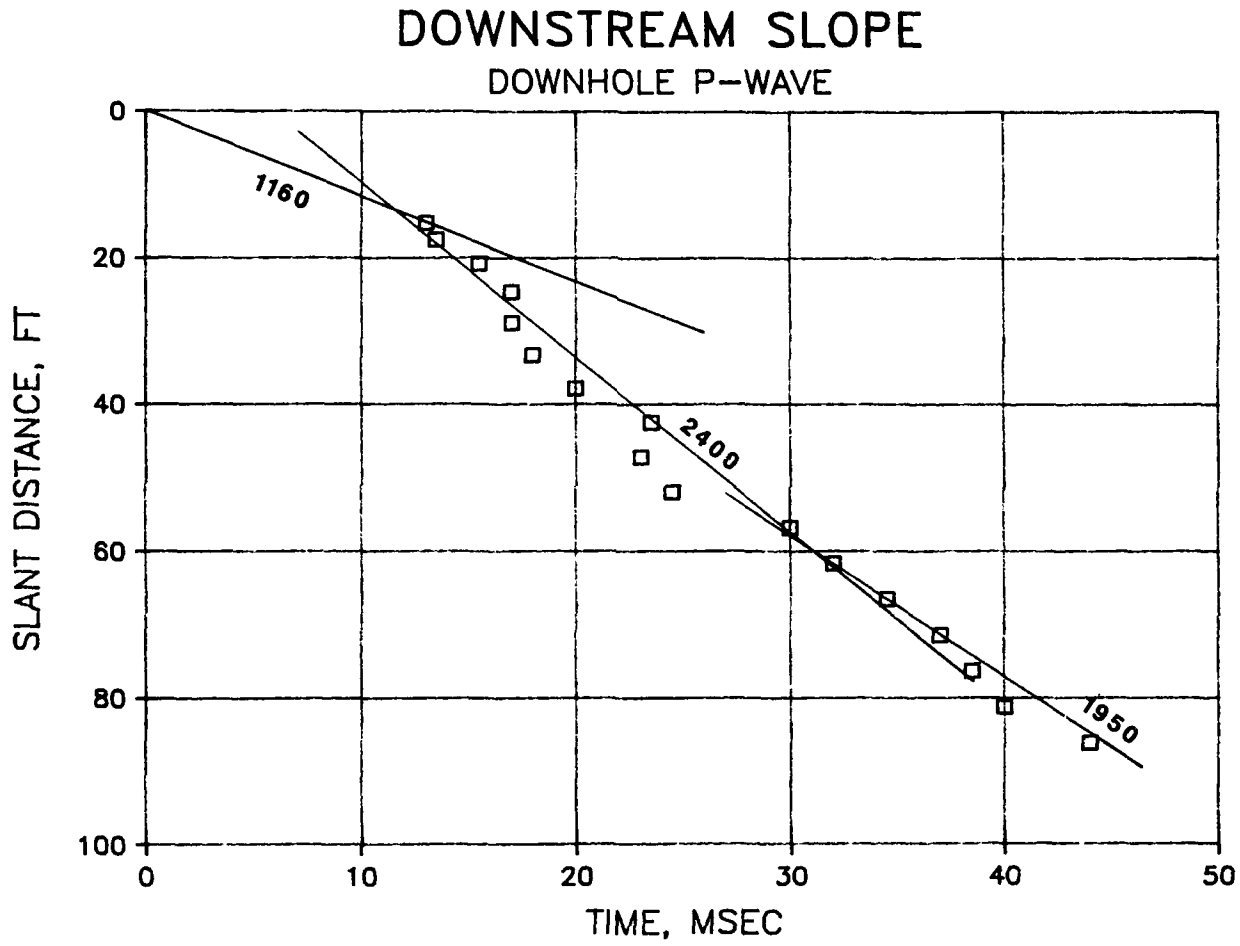

Figure 125. Downhole P-wave results, downstream slope, receiver in SCB5-C, shotpoint SP-A

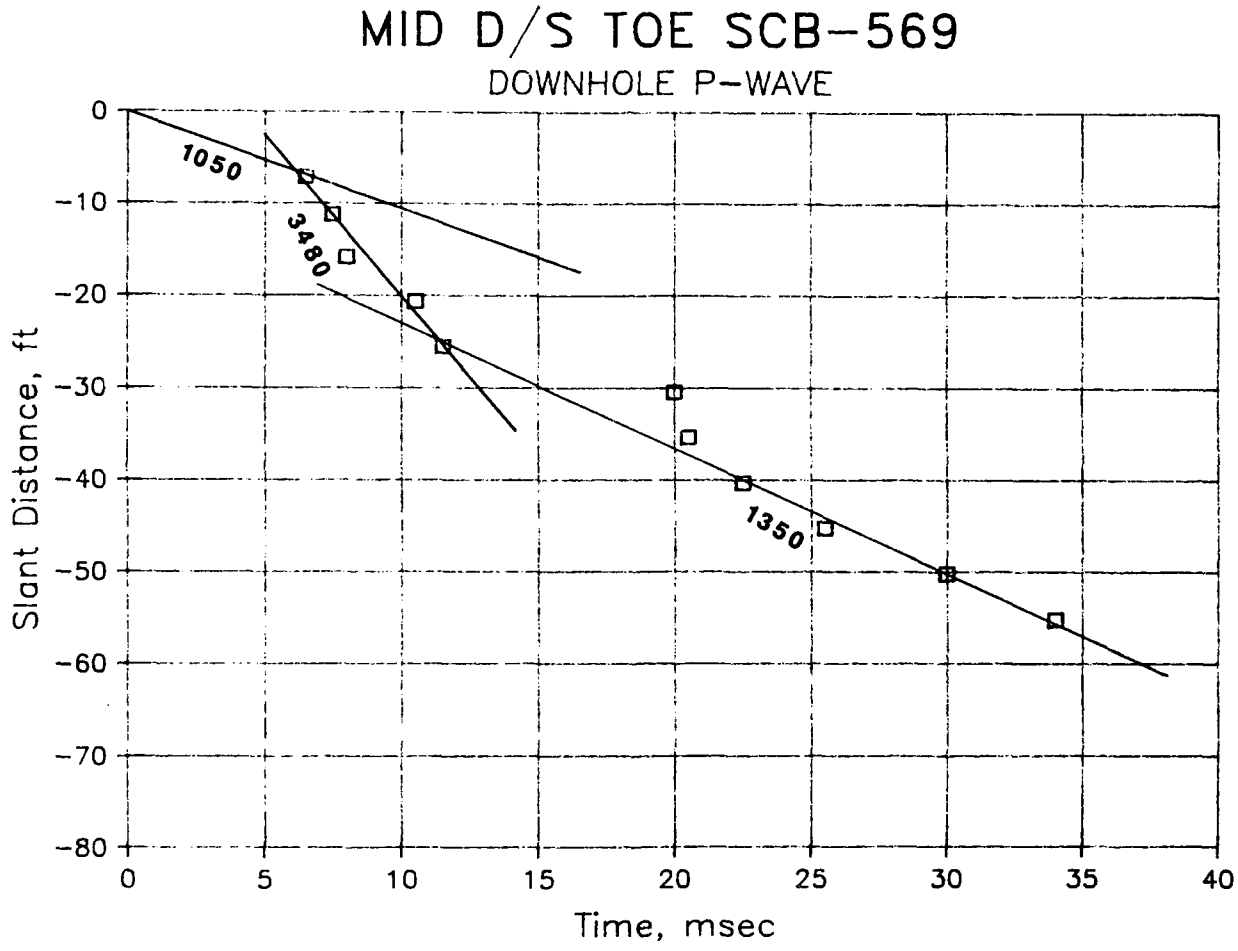

Figure 126. Downhole P-wave results, downstream toe, receiver in SCB-6, shotpoint SP-A

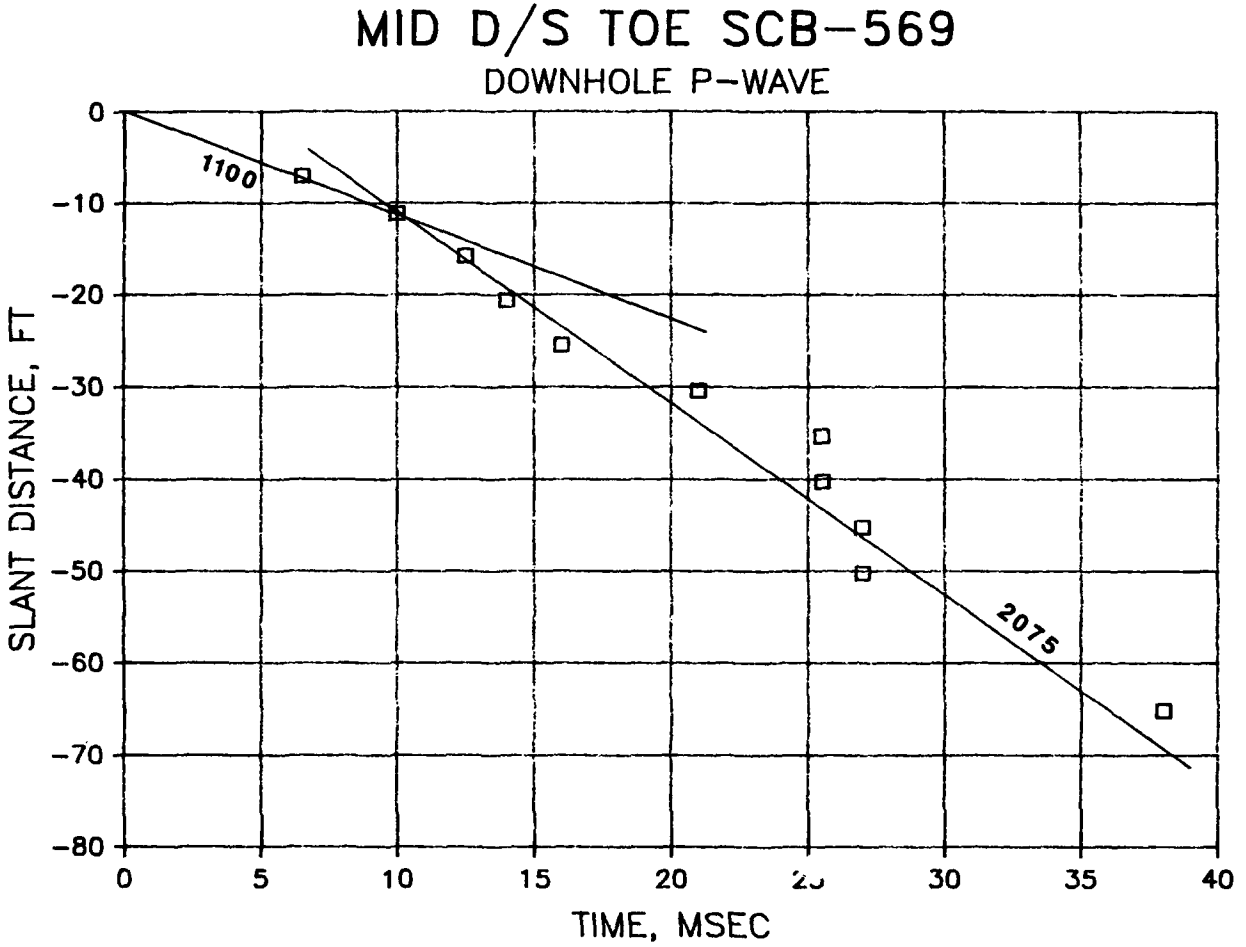

Figure 127. Downhole P-wave results, downstream toe, receiver in SCB-9, shotpoint SP-B

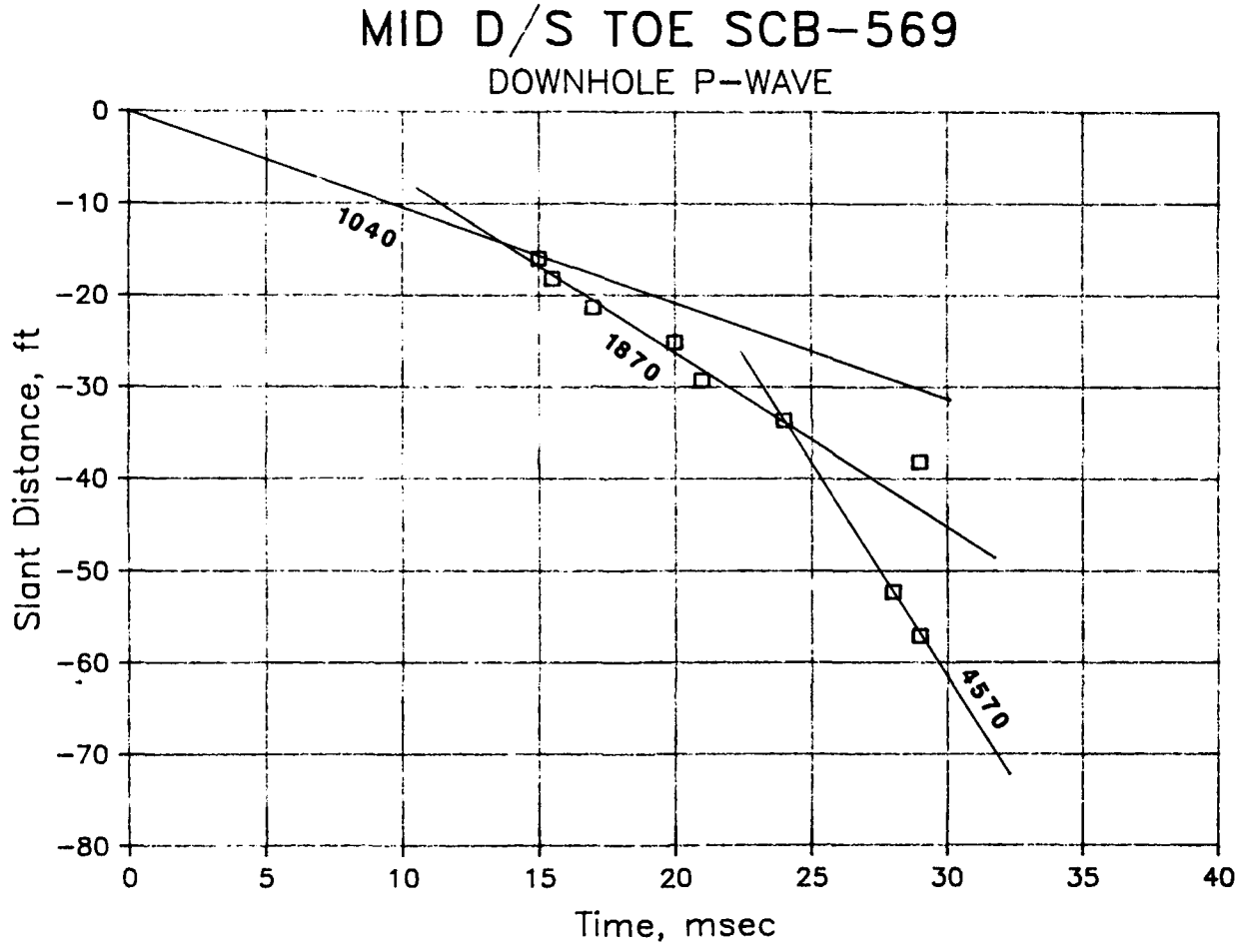

Figure 128. Downhole P-wave results, downstream toe, receiver in SCB-6, shotpoint SP-B

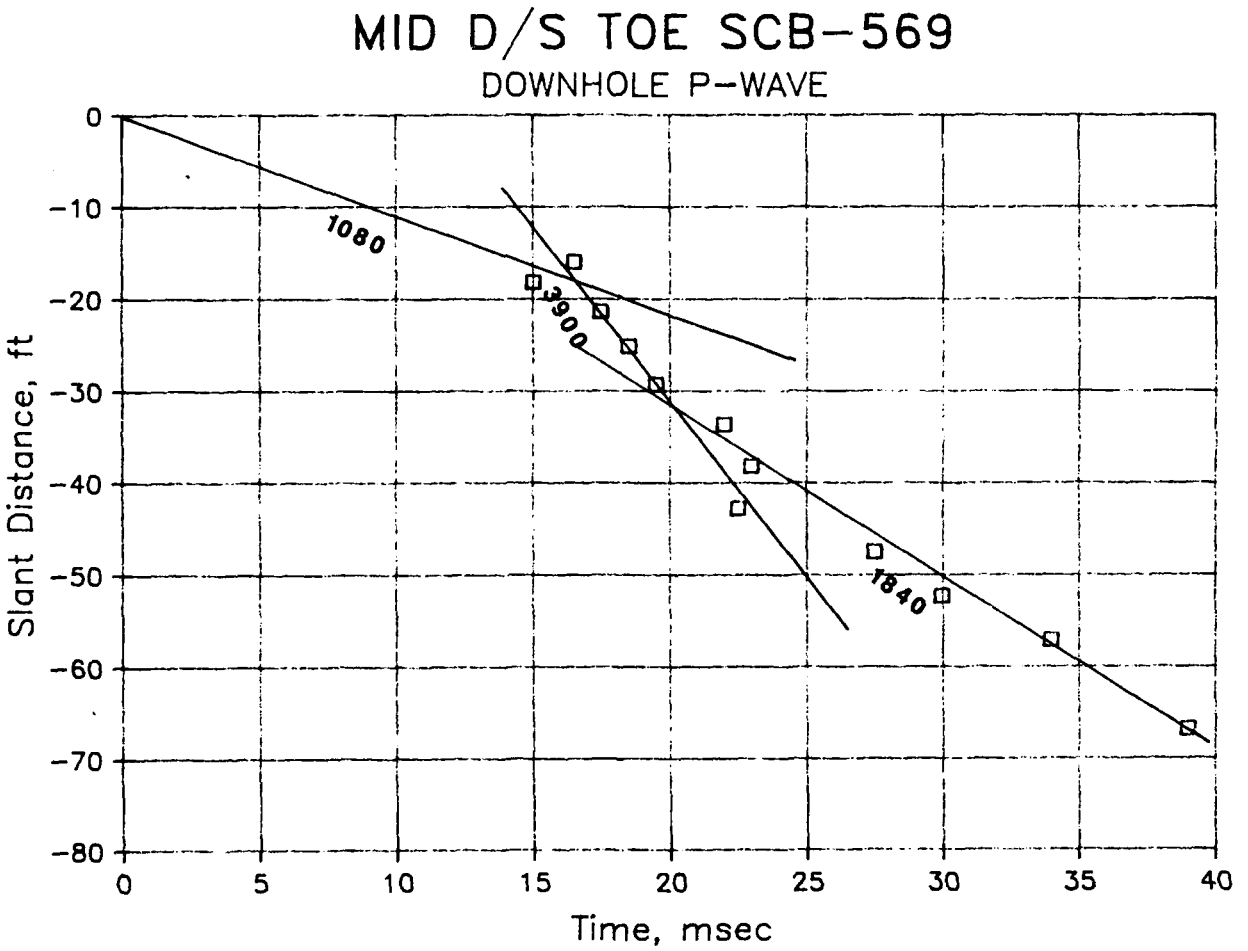

Figure 129. Downhole P-wave results, downstream toe, receiver in SCB-9, shotpoint SP-A

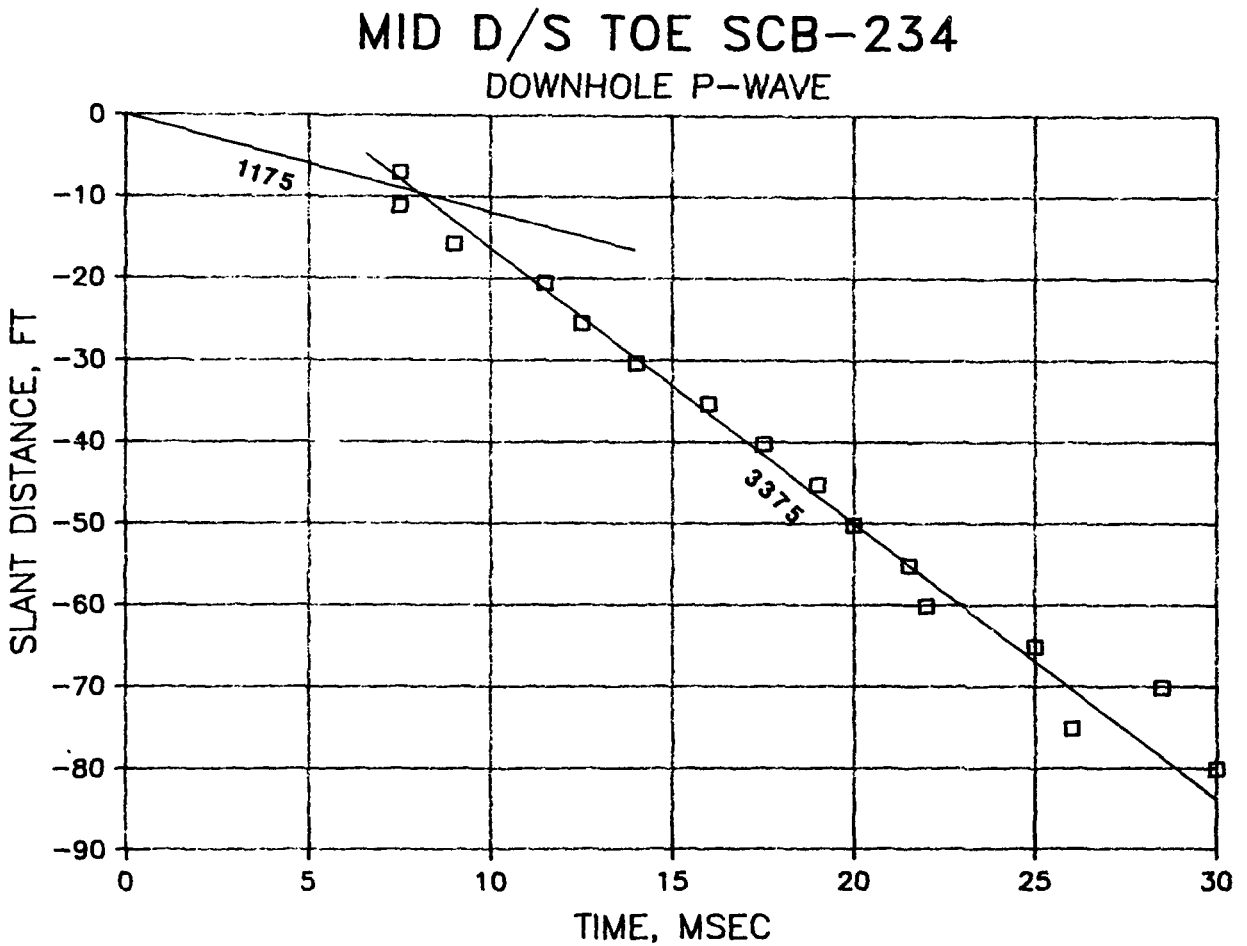

Figure 130. Downhole P-wave results, downstream toe, receiver in SCB-4, shotpoint SP-A

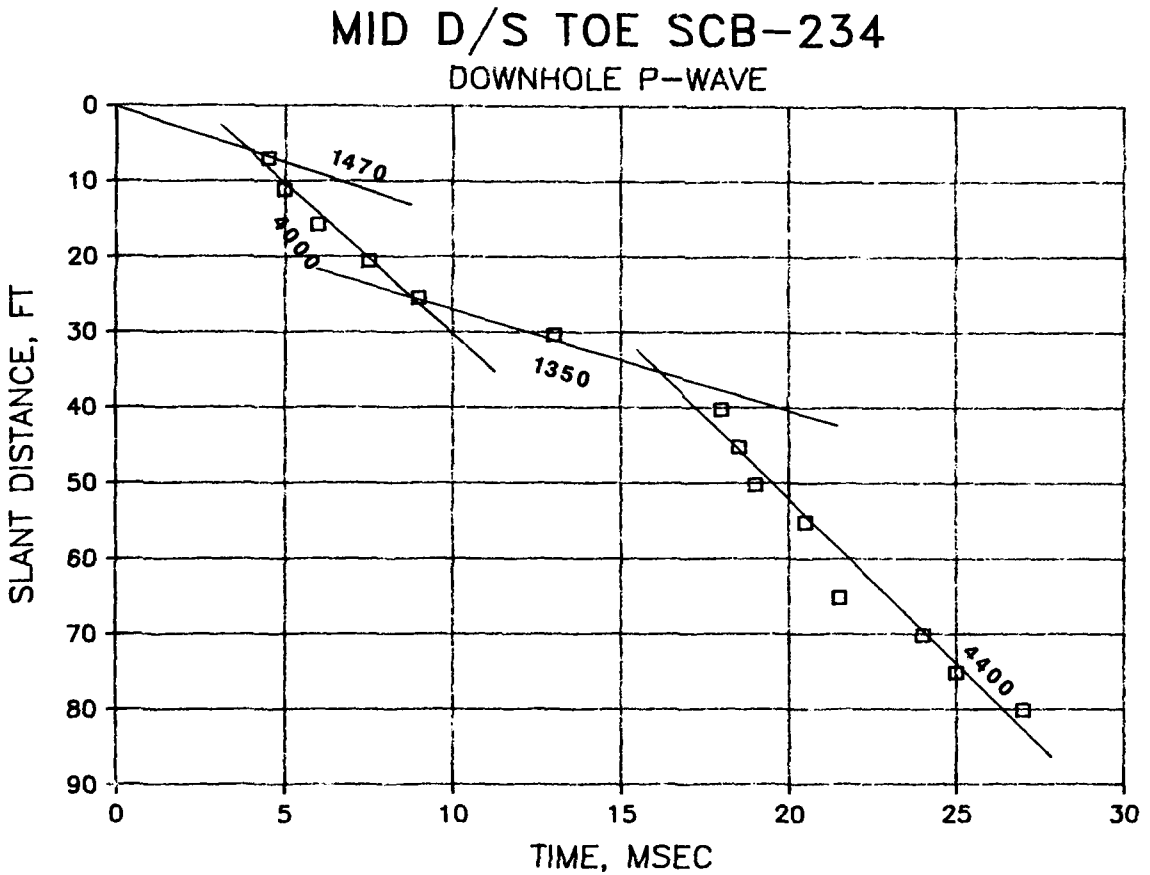

Figure 131. Downhole P-wave results, downstream toe, receiver in SCB-2, shotpoint SP-B

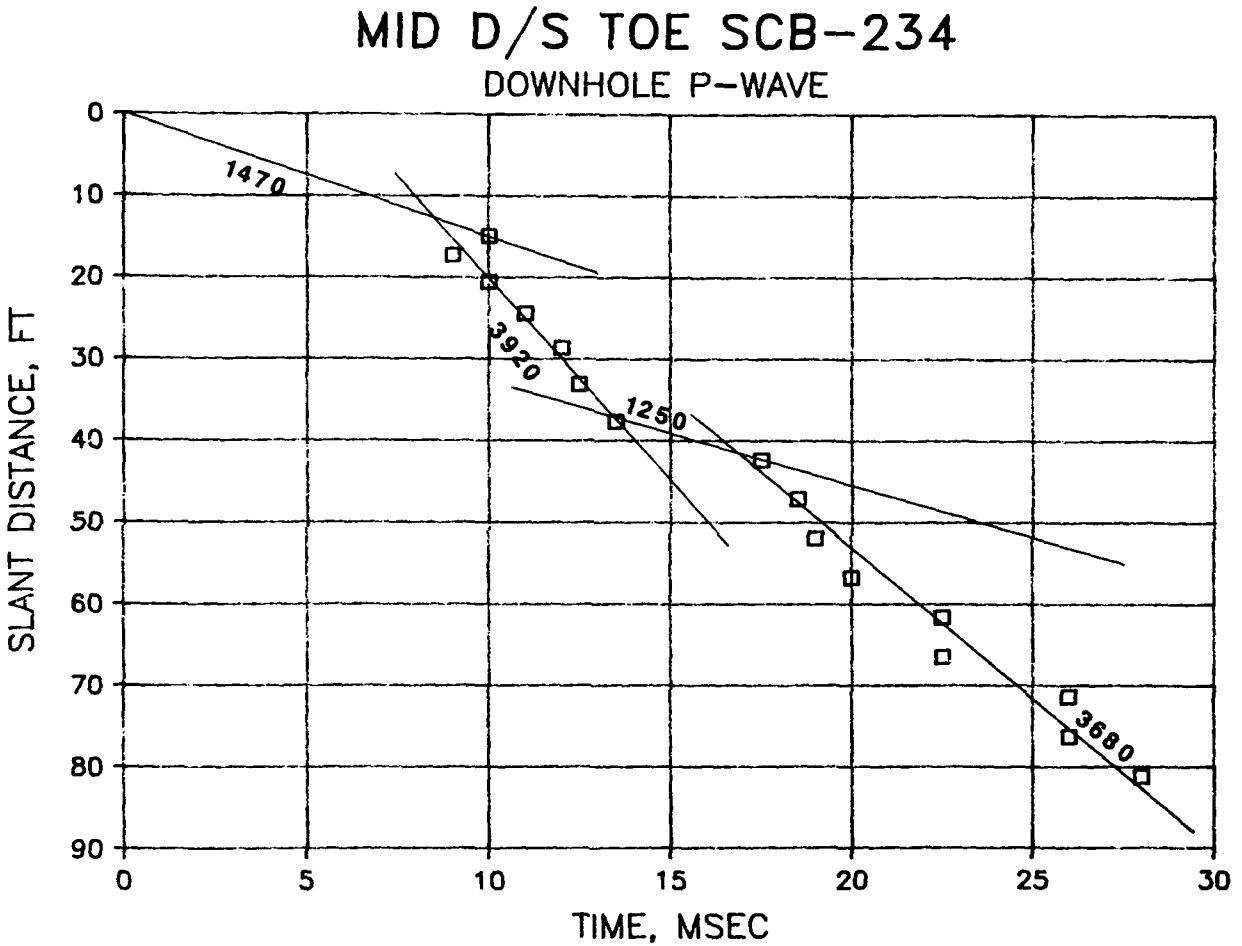

Figure 132. Downhole P-wave results, downstream toe, receiver in SCB-4, shotpoint SP-B

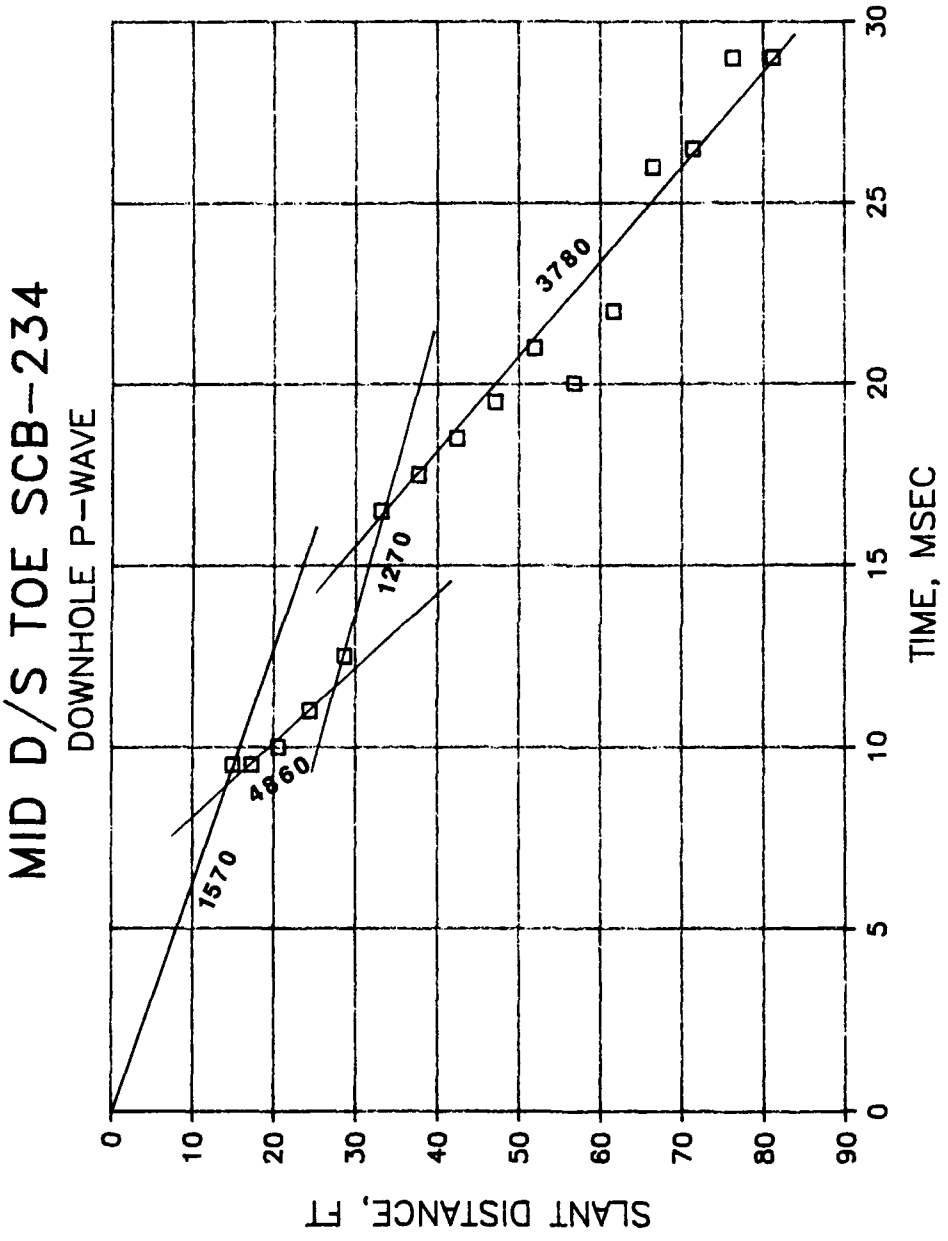

Figure 133. Downhole P-wave results, downstream toe, receiver in SCB-2, shotpoint SP-A

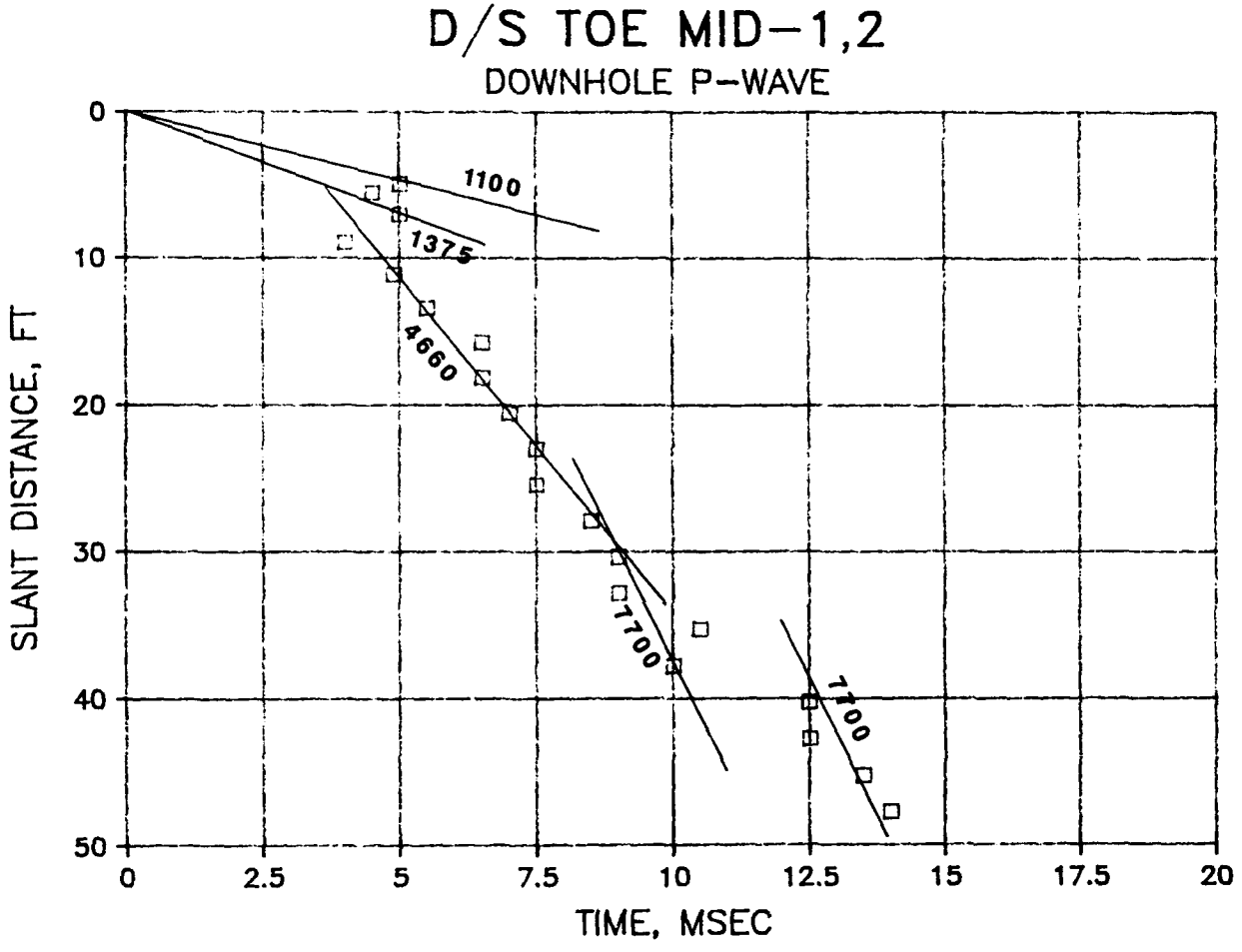

Figure 134. Downhole P-wave results, downstream toe, receiver MID-1

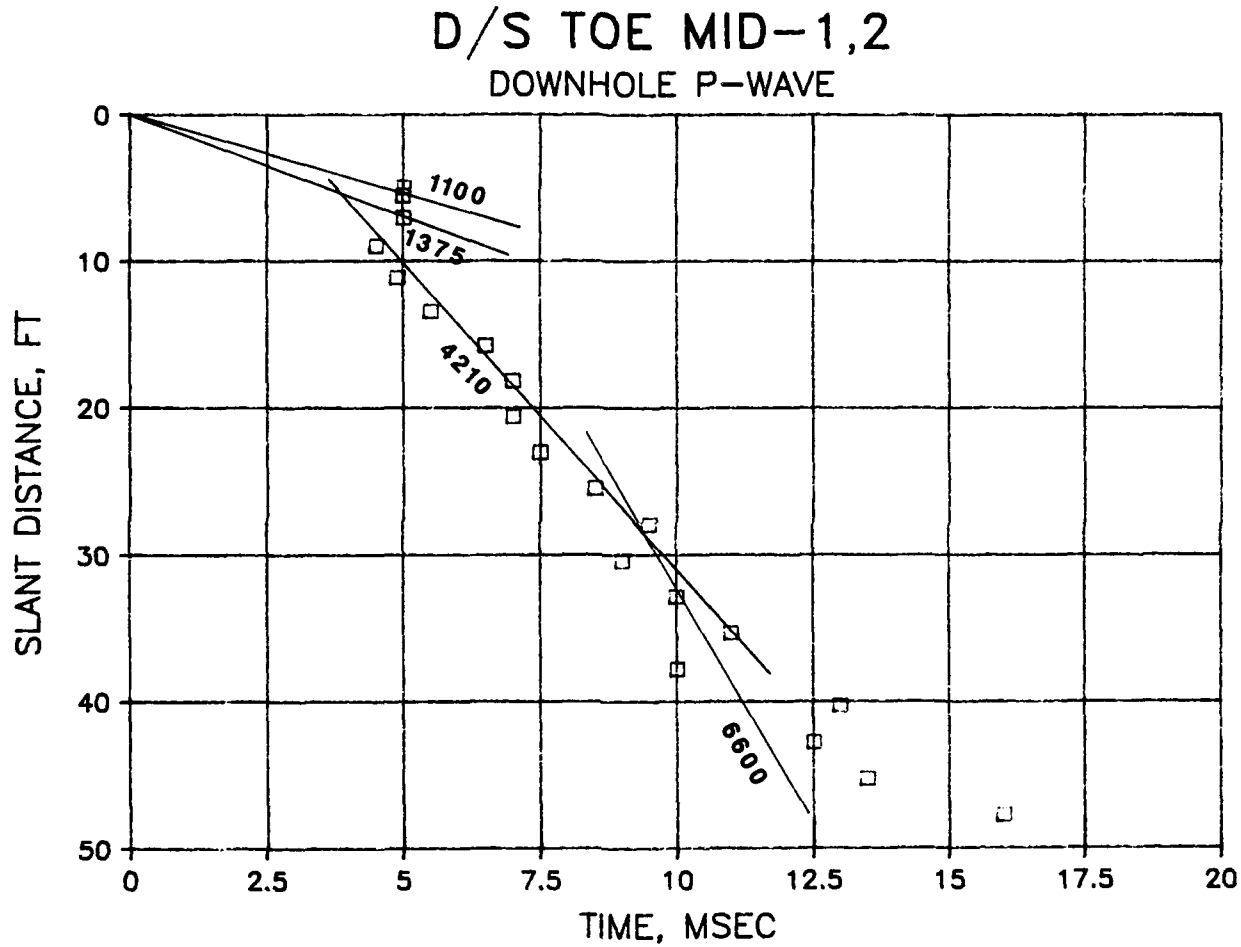

Figure 135. Downhole P-wave results, downstream toe, receiver MID-2

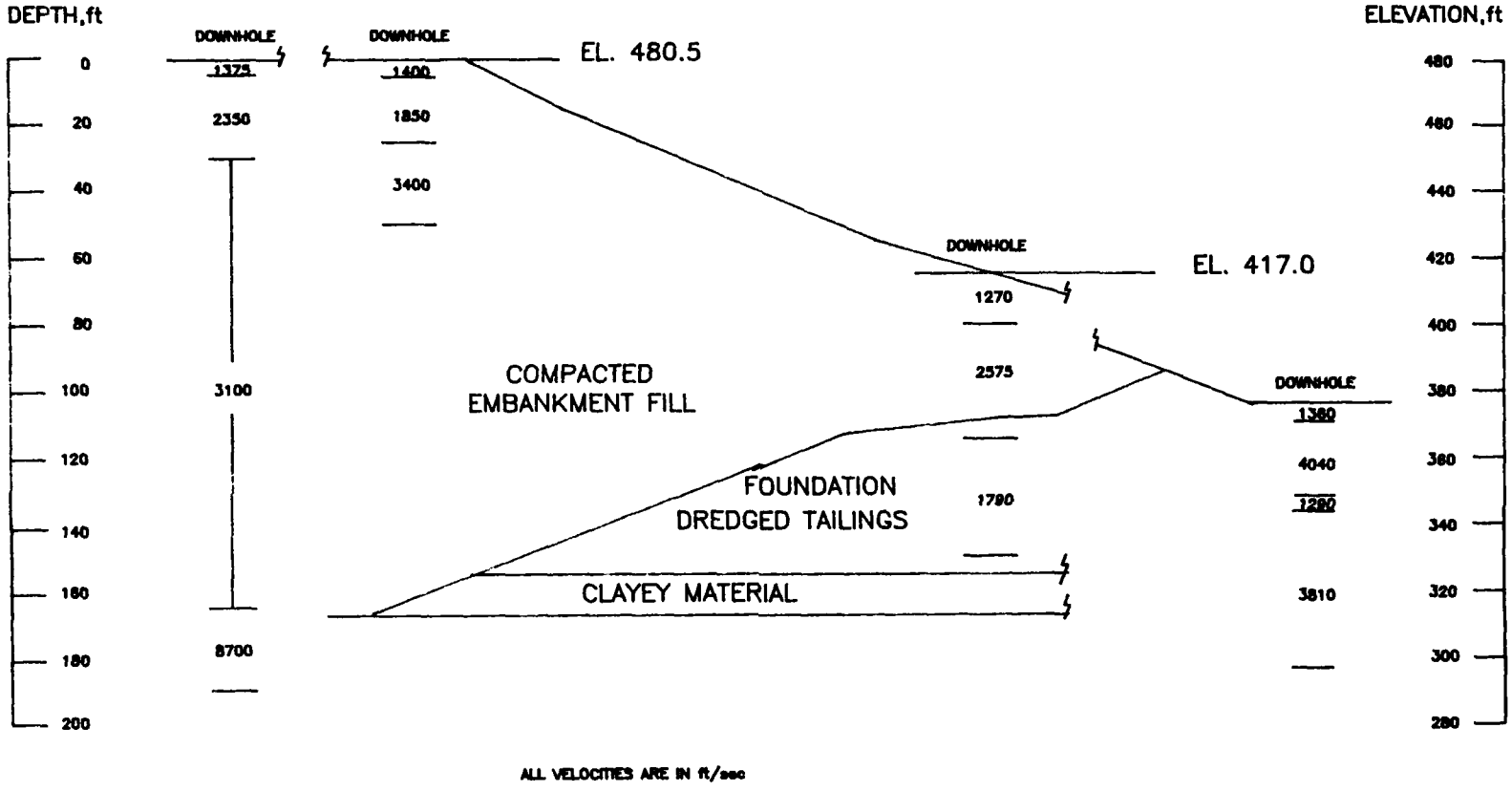

Figure 136. Interpreted P-wave profile from downhole testing for the section through Station 448+00, Mormon Island Auxiliary Dam

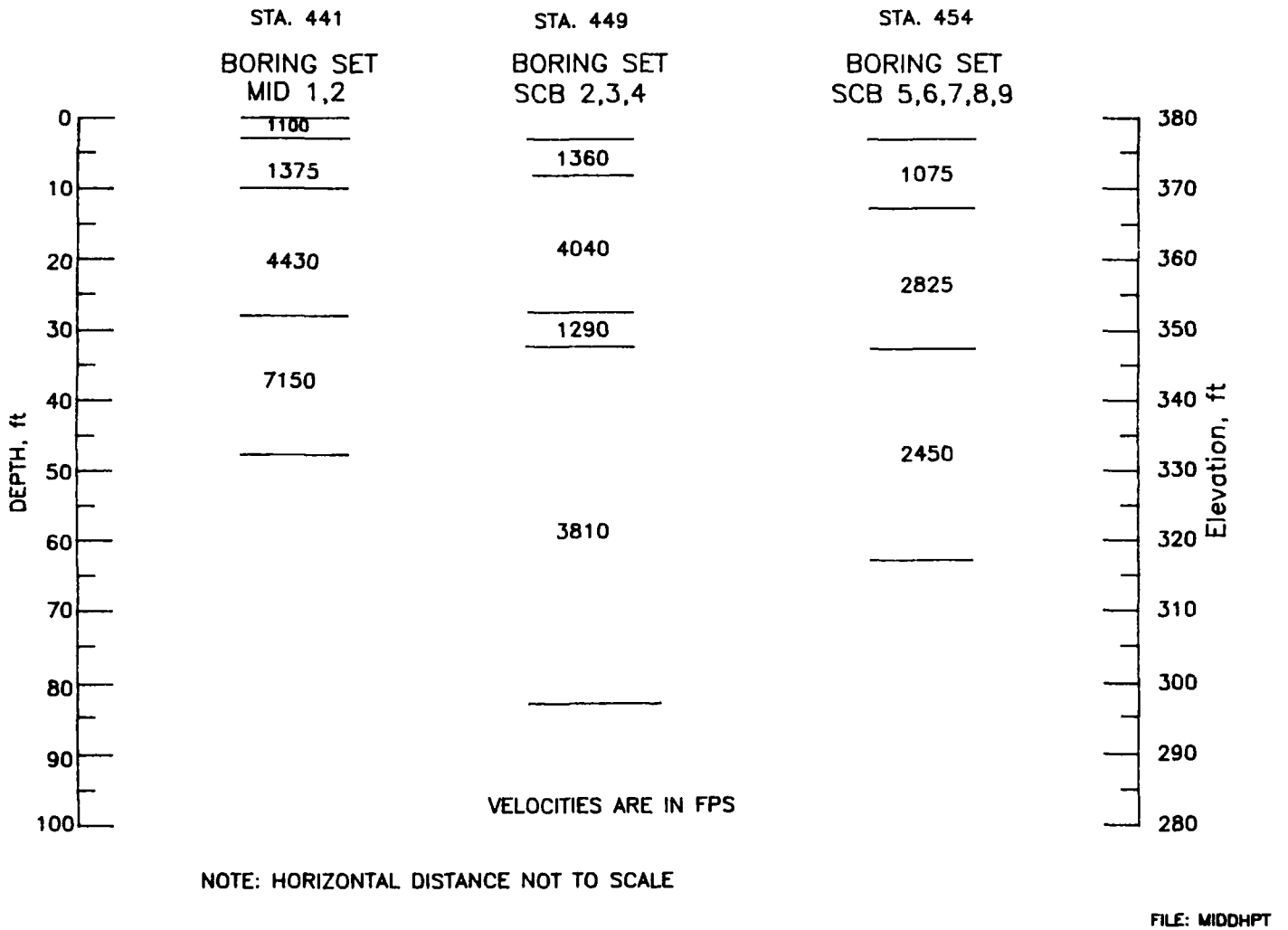

Figure 137. Interpreted P-wave profile from downhole testing along the downstream toe of Mormon Island Auxiliary Dam

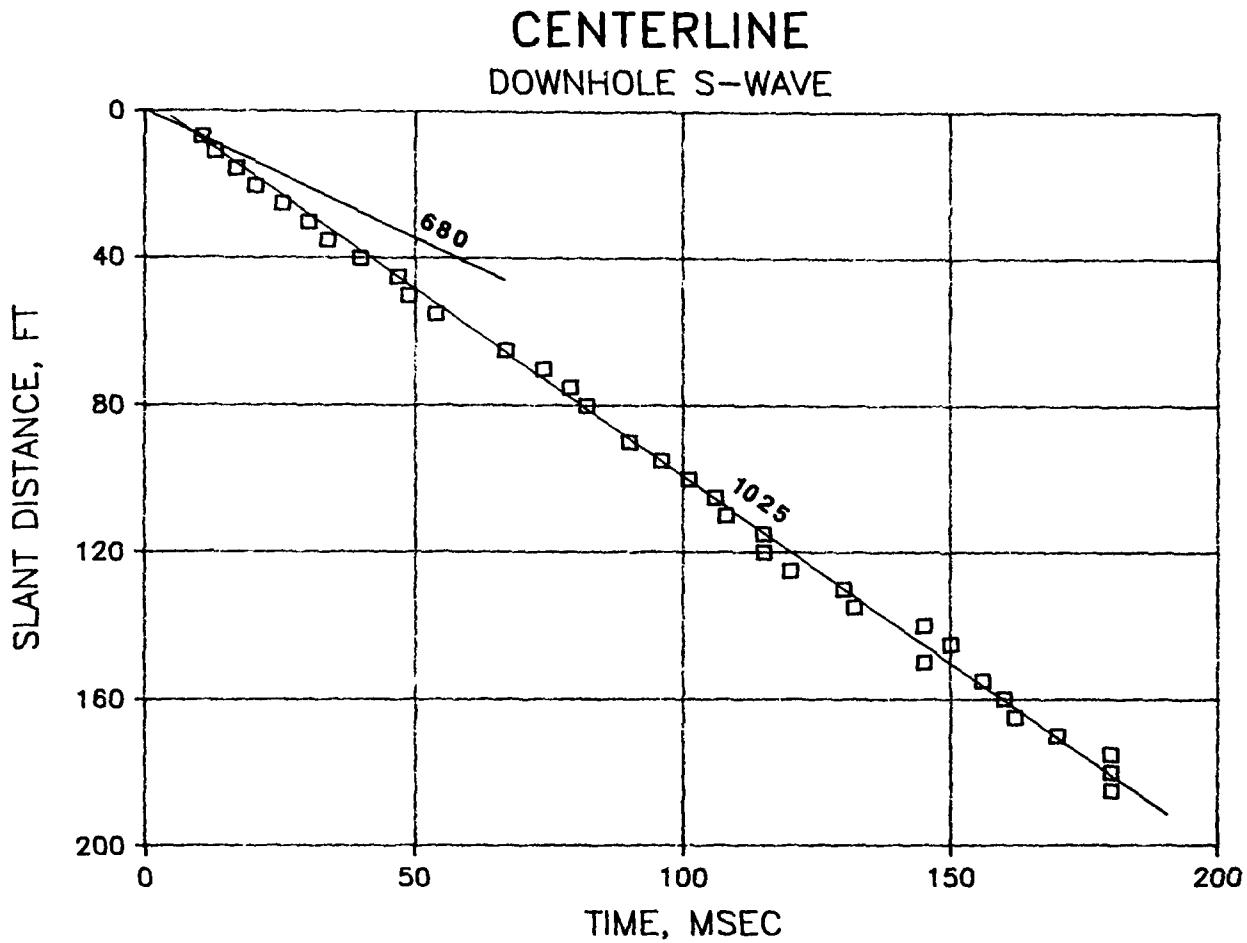

Figure 138. Downhole S-wave results, centerline

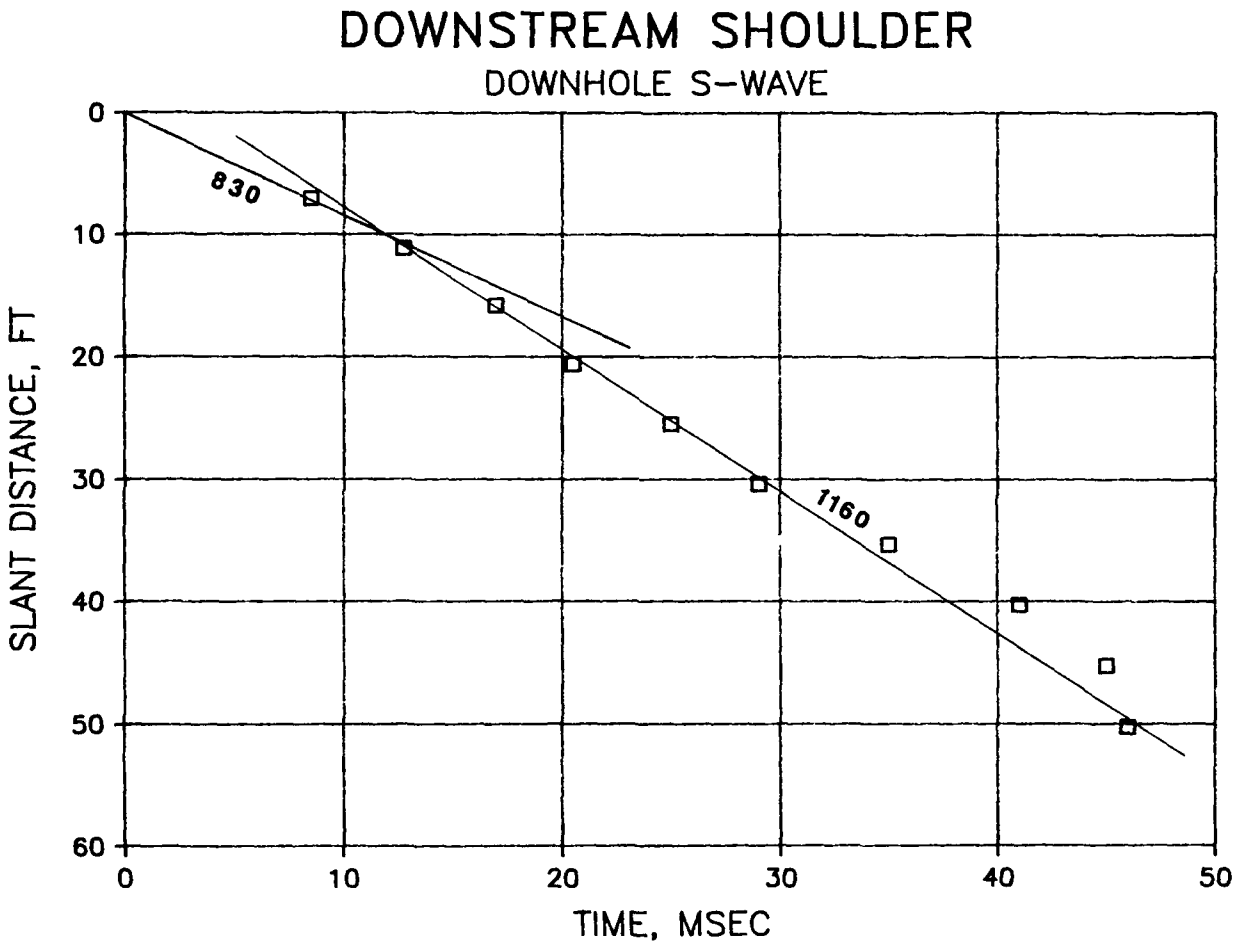

Figure 139. Downhole S-wave results, downstream shoulder

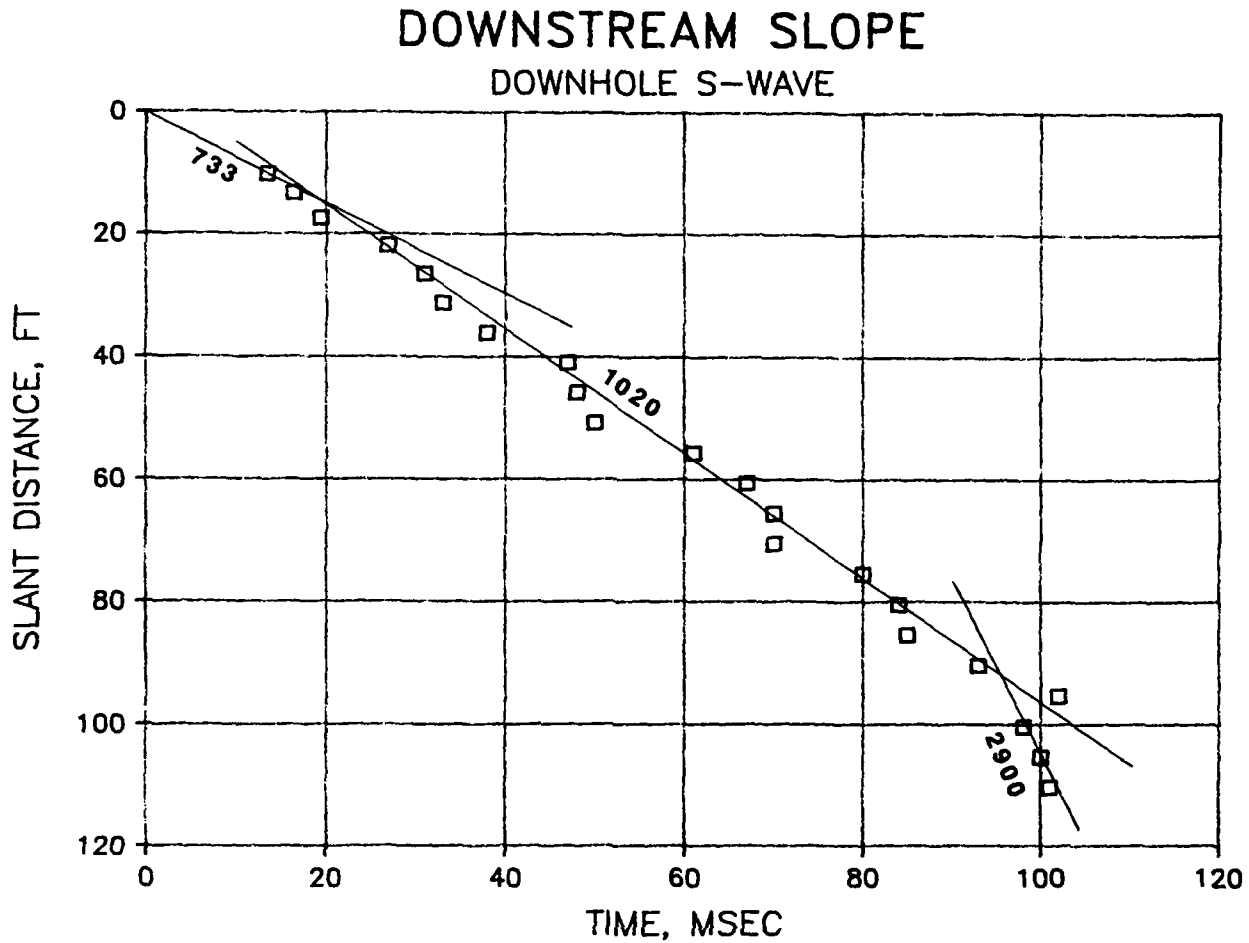

Figure 140. Downhole S-wave results, downstream slope, receiver in SCB5-A

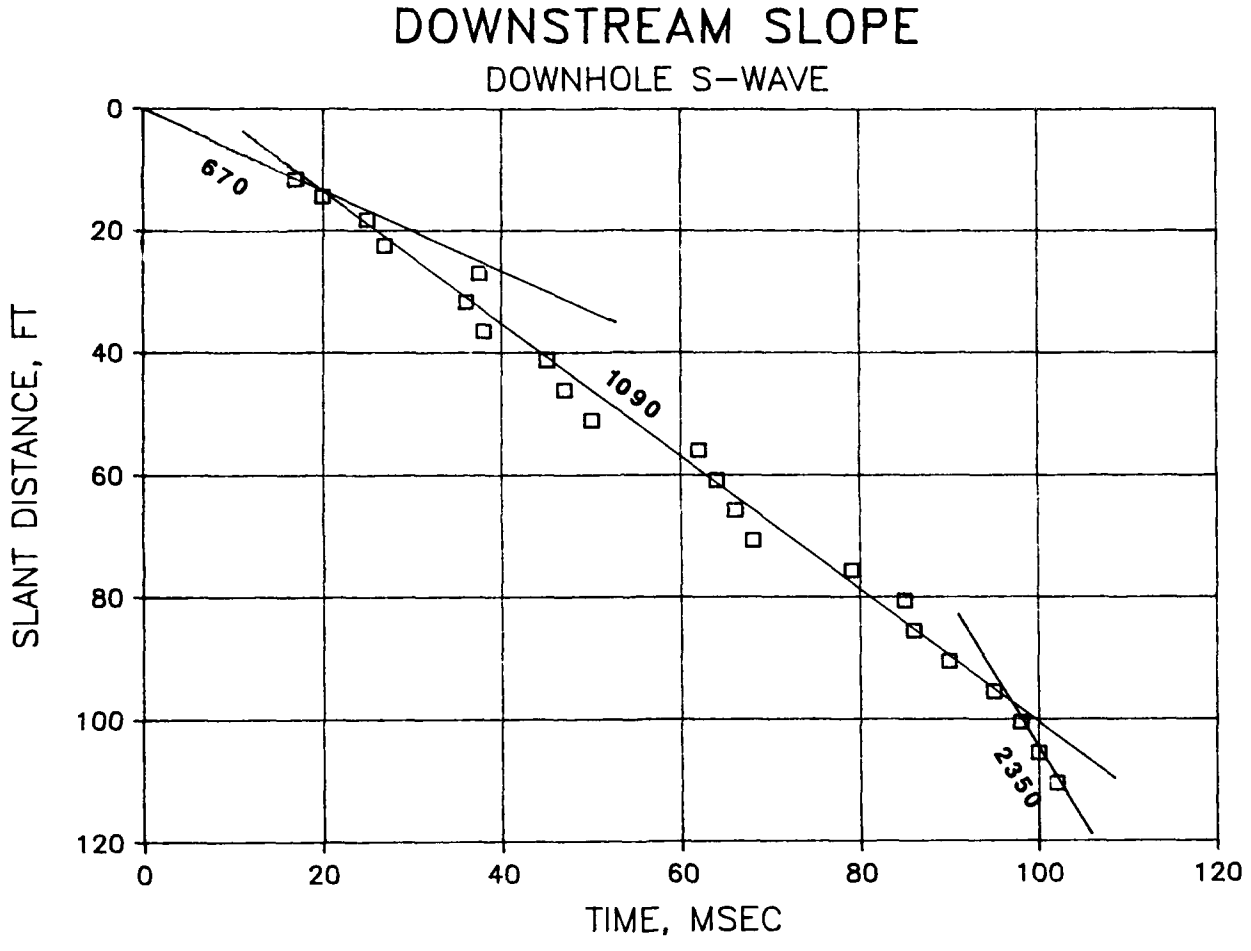

Figure 141. Downhole S-wave results, downstream slope, receiver in SCB5-C

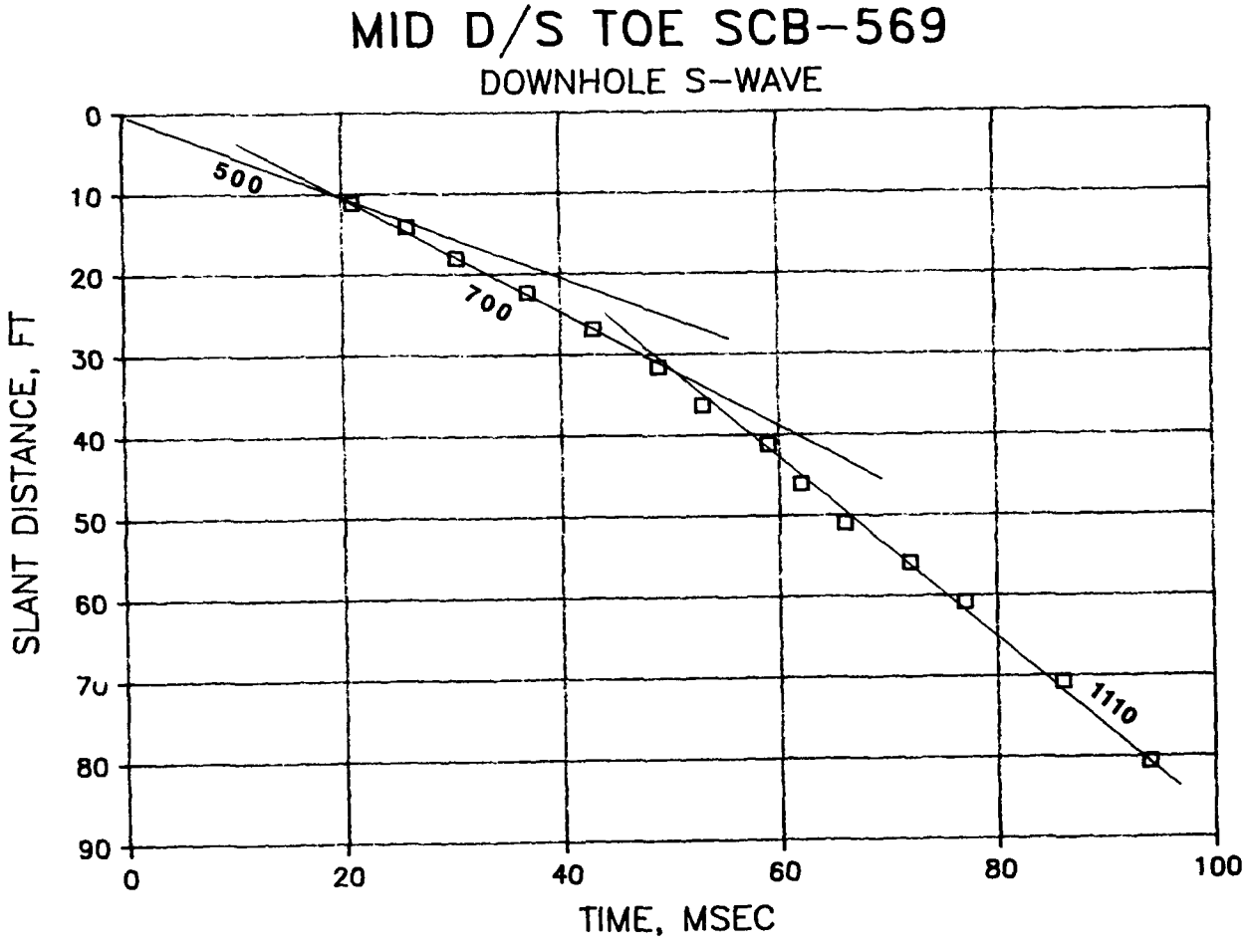

Figure 142. Downhole S-wave results, downstream toe, receiver in SCB-6

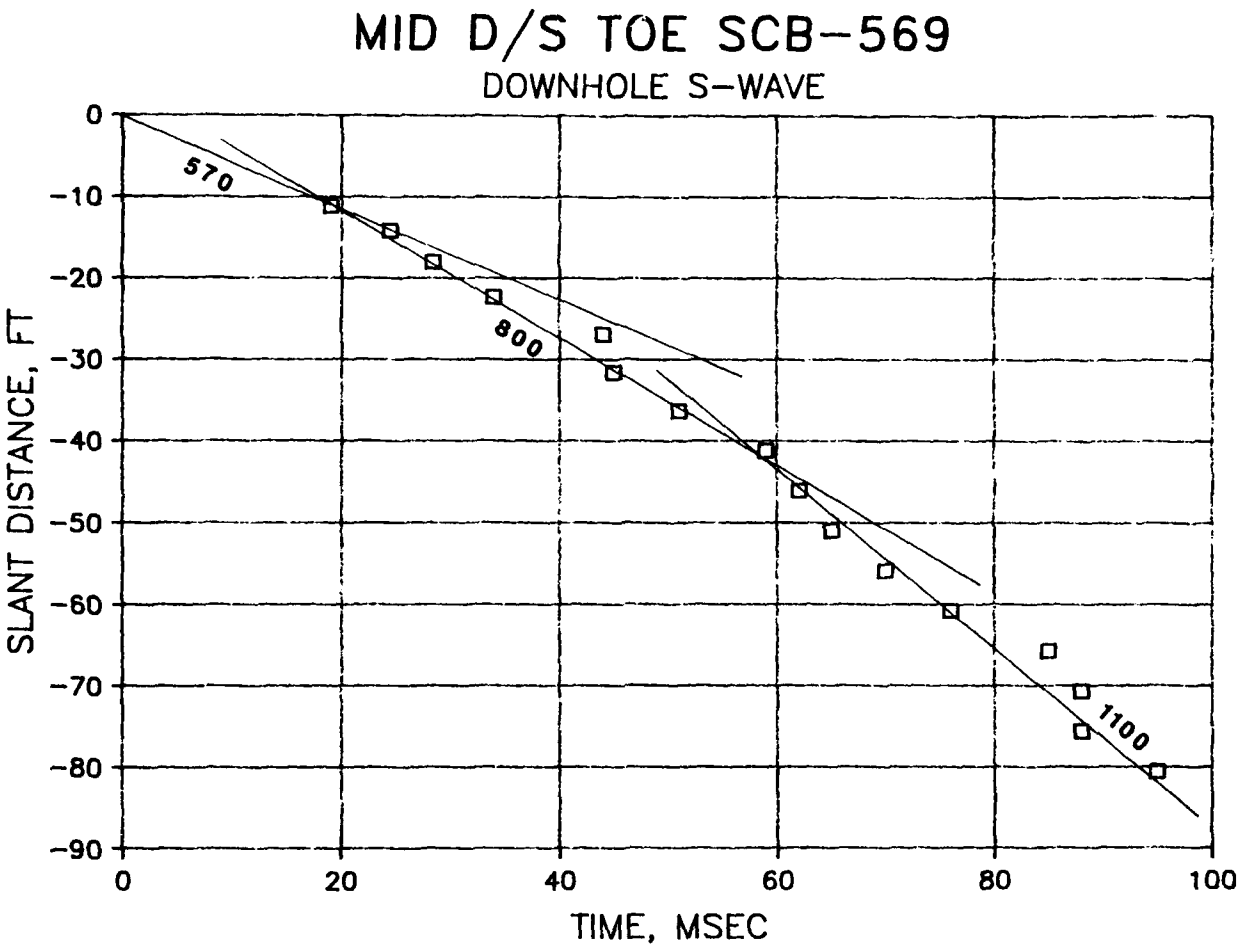

Figure 143. Downhole S-wave results, downstream toe, receiver in SCB-9

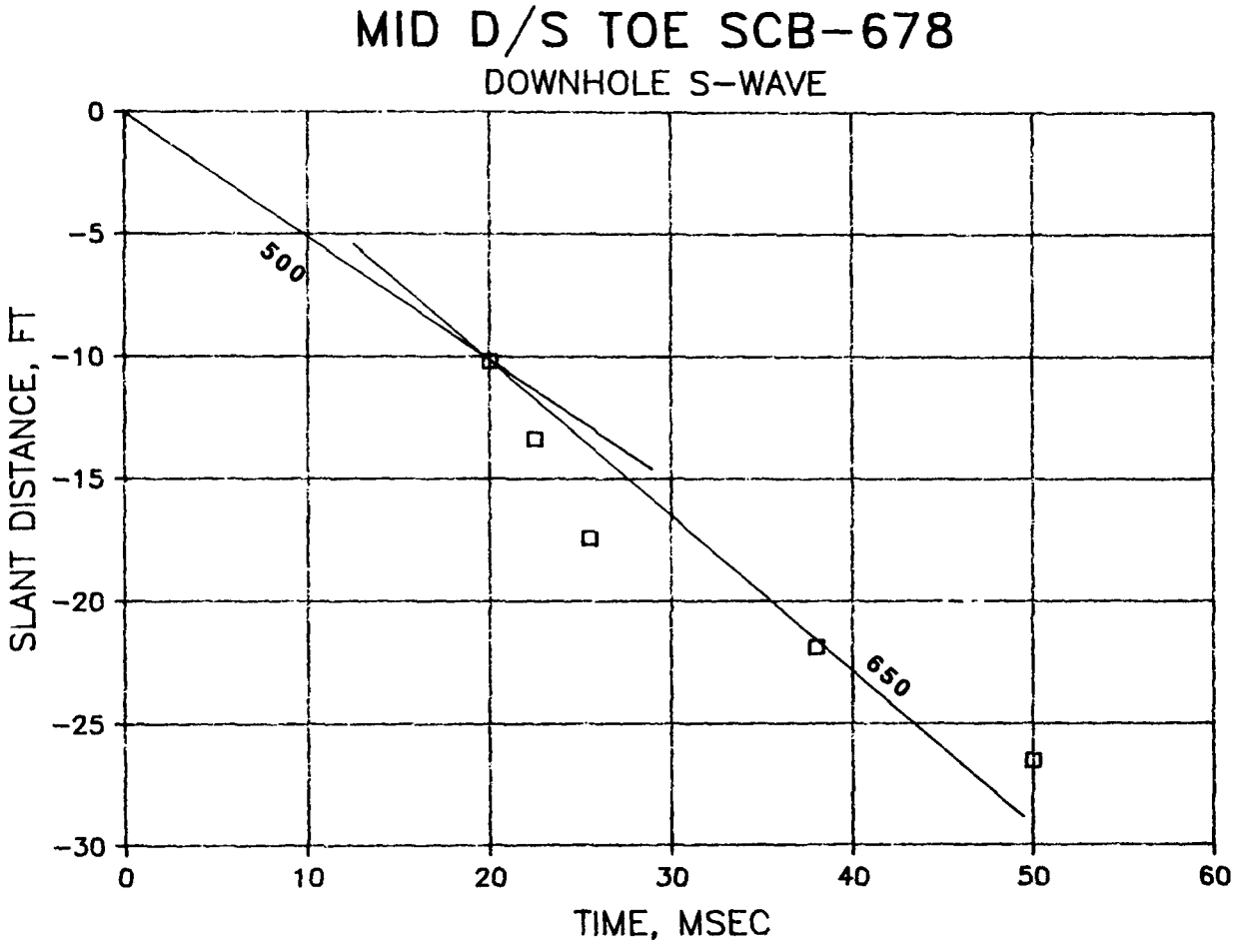

Figure 144. Downhole S-wave results, downstream toe, receiver in SCB-6

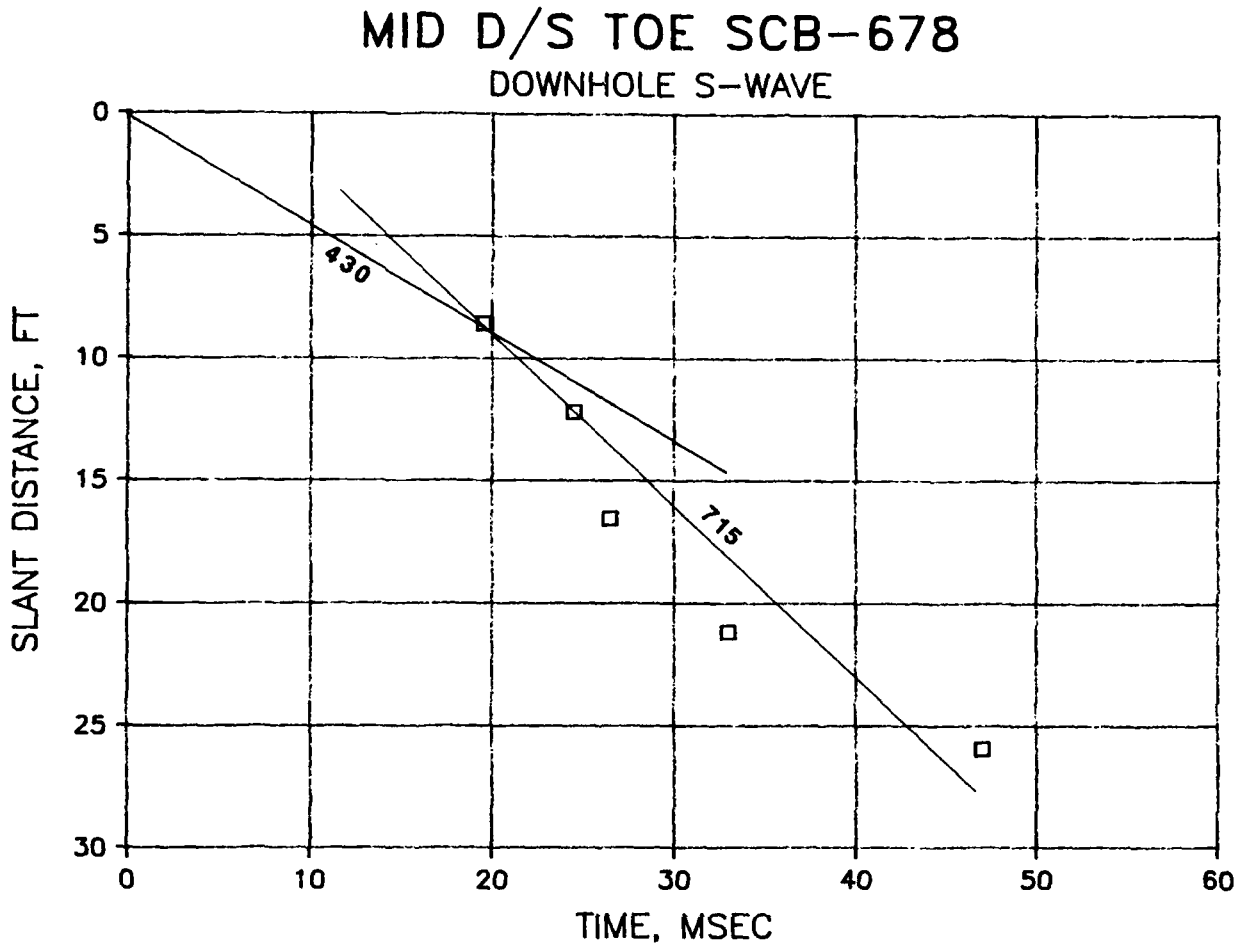

Figure 145. Downhole S-wave results, downstream toe, receiver in SCB-8

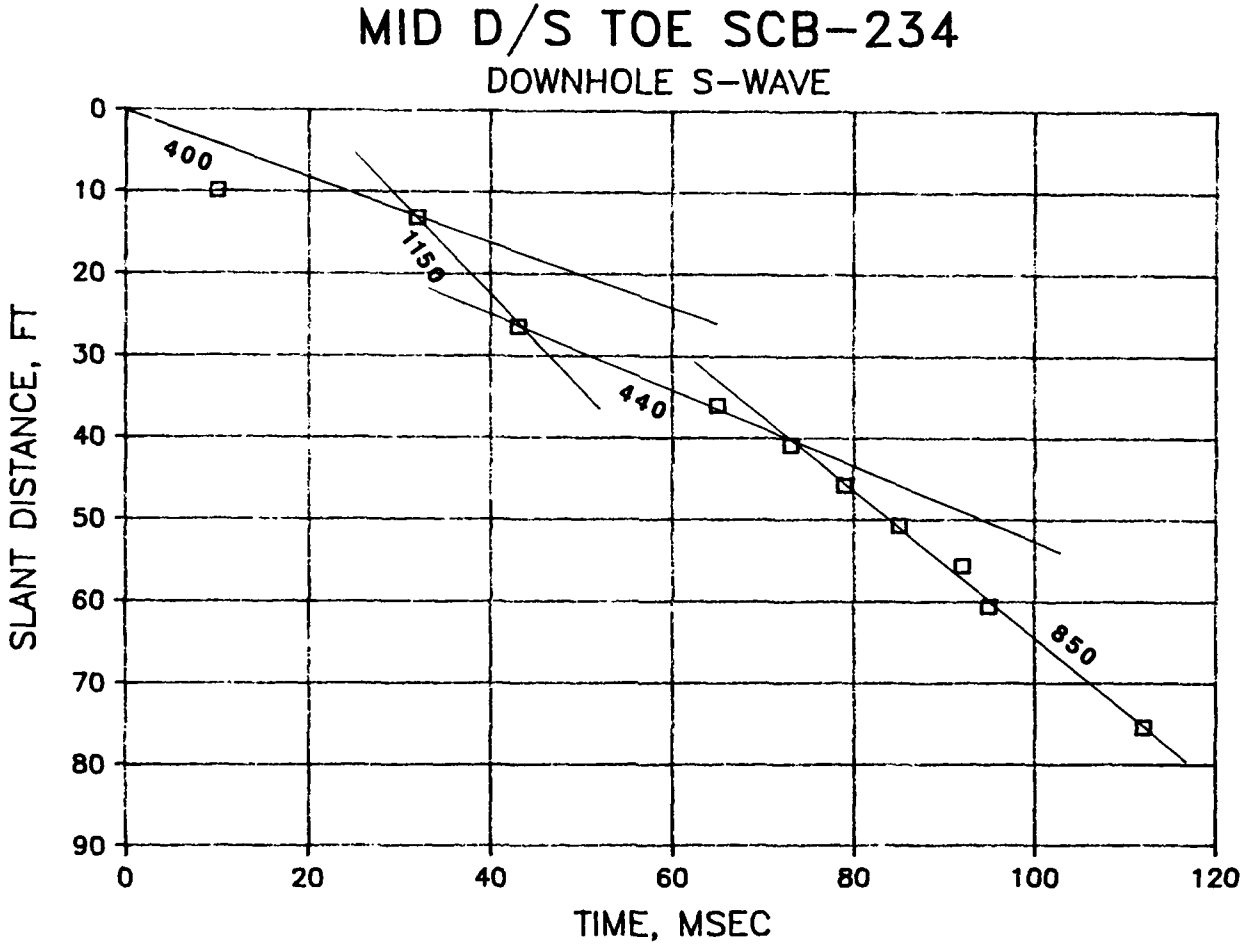

Figure 146. Downhole S-wave results, downstream toe, receiver in SCB-4

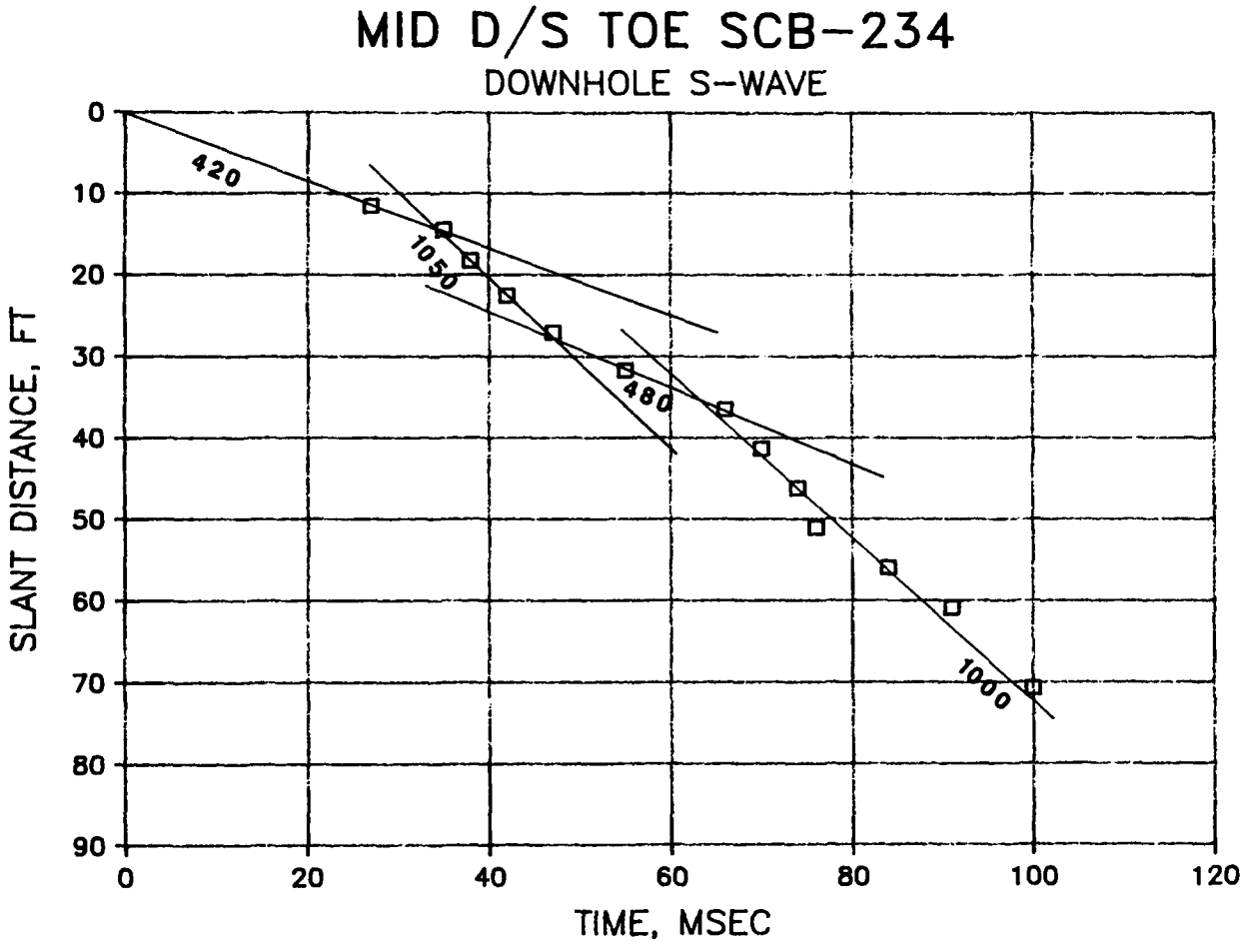

Figure 147. Downhole S-wave results, downstream toe, receiver in SCB-2

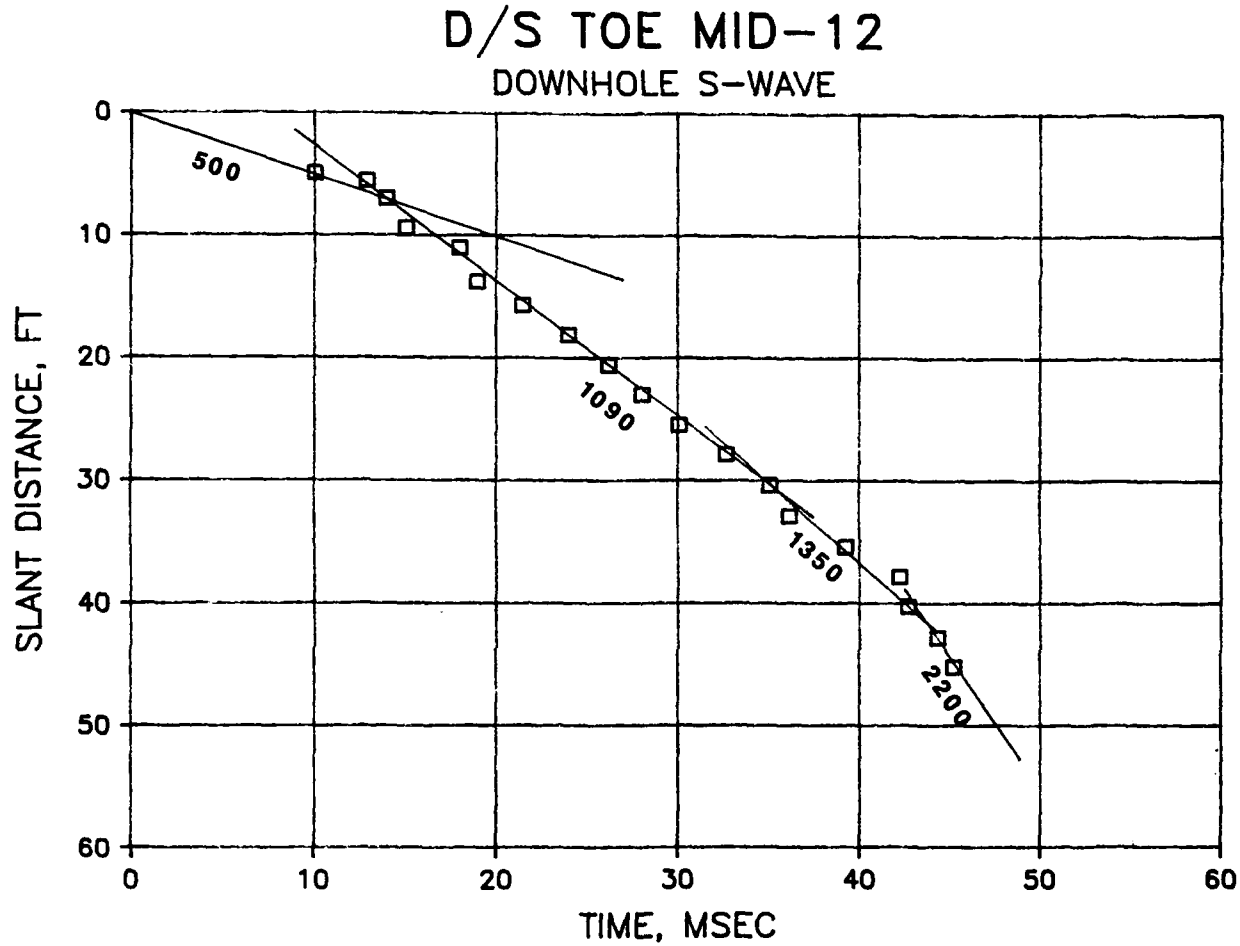

Figure 148. Downhole S-wave results, MID-1,2, downstream toe

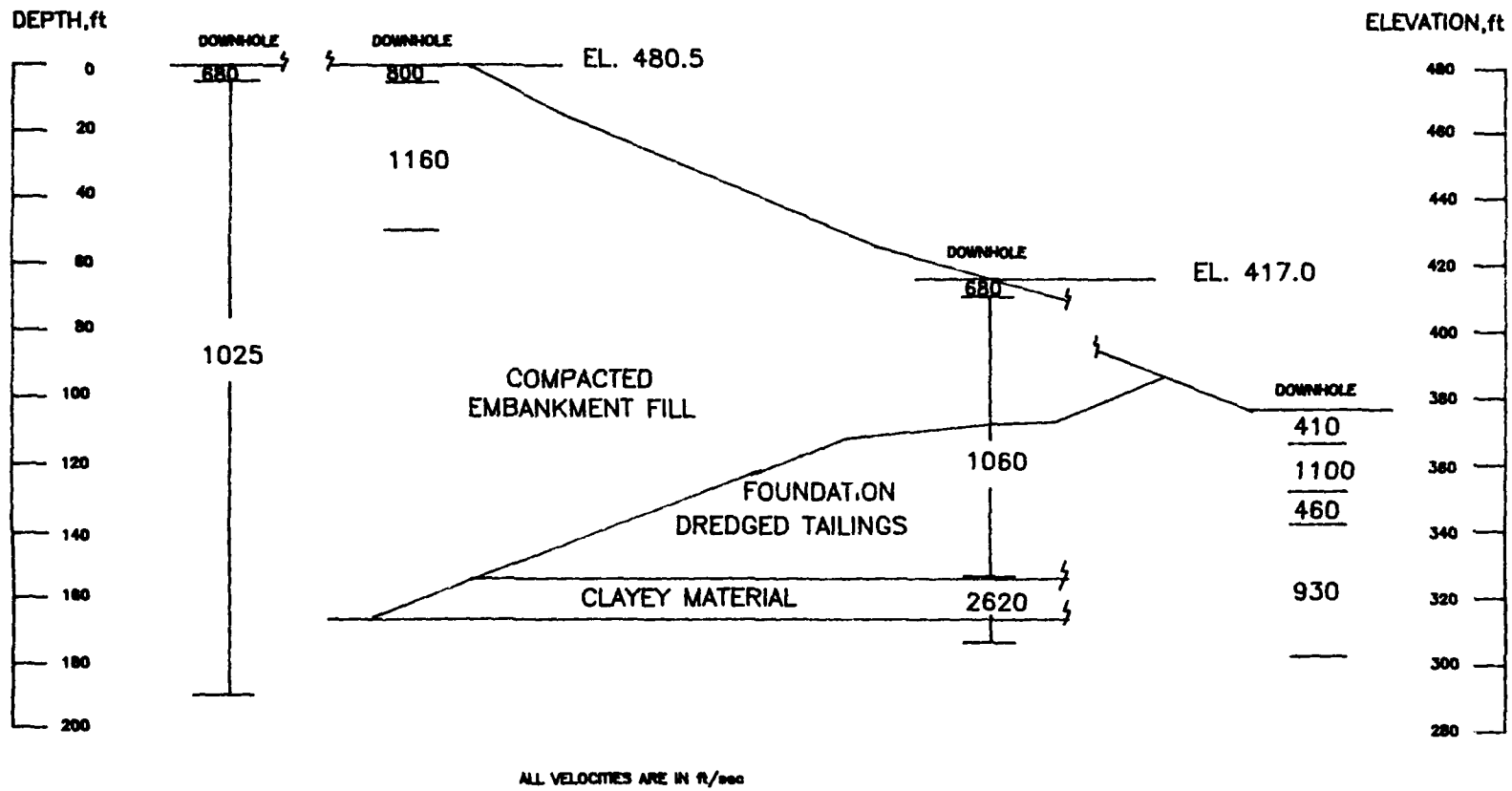

Figure 149. Interpreted S-wave profile from downhole testing for the section through Station 448+00, Mormon Island Auxiliary Dam

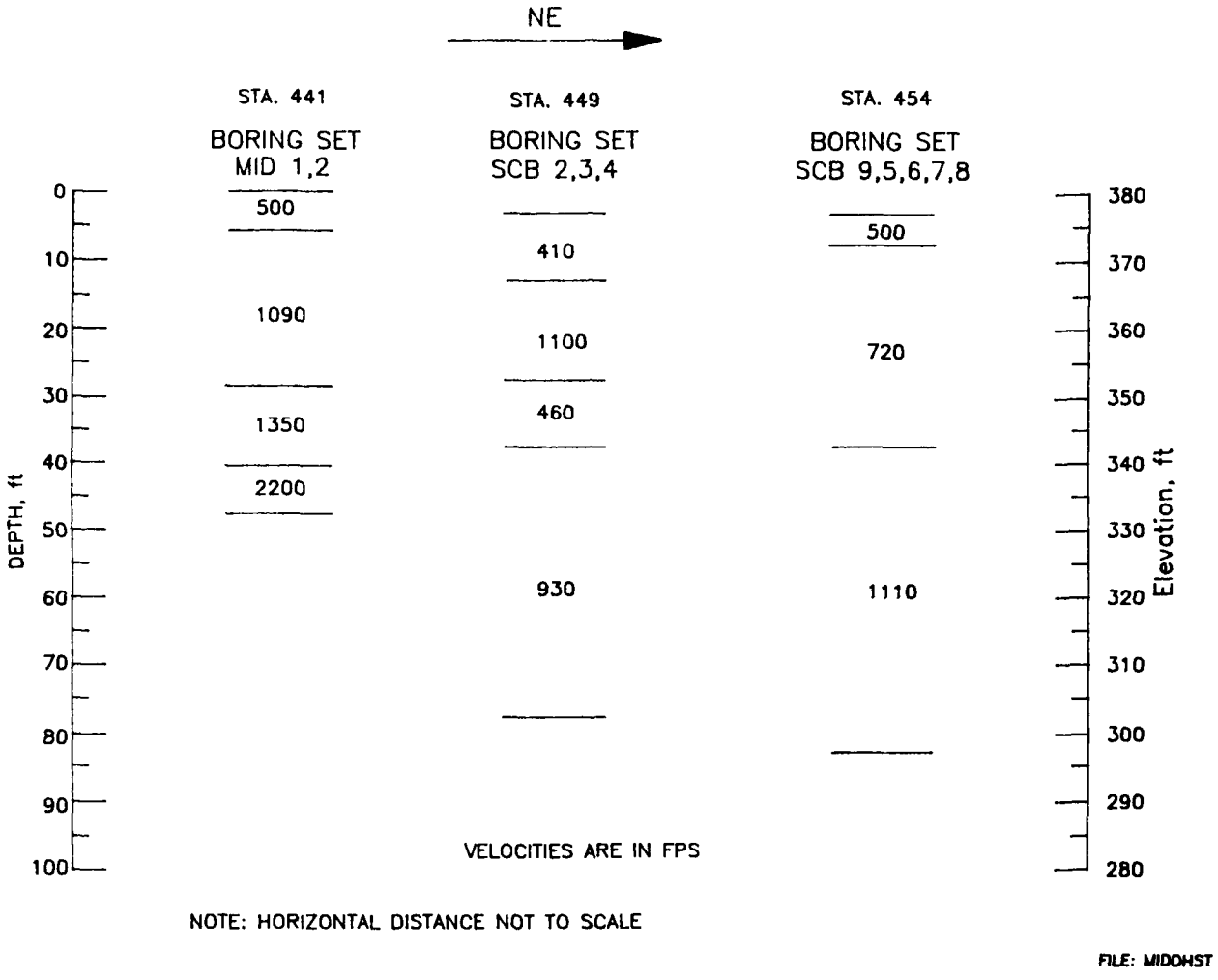

Figure 150. Interpreted S-wave profile from downhole testing along the downstream toe of Mormon Island Auxiliary Dam

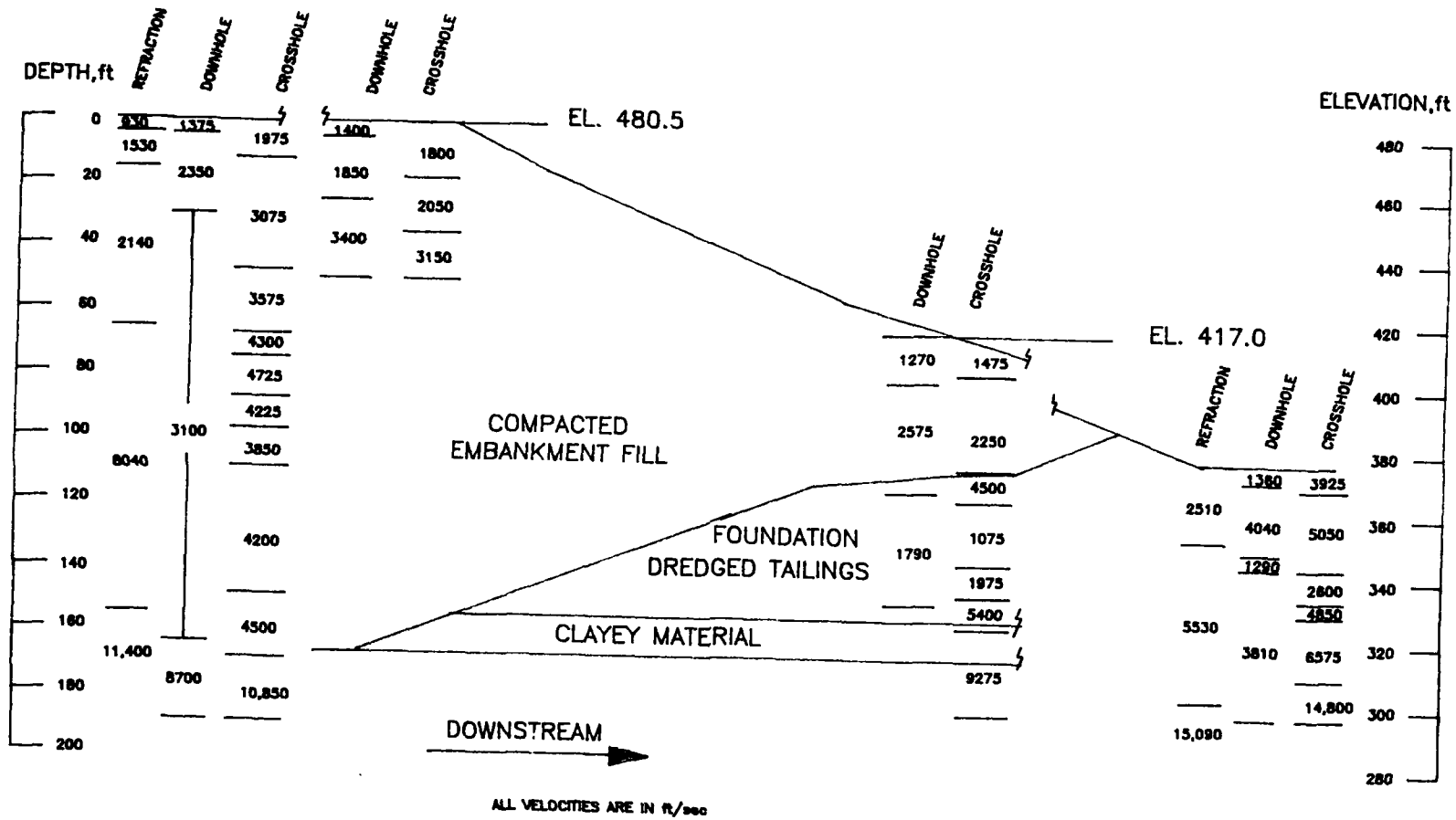

Figure 151. P-wave composite for cross section through Station 448+00, Mormon Island Auxiliary Dam

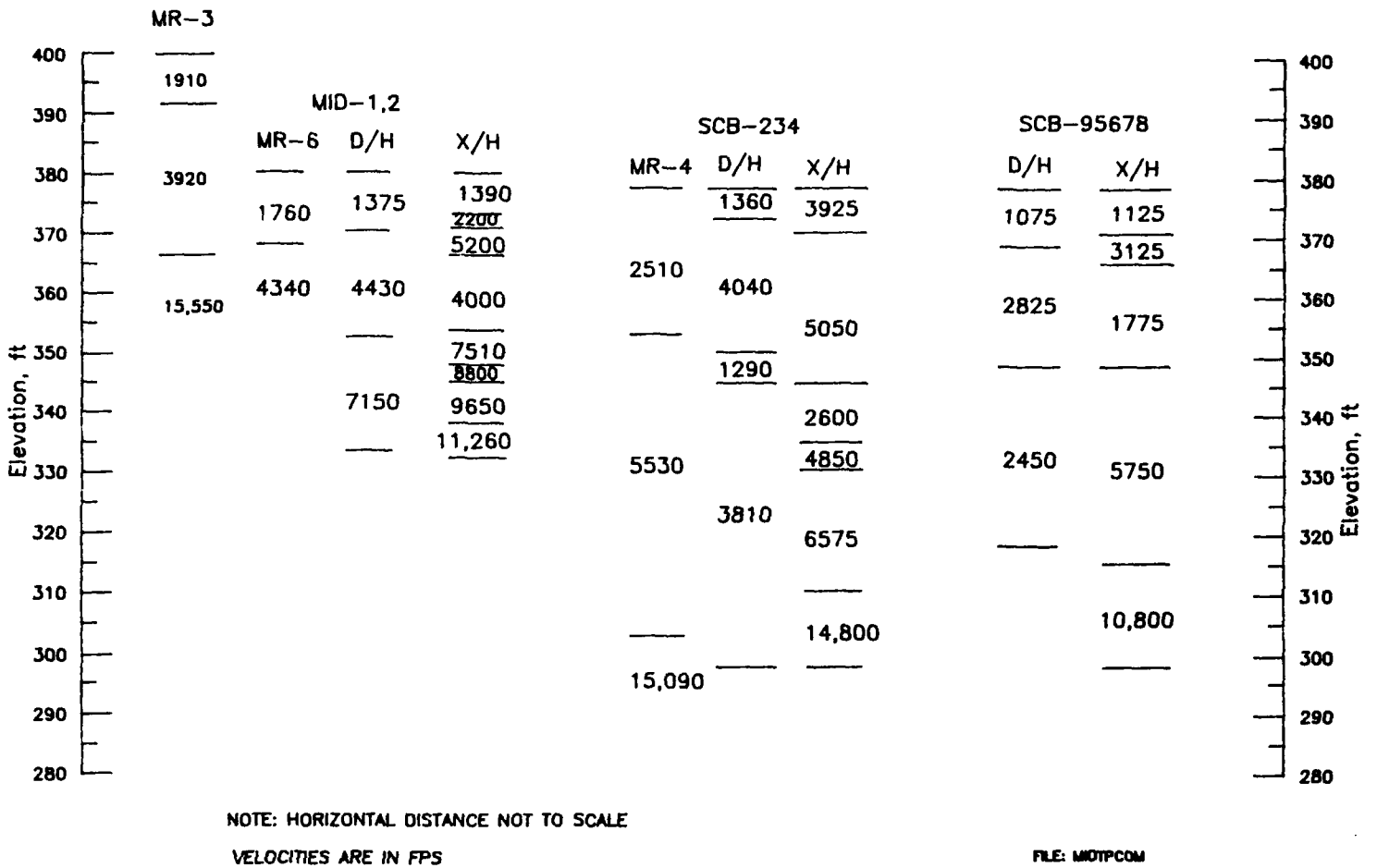

Figure 152. P-wave composite along the toe of Mormon Island Auxiliary Dam

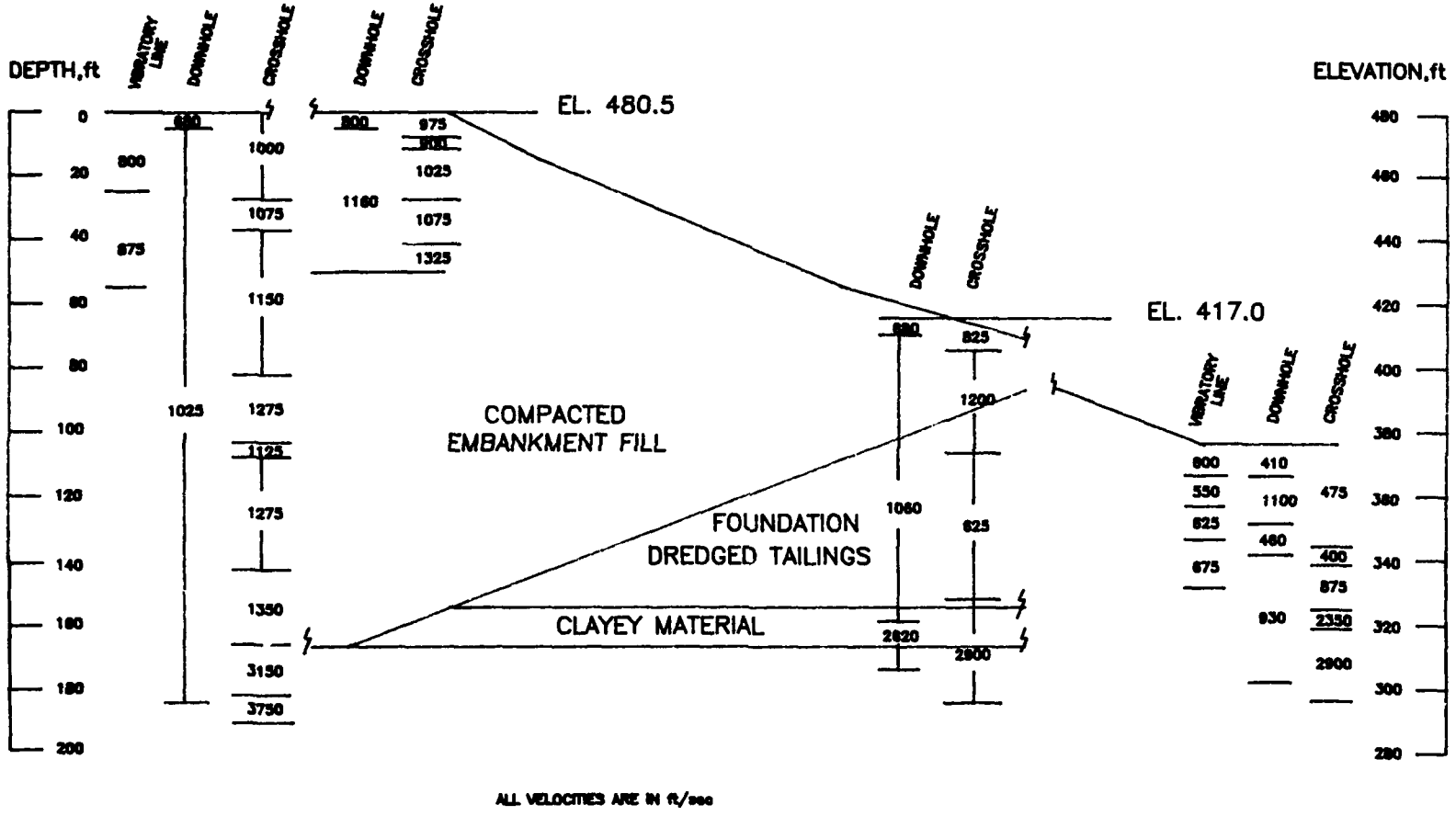

Figure 153. S-wave composite for cross section through Station 448+00, Mormon Island Auxiliary Dam

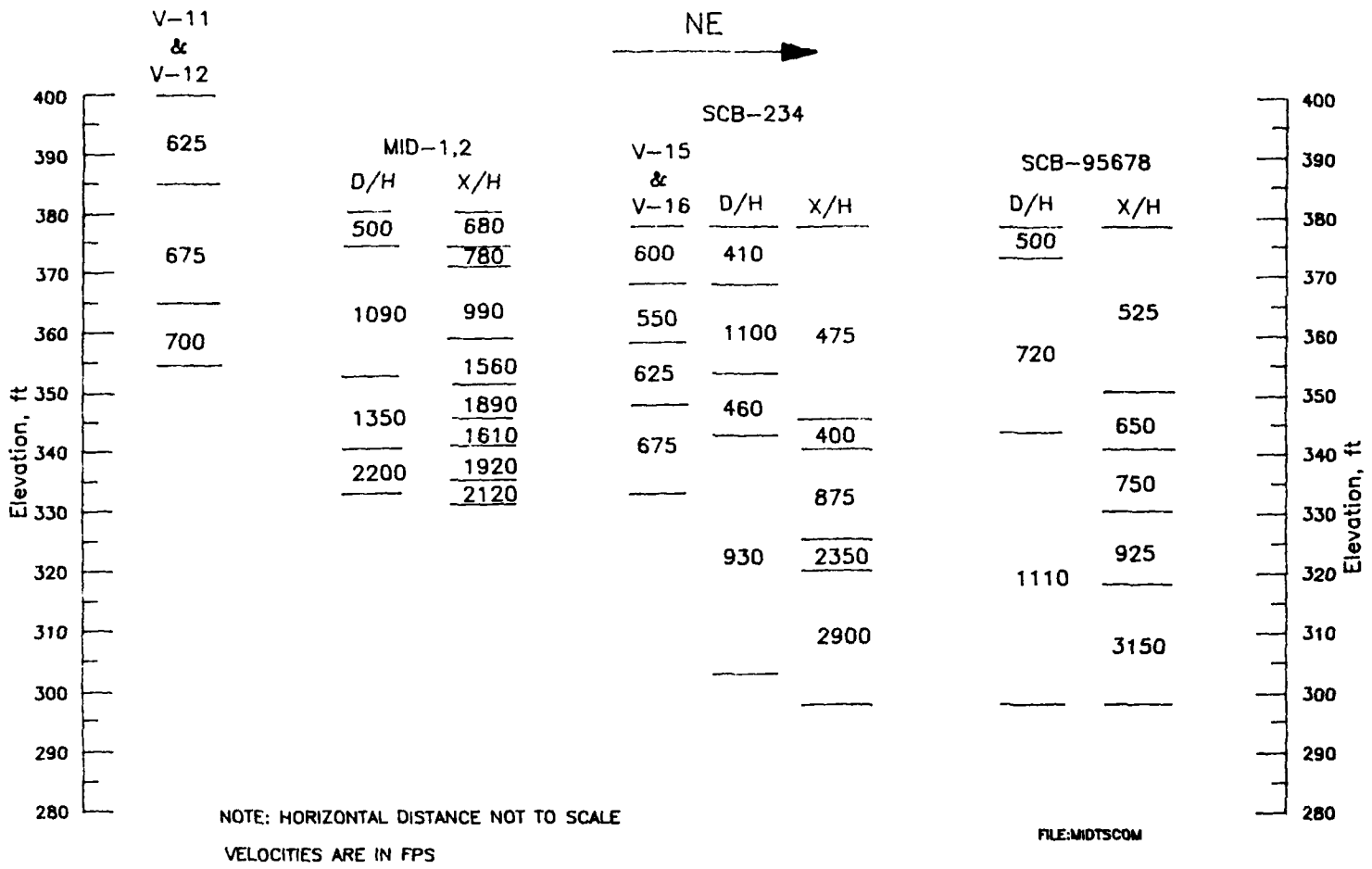

Figure 154. S-wave composite along the toe of Mormon Island Auxiliary Dam

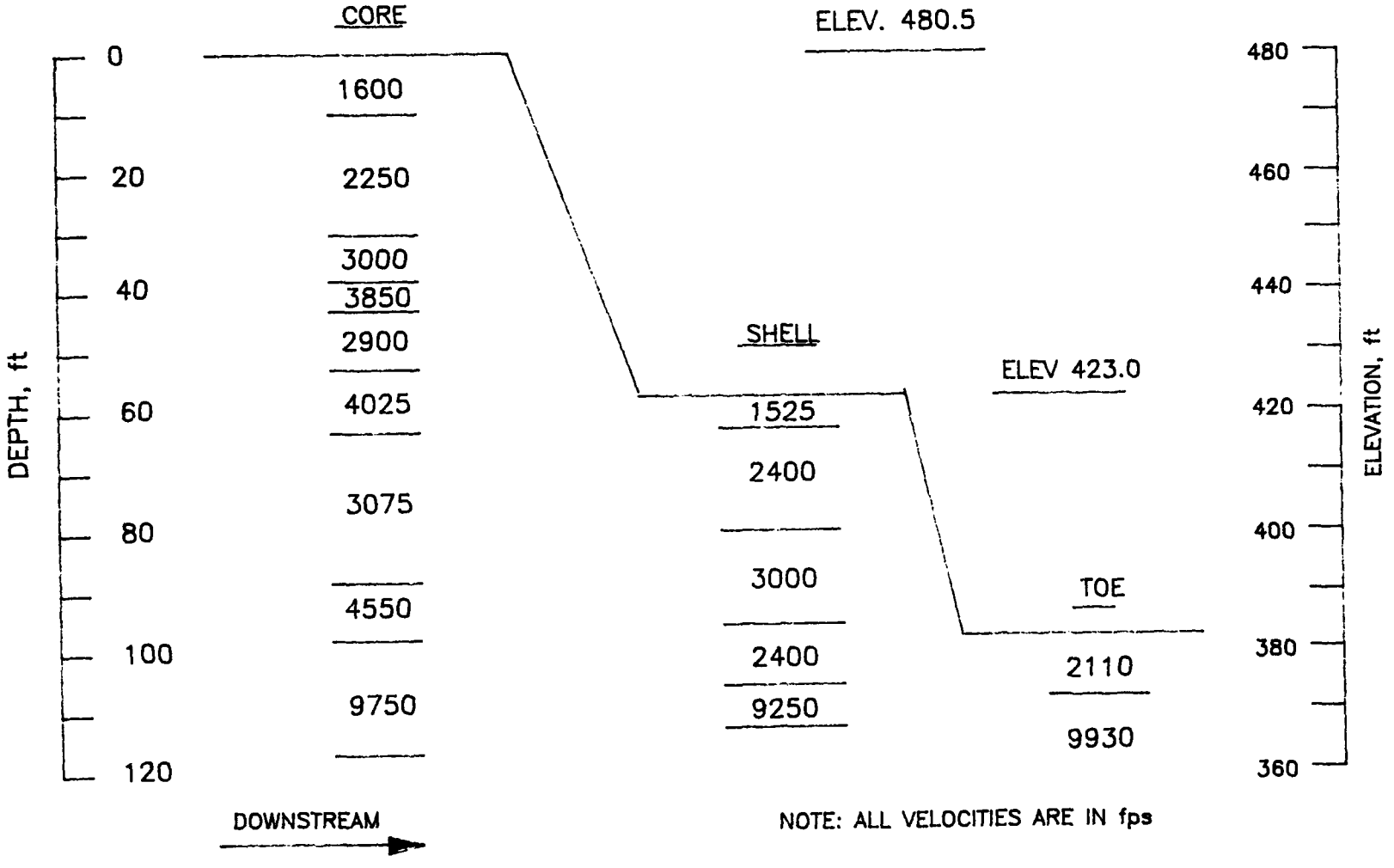

Figure 155. P-wave zonal velocity interpretation for cross section through approximate Station 180+50, Dike 5

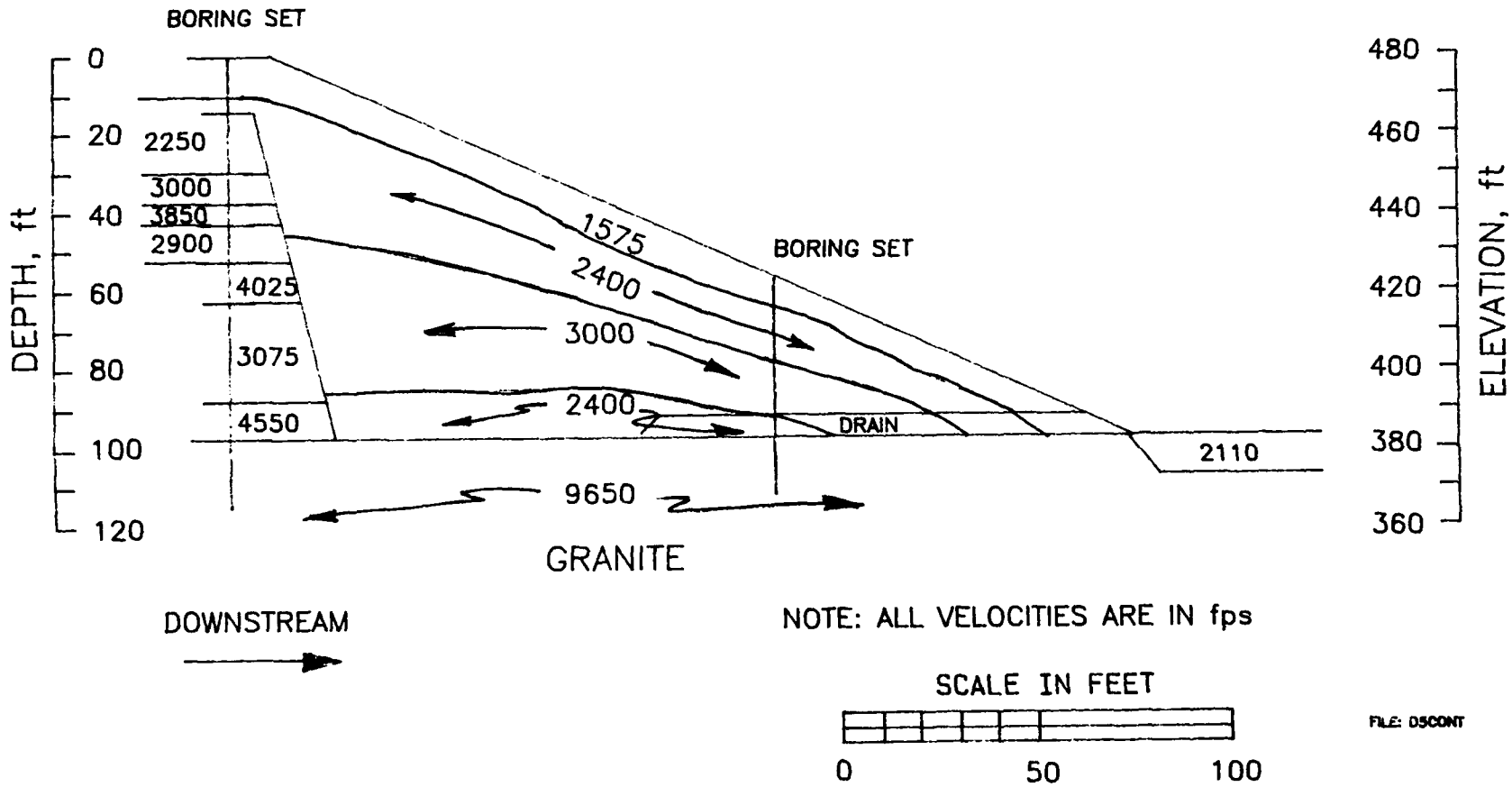

Figure 156. P-wave velocity contours for cross section at approximate Station 180+50, Dike 5

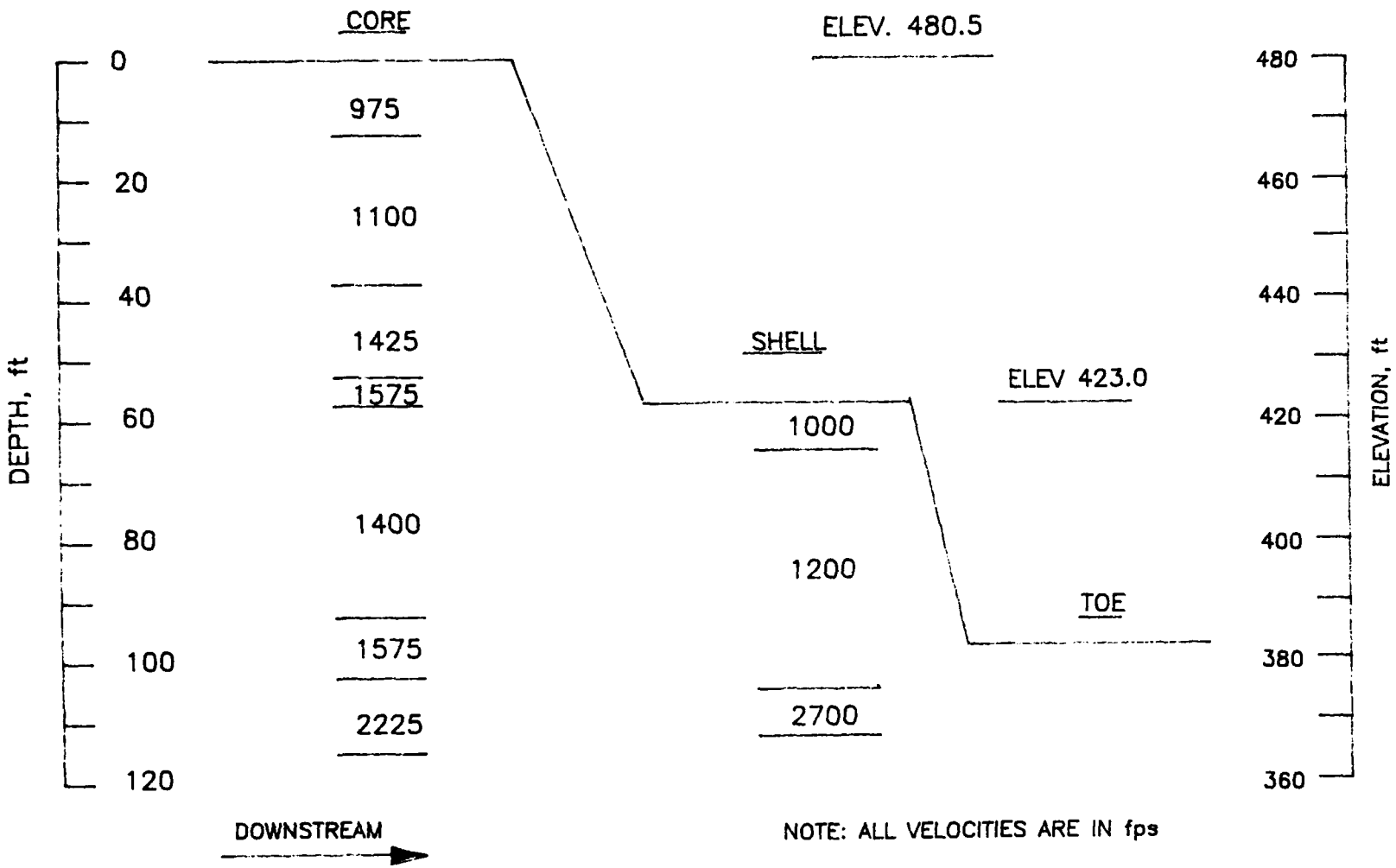

Figure 157. S-wave zonal velocity interpretation for cross section through approximate Station 180+50, Dike 5

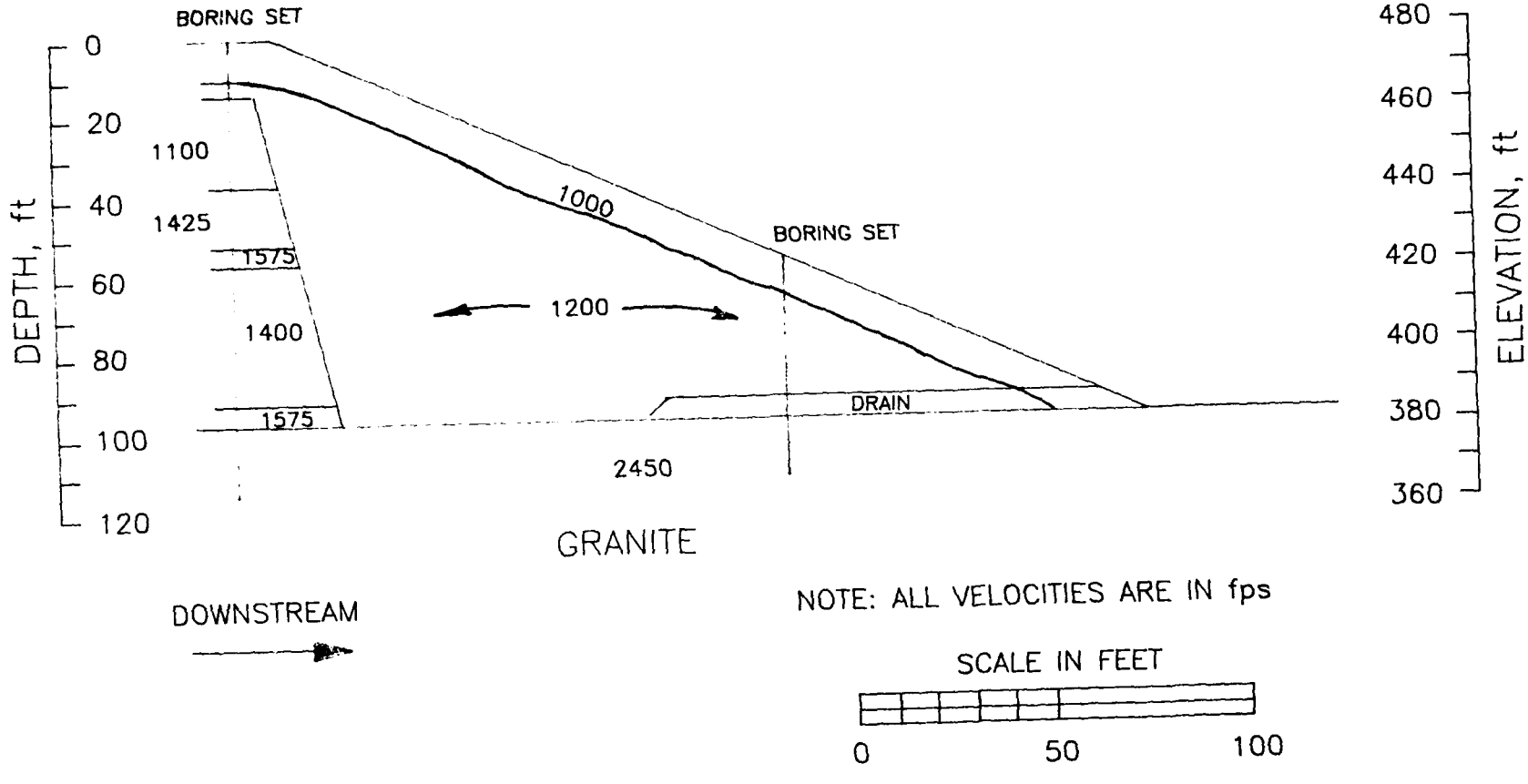

Figure 158. S-wave velocity contours for cross section at approximate Station 180+50, Dike 5

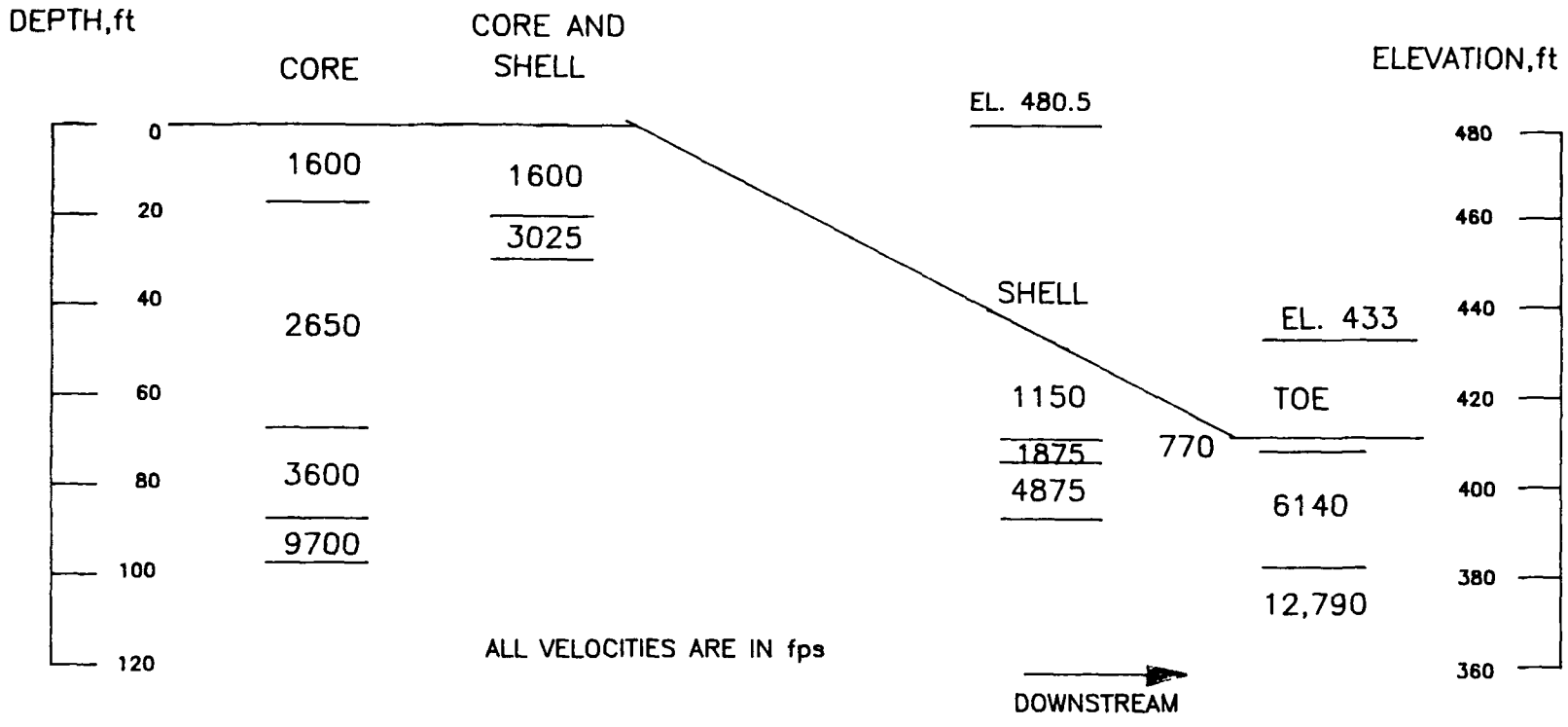

Figure 159. P-wave zonal velocity interpretation for cross section through approximate Station 235+00, Right Wing Dam

RW0235COMP

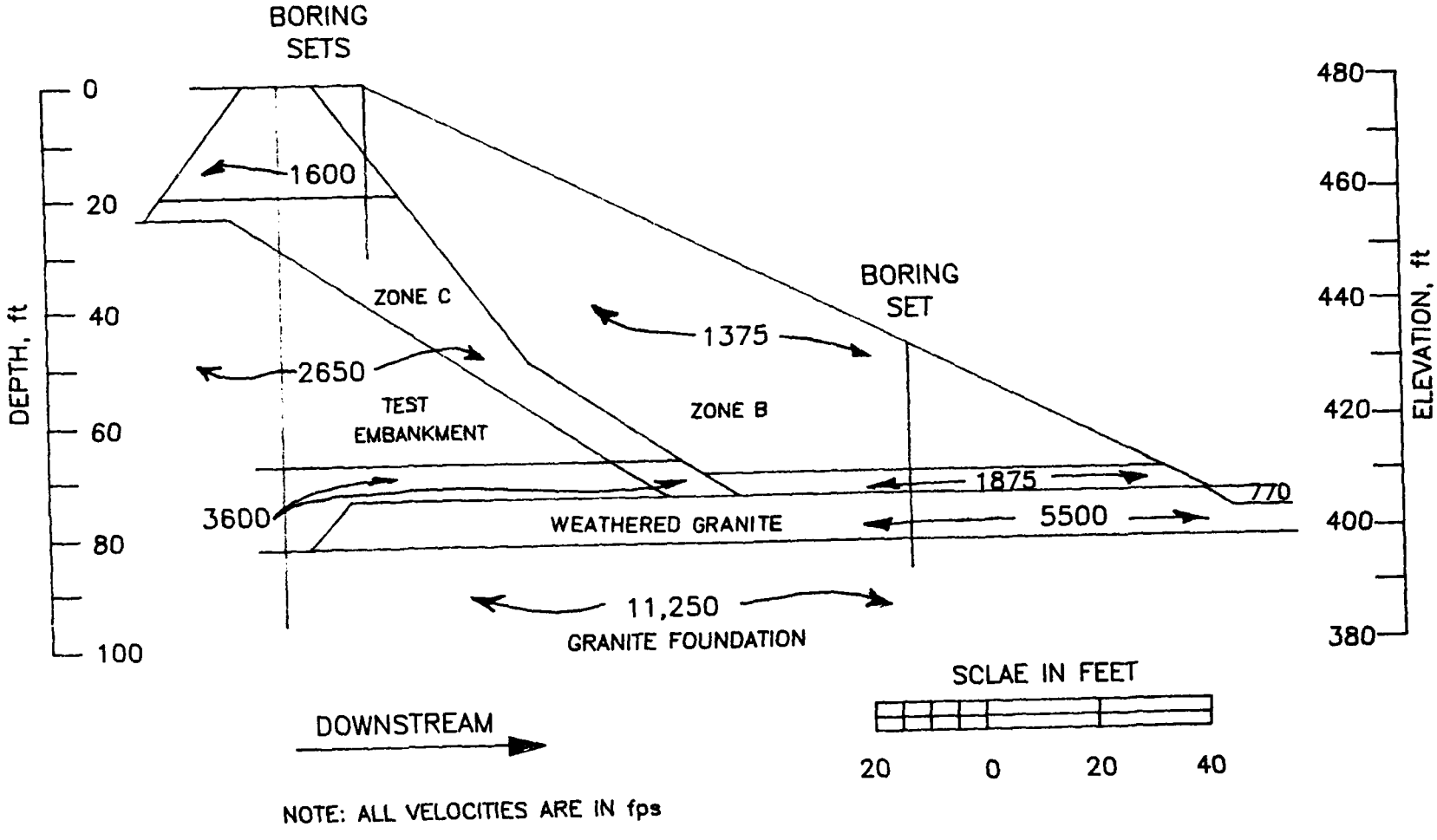

Figure 160. P-wave velocity contours for cross section at approximate Station 235+00, Right Wing Dam

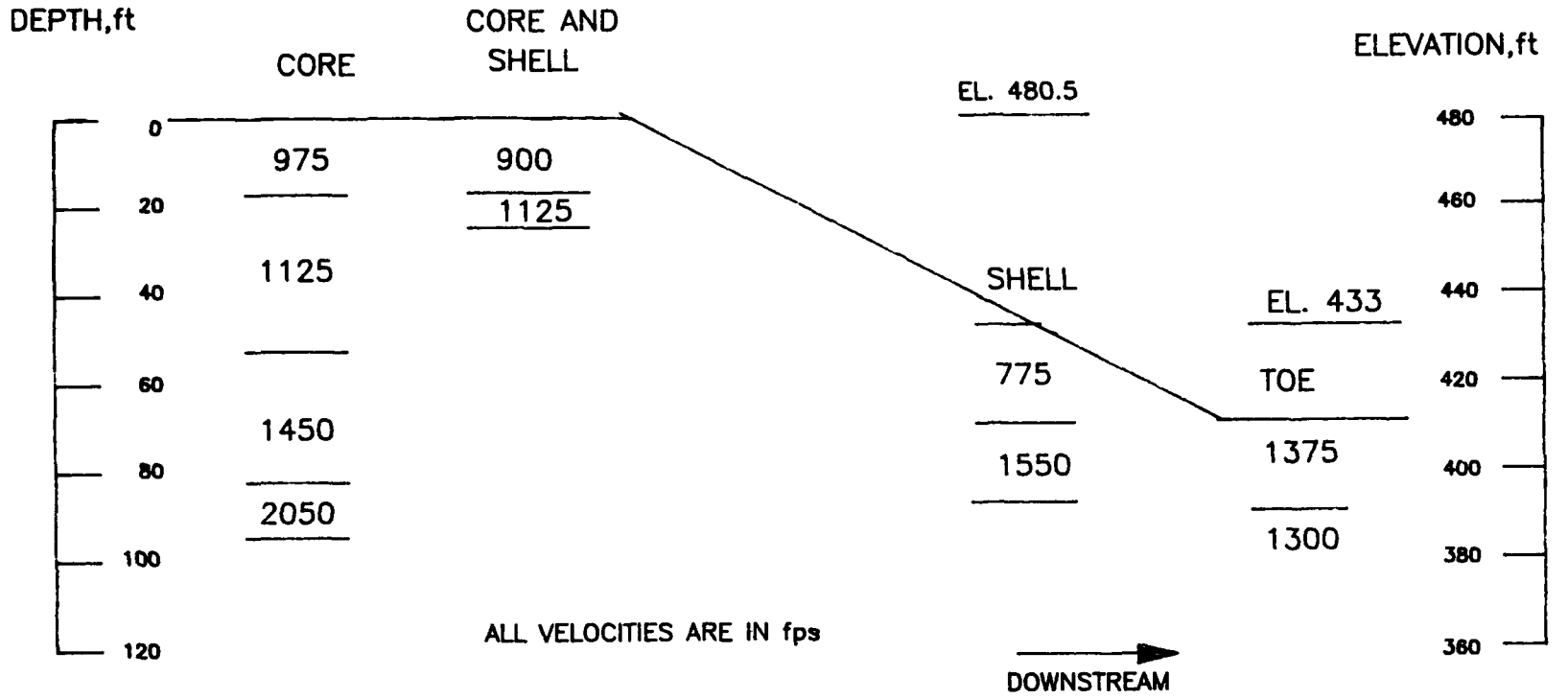

Figure 161. S-wave zonal velocity interpretation for cross section through approximate Station 235+00, Right Wing Dam

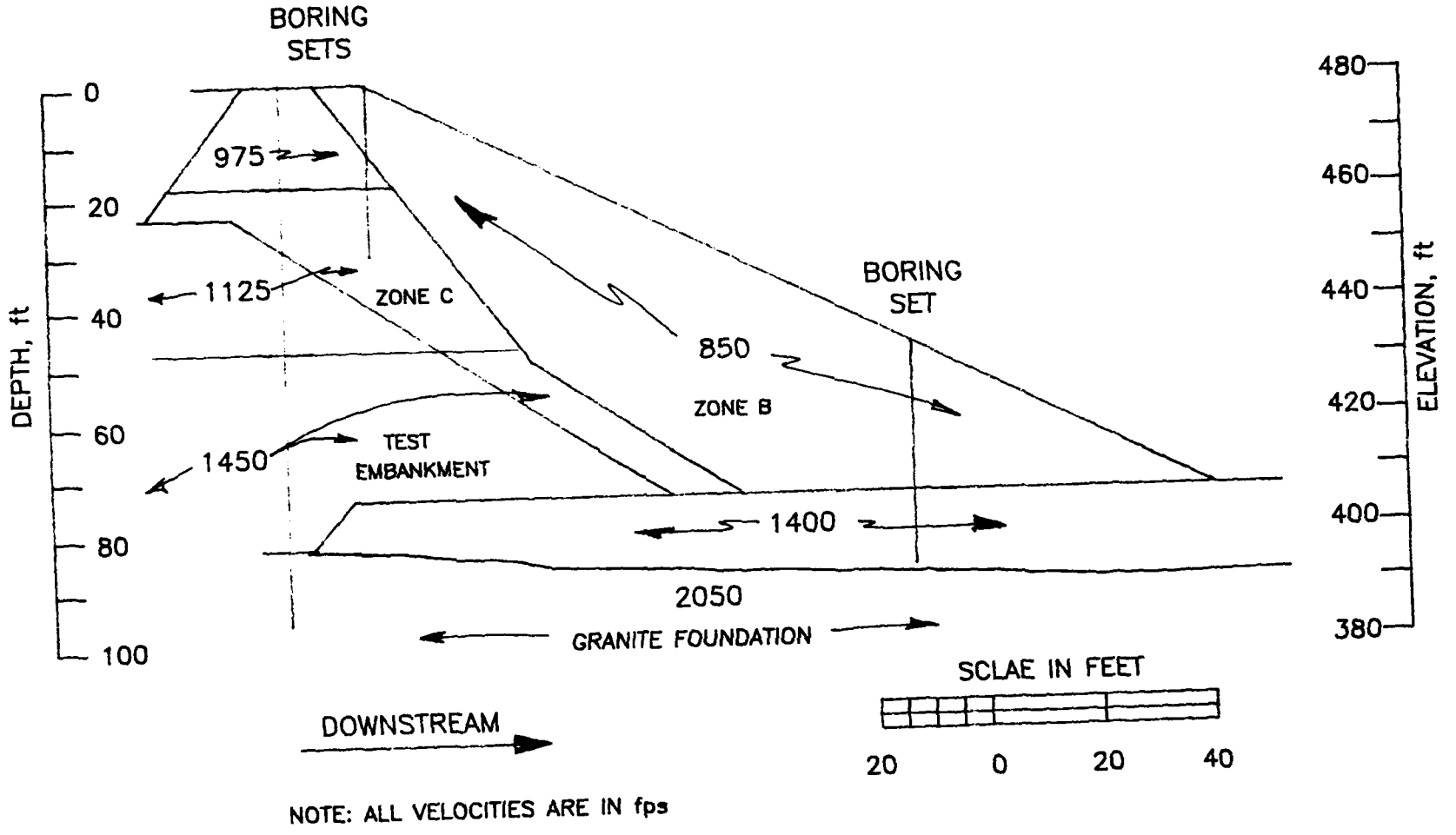

Figure 162. S-wave velocity contours for cross section at approximate Station 235+00, Right Wing Dam

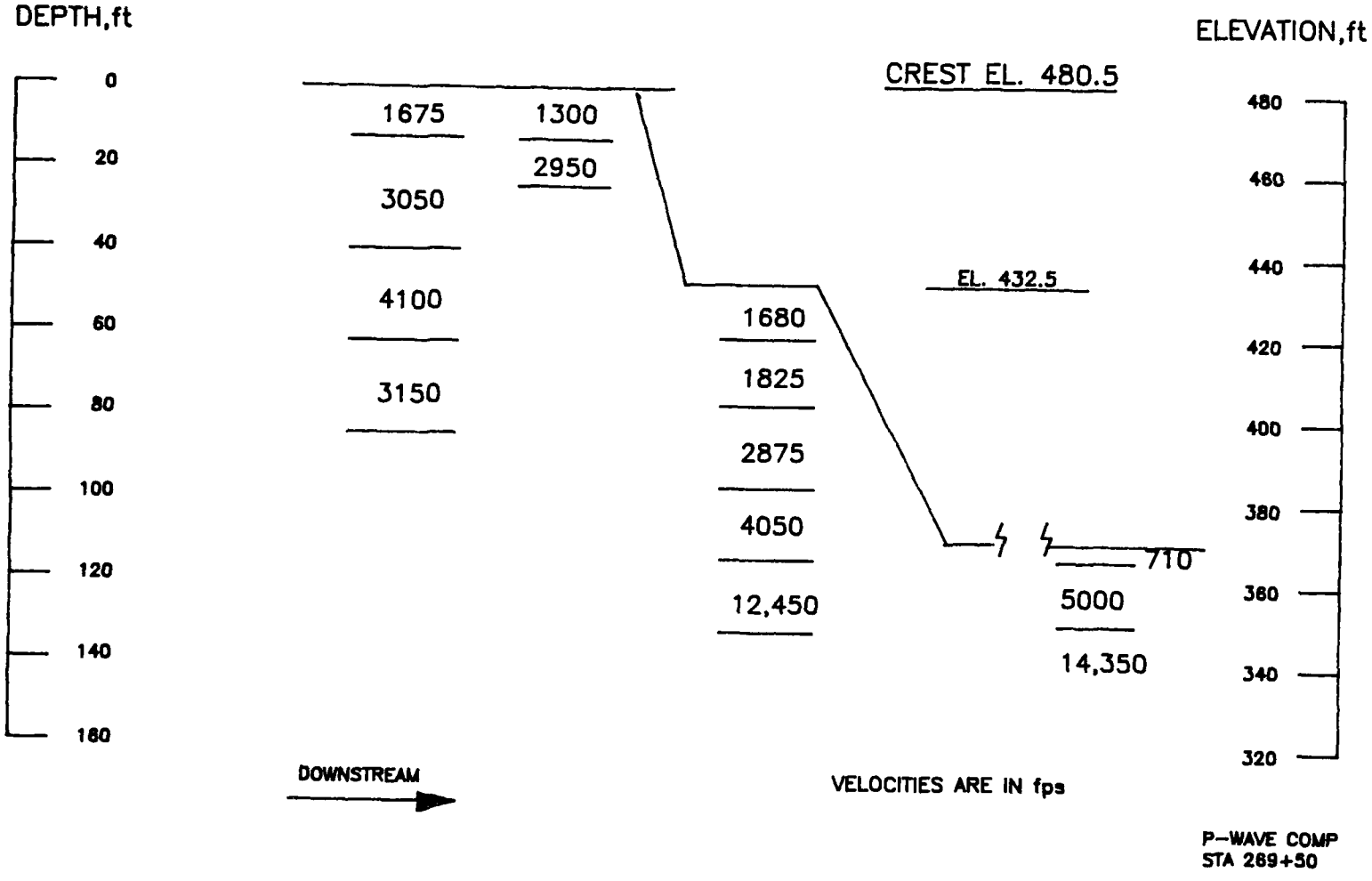

Figure 163. P-wave zonal velocity interpretation for cross section through approximate Station 269+50, Right Wing Dam

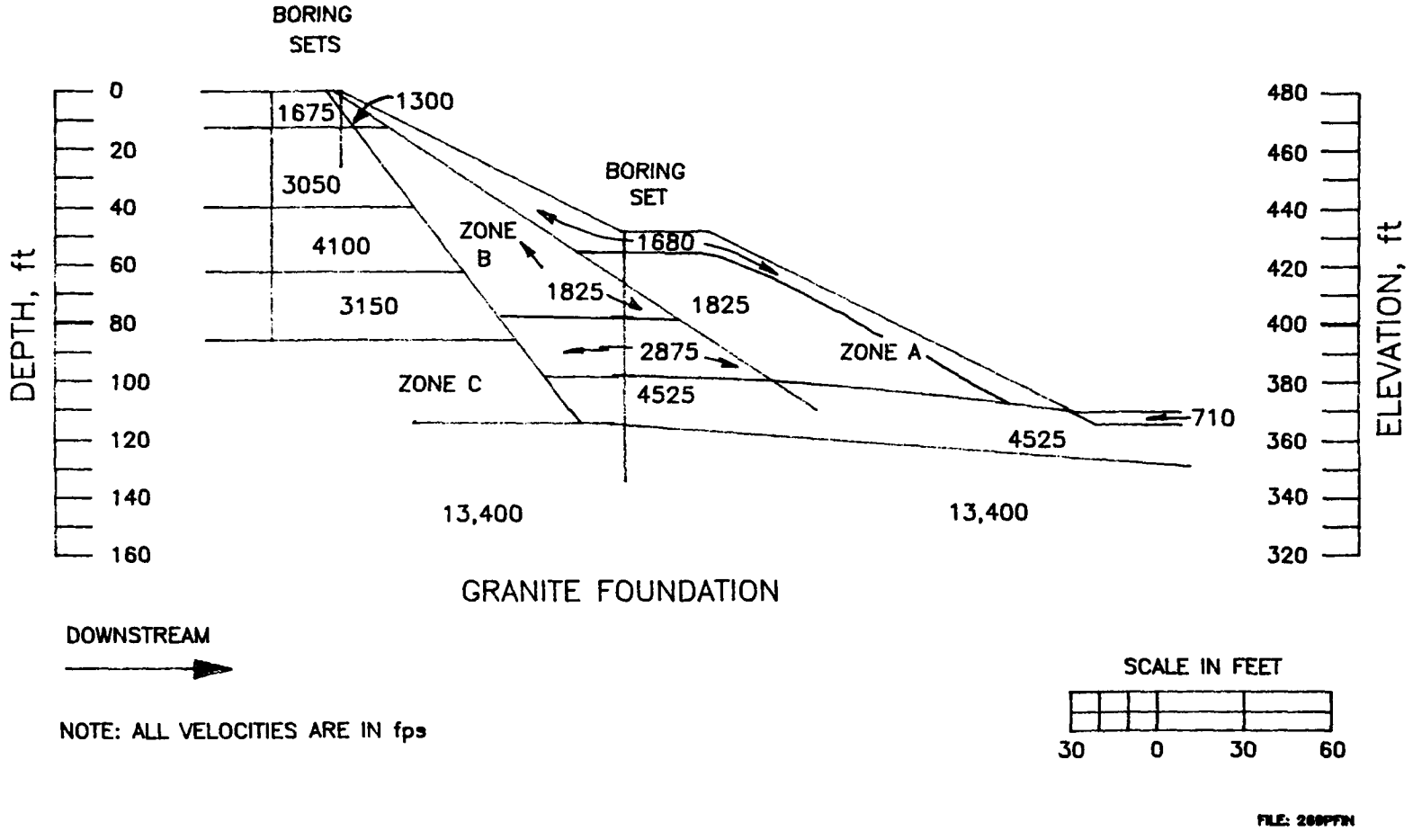

Figure 164. P-wave velocity contours for cross section at approximate Station 269+50, Right Wing Dam

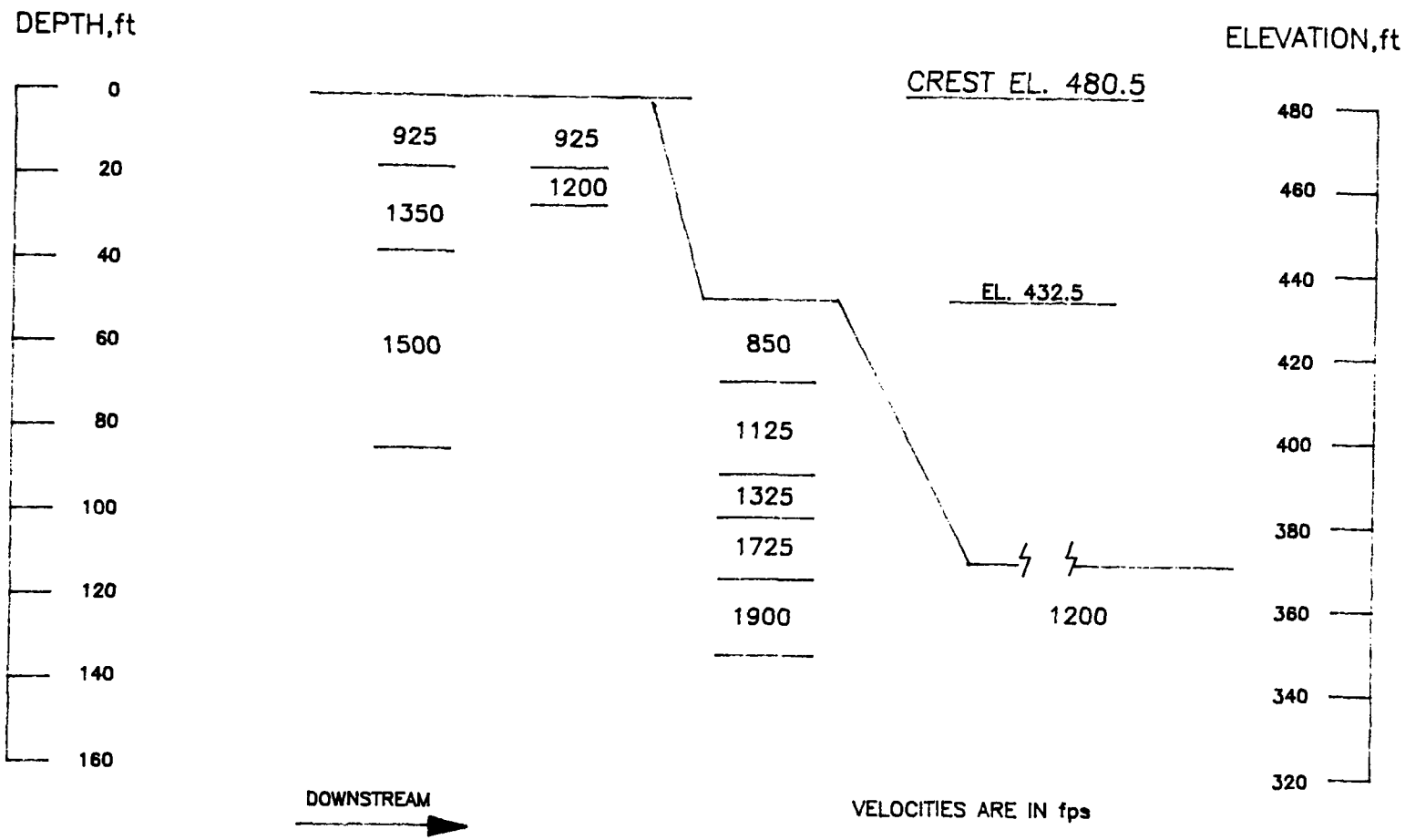

Figure 165. S-wave zonal velocity interpretation for cross section through approximate Station 269+50, Right Wing Dam

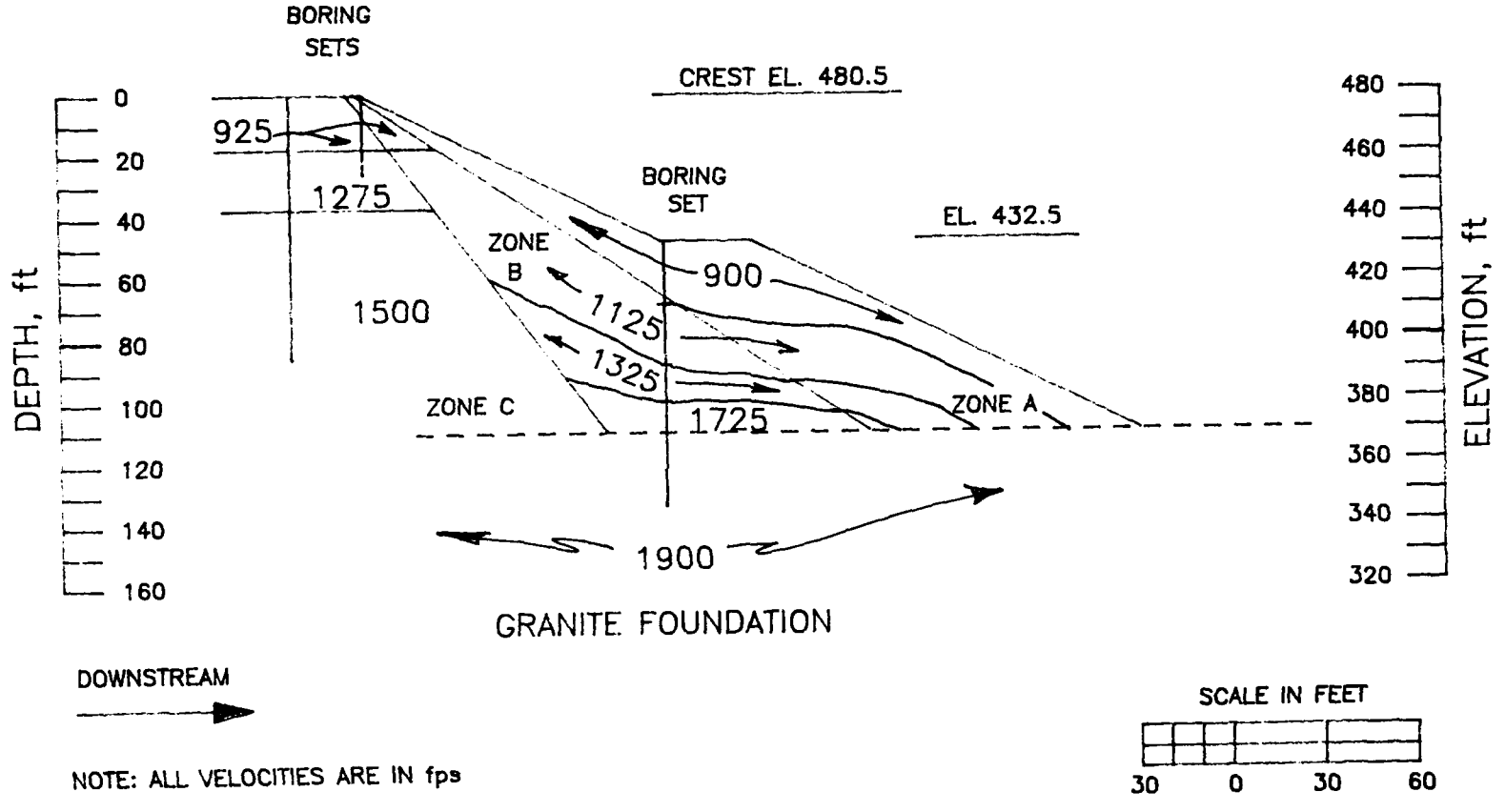

Figure 166. S-wave velocity contours for cross section at approximate Station 269+50, Right Wing Dam

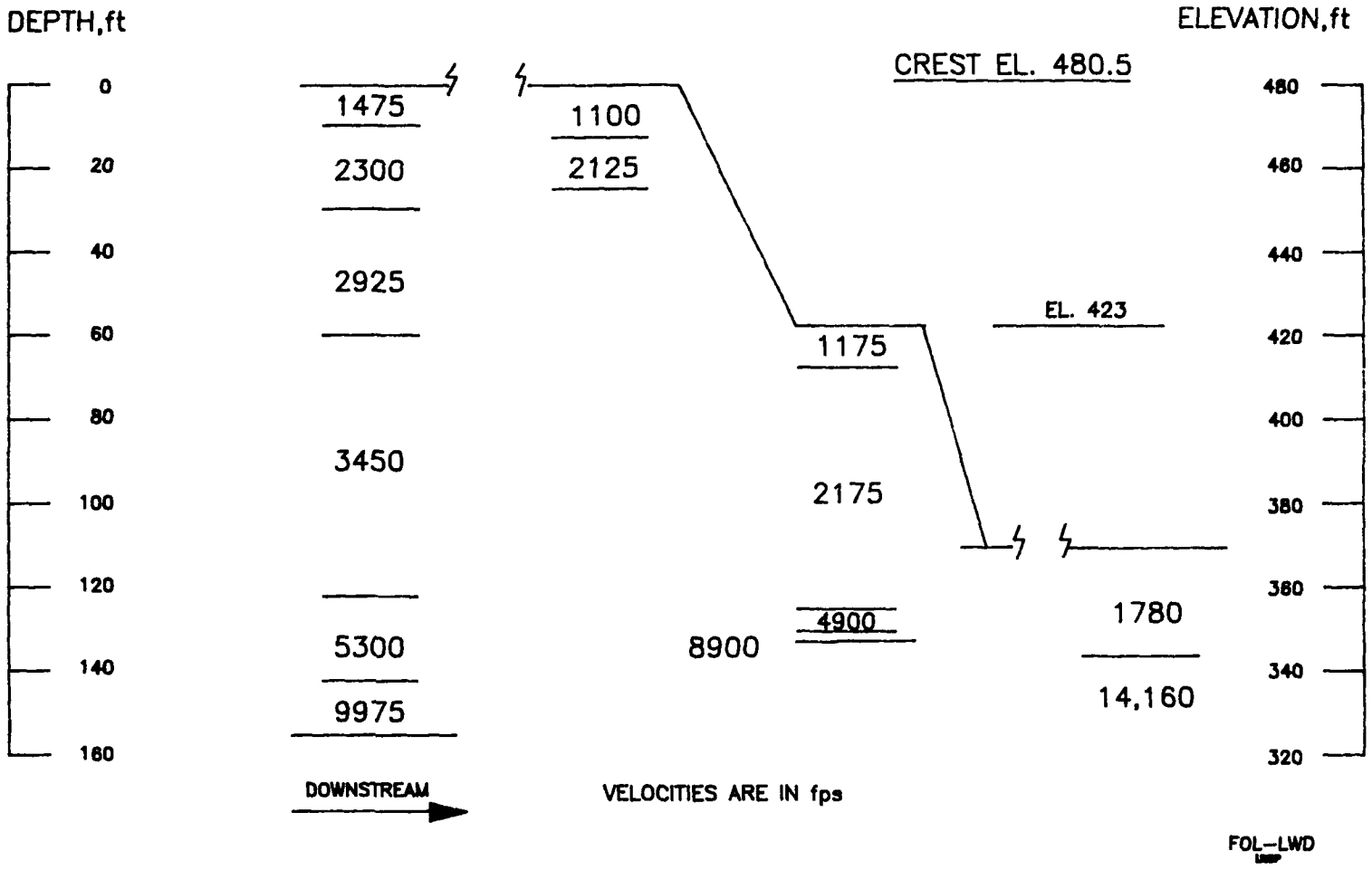

Figure 167. P-wave zonal velocity interpretation for cross section through approximate Station 303+90, Left Wing Dam

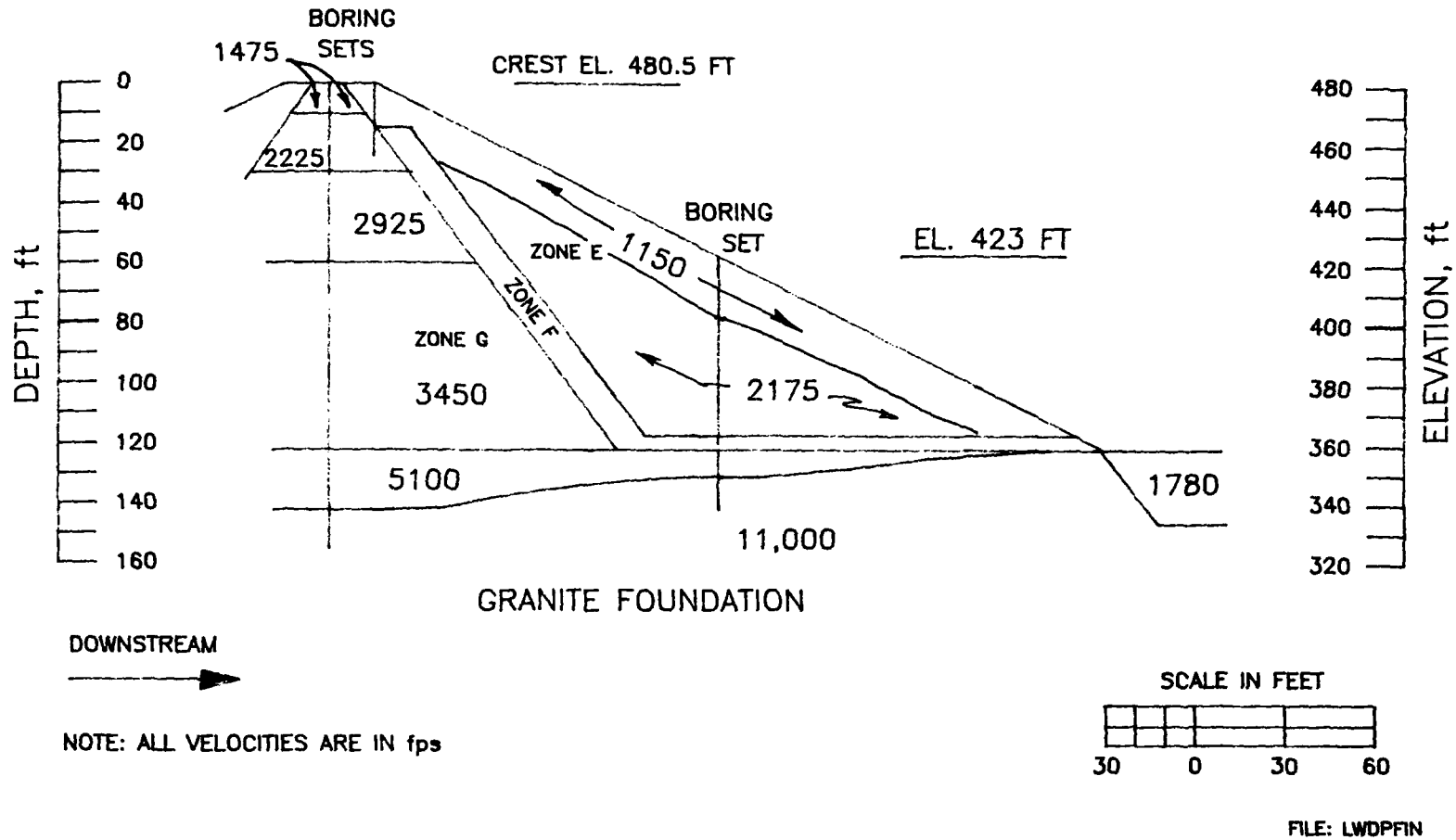

Figure 168. P-wave velocity contours for cross section at approximate Station 303+90, Left Wing Dam

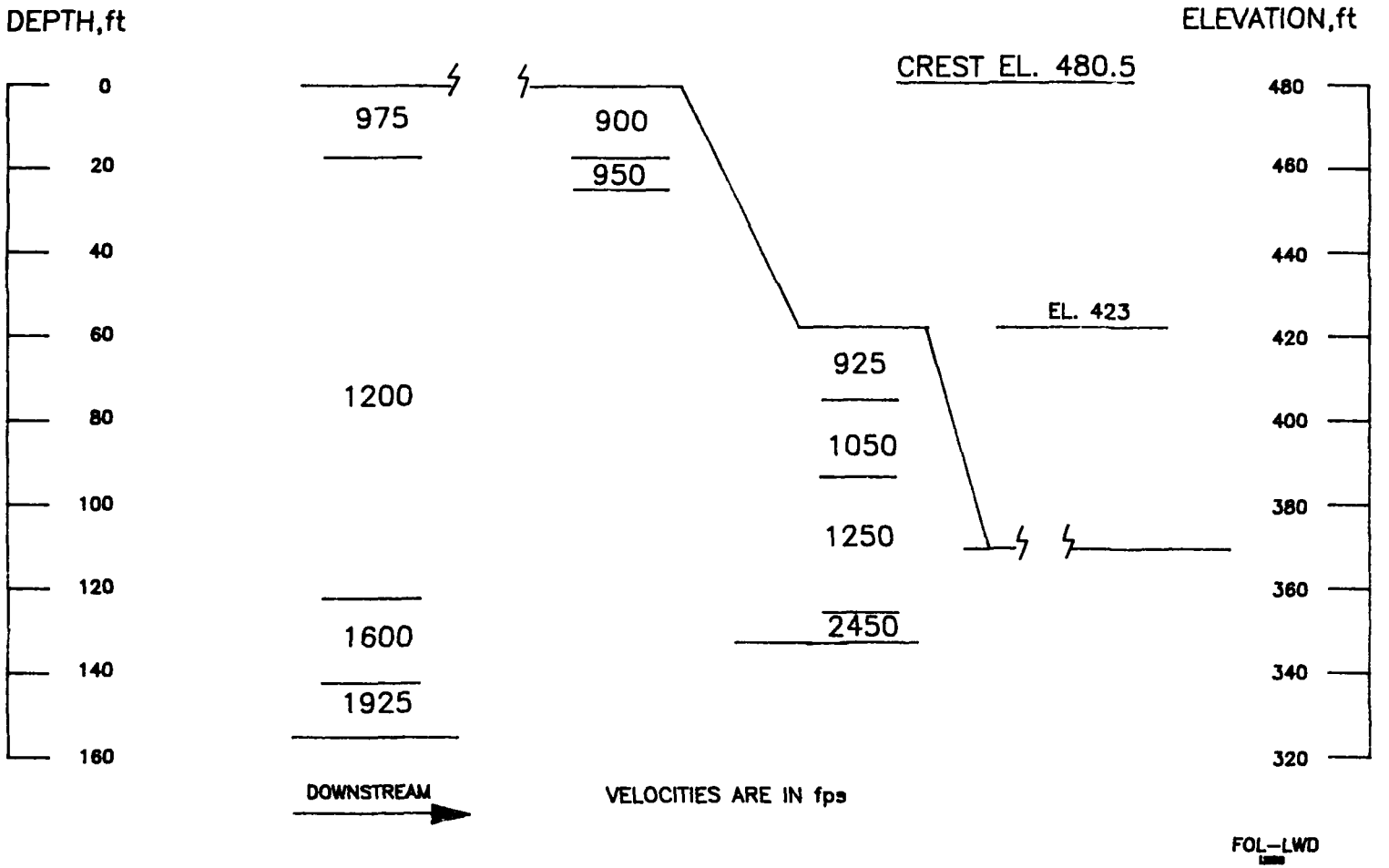

Figure 169. S-wave zonal velocity interpretation for cross section through approximate Station 303+90, Left Wing Dam

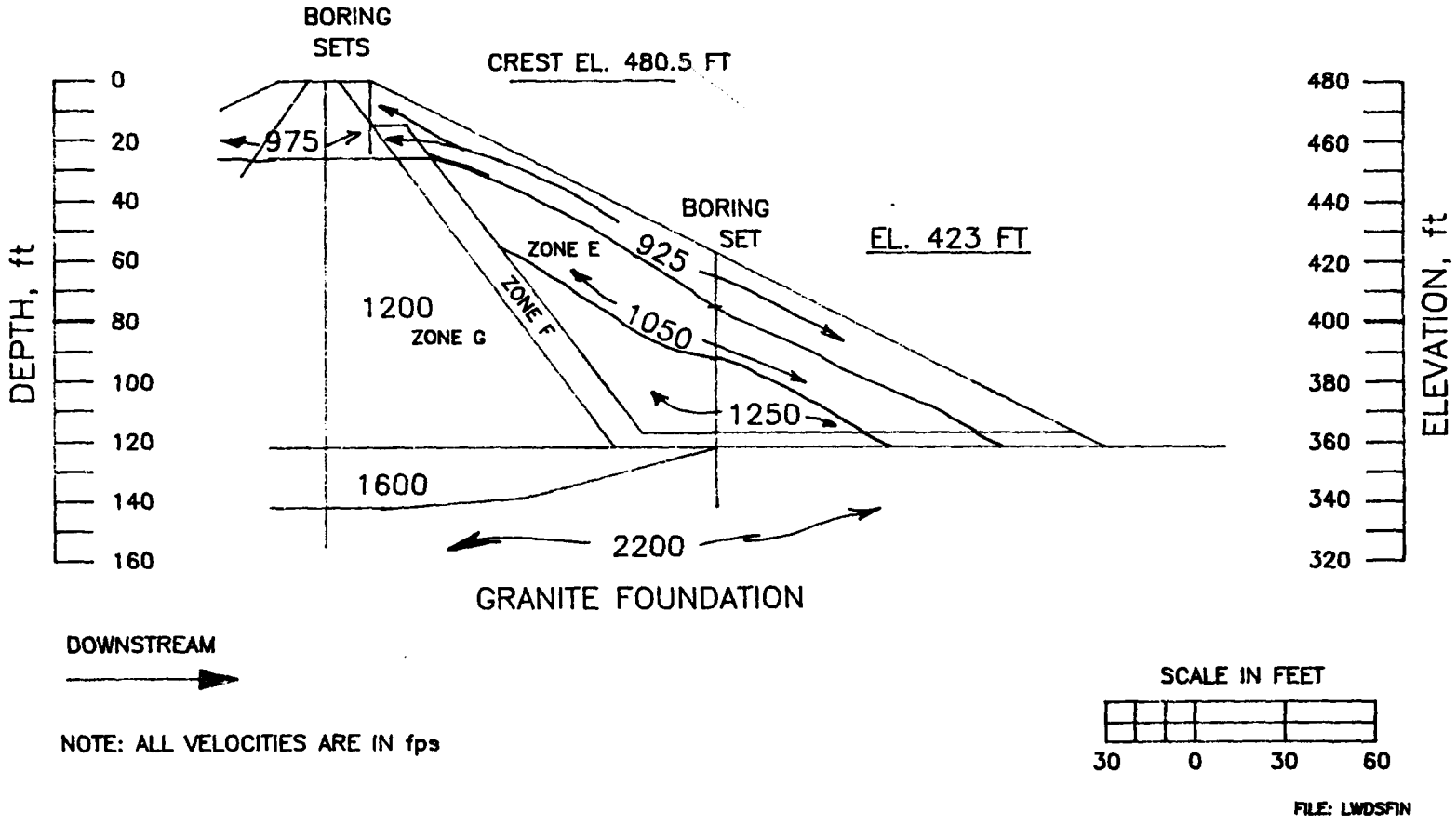

Figure 170. S-wave velocity contours for cross section at approximate Station 303+90, Left Wing Dam

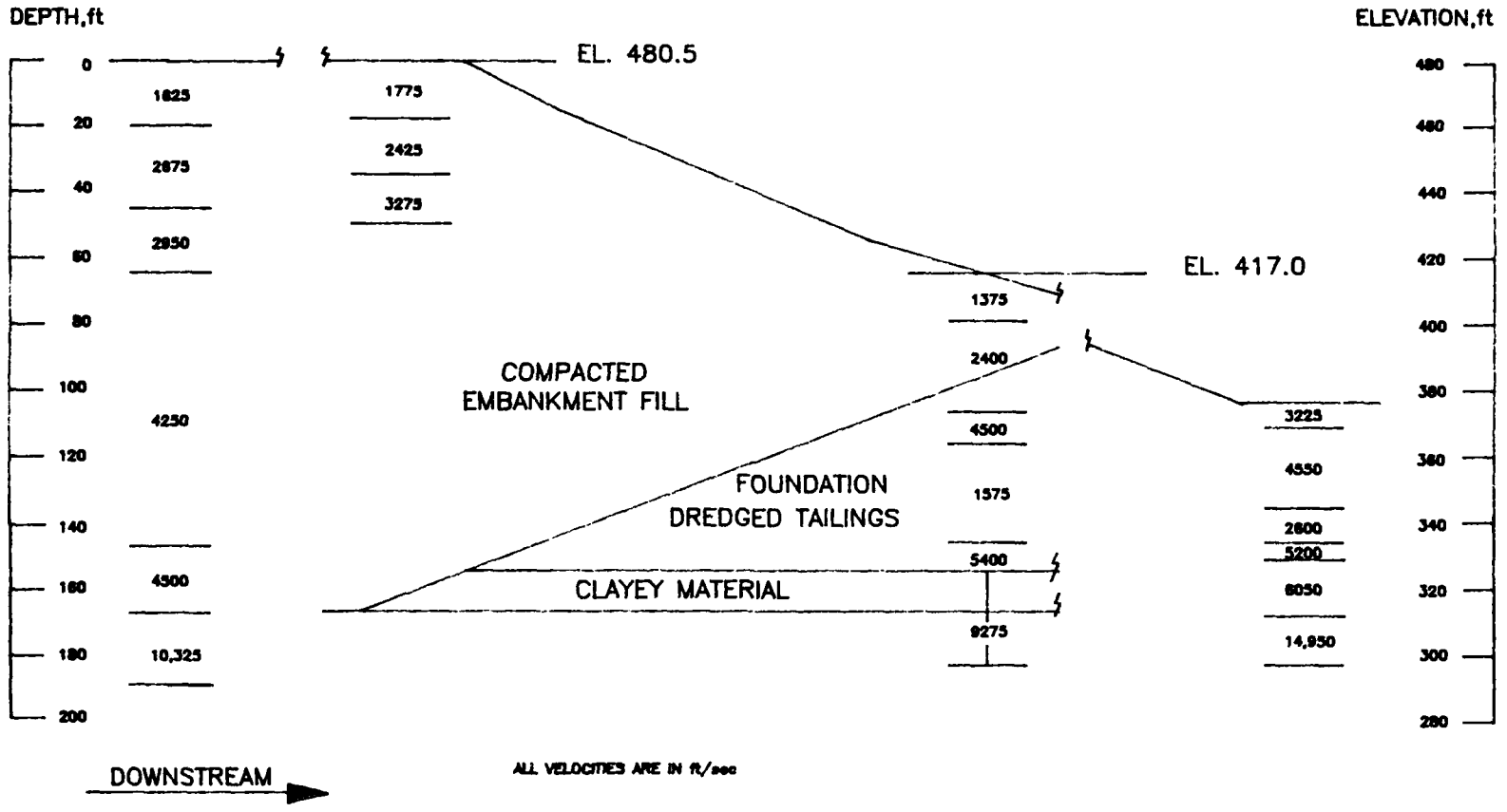

Figure 171. P-wave zonal velocity interpretation for cross section through appropriate Station 448+00, Mormon Island Auxiliary Dam

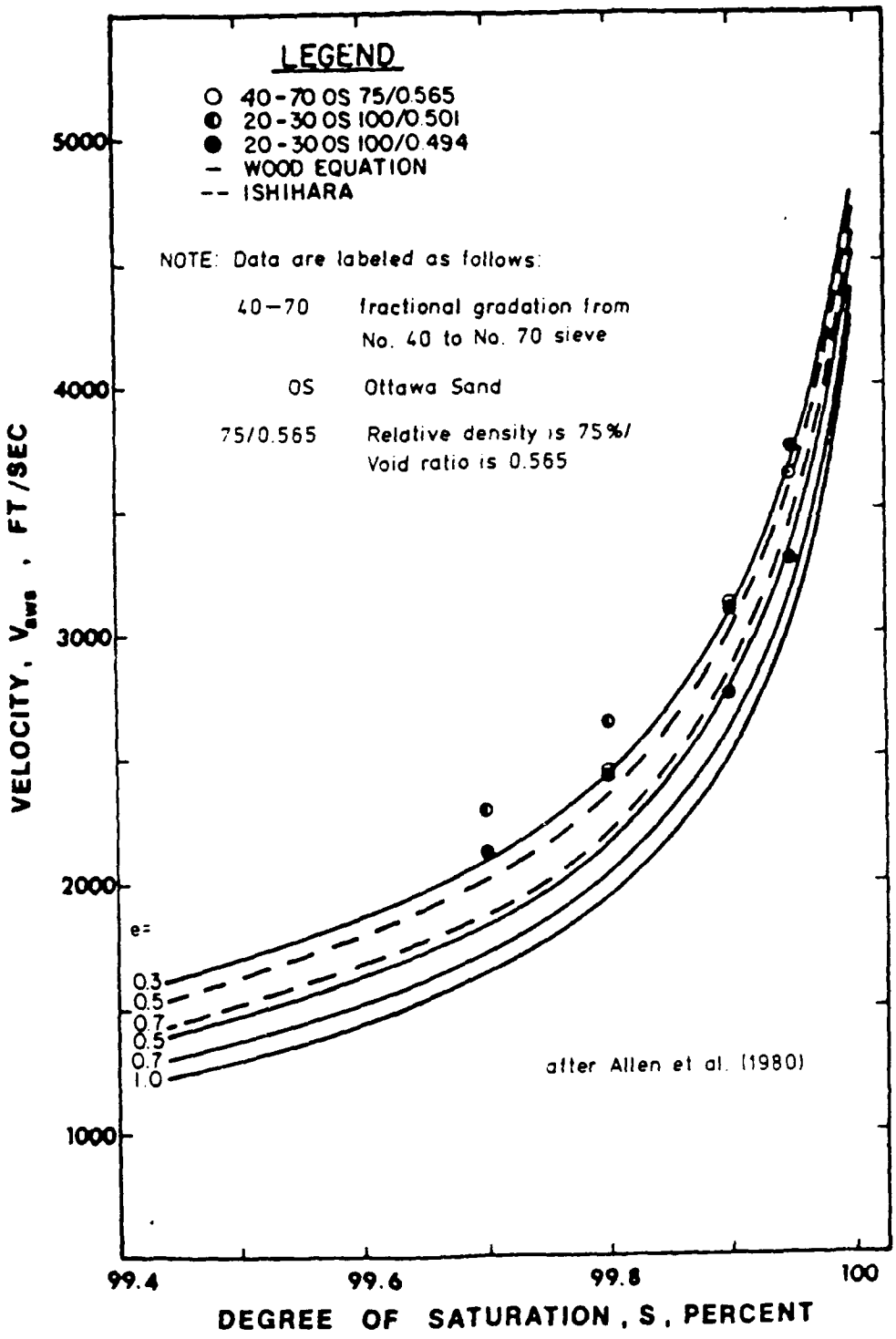

Figure 172. Theoretical and measured relationships between P-wave velocity and degree of saturation for saturated and partially saturated sand

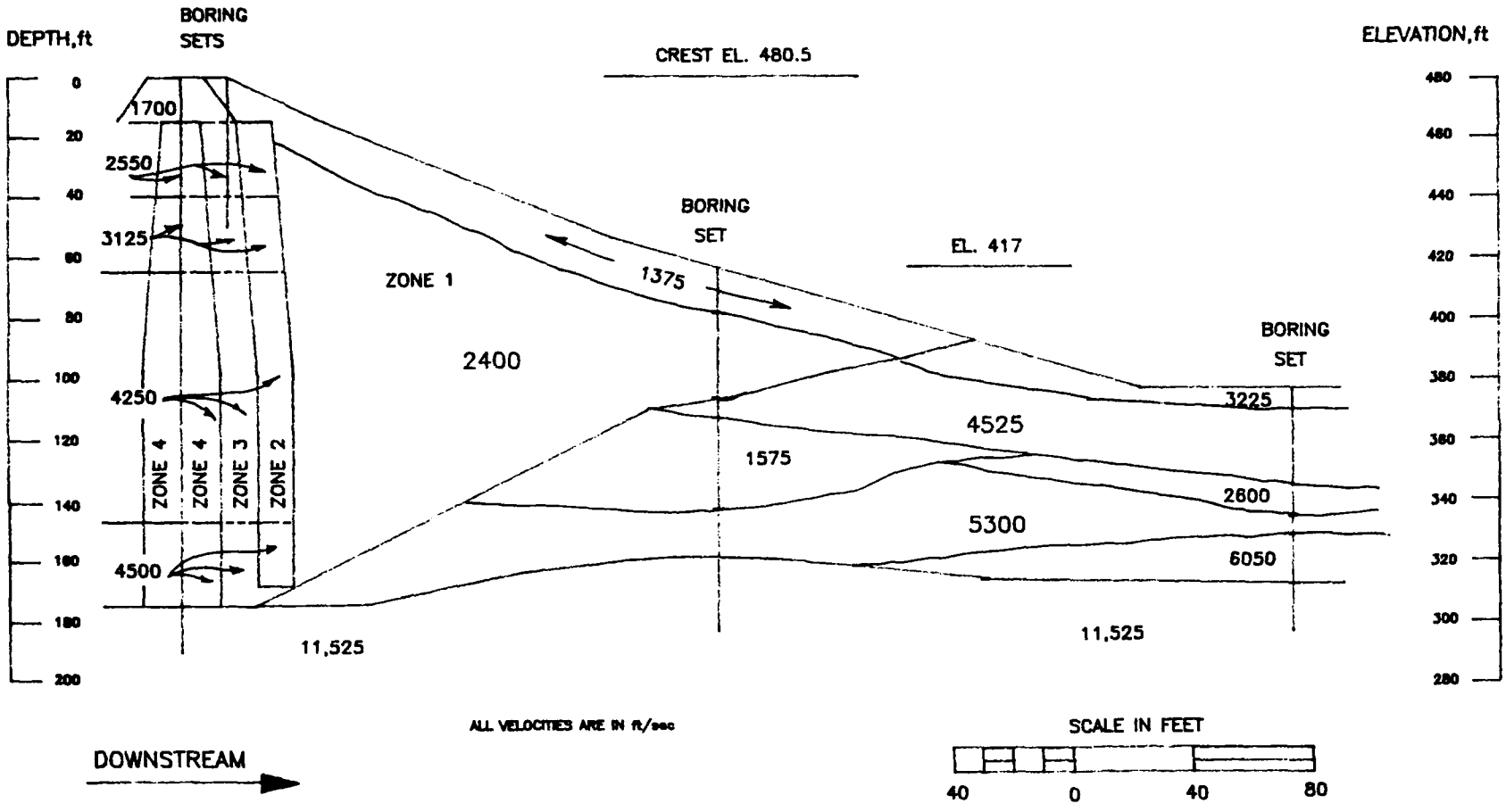

Figure 173. P-wave velocity contours for cross section at approximate Station 448+00, Mormon Island Auxiliary Dam

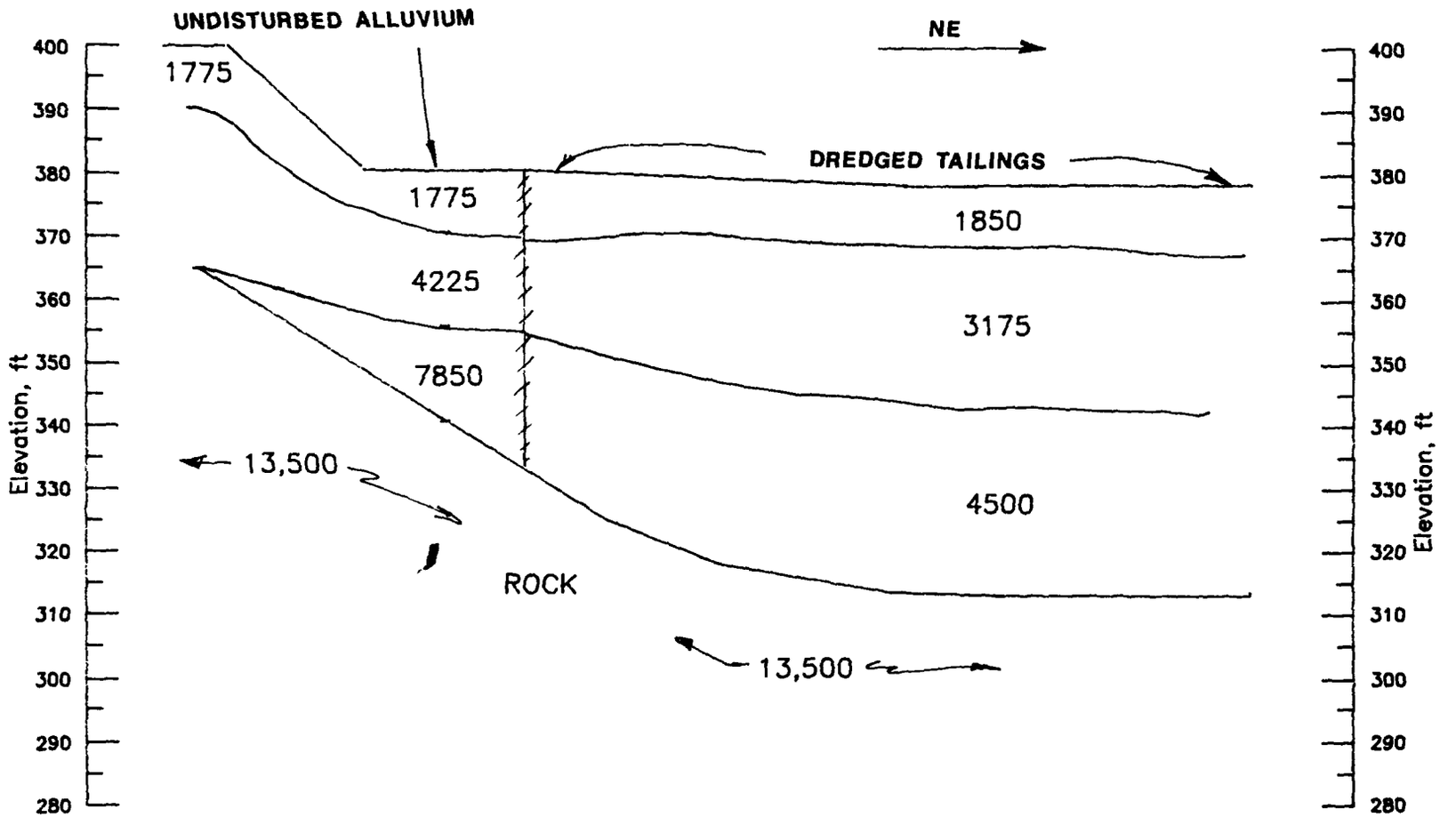

Figure 174. P-wave velocity contours along the downstream toe of Mormon Island Auxiliary Dam

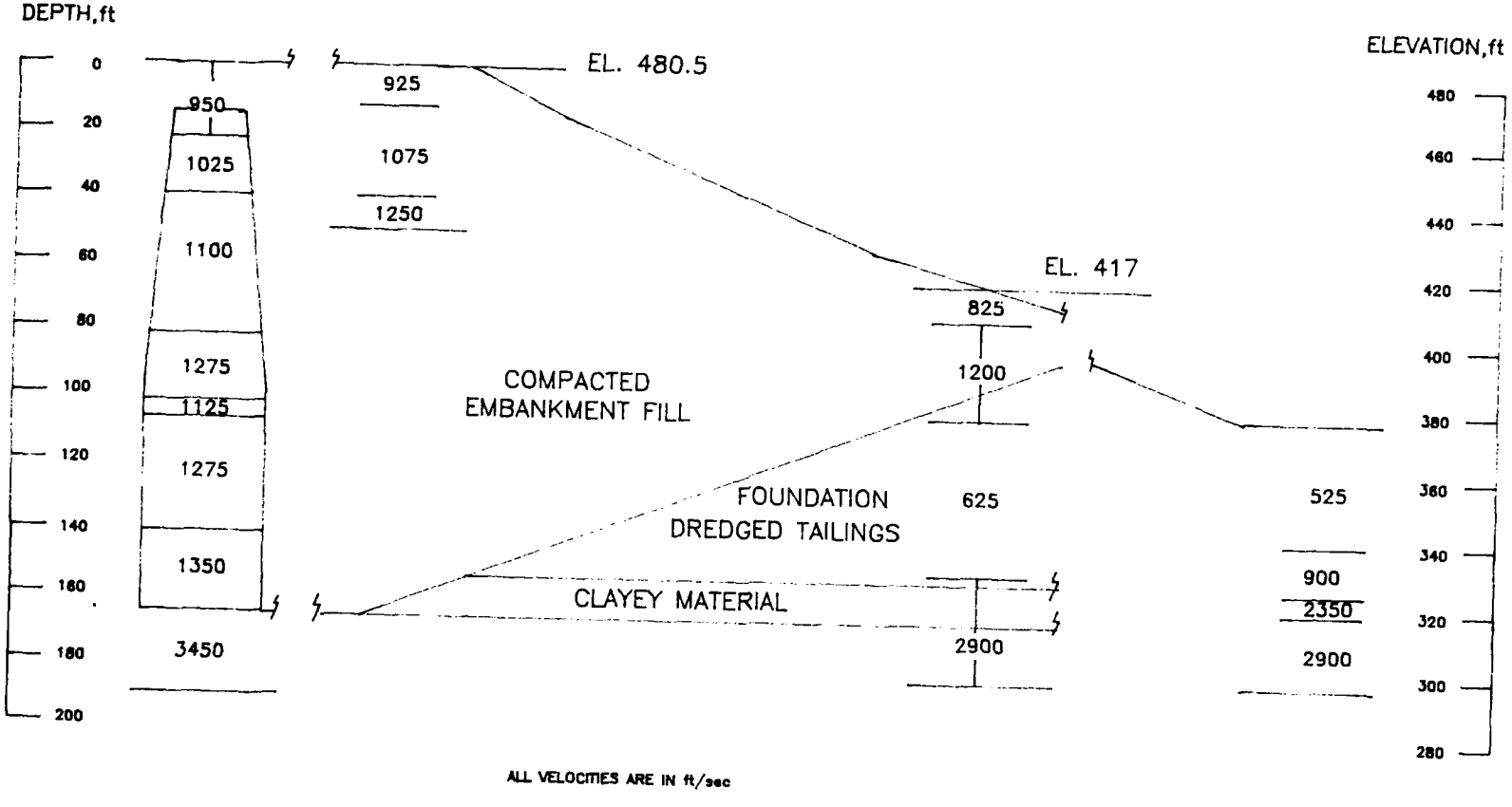

Figure 175. S-wave zonal velocity interpretation for cross section through approximate Station 448+00, Mormon Island Auxiliary Dam

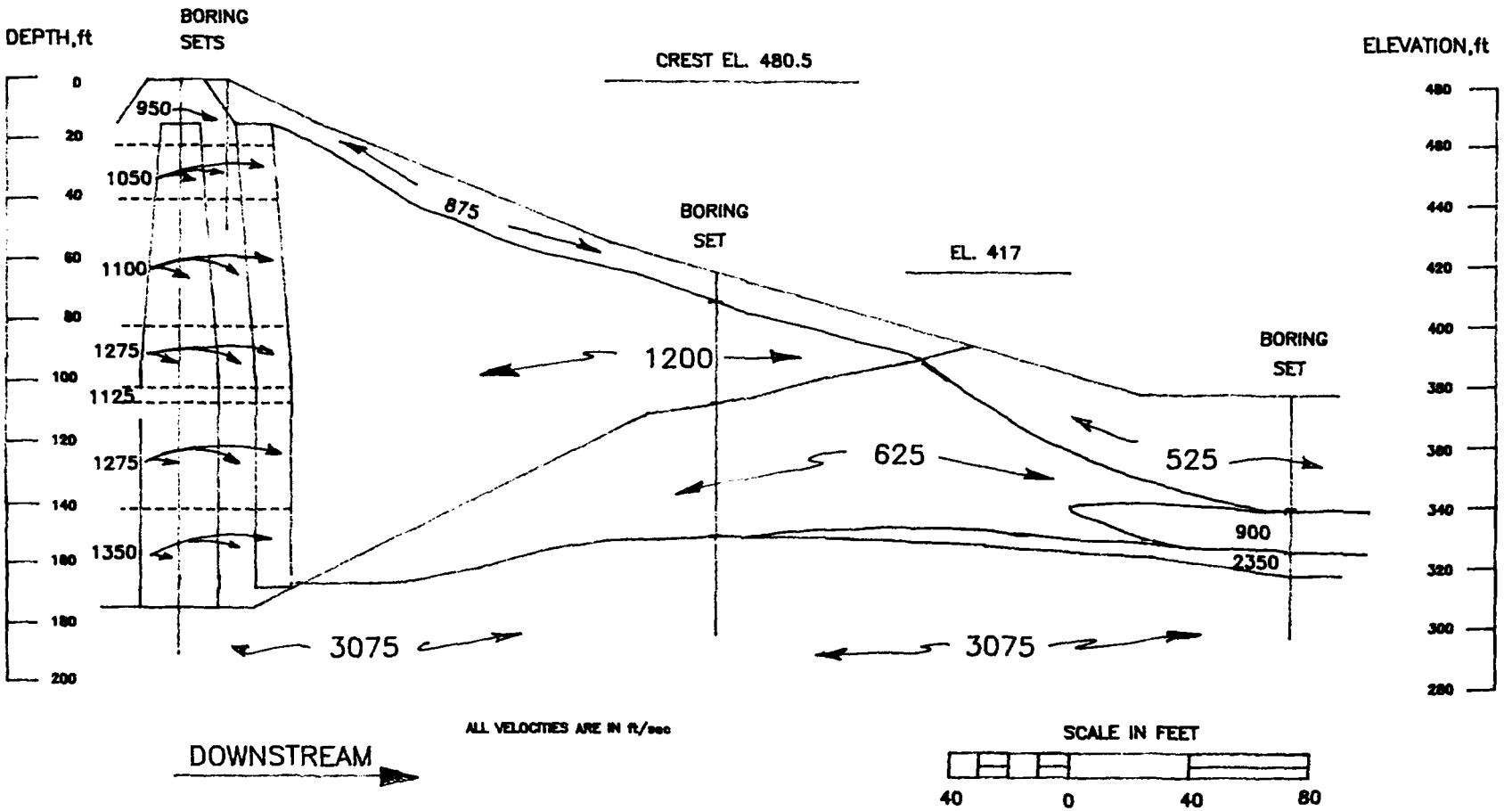

Figure 176. S-wave velocity contours for cross section at approximate Station 448+00, Mormon Island Auxiliary Dam

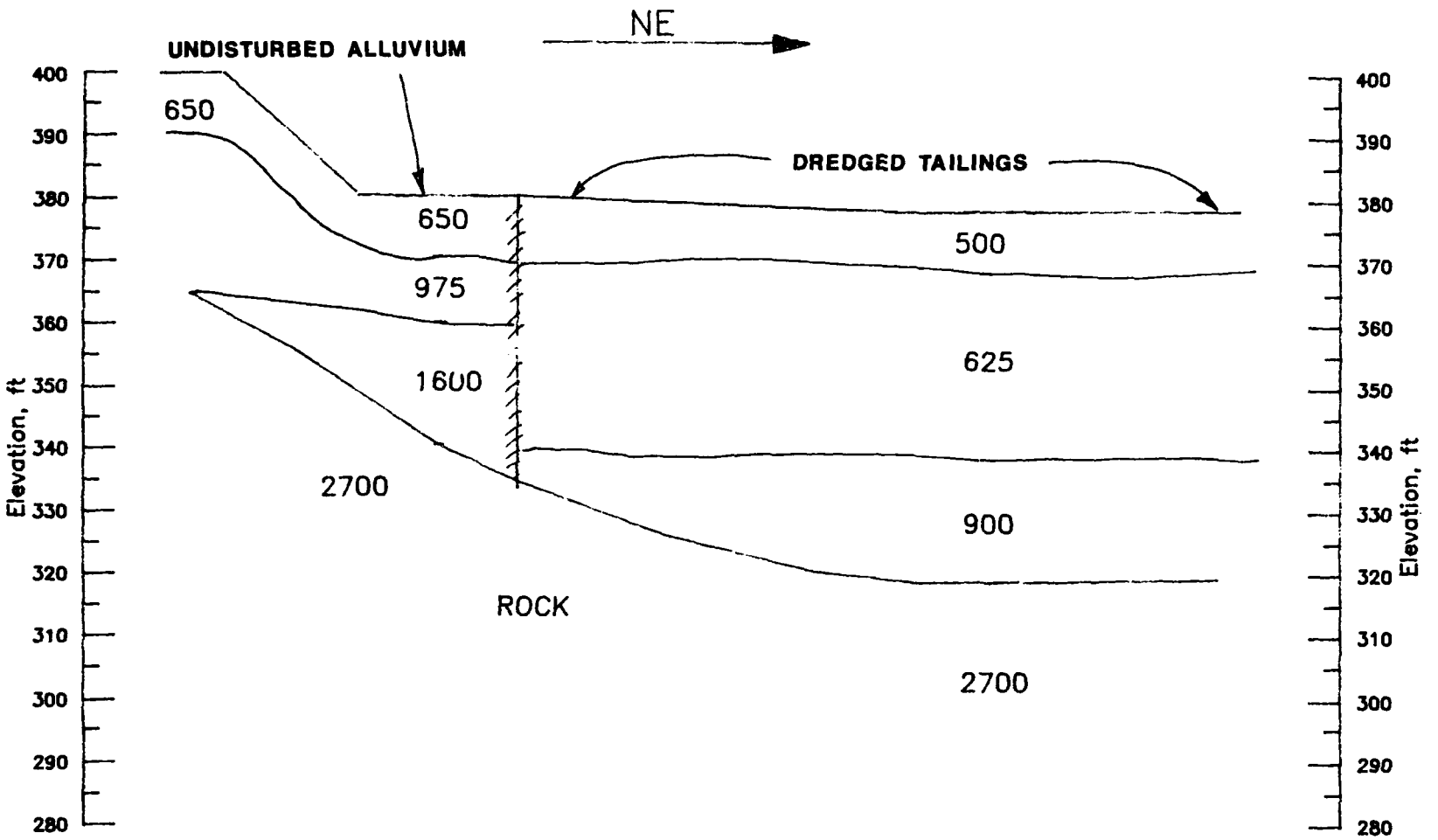

Figure 177. S-wave velocity contours along the downstream toe of Mormon Island Auxiliary Dam